EFFECTS OF CATIONIC ANTIMICROBIAL PEPTIDES ON *CANDIDA* AND *SACCHAROMYCES* SPECIES

Mark R. Harris

A Thesis Submitted for the Degree of PhD
at the
University of St. Andrews
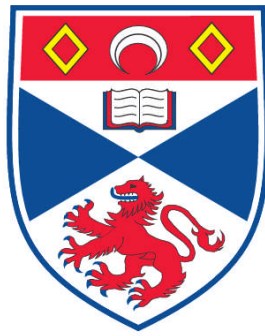
2010

Effects of cationic antimicrobial peptides on *Candida* and *Saccharomyces* species

Mark Harris
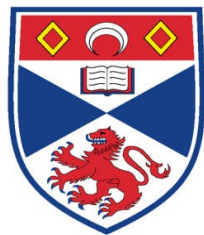
University
of
St Andrews

A Thesis submitted for the degree of Doctor of Philosophy at the University of St Andrews

September 2009

I, Mark Harris, hereby certify that this thesis, which is approximately 44,000 words in length, has been written by me, that it is the record of work carried out by me and that it has not been submitted in any previous application for a higher degree.

I was admitted as a research student in October 2005 and as a candidate for the degree of Ph.D in October 2006; the higher study for which this is a record was carried out in the University of St Andrews between 2005 and 2009.

Date …....................   Signature of candidate …..................................

I hereby certify that the candidate has fulfilled the conditions of the Resolution and Regulations appropriate for the degree of Ph.D in the University of St Andrews and that the candidate is qualified to submit this thesis in application for that degree.

Date …....................   Signature of supervisor …..................................

In submitting this thesis to the University of St Andrews we understand that we are giving permission for it to be made available for use in accordance with the regulations of the University Library for the time being in force, subject to any copyright vested in the work not being affected thereby. We also understand that the title and the abstract will be published, and that a copy of the work may be made and supplied to any bona fide library or research worker, that my thesis will be electronically accessible for personal or research use unless exempt by award of an embargo as requested below, and that the library has the right to migrate my thesis into new electronic forms as required to ensure continued access to the thesis.

Date …................   Signature of candidate …...........................…

                                                  Signature of supervisor ……...........................

Abstract

Antimicrobial peptides (AMPs) are found throughout the animal kingdom and act as a natural defence against a broad spectrum of pathogens. These peptides are toxic to invading organisms without acting on host cells, so are of interest for their potential to act as potent new drugs against pathogenic organisms. AMPs traverse the cell wall and predominantly target the plasma membrane, resulting in destabilisation, leakage of intracellular components and cell death. In this thesis the mode of action of several AMPs was investigated. The role of the cell wall was studied and found to mediate peptide binding, the inhibition of certain cell wall components also increased peptide action, subsequent internalisation events were observed with varying localisation patterns and the effect of several genes that alter cell susceptibility to AMP were examined.

Several *Candida albicans* mutants, each deficient in cell wall protein mannosylation, were tested in relation to their susceptibility to AMPs. It was discovered that cells lacking or deficient in the phosphomannan fraction, with a concomitant reduction in surface negative charge, correlated with reduced susceptibility to AMP action. To ascertain whether peptide binds to negatively charged phosphate, the effect of exogenous glucosamine 6-phosphate (but not glucosamine hydrochloride) was studied demonstrating that peptide efficacy was reduced due to the presence of exogenous phosphate. More specifically, sequestration of the truncated cationic AMP dermaseptin S3 (DsS3(1-16)) was reduced in these phosphomannan deficient mutants. Microscopy

analysis of fluorescein tagged DsS3(1-16) also revealed the differential localisation patterns of this AMP: transiently binding to the plasma membrane, localisation to the vacuole or diffuse distribution throughout the cytoplasm. It is proposed that for these cationic AMPs to exert their full antifungal action they must first bind to the negatively charged phosphate.

The echinocandins are a relatively new class of antifungal that function by inhibiting 1,3-β glucan synthase resulting in reduced 1,3-β glucan in the cell wall. As AMPs have to traverse the cell wall it was postulated that cells lacking this fraction would display increased AMP binding to the membrane. Clinical isolate strains of *Candida* and *Cryptococcus* spp. were acquired to test their susceptibility to AMP and echinocandin combinations. Comparing the fractional inhibitory concentration index (FICI) (supported by viable cell counts and on a solid surface using disc diffusion assays) synergy was observed between caspofungin, anidulafungin and several AMPs *in vitro*. *In vitro* toxicity assays revealed no increase in haemolytic or cytotoxic action on combination. These synergistic combinations could provide a novel treatment against fungal pathogens.

The final area of study was based upon work that identified genes whose expression altered cell susceptibility to AMPs. Three genes were selected for investigation that upon deletion increased the action of DsS3(1-16) or magainin 2 on *S. cerevisiae*. Results from growth analysis, peptide sequestration and cell viability counts confirmed that deletion of *HAL5*, *LDB7* or *IMP2'* did increase susceptibility. Additionally, deletion of

HAL5 increased the probability of cell depolarisation upon peptide exposure. Expression of GFP-tagged Imp2' also increased when cells were exposed to DsS3(1-16). It was concluded that deletion of *HAL5* increases depolarisation due to insufficient potassium efflux, leading to ion leakage and cell death facilitated by AMP action. Double strand break repair and DNA protection are probably compromised upon deletion of *LDB7* and *IMP2',* increasing the inhibitory action of DsS3(1-16) that has previously been shown to bind to DNA.

Acknowledgements

Abbreviations

a.a.	Amino acid
AIDS	Acquired immune deficiency syndrome
AIF	Apoptosis-inducing factor
AMP	Antimicrobial peptide
AU	Absorbance unit
CCCP	Carbonyl cyanide m-chlorophenyl hydrazone
CFU	Colony forming units
CTG	CellTracker™ Green
DAPI	4',6-diamidino-2-phenylindole
diS-C3(3)	3,3'-dipropylthiacarbocyanine iodide
DNA	Deoxyribonucleic acid
DsS3(1-16)	Dermaseptin S3(1-16)-NH_2
FICI	Fractional inhibitory concentration index
Flu-DsS3(1-16)	Fluorescein tagged DsS3(1-16)
G-6-P	Glucosamine 6-phosphate
GFP	Green fluorescent protein
GHCl	Glucosamine hydrochloride
Gom	Gomesin
HAL	HALotolerance
HIV	Human immunodeficiency virus
HS	Human serum
IMP	Inner membrane protease
IZH	Implicated in zinc homeostasis
LB	Luria-Bertani medium
LDB	Low dye binding
Mag 2	Magainin 2
*MAT*a	Mating-type locus
MEB	Malt extract broth
MIC	Minimum inhibitory concentration
MNT	MaNnosylTransferase
MNN	MaNNosyltransferase
MOPS	3-(N-morpholino propane sulfonic acid
OCH	Outer CHain elongation
OD_{600}	Optical density at 600 nm
PBS	Phosphate buffer saline
PCR	Polymerase chain reaction
PI	Propidium iodide
PMR	Plasma Membrane ATPase Related
Rana	Ranalexin
RNA	Ribonucleic acid
RPMI	Roswell Park Memorial Institute medium
SD	Standard deviation
WT	Wild-type
YEPD	Yeast extract peptone dextrose
YNB	Yeast nitrogen base

County/State abbreviations

BRK	Berkshire
BUX	Buckinghamshire
CA	California
CBE	Cambridgeshire
DOR	Dorset
GLR	Gloucester
HFD	Hertfordshire
HPH	Hampshire
IA	Iowa
KNT	Kent
LEC	Leicestershire
MA	Massachusetts
NJ	New Jersey
NY	New York
OFE	Oxfordshire
SCD	Strathclyde
SXW	West Sussex
VT	Vermont
WA	Washington
WLT	Wiltshire
YSS	South Yorkshire

Contents

List of figures

List of tables

Chapter 1

1. General Introduction

1.1 Antimicrobial Peptides

Antimicrobial peptides (AMPs) function throughout the animal kingdom as a means of protection against microbes. Many hundreds of AMPs have now been characterized that have actions against eukaryotic cells, bacteria, fungi and viruses (Giuliani *et al*, 2008). Specificity exists preventing toxic effects on host cells that rely on the core differences found between mammalian and microbial cells. This comprises mainly membrane composition, including expression of lipopolysaccharide, peptidoglycan and sterols (Powers *et al*, 2003). This specificity is strengthened due to interactions with the lipid bilayer through electrostatic interactions arising from mainly cationic AMPs with anionic phospholipids found on target cells (La Rocca *et al*, 1999).

It is becoming clear that AMPs are an integral part of the immune system, providing a fast and effective means of defence against invading organisms. Pathogens frequently enter host organisms via ingestion, inhalation and through wounds. The adaptive immune response does not affect these organisms until they begin to multiply in the body leading to infection (Giuliani *et al*, 2008). The innate immune response is required to combat these pathogens before this occurs. AMPs play an important role in this innate system as a first line of defence and are found in a wide range of organisms from mammals to plants (Hancock *et al*, 1998). They are released after microbial infection and act to kill a broad spectrum of pathogens. AMPs represent ancient elements of the immune responses of a wide spectrum of life (Hancock *et al*, 1998). Throughout the course of evolution they have changed little and have highly conserved induction

pathways in vertebrates, insects, and plants. The majority of these peptides share several common properties: most have a molecular weight below 10 kDa, they are hydrophobic or amphipathic and have an overall positive charge so many are cationic (Bechinger *et al*, 2006).

AMPs are of interest due to the rise in resistance of fungal pathogens against antifungal drugs. Currently around 420 peptides with antifungal action have been identified (Antimicrobial peptide database website, 2009) and can be classified by their secondary structure. These peptides may be linear or cyclic in structure and display hydrophobic or amphipathic (hydrophobic and hydrophilic sections) properties.

Some peptides cause cell lysis by interacting with the membrane lipid bilayer resulting in leakage of certain cellular components (Shai, 1995). This may be due to pore formation (Bechinger, 1997) or interaction with intracellular targets (Hugosson *et al*, 1994). Many of these peptides are disordered in water, but when attached to membranes become ordered and able to exert their killing action. As antifungal peptides have a small size, nuclear magnetic resonance (NMR) has emerged as a useful technique for structural studies of these peptides. This technique has been used for the majority of AMP structures currently known.

1.2 Antimicrobial peptide characterisation

The number and diversity of AMPs discovered thus far makes it problematic to categorise them. This variability is likely to be a result of the species specific microbial environments occupied by pathogenic microorganisms that peptides have evolved to combat. Attempts have been made to group them broadly according to their secondary structure (van't Hof *et al*, 2001). Peptides generally fall into three main categories: linear peptides with an α-helical structure, peptides consisting predominantly of β-strands connected by intramolecular disulphide bridges and peptides characterised by over-representation of one or more amino acids. These categories will be discussed with examples of AMPs representative of each section (Table 1.1).

1.2.1 Linear peptides with an α-helical structure

The majority of peptides discovered thus far have an α-helical structure. These peptides can be divided into; linear helical peptides, helical peptides containing cysteine bridges or a combination of linear and loop structures. They have the propensity to be disordered in aqueous solution but become structured forming amphipathic helices in hydrophobic solvents or when in contact with cytoplasmic membranes (Oren *et al*, 1998). Known as interfacial folding, this is crucial for antimicrobial action as it is required for peptide attachment and insertion into the membrane; e.g., the human cathelicidin LL-37 is disordered in water but in the presence of hydrophobic solvents forms an α-helix. This orientates the residues such that they bind to the lipid head groups and the helix inserts into the membrane. Furthermore, the strength of the helical conformation increases its antimicrobial activity (Johansson *et al*, 1998).

The temporins are a group of small peptides (10-16 a.a.) with a linear α-helical structure (Lu *et al*, 2006). In contrast to other AMPs in this group, they show reduced specificity towards anionic membranes and may target zwitterionic membranes resulting in increased haemolytic and cytotoxic effects (Mangoni *et al*, 2000). Temporin L has the strongest antimicrobial action among the temporins and displays strong lipid binding affinity. The use of CD spectroscopy demonstrated that temporin L formed α-helical conformations more readily and strongly than other temporins (D'Abramo *et al* 2006). This highlights the correlation between peptide conformation in solution and extent of antimicrobial activity.

The helical content of this group of peptides has also been linked to their cytolytic activity. Studies using derivatives of paradaxin and melittin lacking the natural α-helical structure also lack haemolytic activity but still retain their activity against bacteria. This has been demonstrated with model membranes where native melittin binds strongly to both negatively charged and zwitterionic membranes while the analogues bind only to the former (Shai *et al*, 1996; Oren *et al*, 1997). Thus for some peptides in this family, the α-helical conformation is more contributory in determining eukaryotic selectivity than microbial selectivity.

1.2.2 Peptides predominantly consisting of β-strands connected by intramolecular disulphide bridges.

Relative to α-helical AMPs, few peptides adopt a β-sheet conformation. These are longer chain peptides generally over 25 a.a in length to facilitate β-sheet formation. They are structured as β-sheet in aqueous solution that may become strengthened in solvents or membranous environments. The amphipathicity of these peptides is achieved through antiparallel β-sheet and β-hairpin conformations that are essential for antimicrobial action, with hydrophobic residues orientated on one surface and hydrophilic residues on the other. This allows the hydrophilic residues to interact with the lipid head groups while the hydrophobic residues insert and interact with the lipid tail groups.

The defensins are among the most studied and well characterised AMPs in this category and consist mainly of β-sheet (Ganz *et al*, 1985). They are cysteine rich (six cysteines forming three disulphide bonds) and are found in both vertebrates and invertebrates. They function by inserting and forming channels in the membrane leading to efflux of ions (Kagan *et al*, 1990). The cysteine residues are essential for their antimicrobial activity and stability as mutation leads to peptide inactivation.

1.2.3 Peptides characterised by over-representation of one or more amino acids.

Each member of this group is characterised by sequences rich in one or more specific amino acids such as histidine, tryptophan or proline. The amphipathicity of this group originates primarily from their residue distribution. The histatins are a well characterised

group of AMPs produced by the salivary glands and are rich in histidine. They adopt weak amphipathic helical structures in hydrophobic solvents and form transient pores (Helmerhorst *et al*, 1997). They do not cause disintegration of the plasma membrane but instead target the mitochondria (Helmerhorst[a] *et al*, 1999). Tryptophan is an uncommon amino acid in peptides and proteins but is found at a high percentage in indolicidin.

Tryptophan facilitates entry of peptides into the plasma membrane due to the propensity to position itself in or near the lipid bilayer. The mode of action of indolicidin involves pore formation. Using CD spectroscopy it was shown to be unordered in water taking on a more ordered conformation in lipid bilayers (Rozek *et al*, 2000). The bacterial selectivity of indolicidin can be enhanced by the substitution of several tryptophan residues with leucines while retaining specific tryptophans at certain positions (Subbalakshmi *et al*, 2000). Subsequently it was shown that tryptophan mediates interactions with zwitterionic bilayers while the positively charged N-terminus and amidated C-terminus mediate the mode of action of indolicidin with bacterial membranes (Staubitz *et al*, 2001).

Several other AMPs have been identified with differing structures that do not belong to any of the three categories above. These include peptides with a cyclic structure such as gramicidin S and Rhesus theta defensin 1 (RTD-1). The gramicidins are a group of six peptides originally derived from *Bacillus brevis*. Gramicidin S is a derivative forming a cyclic peptide chain constructed from two pentapeptides joined head to tail. Its mode of

action is unclear, however, it has been proposed to induce membrane defects of varying sizes leading to destabilisation of the bilayer (Ashrafuzzaman, *et al*, 2008).

The RTDs were isolated from monkey leukocytes and bone marrow and are short (18 a.a.) cyclic peptides. The cyclic backbone of RTD-1 contains three disulphide bonds producing a β-sheet connected by β-turns (Trabi *et al*, 2001). The cyclic conformation enhances antimicrobial activity as the linear form is 3-fold less active (Tang *et al*, 1999). The RTDs have broad spectrum antimicrobial activity with little cytotoxicity. It was found that this lack of cytotoxicity was not dependent on the cyclic structure. They are thought to cause lysis through pore formation and membrane disruption (Tran *et al*, 2008).

Table 1.1 Classification and origin of structurally representative AMPs.

Group	Name	Sequence	Origin
I α-helix	cathelicidin	LLGDFFRKSKEKIGKEFKRIVQRIKDFLRNLVPRTES	mammalian lysosomes
	DsS3(1-16)	ALWKNMLKGIGKLAGK	*Phyllomedusa sauvagii*
	magainin 2	GIGKFLHSAKKFGKAFVGEIMNS	*Xenopus laevis*
	ranalexin (kinked helix)	FLGGLIKIVPAMICAVTKKC	*Rana catesbeiana*
	temporin L	LLPIVGNLLKSLL-*Am*	*Rana temporaria*
II β-sheet	defensins (eg DEFB1)	DHYNCVSSGGQCLYSACPIFTKIQGTCYRGKAKCCK	human neutrophils
	gomesin	ZCRRLCYKQRCVTYCRGR	*Acanthoscurria gomesiana*
III unusual a.a. composition	histatin-5	DSHAKRHHGYKRKFHEKHHSHRGY	human saliva
	indolicidin	ILPWKWPWWPWRR-*Am*	bovine neutrophils
IV other structures (cyclic)	gramicidin S	cyclo(VOLFP)$_2$	*Bacillus brevis*
	RTD-1	GFCRCLCRRGVCRCICTR	Rhesus macaque monocytes and neutrophils

Am represents an amidated C-terminus.

1.3 Mechanisms of Action

Two general mechanisms were originally proposed to describe the action of AMPs on phospholipid membranes. These were the 'barrel-stave' model (Hogosson *et al*, 1994) and the 'carpet' model (Pouny *et al*, 1992). In the carpet model peptide monomers may also form 'toroidal' pores (Figure 1.1). A third model, aggregate channel formation

(Hancock *et al*, 1999), was also proposed that does not cause significant membrane depolarisation.
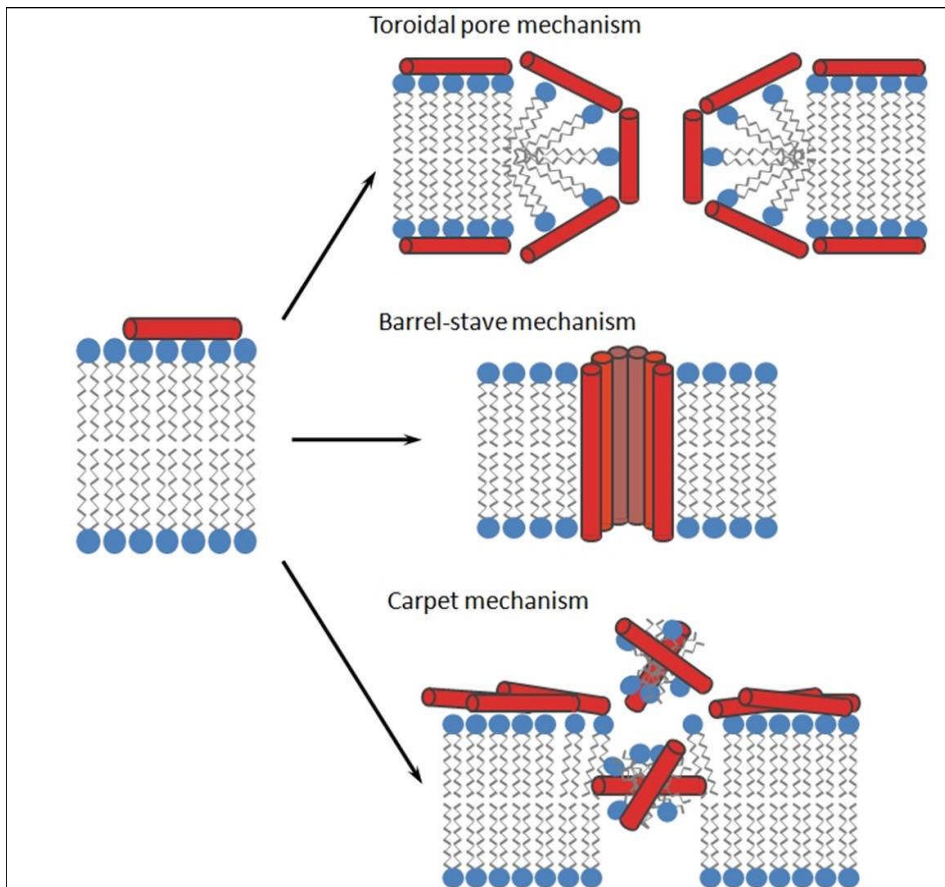
Figure 1.1. The toroidal pore, barrel-stave and carpet models of antimicrobial action. Phospholipid bilayer with peptide monomers represented by red cylinders.

1.3.1 The barrel-stave model

This model was first proposed as the mode of action for α-helical peptides (Boman *et al*, 1993). Peptide monomers first associate with the membrane surface due to electrostatic interactions from the side chains and re-orientate themselves perpendicular to the bilayer and span the membrane. Pore size may increase with the association of additional monomers, however, with certain peptides only three monomers are required for pore formation (Papo *et al*, 2003). Once inserted, the peptides associate

such that their non-polar side chains face the hydrophobic lipid core and the hydrophilic surfaces of the peptides point inward. These pores cause disruption of gradients and leakage of intracellular components ultimately leading to cell death (Shai, 1999). Pore formation can occur on the surface of the membrane or within the core: hydrophobic peptides can span membranes as monomers forming within the core while amphipathic α-helical peptides associate on the surface of the membrane before insertion as it is energetically unfavourable for a single α-helical monomer to insert into the bilayer (Ben-Efraim *et al*, 1993).

Insertion of the peptide into the membrane relies heavily on hydrophobic interactions; it is only the initial interaction with the membrane surface that is controlled by charge interactions. The net charge of the α-helix should be close to neutral to allow pore formation as a result of the proximity of the hydrophilic regions of monomers at the pore centre (Ben-Efraim *et al*, 1997). These properties are thought to result in peptides with decreased cell selectivity making them toxic to both prokaryotic and eukaryotic cells (Shai, 1999).

1.3.2 The carpet model and toroidal pore formation

Some AMPs were found to deviate from the barrel-stave model. The carpet model was first proposed to describe the mode of action of dermaseptin S (Pouny *et al*, 1992) and later applied to other peptides (Gazit *et al*, 1995). In the carpet model peptides are not inserted into the membrane, but are aligned in parallel to the bilayer while remaining in contact with the lipid head groups, thus coating the surrounding area. The peptide binds

to lipid head groups and forms an amphipathic structure. This stage is dependent on target membrane type: the peptide may cover the whole membrane, or alternatively, it may be present in various peptide regions forming local carpets (Oren *et al*, 1998). Peptide monomers align themselves so that the hydrophilic surface is facing the lipid head groups. The hydrophobic residues then interact with the lipid core causing reorientation of the monomers leading to disruption of bilayer curvature. This causes membrane cracks, leakage of cytoplasmic contents, disrupted membrane potential, and eventually the disintegration of the membrane (Oren *et al*, 1998).

Prior to membrane lysis it has been suggested that pores called toroidal pores form to allow the passage of low molecular weight molecules. This was used to describe the mode of action of various AMPs including dermaseptin (Mor[2] *et al*, 1994), and magainin (Ludtke *et al*, 1996). In the toroidal model the lipid bends back on itself like the inside of a torus (a rounded ridge, Figure 1.1) allowing additional peptide monomers to bind to the inner membrane forming a structure of organized holes (Yang *et al*, 2000). The membrane lipids are important as they carry a net negative charge that allows the peptide carpet to form by reducing the positive charge repelling action between peptides. Recently a variation on the toroidal pore model has been proposed in which large pores (>4.6 nm) are formed in bacterial cells sufficient to caused protein leakage (Yoneyama *et al*, 2009).

In the carpet model, when the peptide binds to the membrane, monomers remain in constant contact with the phospholipid head groups throughout the permeation

process. No specific structure needs to be adopted: they can have varying secondary structures, lengths, and can be either linear or cyclic, but they must possess a certain level of hydrophobicity and a number of positive charges (Bechinger *et al*, 2006).

1.3.3 The aggregate channel model

Membrane depolarisation in itself may not be enough to account for the antimicrobial potency of several peptides. For example, studies with gramicidin S against gram positive bacteria showed that at a concentration below the peptides MIC, the target cell displayed the highest levels of membrane depolarisation. This indicates that depolarisation is not necessarily the stage that causes cell apoptosis and so the aggregate channel model was proposed (Hancock *et al*, 1999). In this model, the peptides are allowed to cross the membrane through pores formed by other peptide monomers but also have one or more intracellular targets (Hancock *et al*, 1999). The peptides first bind to the phospholipid head groups and then insert into the lipid bilayer. Unstructured aggregates of peptides then form, spanning the membrane. These are thought to contain water molecules providing channels for leakage of ions and larger molecules through the membrane. This model differs from the previous two in that the clusters that are formed are only present for a short time. These channels allow the peptides to cross the membrane without causing significant membrane depolarization. When the peptides have travelled through the membrane they exert their activity on their specific intracellular targets leading to cell death.

1.3.4 Alternative mechanisms of action

Recently there have been a number of studies that indicate that as well as causing membrane disruption, peptides may also act on intracellular targets including DNA and RNA and interfere with metabolic processes (Morton[a] *et al*, 2007; Hale *et al*, 2007). For example, the peptide PR-39 binds to the membrane of *E. coli* cells but does not cause membrane permeabilisation (Cabiaux *et al*, 1994). Instead it is internalised and interferes with DNA and protein synthesis, killing the bacterial cells (Boman *et al*, 1993). Moreover, peptides may act as signalling molecules to strengthen the immune response. For example, the defensins can increase local neutrophil numbers at sites of host infection (Welling *et al*, 1998).

1.4 Antimicrobial peptides under investigation

Amphibians are a major source of antimicrobial peptides, accounting for over half of the eukaryotic peptides identified. The majority have been isolated from the Hylidae of South Africa and the Ranidae of Asia, Europe and North America. The peptides used in this study, DsS3(1-16), magainin 2 (mag 2) and ranalexin (rana), are cationic, amphipathic and linear in structure ranging from 16 – 23 a.a. in length (Coote *et al*, 1998; Zasloff, 1987; Clark *et al*, 1994). Other peptides of interest in this study are the naturally occurring cyclic peptide gomesin, and the synthetic cyclic peptides; 6752 and GS14K4 (Silva *et al*, 2000; Dartois *et al*, 2005; Kondejewski *et al*, 2002).

1.4.1 DsS3(1-16)

The dermaseptins are a group of polycationic peptides subdivided into S1 – S13 (Nicolas *et al*, 2009). These peptides originated from the South American frog *Phyllomedusa sauvagii.* Dermaseptins are naturally produced and stored in granular glands located on the skin and when ruptured peptide is excreted onto the skin surface. This superfamily has between 25 and 34 a.a. arranged in an amphipathic α-helical structure (Nicolas *et al*, 2009). The first to be identified was dermaseptin S1 in the early 1990s that displays broad spectrum action against bacteria (Mor *et al*, 1991). It was the first eukaryotic peptide with lytic action against pathogenic filamentous fungi to be characterised. Subsequently, other members of the dermaseptin family were rapidly isolated and characterised. The majority display broad spectrum activity against bacteria, fungi and protozoa. Dermaseptins S1-S5 display antiviral activity against herpes simplex virus and HIV-1 (Lorin *et al*, 2005) and S4 has recently been cited for its spermicidal activity as a potential contraceptive (Zairi *et al*, 2008).

The dermaseptins contain a conserved tryptophan residue at position 3 (with the exception of S13) and several lysine residues that contribute to the positive charge (Mor *et al*, 1994). A dermaseptin S1 derivative in which the tryptophan was replaced by a phenyl side chain had reduced antibacterial activity (Savoia *et al*, 2008). This highlights the importance of conserved tryptophan as it is thought to anchor the helix to the membrane. The addition of lysine to the N-terminal also improves antimicrobial action by increasing the net-positive charge of the peptide (Savoia *et al*, 2008). Dermaseptin S4 displays haemolytic activity that can be reduced by decreasing hydrophobicity or by

increasing the net-positive charge. As a result, derivatives have been produced with reduced toxicity towards erythrocytes (Navon-Venezia *et al*, 2002). The antimicrobial activity of this superfamily is thought to arise when the peptides bind to the acidic areas of cell membranes causing destabilisation of the phospholipids when a threshold concentration is achieved, disrupting the osmotic balance of the cell. This results in leakage of cell components and apoptosis (Shai, 2002).

A 16-residue truncation of dermaseptin S3 (DsS3(1-16); Coote *et al*, 1998) that retains its antimicrobial activity was investigated in this study. Much of the antimicrobial potency of dermaseptin S3 is thought to derive from the NH_2-terminal α-helical segment from residues 1-16, because derivatives comprising residues 14-34 lack all antimicrobial potency (Mor and Nicholas, 1994). Shortening of the chain to residues 1-16 did not affect activity. A further reduction in a.a. content reduced activity. However, derivatives with as few as 10 residues remained fully active against several bacterial and fungal strains (Mor *et al*, 1994). DsS3(1-16) monomers are too short to span the membrane but have been proposed to penetrate to the depth of the hydrocarbon layer (Shepherd *et al*, 2003). Simulation studies of DsS3(1-16) indicate that the aromatic residues at the N-terminal region are essential for peptide association with the lipid bilayer, that is driven by the tryptophan residue. The binding of tryptophan to lipid bilayers has been observed (Wimley *et al*, 1996) and is likely to contribute to the hydrophobic binding of the peptide. Simulations also show that the helix increases in rigidity as the chain interacts with the lipid bilayer (Shepherd *et al*, 2003). Recent work shows that DSs3(1-16)

damages DNA indirectly in *S. cerevisiae* and induces programmed cell death via an Aif1p dependent pathway (Morton[a] *et al*, 2007).

In clinical terms, dermaseptins may be useful in combating a variety of opportunistic fungal infections including *Candida* sp., which are prevalent fungal pathogens. Unlike many other AMPs, the dermaseptins do not lyse erythrocytes, greatly increasing their therapeutic applications (Helmerhorst[b] *et al*, 1999). The lack of resistance and rapid killing mechanisms of these peptides make them of interest.

1.4.2 Magainin 2

The magainins are a family of peptides originally isolated from the African clawed frog *Xenopus laevis* (Zasloff, 1987). They are cationic, amphipathic peptides and exhibit both antibacterial and antifungal activity. Interestingly, they also show anti-cancer properties; they kill both hematopoietic and solid tumour cell lines at concentrations that are up to 10-fold lower than concentrations that kill normal human neutrophils and lymphocytes (Jacob *et al*, 1994). Magainin 2 has 23 a.a. that give an well-defined helix comprising residues 4-20 (Figure 1.2). By using NMR it was shown that magainins are randomly coiled in aqueous solution while in the presence of phospholipid bilayers or organic solvents they assume right-handed α-helical conformations. The helix is hydrophilic and cationic on one side and hydrophobic on the other with a net charge of +3 at neutral pH (Bechinger, 1997).
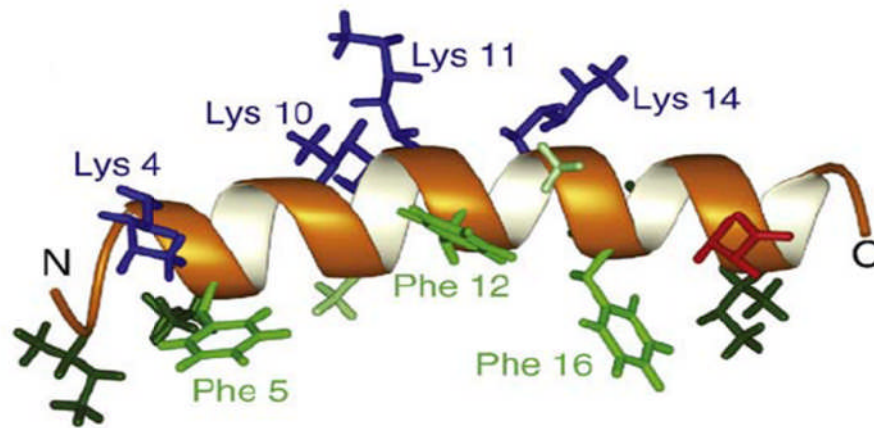
Figure 1.2. Solution structure of magainin 2 which forms a well defined, amphipathic, helix. Hydrophobic residues are green, cationic residues are blue and anionic residues are red. Figure from Haney *et al*, 2009.

Mag 2 inserts into the plasma membrane forming pores that lead to leakage of intracellular components (Bechinger *et al*, 1993). The peptide monomers arrange themselves perpendicular to the lipid bilayer in a helical conformation. These pores are thought to be toroidal with a diameter of 2-3 nm. (Matsuzaki *et al*, 1998). The peptide also internalises into *Bacillus megaterium* and *Escherichia coli* cells as demonstrated by electron microscopy (Haukland *et al*, 2001; Imura *et al*, 2008). Peptides may enter the cell as a result of toroidal pore disintegration or through pores that are wide enough to allow entry of peptide monomers (Imura *et al*, 2008). In order for pore formation and subsequent cell death to occur, a critical concentration of magainin is required (Matsuzaki *et al*, 1995); at low concentrations peptide monomers lie perpendicular to the membrane, as binding increases so the surface pressure and elastic energy of the membrane increases inducing pore formation (Ludtke *et al*, 1996; Tamba *et al*, 2009). Computer simulations have suggested that pore formation can occur with a minimum of four mag 2 monomers (Leontiadou *et al*, 2006). In one study peptide monomers were linked to form multivalent compounds (divalent, tetravalent, octavalent). Leakage from

large unilamillar vesicles was monitored and a large increase in pore formation was observed with the octamer, displaying a 13.4-fold increase in activity compared to native mag 2 (Arnusch *et al*, 2007). The action of mag 2 on the bending rigidity of vesicles has also been studied: it was found that the rigidity was severely reduced at <1% surface area coverage by peptide suggesting membrane integrity is compromised even at low peptide concentrations (Bouvrais *et al*, 2008).

The action of mag 2 has also been observed with mammalian membranes. This mode of action differs from the above: deformation and budding of the membrane was observed, with large molecules (140 kDa) able to enter the cell, suggesting that mag 2 causes a massive disruption of mammalian membranes in a carpet-like mechanism. This is opposed to the toroidal model observed in bacteria.

The antimicrobial activity of magainin has been studied in some detail with the creation of several analogues that aim to maximise this action. For example, the creation of the MSI-78 analogue with increased positive charge (+9) enhanced antimicrobial activity. Increasing the charge from 0 to +6 in these analogues resulted in strengthened binding to phospholipid bilayers. However, if the charge is increased beyond +5 it was found to increase binding to zwitterionic membranes and become significantly haemolytic (Dathe *et al*, 2001). From molecular dynamics simulations of mag 2 and MSI-78 on lipid bilayers it was found that the lysine residues had strongest binding affinity to the oxygens on the lipid head groups. As the MSI-78 analogue has more lysine residues, it showed increased binding and stability. This demonstrates that binding of these peptides is predominantly

mediated by lysine residues forming hydrogen bonds with oxygen atoms on the lipid heads (Kandasamy *et al*, 2004).

1.4.3 Ranalexin

The genus *Rana* is part of the family Ranidae. From this genus at least 36 species are found in North America (Duellman *et al*, 1994). Ranid frogs produce several antimicrobial peptides that are stored in granular glands on the skin and are discharged when these glands are ruptured. The peptides produced by this group vary greatly with no single peptide with the same a.a. sequenced expressed by any two species. The AMPs produced by this genus have been divided into several families (e.g. brevanins, ranateurins) with various isoforms produced in a single species. Despite the structural differences in ranid peptides, the peptide precursors, such as the a.a. sequences of the signal peptide (required for export of the peptide via secretory pathways), are well conserved. These similarities also extend to the Hylidae (including the dermaseptins) which are also structurally dissimilar to the ranid peptides. These two families share structural similarities in peptide precursors indicating all these peptides originated from a common gene in a shared ancestor (Vanhoye *et al*, 2003).

Ranalexin (rana) is a cationic peptide first isolated from the North American bullfrog *Rana catesbeiana* (Clark *et al*, 1994) and has potent antimicrobial action against gram-positive bacteria and fungi (Giacometti *et al*, 2000). It shows less activity against gram-negative bacteria and is inactive against infectious strains such as *Proteus mirabilis*

(Giacometti *et al*, 1998). Three isoforms have been identified that are found in *Rana grylio* and *Rana clamitans*. The primary structures are similar with only minor substitutions of hydrophobic a.a. (Conlon *et al*, 2004).

Ranalexin contains 20 a.a. structured to form a cyclic heptapeptide ring from a single intramolecular disulphide bond (Figure 1.3). This bond does not have a large effect on antimicrobial activity or the conformation of the peptide (Vignal *et al*, 1998). Rana is unstructured in water but forms an α-helical conformation when in hydrophobic solvents. It is amphipathic in nature with a lysine residue present in the hydrophilic face and hydrophobic residues grouped in a hydrophobic face that form the α-helix (Clark *et al*, 1994). Removal of any of these hydrophobic a.a. negates the antimicrobial activity of the peptide. Deletion of the cysteine required for the ring structure results in reduced potency, suggesting it is needed for optimal peptide action (Clark *et al*, 1994). The mode of action of this peptide still remains unclear but it has been proposed that the basic a.a. residues are involved in the binding and transport across the phospholipid membrane while the hydrophobic residues cause disruption of the membrane leading to cell death (Conlon *et al*, 2004). Rana is similar in structure to the polymyxin antibiotics that also target cell membranes. Polymyxin also has a ring structure that is important for antimicrobial activity. Within the ring there are several residues that are present in both rana and polymyxin, in particular the positively charges lysine residues (Kurihara *et al*, 1972). It has been proposed that they may share similar modes of action (Clark *et al*, 1994). Studies on rats show that rana can reduce mortality from septic shock, retaining

its antimicrobial efficacy *in vivo* (Ghiselli *et al*, 2001). This indicates that rana has the potential for development into a novel antimicrobial treatment.

A.

B.
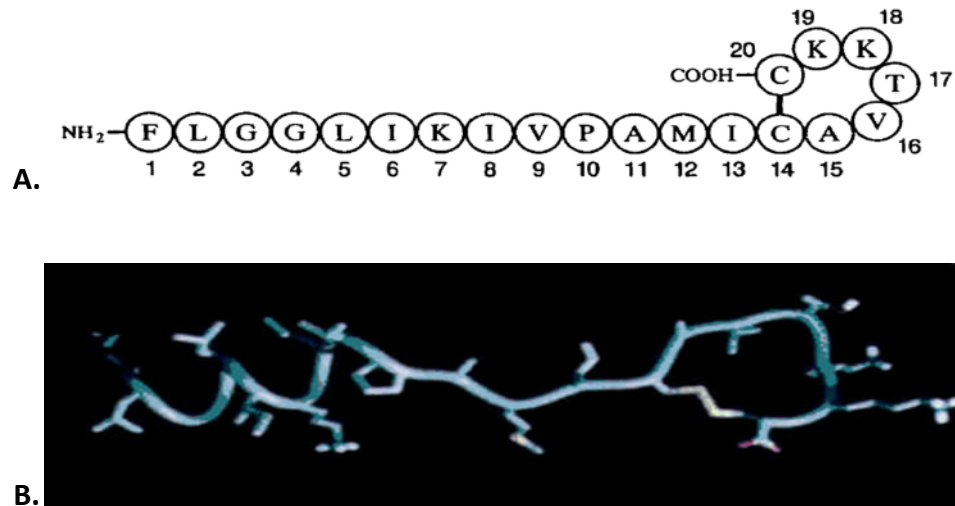
Figure 1.3. The amino acid sequence (A) and solution structure (B) of ranalexin showing the loop structure from the disulphide bond. From Clank *et al*, 1994.

1.4.4 Cyclic peptides: gomesin, 6752 and GS14K4

Gomesin is a cationic AMP that was isolated from the haemocytes of tarantula spider *Acanthoscurria gomesiana*. Gomesin has a sequence of 18 a.a. and contains two disulphide bridges ($Cys^{2,15}$, $Cys^{6,11}$) that allow it to adopt a well-defined β-hairpin structure (Mandard *et al*, 2002). This cyclic peptide is similar in structure to androctonin and tachyplesin (Mandard *et al*, 1999; Fahrner *et al*, 1996). Gomesin and the protegrins share structural similarities (short chained with two disulphide bridges) so may share a similar mode of action (Sokolov *et al*, 1999). Gomesin has an N-terminal pyroglutamic acid and a C-terminus arginine α-amide. The pyroglutamic acid and disulphide bonds help to stabilise the peptide, preventing degradation by proteases. The a.a. side chain also includes six positively charged residues (five Arginine and one Lysine) (Silva *et al*, 2000). It was found to show strong fungicidal activity on all filamentous fungi tested

with MICs <3.15 μM. These included *Aspergillus fumigatus*, *Fusarium culmorum* and *Nectria haematococca*. Gomesin also has a marked activity against various yeast strains including *Candida tropicalis, Saccharomyces cerevisiae* and *C. albicans* all with MICs <6.25 μM (Silva *et al*, 2000). However, it demonstrates haemolytic activity at low concentrations (16 % haemolysis at 1 μM).

CD spectroscopy showed that removal of both disulphide bonds resulted in reduced antimicrobial and haemolytic activity. Both are required for optimal antimicrobial potency and stability in human serum. The presence of a single disulphide bond resulted in a structure similar to that of native gomesin (Fazio *et al*, 2006). Several gomesin analogues have been designed that adopt an α-helical conformation. These were slightly less active against bacteria but as active against *C. albicans* and 3-fold less haemolytic. A single analogue was also as stable in human serum as the native gomesin (Fazio *et al*, 2006).

Gramicidin S is a cyclic β-sheet peptide and has wide spectrum antimicrobial activity but also targets human erythrocytes. In an attempt to decrease haemolytic activity the ring size was increased from 10 a.a. to 14 a.a., producing the peptide GS14. Further changes were made to increase specificity for microbial membranes by substituting enantiomers (D-lysine at position 4) to decrease amphipathicity producing the peptide GS14K4 (Kondejewski *et al*, 2002). In this peptide class high amphipathicity results in high haemolytic activity so GS14K4 was synthesized with reduced haemolytic activity producing a peptide with optimal hydrophobicity maintaining antimicrobial potency. The

mode of action of GS14K4 has not been reported, however, gramicidin S induces membrane defects of varying sizes leading to destabilisation of the bilayer (Ashrafuzzaman *et al*, 2008). This cyclic peptide has a higher therapeutic index (propensity to act on microbial rather than mammalian membranes) than gramicidin S (Lee *et al*, 2003) and exhibits strong antimicrobial action against a range of bacteria and fungi including *Staphylococcus aureus*, *S. epidermis* and *C. albicans* (Kondejewski *et al*, 2002).

The screening of combinatorial libraries of cyclic D,L-α-peptides (alternating D- and L-α-amino acids) for antimicrobial activity yielded six peptides that were optimised with substitutions for selectivity towards bacterial membranes. From this group the D,L-α-peptide '6752' was active at 8 μg/ml against *S. aureus* and displayed favourable tolerances with an *in vivo* thigh model of *S. aureus* infection. It was shown to be systemically active for as long as vancomycin with good stability and resistance to proteolytic degradation in serum (Dartois *et al*, 2005). D,L-α-peptides are thought to self-assemble at lipid bilayers and form multimeric pores through a carpet-like mechanism causing loss of membrane gradients leading to cell death (Fernandez-Lopez *et al*, 2001).

1.5 Antifungal drugs

The previous two decades have seen an increasing occurrence of invasive fungal infections. These infections are primarily found in patients with HIV, cancer, transplantation and other medically invasive procedures where suppression of the immune system exists. Current antifungal drugs include the polyenes, the azoles and the echinocandins (Figure 1.4) (Kleinberg, 2006; Chen *et al*, 2005; Denning, 2003).

1.5.1 Polyenes

The polyenes are a group of antifungals containing a cyclic ester ring with multiple carbon-carbon double bonds. They are used to treat systemic or oral fungal infections and include amphotericin B, nystatin and natamycin. Discovered in 1955, several amphotericin compounds were developed but only amphotericin B is used today due to its higher activity (Oura *et al*, 1955). Amphotericin B does display nephrotoxicity (leading to renal failure) but because of its high antifungal activity and broad spectrum of action (candidiasis, blastomycosis, coccidioidomycosis, cryptococcosis, aspergillosis, zygomycosis, sporotrichosis, fusariosis and phaeohyphomycosis) is one of the most frequently used antifungals. Additionally, it initiates very low levels of fungal resistance. Amphotericin B functions by interacting with ergosterol at the fungal cell membrane, forming trans-membrane pores inducing leakage of cations, reduction in intracellular potassium levels, and cell death (Baginski *et al*, 2005). Amphotericin B has a strong affinity for ergosterol but may also bind to the sterols present on mammalian cells increasing its toxicity. There have been several preparations developed to reduce toxicity that have been approved by the Food and Drug Administration (FDA) including

liposomal amphotericin B (Wong-Beringer *et al*, 1998). The liposomal formulation allows increased dosages and high tissue concentrations but its use is hampered due to high production costs. Liposomal treatments display reduced nephrotoxicity although this still limits treatment compared to other antifungal drugs (Wong-Beringer *et al*, 1998). A drawback of amphotericin B treatment is the lack of an oral preparation as it has to be administered intravenously although oral administration is in development (Wasan *et al*, 2009).

1.5.2 Azoles

Azoles interfere with the synthesis of ergosterol, a constituent of fungal cell membranes. Azole treatment displays low toxicity with no nephrotoxic effects and was commonly used to treat invasive fungal infections. The azole antifungal agents can be split into two groups: the imidazoles (miconazole and ketoconazole) and the triazoles (fluconazole, itraconazole, voriconazole and posaconazole). The imidazoles have replaced the triazoles in the treatment of systemic fungal infections as they display increased pharmacokinetics and safety profiles (Kauffman *et al*, 1997). Their mode of action involves inhibiting the cytochrome P_{450} enzyme that is required for the conversion of lanosterol to ergosterol (Chen *et al*, 2007). As the imidazoles have less affinity for this enzyme in fungal models a higher dosage is required. They are mainly used for the treatment of superficial skin or mucosal infections. However, resistance to this class is becoming common and the mortality rate from such infections remains high (Mareş *et al*, 2008). Resistance mechanisms include overexpression of drug efflux pumps encoded by *CDR1*, *CDR2* and *MDR1* and overexpression of *ERG11* that encodes 14-α lanosterol

demethylase (Sanglard *et al*, 1997; Sanglard *et al*, 1995; White *et al*, 1998). Azole resistance is also associated with polyene resistance originating from lack of ergosterol (Sanglard *et al*, 2003). This ergosterol reduction decreases the role of cytochrome P_{450}, reducing the action of azoles on cell viability.

Several side-effects have been reported that depend on the preparation administered. Itraconazole has been associated with peripheral oedema and hepatic failure while fluconazole may cause chapped lips and skin dryness (Tan *et al*, 2006). Liver toxicity is the main adverse reaction associated with all azoles. This can range from elevated levels of transaminases to clinical hepatitis and liver failure. These cases are rare with only 5 % of patients requiring treatment termination (Sheehan *et al*, 1999). The azoles also display drug-drug interactions with many other treatments due to the mode of action with cytochrome P_{450}. Inhibition of these enzymes results in elevated levels of drug metabolism resulting in additional toxicity (Gubbins *et al*, 2005).
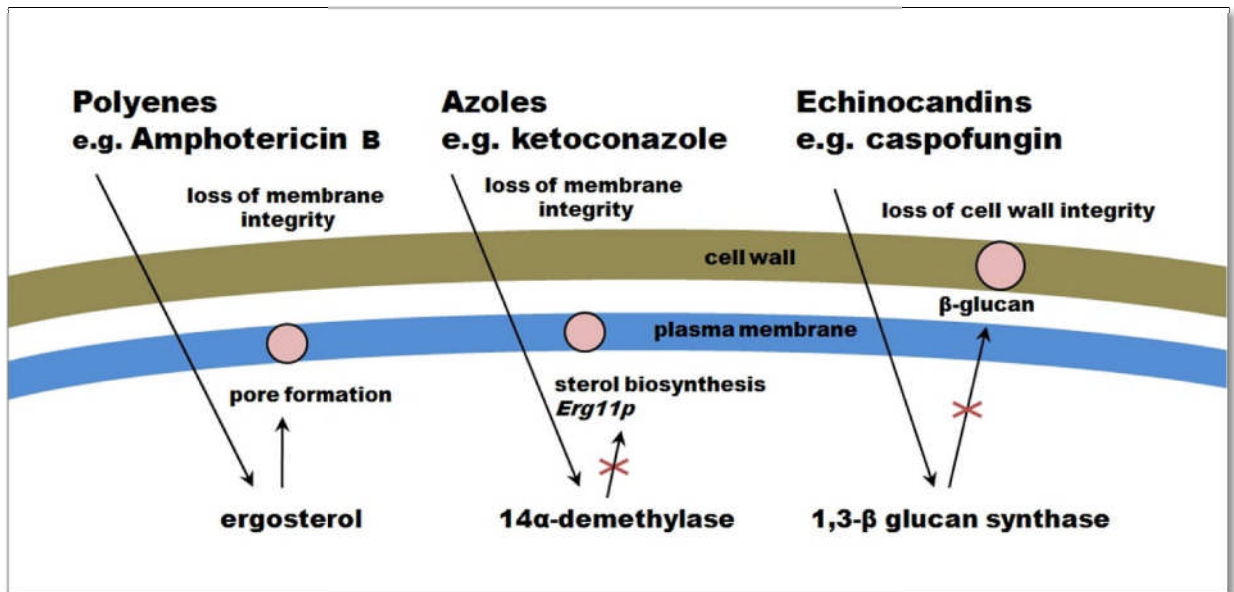
Figure 1.4. Mode of action of the polyene, azole and echinocandin classes of antifungals. The polyenes associate with ergosterol inducing the formation of transmembrane pores. The azoles inhibit 14α-demethylase, reducing ergosterol levels that are required for normal plasma membrane function. The echinocandins inhibit 1,3-β glucan synthase, reducing 1,3-β glucan, an essential component of the fungal cell wall.

1.5.3 Echinocandins

The most recent class of antifungal drug to be introduced for clinical use are the echinocandins. There are currently three echinocandins that have been approved by the FDA in 2002, 2005 and 2006 respectively for use in the USA: caspofungin, micafungin and anidulafungin (Figure 1.5). They have recently been granted licenses by the European Medicines Evaluation Agency (EMEA). Their structure incorporates a cyclic hexapeptide that is linked to a fatty acyl chain. The echinocandins have a novel mode of action whereby they inhibit the synthesis of 1,3-β glucan in the fungal cell wall by targeting 1,3-β glucan synthase (Douglas, 2001). These linkages are not present in mammalian cells. This enzyme is composed of several subunits and catalyses the transfer of sugars from donor to acceptor molecules forming glycosidic bonds. The enzyme requires a minimum of two subunits named Fks1 and Rho. Fks1 functions as the catalytic subunit while Rho regulates the activity of glucan synthase (Schimoler-O'Rourke

et al, 2003). The echinocandins are fungicidal against a wide range of species and fungistatic against moulds as they block hyphal tip growth and are also effective against biofilms (Bachmann *et al*, 2002; Douglas, 2006). They show reduced efficacy (MIC >16 μg/ml) against *Cryptococcus neoformans* and *Fusarium, Scedosporium* and *Zygomycetes* sp. (Denning, 2003; Pfaller *et al*, 1998). They are as effective as amphotericin B and some studies show them to be more so (Villanueva *et al*, 2002; Arathoon *et al*, 2002). The echinocandins are also effective against strains of *Candida* that display resistance to amphotericin B and azoles such as *Candida glabrata*, *Candida tropicalis* and *Candida krusei* (Zaoutis *et al*, 2005). As the echinocandins are not metabolised via cytochrome P_{450} there show minimal drug-drug interactions. An exception is cyclosporine as the combination results in elevated transaminase levels (Denning, 2003). In comparison to other antifungal drugs, the echinocandins have extremely low levels of toxicity. The most common side-effects reported are urticaria (hives), pruritus (itching) and elevation in transaminase levels (Cappelletty *et al*, 2007).
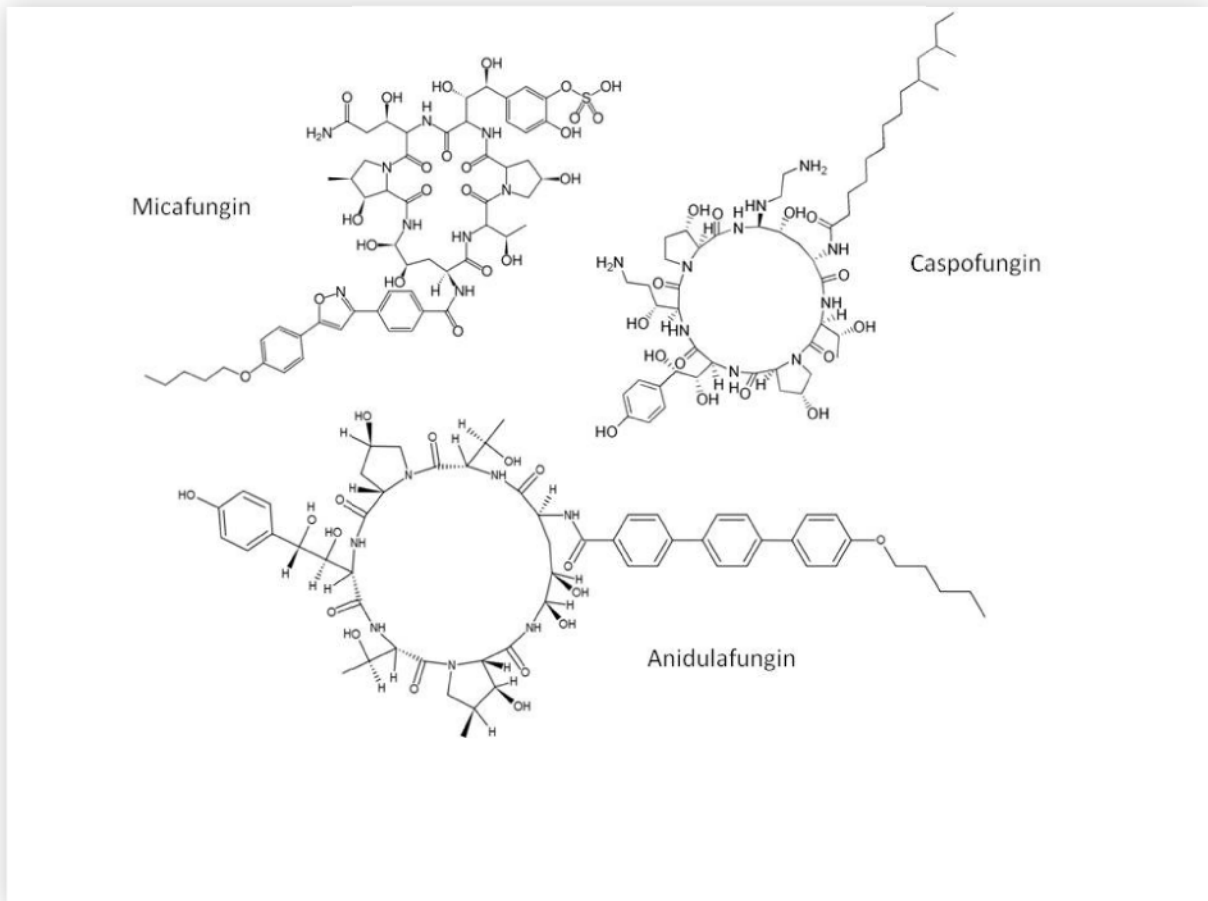
Figure 1.5. Structural diagrams of micafungin, caspofungin and anidulafungin (adapted from en.wikipedia.org). They are structured into large cyclic heptapeptides linked to a long chain fatty acid.

1.6 Fungal pathogenicity and drug susceptibility

1.6.1 *C. albicans*

Clinical isolate strains of *C. albicans*, *C. glabrata* and *C. neoformans* were acquired to test their susceptibility to antimicrobial peptides. *C. albicans* is a common commensal fungus that can become pathogenic, usually in immunocompromised patients or those undergoing invasive surgery. *C. albicans* cells can have one of three morphogenic forms: yeast (cells grow and bud daughter cells that dissociate), pseudohyphae (elongated cells that bud, forming chains and remain attached), and true hyphae (long elongated cells with a continuous growing tip separated by septa). Colonies are naturally found as

commensals in the gastrointestinal tract and oral cavity (Calderone, 2002). The key to its pathogenicity is the ability to colonise available niches within the host facilitated by phenotypic switching between morphogenic forms. When conditions are favourable they can invade the oral and vaginal epithelium and in severe cases can invade the blood stream and disseminate, leading to a systemic infection (Calderone, 2002).

To combat candidiasis several classes of drug have been developed that act on the cell membrane or cell wall to exert their antifungal action (Denning, 2003; Chen *et al*, 2005; Kleinberg, 2006). As *C. albicans* can survive in a variety of niches within the host it has a series of well characterised stress responses that are activated during changes in temperature, pH and osmolarity (Cannon *et al*, 2007). These stress responses contribute to resistance from host defence mechanisms. Resistance is frequently due to genetic mutation targeted by these drugs or enzymes involved in metabolic pathways. For example, the cell wall integrity pathway is responsible for glucan synthesis and cell wall repair (Navarro-Garcia *et al*, 1998). A change in this pathway can lead to echinocandin resistance. Resistant strains have mutations in the 1,3-β glucan synthase subunits *Fks1p* and *Gsc1p* (Balashov *et al*, 2006; Baixench *et al*, 2007). However, resistance to the echinocandins has been reported only rarely, this could be due to their relatively recent introduction (Perlin, 2007). The increase in MIC associated with a decrease in susceptibility is greater with caspofungin and micafungin than anidulafungin. The reason for these differences is not yet fully understood. *C. albicans* strains that show azole resistance may display mutations in *ERG3,* lowering the ergosterol content in the membrane and so reducing the effectiveness of both the azoles and amphotericin B

(Sanglard, 2003). *Erg11p* is the target of azole drugs and point mutations in this gene reduce drug affinity leading to resistance (White *et al*, 1998). The regulators of *ERG* genes have also been implicated in resistance, for example, deletion of *UPC2* resulted in *C. albicans* cells that were hypersensitive to fluconazole and ketoconazole, whereas overexpression increased resistance to these drugs (MacPherson *et al*, 2005). Clinical strains of *C. albicans* also over-express *Cdr1p* and *Cdr2p*, two phospholipid transporters that can increase azole resistance, indeed, deletion of these genes decreases azole action by 8-fold (Tsao *et al*, 2009). It has also been reported that inactivation of a sterol ($\Delta^{5,6}$-desaturase) involved in the final stage of ergosterol synthesis decreases azole susceptibility (White, 2007).

C. albicans resistance to amphotericin B is rare and not fully understood. A decrease in ergosterol content decreases susceptibility and is thought to be associated with mutations in the genes involved with the regulation of ergosterol production. The susceptibility of *C. albicans* biofilms has also been investigated and it was found that several genes encoding enzymes of the ergosterol (*ERG1*, *ERG2*) and β-1,6-glucan (*SKN1*, *KRE1*) pathways were differentially regulated. It was hypothesised that changes to susceptibility originate from changes to both the cell membrane and cell wall (Khot *et al*, 2006).

As cases of resistance have been reported in all the major drug groups introduced to combat Candidiasis, it is important that new treatments are pursued. Antimicrobial peptides have the potential to act as this new form of defence as they display potent

antimicrobial action against a range of pathogenic microbes including *Candida* sp*.* (Giuliani *et al*, 2008).

1.6.2 *C. glabrata*

C. glabrata has only recently been recognised as a human pathogen as it was previously considered a non-pathogenic component in the microbial flora of healthy individuals (Stenderup *et al*, 1962). Thus far no sexual phase has been reported and it is thought that this species reproduces clonally. *C. glabrata* causes mucosal and bloodstream infections and is commonly isolated in combination with *C. albicans* (Redding *et al*, 1999). It is becoming increasingly infectious, especially in immunocompromised patients suffering from AIDS or cancer. As with *C. albicans*, *C. glabrata* can undergo phenotypic switching and hyphal transformation which contributes to pathogenicity, allowing colonies to rapidly adapt in response to antifungal treatment or the host immune response (Lachke *et al*, 2000).

C. glabrata is increasing in prevalence but is still very difficult to treat, even more so when it is found in combination with other *Candida* strains (Redding *et al*, 2000; 2002; 2004). Although *C. glabrata* is classified with other *Candida* sp. it is genetically quite dissimilar, based on analysis of 204 related species (Kurtzman *et al*, 1997). As a result, conventional antifungal agents effective against *C. albicans* have reduced or abolished efficacy against *C. glabrata*. For example, *C. glabrata* is resistant to several cationic AMPs including the histatins and magainins (Helmerhorst *et al*, 2005). When exposed to

human β-defensins 2 and 3, membrane disruption was observed with *C. albicans* but not *C. glabrata* suggesting a species specific mechanism (Feng *et al*, 2005). Colonies show resistance to the azole drug class including fluconazole and ketoconazole (Rex *et al*, 1995). Azole resistance is similar to that of *C. albicans* and has been linked to overexpression of drug efflux pumps encoded by *CgCDR1*, *PDH1* and *CgCDR2* (Kanafani *et al*, 2008). This could also account for their resistance to cationic AMPs (Helmerhorst *et al*, 2005). Additionally, expression of *CgPDR1* increases azole resistance by regulating the expression of drug efflux pumps (Tsai *et al*, 2006).

C. glabrata is responsible for both systemic and mucosal Candidiasis and is most frequently found colonising the oral cavity. The occurrence of such infections has been shown to increase with age due to the changing microenvironment (Qi *et al*, 2005). Systemic infections have a high mortality rate and are difficult to treat due to increasing resistance to azole drugs. Amphotericin B is commonly used to treat infection, especially in immunocompromised patients. However, it has recently been reported that several hospital isolates are now amphotericin B resistant (Rezusta *et al*, 2008). Resistance to the polyenes is still rare so these resistance mechanisms are poorly understood. One study focused on a resistant strain that displayed pseudohyphal growth. A mutation in *CgERG6* was found to disrupt the ergosterol biosynthesis pathway, resulting in amphotericin resistance (Vandeputte *et al*, 2007). Caspofungin appears to be a viable alternative to amphotericin B and is more effective, reducing toxicity in clinical trials against invasive candidiasis (Mora-Duarte, 2002). Resistance to

the echinocandins is similar to that of *C. albicans* and involves mutations in *FKS2* the subunit of 1,3-β glucan synthase (*FKS1* homologue) (Katiyar *et al*, 2006).

1.6.3 *C. neoformans*

C. neoformans is a budding yeast that has a worldwide distribution and is often found naturally in the soil. There are three variants (*v*) of this species with differences in virulence: *C. neoformans, v. grubii, v. gattii* and *v. neoformans*. *V. grubii* accounts for the majority of Cryptococcal infections that are predominantly found in immunocompromised hosts and cause subacute meningitis and meningoencephalitis (Casadevall *et al*, 1998). *V. gattii* and *v. neoformans* infections are less common, however, *v. gattii* can also infect immunocompetent individuals. Several virulence factors have been documented including capsule size, laccase expression (leading to polymerised melanin) and sporulation (leading to lung infection) (Kwon-Chung *et al*, 1986; Wang, 1994; Salas *et al*, 1996). The sequencing of the genome in 2005 has provided initial understanding of virulence factors, stress responses and translation repression required for such responses (Loftus *et al*, 2005; Brown *et al*, 2007). The presence of the capsule makes it unique among eukaryotic pathogens and is estimated to play the largest roll in *C. neoformans* virulence (McClelland *et al*, 2006).

C. neoformans is resistant to echinocandins by a mechanism that is not completely understood. This resistance is not similar to the *Candida* mechanism as it has been demonstrated that *C. neoformans* 1,3-β glucan synthase is sensitive to caspofungin

(Maligie *et al*, 2005). This indicates a different resistance mechanism is present that may include the action of efflux pumps or degradation pathways (Feldmesser *et al*, 2000). Serious cases of Cryptococcus are treated with liposomal amphotericin at 0.6 - 1.0 mg/kg per day. This lessens the side effects in AIDS patients but has a high cost and problems associated with toxicity so limits its use (Bohde, 2002). Amphotericin B resistant strains are uncommon but have reduced ergosterol content (Dick *et al*, 1980). Side effects include: drug-related fever, nausea, kidney problems and anaemia. Thus it remains important to investigate potential new drug treatments.

1.6.4 *S. cerevisiae* as a model organism

S. cerevisiae is a budding yeast and an intensely studied model organism. The genome of this eukaryote was the first to be sequenced and contains 5885 potential protein-encoding genes (Goffeau *et al*, 1996). It is advantageous to study this yeast as it shares many cell processes with metazoan cells and similarly contains Mitochondria, Golgi, Nucleus and Endoplasmic Reticulum. The *Saccharomyces* genome database (www.yeastgenome.org) is an invaluable tool for understanding the genetics and physiology of eukaryotic cells and is the accumulation of years of intensive research. Therefore, it is the ideal organism for molecular techniques and genetic manipulation. These, usually haploid, cells have a short generation time of ~2 hours in optimal growth conditions and can be stored at low temperature (typically -70 °C) without affecting viability. *S. cerevisiae* is a very uncommon source of infection in humans, but several cases have emerged within the last decade displaying various forms of invasive infection (McCullough *et al*, 1998; Cassone *et al*, 2003; Graf *et al*, 2007). It has been estimated to

be responsible for up to 3.6 % of fungemic infections (Lherm *et al*, 2002). Over 60 cases of *S. cerevisiae* infection have been reported ranging from isolated fungemia, endocarditis, disseminated disease and liver abscesses. Fluconazole and amphotericin B are generally used to combat infection although it is becoming increasingly resistant to the azole class (Salonen *et al*, 2000). Infection carries a relatively high mortality rate of 28 % (Munoz *et al*, 2005).

1.7 Aims of this study

The main aim of this study is to gain insight into the mode of action and efficacy of antimicrobial peptides against pathogenic fungi. More specifically, areas of study include the role of the cell wall in mediating antimicrobial activity, the use of antimicrobial peptides when combined with currently available treatments for fungal infections, the analysis of genes whose expression confers susceptibility changes to antimicrobial action and assessment of the viability of antimicrobial peptides as new clinical therapeutics.

Chapter 2

2. Materials and Methods

2.1 Yeast and bacterial strains

The strain of *S. cerevisiae* used in this study was BY4741, a derivative of S288C (genotype *MAT*a *his3Δ1 leu2Δ0 met15Δ0 ura3Δ0*) obtained from the Research Genetics BY4741 *MAT*a haploid genome deletion set. Gene deletion mutants were from the Research Genetics BY4741 *MAT*a haploid genome deletion mutant set (Table 2.1). Deletion strains were selected on yeast extract peptone dextrose agar (YEPD; 2 % glucose, 2 % agar, 1 % bactopeptone, 1 % yeast extract) with 150 µg/ml geneticin (Sigma-Aldrich Ltd, DOR, UK).

Table 2.1. *S. cerevisiae* deletion strains used in this study.

Strain	Genotype
BY4741a	*MAT* a hisΔ1 leu2Δ0 met15Δ ura3Δ0
hal5 Δ	BY4714a *hal5* Δ::*KanMX4*
HAL5-GFP	BY4741a *HAL5-GFP* ::HIS3
ldb7 Δ	BY4714a *ldb7* Δ::*KanMX4*
LDB7-GFP	BY4741a *LDB7-GFP* ::HIS3
imp2' Δ	BY4714a *imp2'* Δ::*KanMX4*
IMP2'-GFP	BY4741a *IMP2'-GFP* ::HIS3
izh2 Δ	BY4714a *izh2* Δ::*KanMX4*
Izh2 comp	BY4714a *izh2* Δ::*KanMX4* [pRS313::IZH2]
Izh2 ovexp	BY4714a *izh2* Δ::*KanMX4* [pRS423::IZH2]
wt313	BY4741a [pRS313]
wt423	BY4741a [pRS423]

Clinical isolates of *C. albicans*, *C. glabrata* and *C. neoformans* were provided by Dr. Cyril Lafong (Fife Area Laboratory, Victoria Hospital, Kirkcaldy). *C. albicans* SC5314 was provided by Prof. Frank Odds (School of Medical Sciences, University of Aberdeen). CAI-4 and cell wall deletion mutants were provided by Prof. Neil Gow (School of Medical Sciences, University of Aberdeen) (Table 2.2).

Table 2.2. CAI-4 cell wall mutants used in this study.

Description	Strain	Phenotype	Source
CAI-4+Clp10	NGY152	parent strain	Brand et al, 2004
mnt1 Δ+Clp10	NGY158	reduced Man$_2$-Man$_5$ residues	Munro et al, 2005
mnt1 Δ+Clp10-*MNT1*	NGY148	parent strain phenotype	Munro et al, 2005
mnt2 Δ+Clp10	NGY145	reduced Man$_2$-Man$_5$ residues	Munro et al, 2005
mnt2 Δ+Clp10-*MNT2*	NGY149	parent strain phenotype	Munro et al, 2005
mnt1-mnt2 Δ+Clp10	NGY337	reduced Man$_2$-Man$_5$ residues, inc Man$_1$ residues	Munro et al, 2005
mnt1-mnt2 Δ+Clp10-*MNT1*	NGY335	parent strain phenotype	Munro et al, 2005
mnt1-mnt2 Δ+Clp10-*MNT2*	NGY336	parent strain phenotype	Munro et al, 2005
mnn4 Δ+Clp10	CDH15	severe mannosylphosphate reduction	Hobson et al, 2004
mnn4 Δ+Clp10-*MNN4*	CDH13	parent strain phenotype	Hobson et al, 2004
pmr1 Δ+Clp10	HGY355	severe mannose reduction	Bates et al, 2005
pmr1 Δ+Clp10-*PMR1*	NGY356	parent strain phenotype	Bates et al, 2005
och1 Δ+Clp10	NGY357	no α-1,6-linked polymannose	Bates et al, 2006
och1 Δ+Clp10-*OCH1*	NGY358	parent strain phenotype	Bates et al, 2006
mnt3 Δ *mnt5* Δ+Clp10	NGY1227	mannosylphosphate reduction	Mora-Montes & Gow, unpublished
mnt3 Δ *mnt5* Δ+Clp10-*MNT3*	NGY1228	parent strain phenotype	Mora-Montes & Gow, unpublished
mnt3 Δ *mnt5* Δ+Clp10-*MNT5*	NGY1229	parent strain phenotype	Mora-Montes & Gow, unpublished

The *E. coli* strain used for transformations was DH5α (Invitrogen Inc., SCD, UK).

All yeast and *E. coli* cultures were prepared with 15 % (v/v) glycerol and stored at –80 °C.

Vero cells (African green monkey kidney cells, 'fibroblast-like', non-cancerous (Health Protection Agency Culture Collections, WLT, UK)) were cultured in RPMI-1640 medium (Sigma-Aldrich Ltd, DOR, UK) supplemented with 10 % bovine calf serum (Cambrex, IA, USA) and 0.3 % Penicillin/Streptomycin (Sigma-Aldrich Ltd, DOR, UK).

2.2 Growth Media

Malt extract broth [pH 7] (MEB; 1 % glucose, 0.6 % malt extract, 0.12 % yeast extract) (Difco Laboratories, OFE, UK).

Malt broth agarose plates [pH 7] (2% agarose).

RPMI-1640 Media [pH 6.4] (Sigma-Aldrich Ltd, DOR, UK) with addition of 2 % 3-(N-morpholino) propane sulfonic acid (MOPS; Sigma-Aldrich Ltd, DOR, UK), 10 % bovine calf serum (Cambrex, IA, USA).

RPMI-1640 agarose plates [pH 7] (2 % agarose, 1 % RPMI-1640 medium Auto-mod^{TM} (Sigma-Aldrich Ltd, DOR, UK), 0.4 % Sodium bicarbonate (Sigma-Aldrich Ltd, DOR, UK), 2 % MOPS (Sigma-Aldrich Ltd, DOR, UK)).

YEPD agar (2 % glucose, 2 % agar, 1 % bactopeptone, 1 % yeast extract).

Luria-Bertani media (LB; 1 % Bacto-peptone, 0.5 % Bacto-yeast extract, 1 % NaCl).

Minimal yeast nitrogen base agarose [pH7] (YNB; 2 % glucose, 2 % agarose, 5 g/L ammonium sulphate, 5 mg/L potassium dihydrogen orthophosphate, 1 mg/L magnesium sulphate, 0.2 mg/L sodium chloride, 0.002 mg/L biotin, 0.4 mg/L Ca-panthotenate, 0.002 mg/L Folic acid, 2 mg/L inositol, 0.4 mg/L nicotinic acid, 0.2 mg/L p-aminobenzoic acid, 0.4 mg/L pyridoxine-HCl, 0.2 mg/L riboflavin, 0.4 mg/L thiamine HCl, 0.5 mg/L boric acid, 0.04 mg/L copper sulphate, 0.1 mg/L potassium iodide, 0.2 mg/L ferric chloride, 0.4 mg/L manganese sulphate, 0.2 mg/L sodium molybdate, 0.4 mg/L Zinc sulphate).

2.3 Optical density versus viable cell number calibration curves

Yeast strains were cultured in MEB from a single colony in 100 ml flasks (30°C, 200 rpm). Cell viability was measured by serial dilution in fresh media and plating onto YEPD agar. Plates were incubated at 30 °C for 24 h. Numbers of yeast cells were calculated by constructing calibration curves plotting each cultures optical density at 600 nm (OD$_{600}$) against viable cell number per ml. Cultures were sampled every 30 min (MEB, pH 7, 100ml flasks, OD$_{600}$) and viable cell numbers determined (Table 2.6 and Figures 2.6 – 2.15).

2.4 Antifungal peptides and echinocandins

Peptides were synthesised (Peptide Protein Research Ltd, HPH, UK) to a purity of >95% (verified by HPLC and mass spectrometry) (Table 2.3).

Table 2.3. Antimicrobial peptides used in this study.

Antimicrobial Peptide	Abbreviation	Amino Acid Sequence
Dermaseptin S3(1-16)-NH$_2$	DsS3(1-16)	ALWKNMLKGIGKLAGK
Magainin 2	Mag 2	GIGKFLHSAKKFGKAFVGEIMNS
Ranalexin	Rana	FLGGLIKIVPAMICAVTKKC
Gomesin	Gom	ZCRRLCYKQRCVTYCRGR
6752	6752	cyclo (SwFkTkSk)
GS14K4	GS14K4	cyclo (VKLkVyPLKVKLyP)

6752 and GS14K4: residues with D stereochemistry are in lowercase.

In addition, DsS3(1-16) was synthesised with a fluorescein tag attached to the N-terminal lysine (Flu-DsS3(1-16)). The attached fluorescein adds 17.2 % to the overall weight of the peptide, and so, peptide concentrations were adjusted to account for this. Peptides were solubilised in distilled water (dH$_2$O) and stored at -80°C.

Linear peptides were solubilised in dH$_2$0, cyclic peptides were solubilised in Dimethyl sulfoxide (Fisher Scientific Ltd., LEC, UK) (50 mg/ml, stored at -80 °C).

Caspofungin (Merck & Co., NJ, USA) and micafungin (Astellas, MIDDX, UK) were diluted into 10 mg/ml aliquots with ddH$_2$O.

Anidulafungin (Pfizer Inc., NY, USA) was diluted into 10 mg/ml aliquots with 20 % (v/v) ethanol.

2.5 MIC determination

To each well of a 96-well microtitre plate (Greiner Bio-one Ltd, GLR, UK) was dispensed 150 µl sterile MEB or RPMI-1640 in the presence or absence of glucosamine hydrochloride (Sigma-Aldrich Ltd, DOR, UK) or glucosamine 6-phosphate (Sigma-Aldrich Ltd, DOR, UK) (Section 3.2.6) or in the presence or absence of echinocandin (Sections 4.2.1 - 4.2.3). Various concentrations of AMP were added to wells that were then inoculated to 1.0×10^3 cells per well with yeast cells from a mid-exponential culture and plates were incubated (30 °C, 48 h, 200 rpm). Plates were then scanned using an ImageScanner (GE Healthcare UK Ltd, BUX, UK) with ImageMaster Labscan v.3 software (GE Healthcare UK Ltd, Chalfont St. Giles, UK) and MIC determined by visible growth.

2.6 Synergy studies

Checkerboard assays were performed with various drug combinations to determine if each displayed more antimicrobial activity than the sum of their effects alone. In these assays increasing concentrations of two antimicrobial agents were added to a 96-well microtitre plate so that each row or column contained a defined amount of one drug and increasing amounts of the second drug. There are various patterns of inhibition that were encountered when performing these assays (Figure 2.1). If the combined agents have no interaction then inhibition would be proportional to drug concentration. If synergy were present then increased inhibition would occur forming a concave pattern. If the combination was antagonistic then wells containing growth would form a convex pattern. The extent of concavity or convexity is also indicative of the extent of synergy or antagonism respectively.
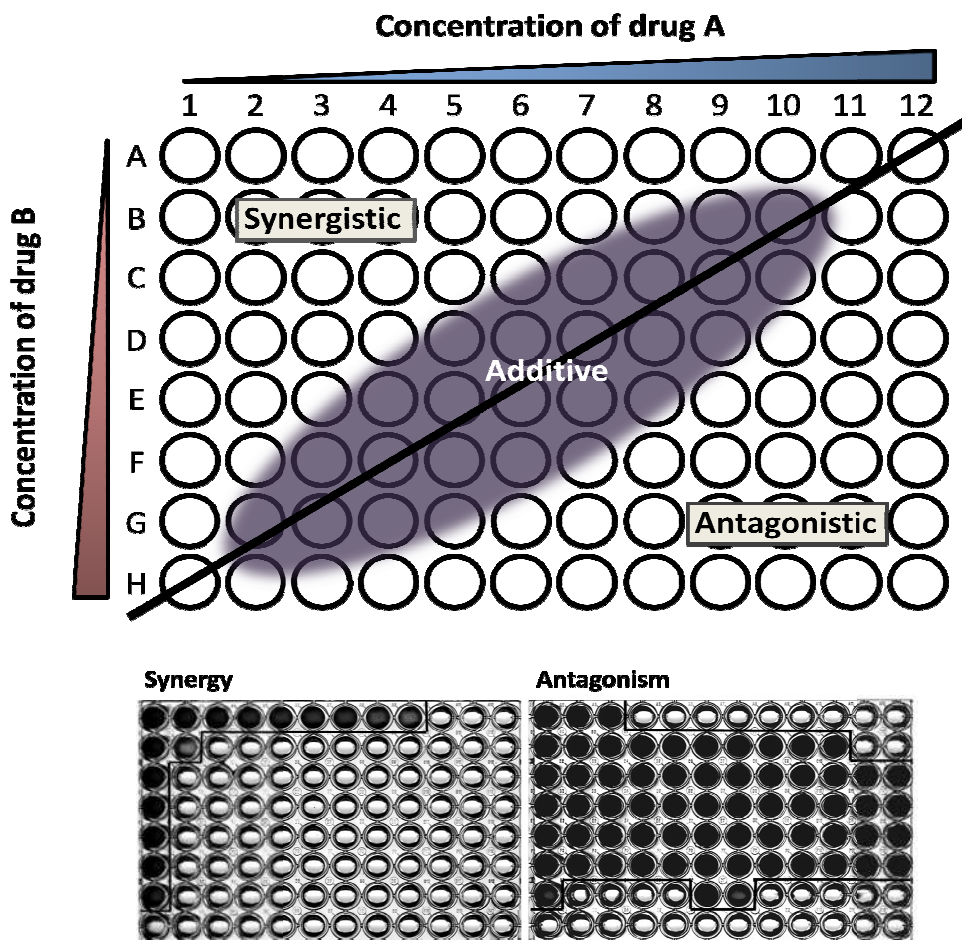
Figure 2.1. Synergistic, additive and antagonistic growth patterns. A 96-well plate (top) displaying inhibition patterns indicative of synergy (concave), antagonism (convex) and additive where no interaction occurs. Plates below are representative of synergistic and antagonistic growth patterns.

Data from all checkerboard work was gathered to calculate the corresponding fractional inhibitory concentrations (FIC) displayed by each combination of echinocandin and AMP. Results were calculated for each strain in MEB or RPMI-1640 media from the 96-well growth inhibition studies. The fractional inhibitory concentration index (FICI) is an interaction coefficient indicating whether the combined inhibitory effect of antimicrobial agents is synergistic, additive or antagonistic. Its use in chapter 4 was to elucidate the results gathered through the checkerboard assays distinguishing combinations that displayed synergy from those that did not.

The methodology is as follows:

fractional inhibitory concentration = A + B

where:

A = (MIC of drug X combination) / (MIC of X alone)

B = (MIC of drug Y combination) / (MIC of Y alone)

Results should be interpreted as synergy with FIC ≤ 0.5, antagonism with FIC > 4.0 and no interaction (additive) with FIC > 0.5 – 4.0 (Odds, 2003).

2.7 Effect of salt, pH, temperature and human serum on AMP viability.

To each well of a 96-well microtitre plate (Greiner Bio-one Ltd, GLR, UK) sterile MEB (150 µl) was added with Human serum (HS; Lonza biologics plc., BRK, UK) or NaCl and AMP. Wells were inoculated with yeast cells from a mid-exponential culture (1.0×10^3 cells per well) and plates were incubated (30 °C, 48 h). Images were captured as described previously (Section 2.5). HS was inactivated at 56 °C for 30 min. The pH of MEB was adjusted using HCl (Fisher Scientific Ltd., LEC, UK) or NaOH (Fisher Scientific Ltd., LEC, UK).

2.8 Disc diffusion assay of yeast growth inhibition

Sterile paper discs (6mm, Aa, Whatman International Ltd., KNT, UK) were impregnated with peptide in the presence or absence of echinocandin. These were left overnight to dry at room temperature. A 100 µl volume of mid-exponential phase cultures (OD_{600} = 0.3 for *S. cerevisiae*, OD_{600} = 0.6 for *C. albicans* and *C. glabrata*) was spread onto MEB or RPMI-1640 agarose plates and left to dry for 1 h at room temperature. The discs were then applied to the surface and the plates and incubated (30 °C, 48 h). Images of plates were acquired as described previously (Section 2.5).

2.9 Growth of yeast strains

Cells (cultured as Section 2.3) were used to inoculate each well of a 48-well plate (Greiner Bio-one Ltd, GLR, UK) so that each well contained 300 µl MEB and 2 x 10^3 cells. Peptide was added to the required concentration. Plates were incubated (30 °C, 48 h, shaking intensity of '2') and OD_{600} readings were taken every 15 min on a PowerWave XS automated microplate spectrophotometer (Bio-tek Instruments Inc., VT, USA).

2.10 Yeast cell viability

Yeast strains were incubated overnight (100 ml flasks, 20 ml MEB, 30 °C, 200 rpm) and inoculated into fresh MEB or RPMI-1640 in the presence or absence of 15 mM glucosamine hydrochloride or 15 mM glucosamine 6-phosphate (Chapter 3), to 1.0 x 10^6 cells ml^{-1}. Cultures were then exposed to peptide in the presence or absence of echinocandin (Chapter 4). The cultures were incubated as Section 2.3 and OD_{600} readings

were taken every 60 min until an optical density of 0.3 (*S. cerevisiae* mid-exponential) or 0.6 (*Candida* mid-exponential) was attained. Viability assays at each time point were determined by serial dilutions that were plated onto YEPD agar plates (30 °C, 48 h).

2.11 Population viability using fluorescence microscopy

To monitor cell viability visually, CellTracker[TM] Green 5-chloromethylfluorescein diacetate (CTG; Invitrogen Ltd., SCD, UK) was used to label metabolically active cells (FITC filter - excitation λ = 490/520 nm; emission λ = 528/38 nm), propidium iodide (PI; Invitrogen Ltd., SCD, UK) was used to stain cells with compromised membranes (RD-TR-PE filter - excitation λ = 490/520 nm; emission λ = 528/38 nm) and CellTracker[TM] Blue 7-amino-4-chloromethylcoumarin (CMAC; Invitrogen Ltd., SCD, UK) was used to stain yeast vacuoles (Makrantoni *et al*, 2007). Images were captured on an Olympus IX70 DeltaVision microscope (Applied Precision Inc., WA, USA) and image processing and analysis performed using SoftWoRx Explorer 1.3 (Applied Precision Inc., WA, USA).

Prior to staining, yeast cells (cultured to mid-exponential phase as Section 2.3) were harvested and diluted into 1 ml aliquots with MEB to 2×10^6 cells ml^{-1}. DsS3(1-16) was added to give various concentrations and then incubated (30 °C, 5 min). PI (stock of 3.75 mM in ethanol) and CTG (stock of 10 mM in DMSO) were added to give concentrations of 1.8 μM and 10 μM respectively. The 1 ml reaction mixture was then incubated in the dark (30 °C, 25 min). Unbound dye was removed by centrifugation (1 min, 12,000 x g). The resulting pellet was washed with 500 μl dH_2O, centrifuged (1 min, 12,000 x g) and re-suspended in 20 μl MEB. Two microlitre aliquots of the stained cells were fixed with 2

µl 1 % low-melting-point agarose (Biogene Ltd., CBE, UK). Samples were placed on ice and kept in the dark until inspected as above.

In addition, Flu-DsS3(1-16) (FITC filter) was added to cells prepared as above at various concentrations and incubated in the dark (30 °C, 30 min). Unbound peptide was removed by centrifugation (8 min at 3,000 x g), washing in 500 µl dH$_2$O, centrifugation (8 min at 3,000 x g) and re-suspension in 20 µl MEB. Samples were fixed as above.

2.12 Quantification of Flu-DsS3(1-16) binding and internalisation

Fluorescence emission spectra of Flu-DsS3(1-16) was measured on a Cary Eclipse Fluorescence Spectrophotometer (Varian Inc., CA, USA) equipped with a xenon lamp. Excitation and emission wavelengths were 494 nm and 521 nm, respectively. Readings were taken in a Quartz SUPRASIL Micro cuvette (700 µl volume) (Perkin Elmer, MA, USA). Peptide bound to cells was calculated via a calibration curve with increasing concentrations of Flu-DsS3(1-16) in MEB, against fluorescence intensity (a.u.). One millilitre of cells (OD$_{600}$ = 0.3 for *S. cerevisiae*; OD$_{600}$ = 0.6 for *C. albicans*) was aliquoted and Flu-DsS3(1-16) added at various concentrations. Cells were incubated in the dark (30 °C, 30 min). The suspension was centrifuged (10,000 x g, 2 min) to remove the cells and bound peptide. Residual fluorescence remaining in the supernatant was measured.

A concentration to fluorescence ratio was calculated so that when a known concentration of peptide was added, the sequestered peptide could be calculated based

on the fluorescent intensity of the media. Flu-DsS3(1-16) was added to MEB at 5, 10, 15 and 20 µg/ml concentrations and the fluorescent intensity was measured. Each condition was performed in duplicate and a mean was calculated. These data produced a direct correlation between peptide alone and fluorescence (Figure 2.2). It was calculated that 1 µg/ml Flu-DsS3(1-16) was equal to a fluorescent intensity (a.u.) of 33.05.
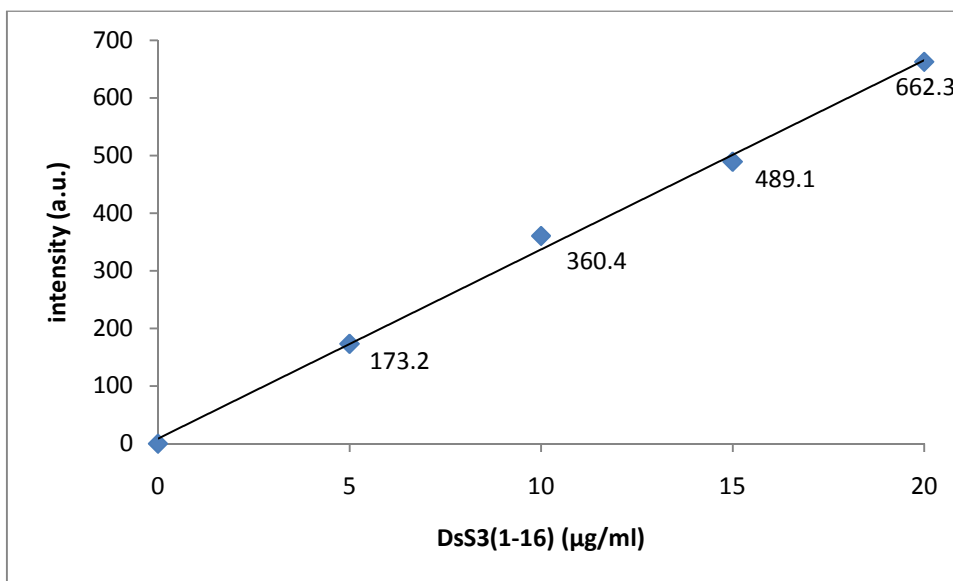
Figure 2.2. Fluorescent intensity of Flu-DsS3(1-16) in MEB. The average reading from each concentration was plotted. A line of best fit was placed over the points with the equation showing above. From this the Flu-DsS3(1-16) / fluorescent intensity ratio was calculated to be: 1 µg/ml = 33.05 a.u; n = 2.

2.13 Intracellular localisation of Flu-DsS3(1-16) using fluorescence microscopy.

The phase-contrast and fluorescent peptide images were generated using the FITC filter (Ex λ = 490/20 nm, Em λ = 528/38 nm). P.I. (Invitrogen Ltd., SCD, UK) was used to identify dead cells (RD-TR-PE, Ex λ = 490/20 nm, Em λ = 528/38 nm). Cells were cultured in MEB and harvested at mid exponential phase. A volume equivalent to 2×10^6 cells/ml was removed from each assay, centrifuged (2 min, 12,000 x g), washed in 500 µl dH$_2$O and resuspended in 1 ml of RPMI-1640 or MEB. The desired concentrations of echinocandin

in the presence or absence of Flu-DsS3(1-16) were added with P.I. (1.8 µM) and incubated (2 h, 30 $^{\circ}$C, in dark). The unbound dye and peptide were removed by centrifugation (8 min, 3,000 x g). The resulting pellet was washed in dH$_2$O, centrifuged (8 min, 3,000 x g) and resuspended in 20 µl RPMI-1640 or MEB. Two microlitre aliquots of the stained cells were fixed with 2 µl of 1 % low-melting-point agarose (Biogene Ltd., CBE, UK). Samples were placed on ice and kept in the dark until analysis. Images were captured and edited as described previously (Section 2.11).

2.14 GFP-tagging of *LDB7*, *IMP2'* and *HAL5*

HAL5, *LDB7* and *IMP2'* were chromosomally tagged at the 3' end with GFP-*HIS1* cassettes using the method of Sheff and Thorn (2004). The pKT209 plasmid (Appendix I) was amplified and tagging was verified by diagnostic PCR. Primers were designed using Integrated DNA Technologies software (http://eu.idtdna.com/Scitools/Scitools.aspx) and synthesized by Eurofins MWG Operon, Germany (Table 2.4). Gels were visualised using a UV transiluminator (Ultra-Violet Products Ltd**.,** CBE, UK), and photographed with a BioDoc-It™ imaging system (Ultra-Violet Products Ltd**.,** CBE, UK) (Figure 2.3).

Table 2.4. Sequences used to generate GFP- tagged *HAL5*, *LDB7* and *IMP2'* strains. Forward (F) and reverse (R) oligos.

Oligo		Sequence (5'-3')
HAL5	F	CTGTGTAGTTTATAGACACTTACATACCAAGGTTAGTAAAGGTGACGGTGCTGGTTTA
	R	GTAATAATAAATACTTAAGCATTTTTTGTTTTGTATATCTTCGATGAATTCGAGCTCG
LDB7	F	CCATAGGCGGTCTCAACTTAGAGAACATGCCTGCGTAGATGGTGACGGTGCTGGTTTA
	R	TTTCTACGAAGCAACATTCTACCTCTATCAATTACATGGTTCGATGAATTCGAGCTCG
IMP2'	F	CTGAAACGTGCCAAGCGCAAGGGCATCAGCGAGTGACCAAGGTGACGGTGCTGGTTTA
	R	TATATAAGTATGTGTTGCTAAAAAGGAATTAGTGCAGTGATCGATGAATTCGAGCTCG
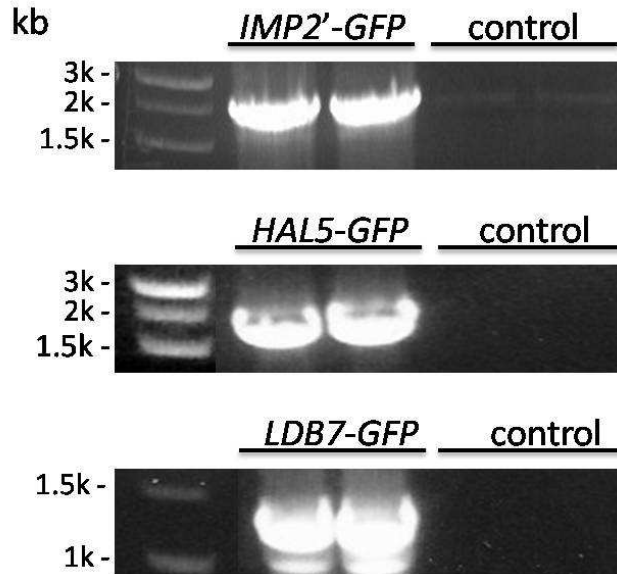
Figure 2.3. Images from gel electrophoresis of GFP PCR products showing approximate sizes of the constructs. *HAL5-GFP* ~2.3 kb, *IMP2'-GFP* ~1.6 kb, *LDB7-GFP* ~1.3 kb.

Localisation and expression of GFP-tagged Hal5, Ldb7 and Imp2' images were acquired as described above using the FITC and DAPI filters. Briefly, yeast cultures were harvested at mid-exponential phase (OD_{600} 0.3) and diluted with MEB to give 2 x 10^6 cells ml^{-1}. Cells were incubated in the presence or absence of peptide (60 min, 30 °C) and fixed with 10 µl *Mowiol-DAPI* solution (10% *Mowiol* (Sigma-Aldrich Ltd, DOR, UK), 25% glycerol, 100 mM Tris–HCl, 1µg/ml *DAPI* (Sigma-Aldrich Ltd, DOR, UK)) prior to image acquisition.

2.15 Cytometric analysis of membrane potential

Stock solution of 3,3'-dipropylthiacarbocyanine iodide (diS-C$_3$(3)) was prepared (10^{-4} M in ethanol). Cells were cultured (MEB, OD$_{600}$ = 0.3), then harvested by centrifugation (3,000 rpm, 10 min) and washed in dH$_2$O. Cells were resuspended in citrate-phosphate buffer (1 M citric acid (Sigma-Aldrich Ltd, DOR, UK), 1M Na$_2$HPO$_4$ (Sigma-Aldrich Ltd, DOR, UK), pH6.5) to a final concentration of 5 x 10^6 cells/ml. Cells were labelled with diS-C$_3$(3) giving a working concentration of 2 x 10^{-7} M. The time needed for probe equilibrium in suspensions of *S. cerevisiae* is 20 min (Gaskova *et al*, 1998). Peptide was added to the desired concentration and incubated for a further 20 min. Cultures were vortexed prior to cytometry to dissipate any aggregates. An Epics XL-MCL flow cytometer (Beckman Coulter Ltd, BUX, UK) with Expo32 ADC software (Applied Cytometry, YSS, UK) was used. Prior to sampling, dH$_2$O was passed through until no artefacts were observed. Flow rate was adjusted to keep readings below 1,000 events per second during analysis. A total of 10,000 cells were counted for each assay to generate data. Fluorescence of diS-C$_3$(3) was monitored in fluorescence channel FL2 (CT-SNARF, BR, PKH-26). Amphotericin B was used as a control as it causes significant membrane depolarisation so a consequent reduction in fluorescent maximum would be expected, caused by probe outflow from the cell (Henry-Toulmé *et al*, 1989).

2.16 *In vitro* haemolytic assay of echinocandins and AMPs

Defibrinated horse blood (2 %) (Oxoid Ltd, HPH, UK) was diluted in phosphate buffer saline (PBS). Horse blood (2 %) in dH$_2$O was used as a positive control. To each well of a 96-well microplate, 150 µl of blood was added with appropriate concentrations of

echinocandin or AMP. Blood cell turbidity was measured spectrophotometrically (570 nm) every 15 min over 4 h. A reduction in OD_{570} deviating from the control would indicate haemolysis of erythrocytes.

2.17 *In vitro* mammalian cell cytotoxicity assay of echinocandins and AMPs

The method is as described by Yang *et al.* (2006). *Vero* cells were cultured in 75 cm^2 culture flasks (Greiner Bio-one Ltd, GLR, UK) (37 °C, 95% humidity, 5% CO_2). Cells (25,000 per well) were dispensed into microplate wells and incubated (37 °C, 24 h). Appropriate concentrations of echinocandins, AMPs or combinations were prepared in RPMI-1640, added to the wells and incubated for 48 h. The proportion of viable cells was determined by neutral red (Sigma-Aldrich Ltd, DOR, UK) procedure (10 mg/ml stock in PBS) adapted from that described by Borenfreund and Puerner (1984). After incubation with the antifungals, cells were washed with PBS and incubated (37 °C, 90 min) with RPMI-1640 media containing neutral red (166 µg/ml). The plate was then washed to remove extracellular dye prior to the addition of acidified isopropanol (Fisher Scientific Ltd., LEC, UK) (0.33% HCl) to lyse the viable cells and release any retained neutral red. Released dye was measured spectrophotometrically at 540 nm. Viable cells were expressed as the proportion retaining neutral red after exposure to antifungals relative to untreated controls. Carbonyl cyanide m-chlorophenyl hydrazone (CCCP; Sigma-Aldrich Ltd, DOR, UK) was used as a positive control (0.15 µg/ml).

2.18 Efficacy *in vivo* of the combination of caspofungin with ranalexin in a murine model of disseminated Candidiasis

This work was performed by Prof. Frank Odds group, School of Medical Sciences, University of Aberdeen. Basic details of the intravenous challenge model for disseminated *C. albicans* infection have been published previously (MacCallum *et al*, 2005). Briefly, female BALB/c mice were infected intravenously (IV) with *C. albicans* at a dose of $3\pm1 \times 10^4$ CFU/g body weight. Animals were humanely terminated 72 h after challenge, and body weight changes (which correlate with survival times and fungal burdens in kidney homogenates) were determined. Caspofungin IV preparation was diluted in saline as required. Combination therapy with caspofungin and ranalexin was investigated in two experiments. In the first, caspofungin was dosed at 0.01 mg/kg intraperitoneal (IP), every day (qd), and ranalexin at 10 mg/kg IV, qd. Saline IV and IP were used as placebo, and animals given caspofungin or ranalexin monotherapy were concomitantly dosed with saline by the IV and IP routes, respectively. The first treatments were given 1 h after challenge and repeated at 24 and 48 h. In the second experiment, caspofungin was dosed at 0.05 mg/kg IV, qd, and ranalexin was dosed IV at 10 mg/kg bid. The first treatments were given 1 h after challenge. Saline IV was used as placebo. All animal experimentation was approved by the local ethical review committee and was performed under UK Home Office regulations. Statistical analysis of the data was by Mann-Whitney *U*-test.

2.19 Expression analysis of *IZH2* (Appendix VII)

2.19.1 *S. cerevisiae* gene cloning and PCR amplification of *IZH2*

The *IZH2* gene from *S. cerevisiae* was cloned under the control of its own promoter into the pGEM-T® Easy Vector (Promega, HPH, UK; Appendix I) and then into the single copy pRS313 vector according to the method of Sambrook *et al*, 1989. *IZH2* was amplified from *S. cerevisiae* genomic DNA using Taq polymerase (Promega, HPH, UK) with gene specific primers (Table 2.5). The control contained no template DNA. PCR products were added to a 1 % agarose gel and the resulting *IZH2* DNA was excised and extracted using a gel extraction kit (Qiagen Ltd., SXW, UK) according to manufacturer's instructions. The extracted DNA was ligated into the linearised pGEM-T® Easy Vector using: 1 x ligation buffer, 100 ng pGEM-T® Easy Vector, 1 µl T4 DNA ligase, 100 ng *IZH2* DNA (control contained no DNA) and incubated overnight at 4 °C.

Table 2.5. Sequences used to amplify *IZH2* gene.

Oligo	Sequence (5'-3')	Product Length
IZH2 Forward	CGGTCTTCCGTTGTTGAGCTCTTT	1272 bp
IZH2 Reverse	GTGCACAAATCCTGCTTCCCTTCT	

The resulting ligation mix (10 µl) was added to 100 µl competent *E. coli* and left on ice for 30 min before heat shocking (42 °C, 90 s). The mixture was placed on ice for 2 min before 500 µl of LB was added and incubated (37 °C, 1 h). Cells were harvested by centrifugation (13,000 rpm, 30 s) and resuspended in 100 µl dH$_2$O. Cells were then plated onto LB agar plates with 100 µg/ml ampicillin and incubated (37 °C overnight). *IZH2* gene insertions were verified by PCR. *IZH2* transformed *E. coli* cells were used

instead of template DNA. Products were confirmed using 1 % agarose gel displaying either amplification of *IZH2* into pGEM-T® Easy Vector.

2.19.2 Reintegration of *IZH2*

IZH2 was reintegrated into the respective deletion strain using pRS313 (New England Biolabs, HFD, UK; Appendix I). Initially the *IZH2* gene was cut using the restriction enzyme Not 1 (Promega, HPH, UK). Digestion of *IZH2* pGEM-T with pRS313 was performed with: 1 x reaction buffer, 0.5 µl Not 1, 1 µg *IZH2* pGEM-T plasmid and pRS313 DNA. This was incubated overnight (37 °C) and run on a 1 % agarose gel before the *IZH2* gene and pRS313 DNA bands were excised using a QIAquick Gel extraction kit (Qiagen Ltd., SXW, UK) (Figure 2.4) following the manufacturer's instructions.

The *IZH2* gene and pRS313 vector ligation was prepared with a control lacking *IZH2* DNA. The reaction mixture was as follows: 1 x reaction buffer, 100 ng pRS313 vector, 100 ng *IZH2* DNA, 1 µl ligase. The mixture was incubated for 2 h at room temperature before transformation into competent yeast cells (BY4741a) using the method of Gietz *et al*, 1995 and selected using the His 3 marker. Integration was confirmed using PCR.
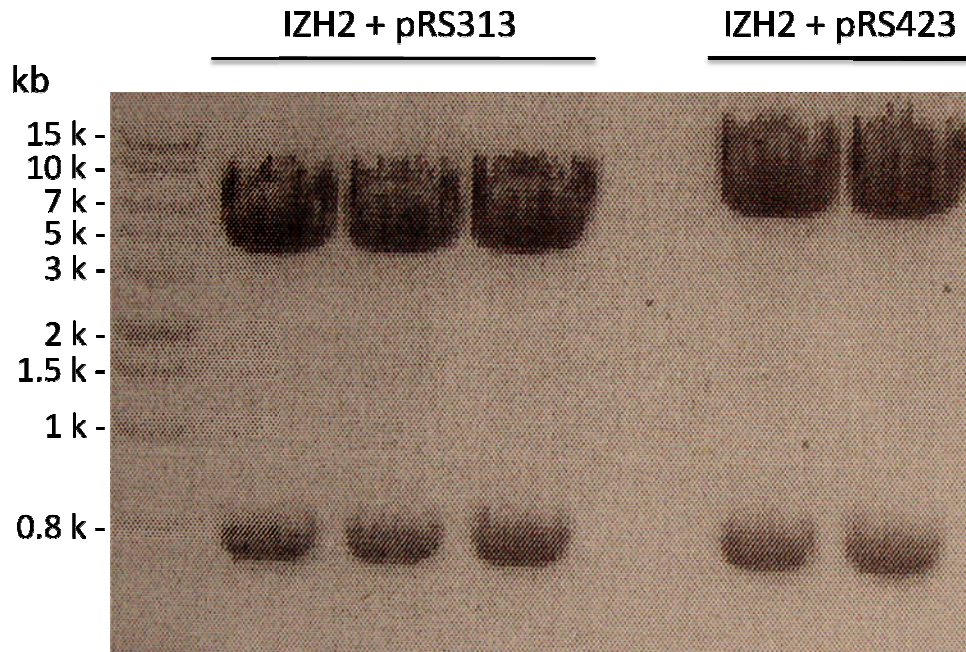
Figure 2.4. Images from gel electrophoresis of *IZH2* DNA (bottom row) and pRS313 or pRS423 (top row) products showing approximate sizes.

2.19.3 Overexpression of *IZH2*

IZH2 was cloned into the 2 μ-based multi-copy vector pRS423 (New England Biolabs, HFD, UK; Appendix I) following the method of Sambrook *et al*, 1989. The pRS423::IZH2 constructs were then transformed into the *izh2Δ* strain.

2.19.4 Transformant growth analysis

A dilution series from 5×10^{6} to 5×10^{3} cells per ml was prepared for each transformation. Suspensions were then spotted (10 μl) into wells of a 24-well microtitre plate (Greiner Bio-one Ltd, GLR, UK) containing YNB agarose with or without 100 μl DsS3(1-16). These were incubated at 30˚C for 48 h. YNB salt concentrations were reduced to 5 % Potassium dihydrogen orthophosphate and 2 % of Magnesium sulphate,

Sodium chloride and Calcium chloride of their original concentration to minimise peptide

interactions.

2.20 Growth and cell number of all yeast strains

Cells used in viability studies were from mid-exponential phase cultures. Periods of

exponential growth were determined from optical density versus cell number calibration

curves (Figures 2.6 - 2.15). Exponential growth was recorded for all strains between ~0.2

- 1.0 and cells were selected for experimentation at OD_{600} = 0.6 (Table 2.6). *S. cerevisiae*

exponential growth was recorded at a reduced OD_{600}, therefore cultures were selected

for analysis at OD_{600} = 0.3. *C. glabrata* had the greatest number of cells present per ml of

culture at OD_{600} = 0.6. All cell wall mutant *C. albicans* strains had a reduction in cell

number at OD_{600} compared to the CAI-4 parent strain.

Table 2.6. Exponential growth period of all strains in MEB with CFU/ml at OD_{600} = 0.6 (OD_{600} = 0.3 for *S. cerevisiae*).

strain	exponential growth	cfu/ml
S. cerevisiae	0.14-0.47	3,913,304
C. albicans isolate	0.29-1.01	7,208,009
CASC5314	0.22-1.02	10,345,819
C. glabrata	0.34-1.22	30,713,409
C. neoformans	0.21-0.97	13,408,926
CAI-4(Clp10)	0.31-1.39	5,937,039
mnt1-mnt2Δ(Clp10)	0.22-1.35	2,437,209
mnt3/mnt5Δ (Clp10)	0.18-1.15	3,679,252
och1Δ(Clp10)	0.16-1.43	4,033,131
pmr1Δ(Clp10)	0.16-0.63	2,505,017
mnn4Δ(Clp10)	0.28-2.22	4,700,541
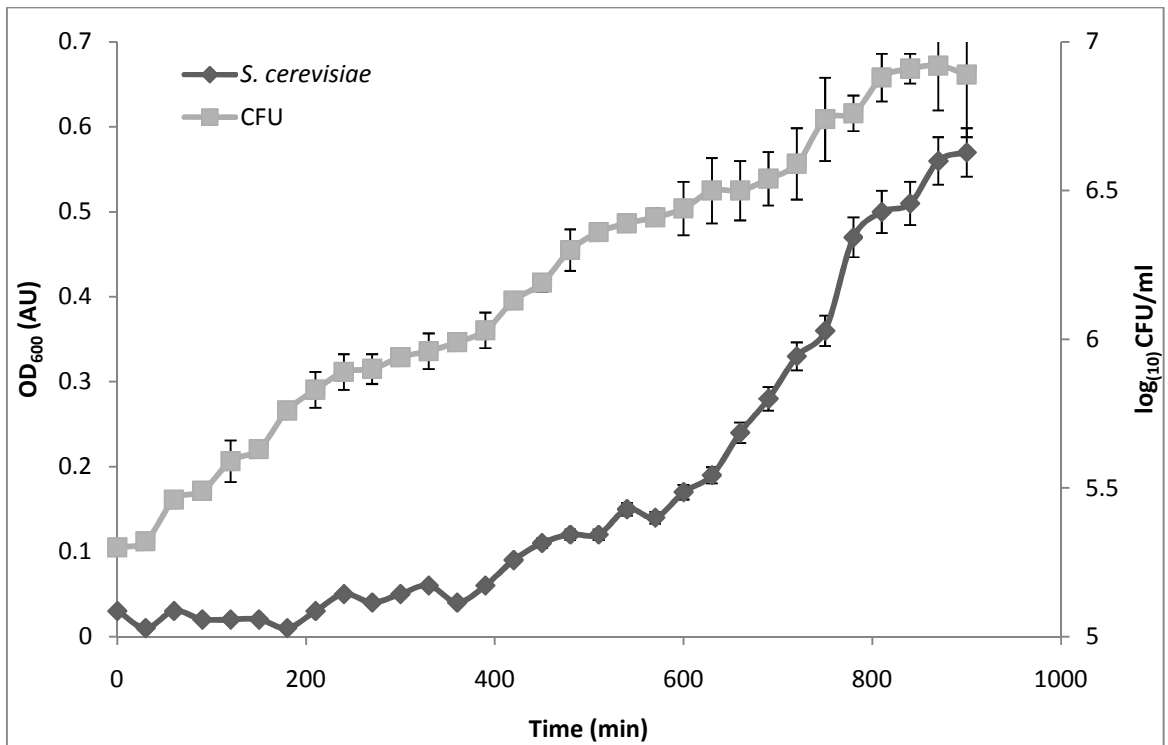
Figure 2.5. Growth of *S. cerevisiae* in MEB. Cell density was measured every 30 min over a 900 min period; n = 3 mean ± 2 SD.
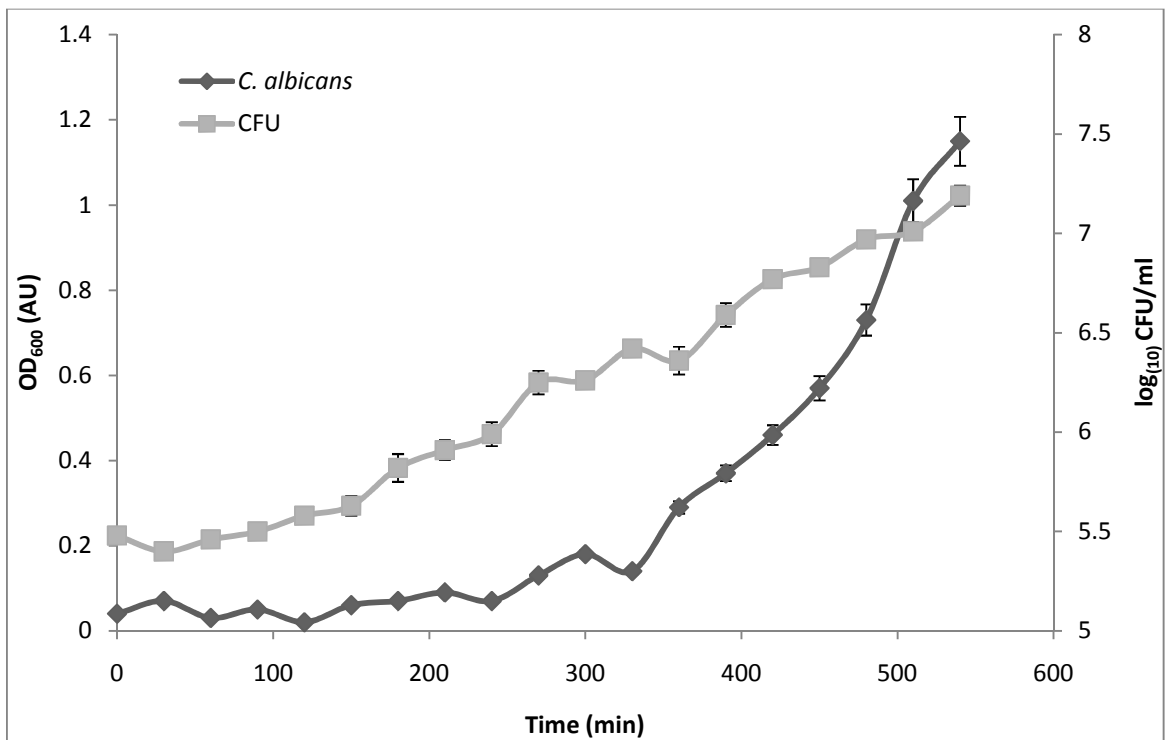
Figure 2.6. Growth of *C. albicans* in MEB. Cell density was measured every 30 min over a 540 min period; n = 3 mean ± 2 SD.
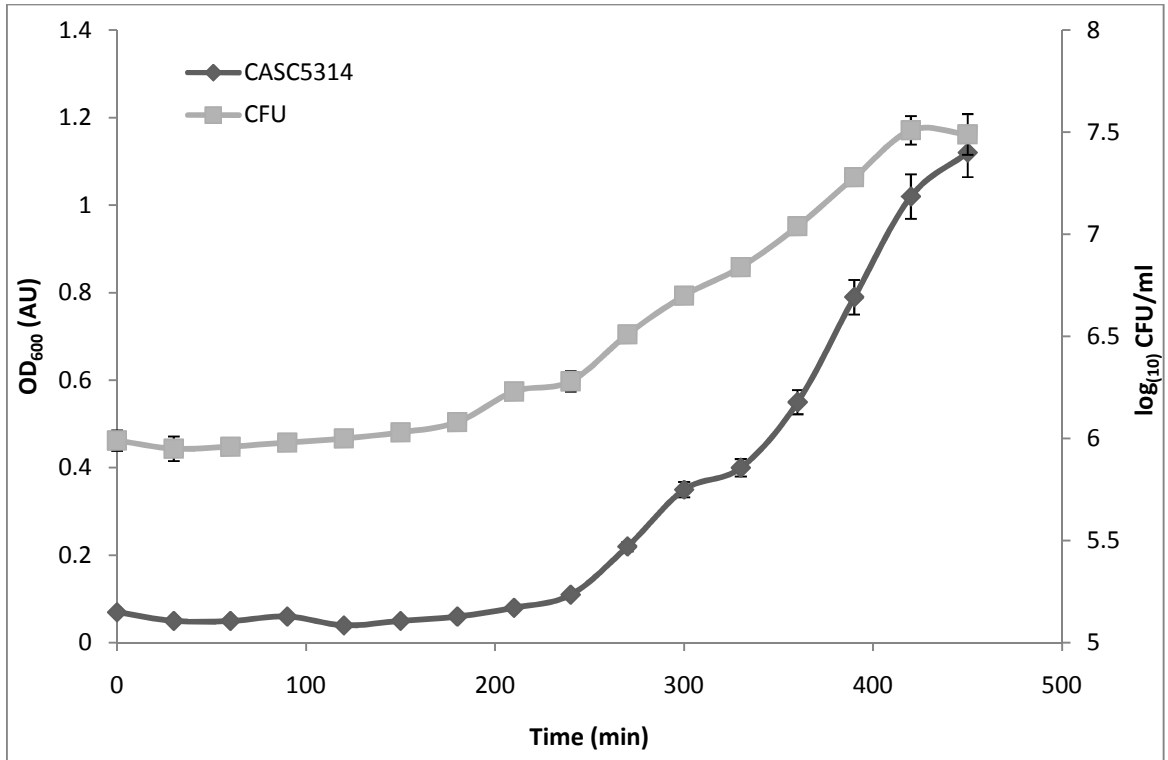
Figure 2.7. Growth of *C. albicans* SC5314 in MEB. Cell density was measured every 30 min over a 450 min period; n = 3 mean ± 2 SD.
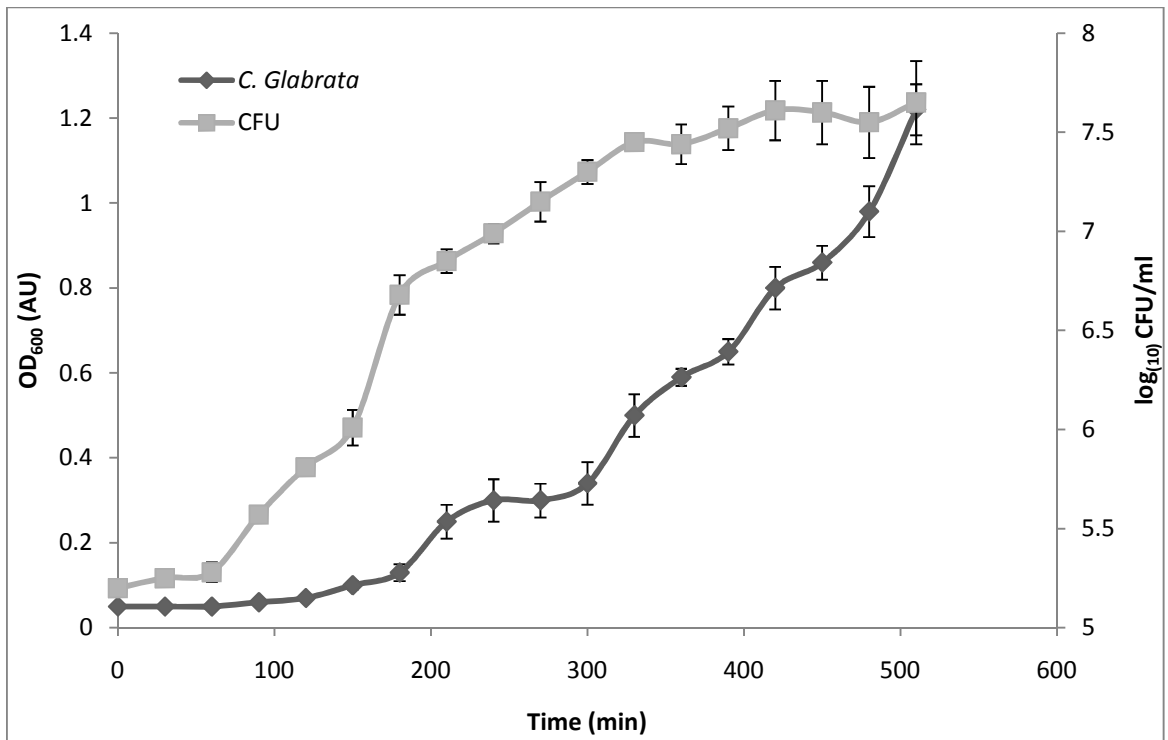
Figure 2.8. Growth of *C. glabrata* in MEB. Cell density was measured every 30 min over a 510 min period; n = 3 mean ± 2 SD.
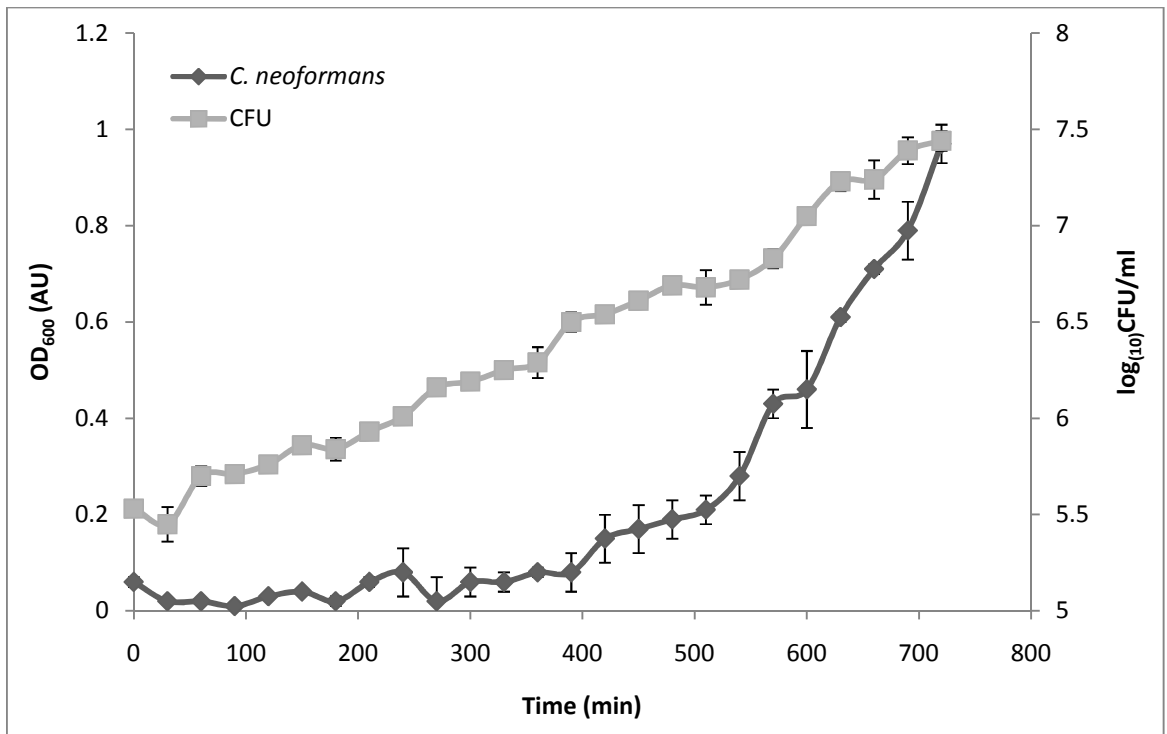
Figure 2.9. Growth of *C. neoformans* in MEB. Cell density was measured every 30 min over a 720 min period; n = 3 mean ± 2 SD.
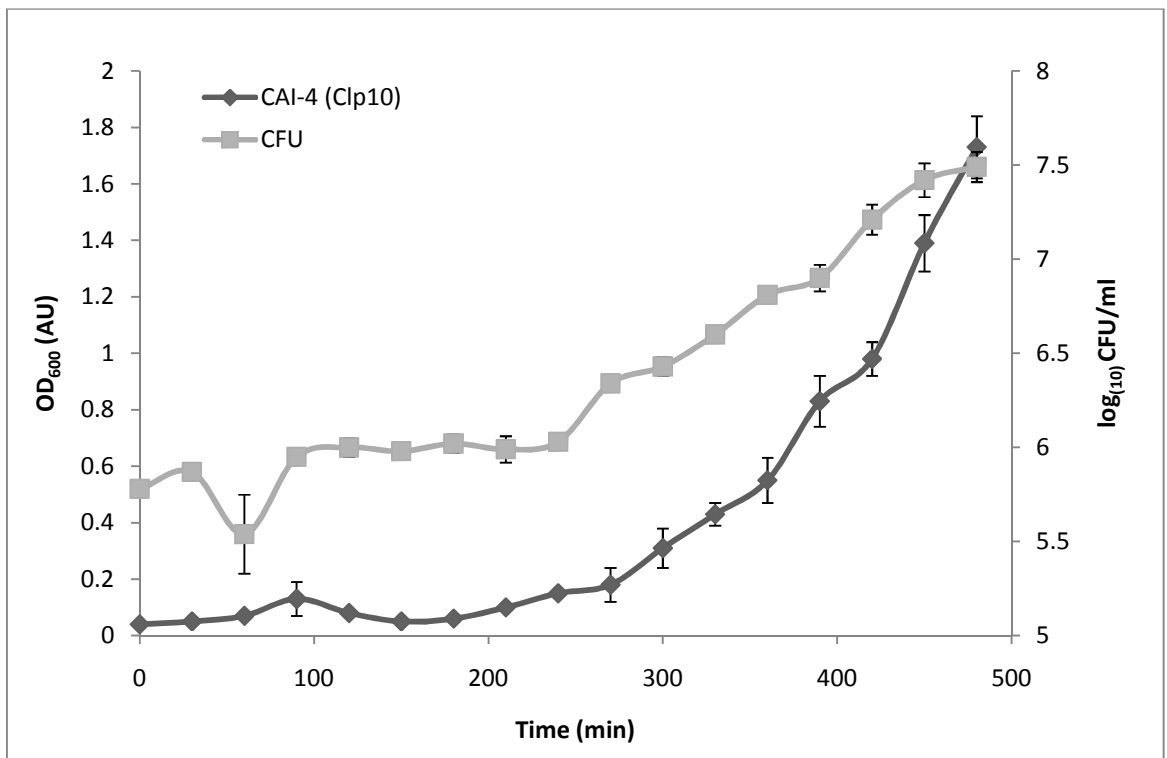
Figure 2.10. Growth of CAI-4(Clp10) in MEB. Cell density was measured every 30 min over a 480 min period; n = 3 mean ± 2 SD.
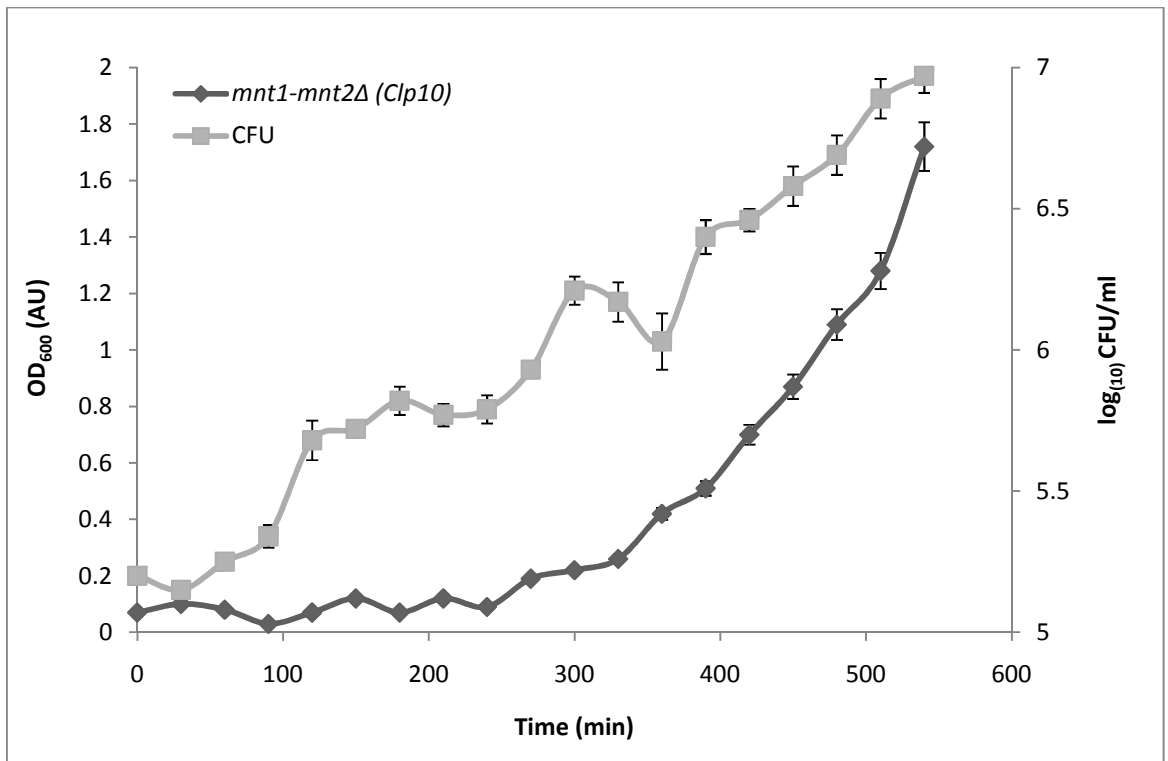
Figure 2.11. Growth of *mnt1-mnt2*Δ(Clp10) in MEB. Cell density was measured every 30 min over a 540 min period; n = 3 mean ± 2 SD.
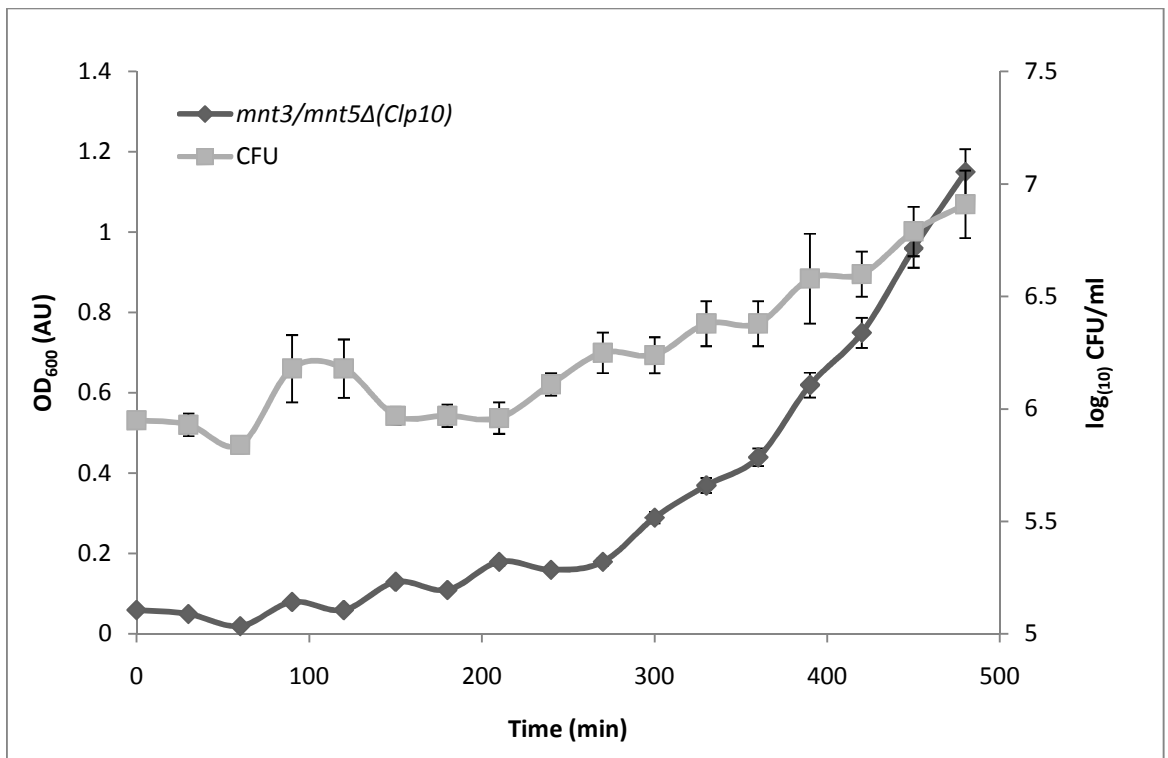
Figure 2.12. Growth of *mnt3/mnt5*Δ(Clp10) in MEB. Cell density was measured every 30 min over a 480 min period; n = 3 mean ± 2 SD.
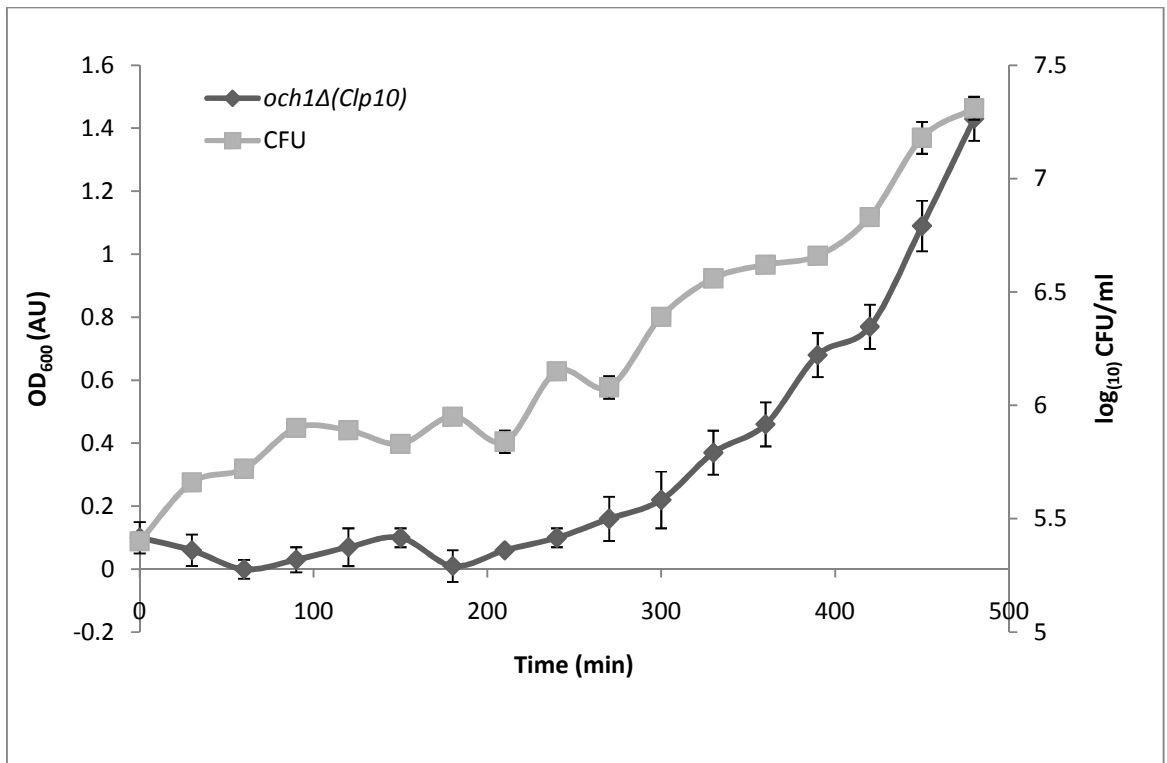
Figure 2.13. Growth of *och1*Δ(Clp10) in MEB. Cell density was measured every 30 min over a 480 min period; n = 3 mean ± 2 SD.
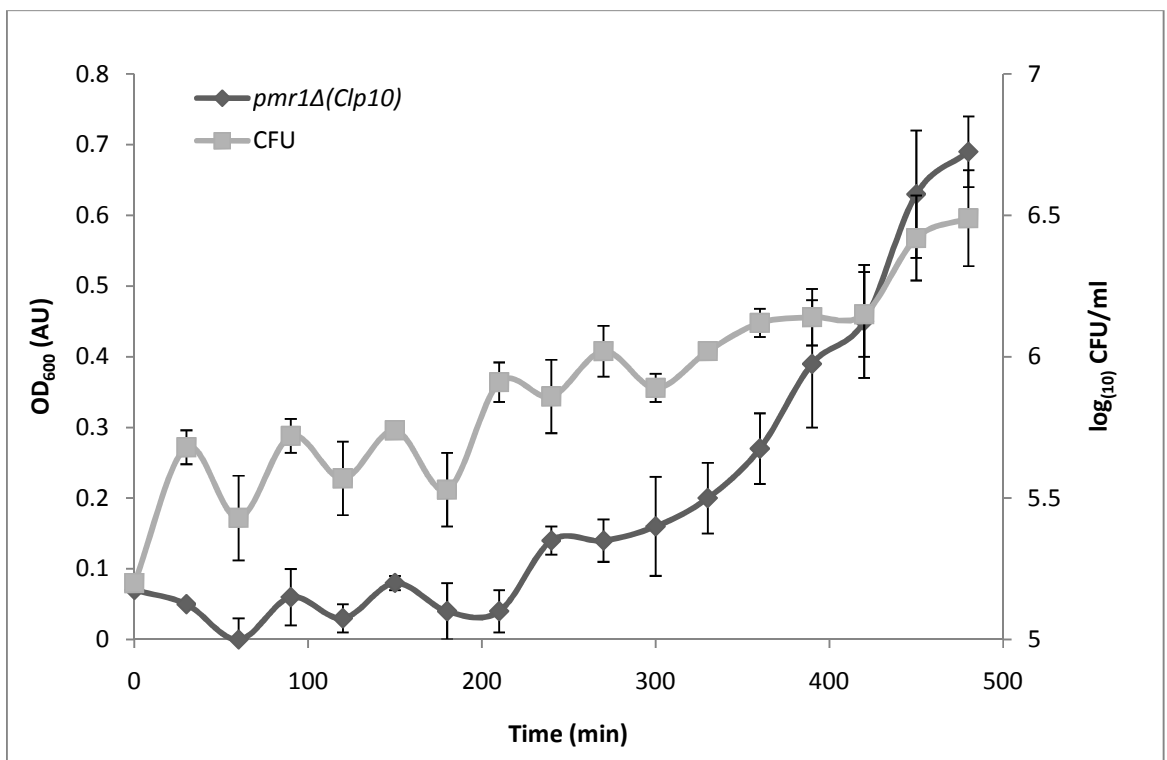
Figure 2.14. Growth of *pmr1*Δ(Clp10) in MEB. Cell density was measured every 30 min over a 480 min period; n = 3 mean ± 2 SD.
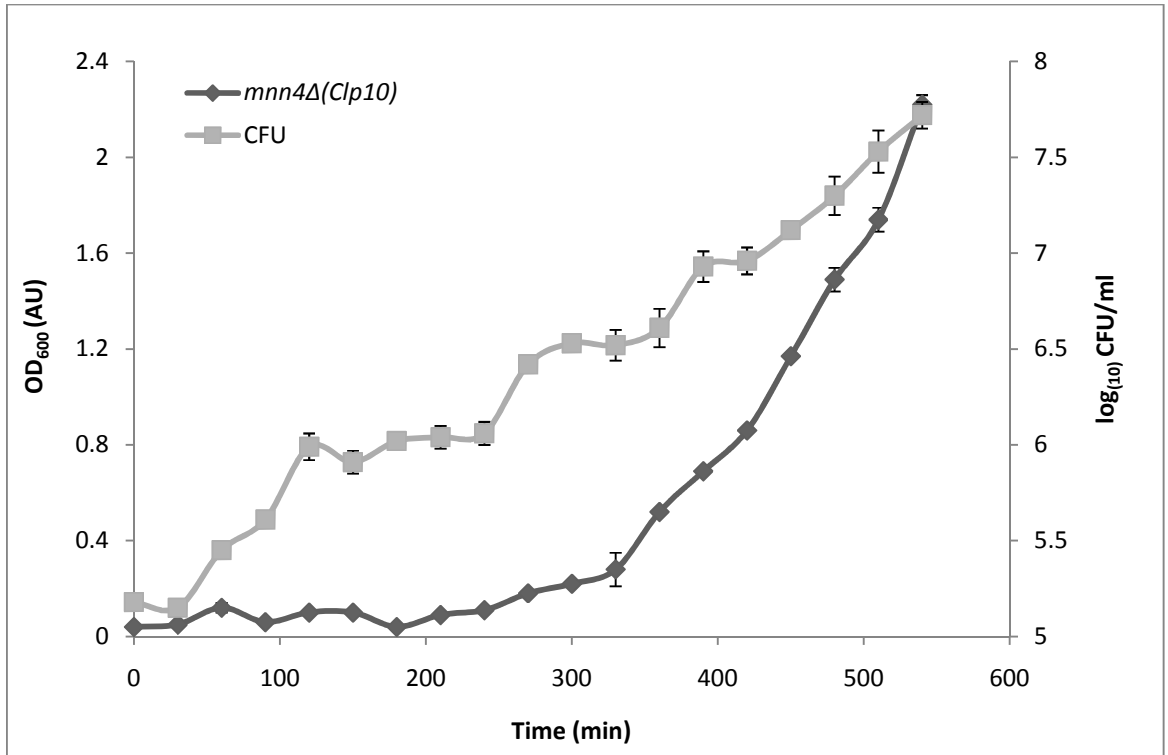
Figure 2.15. Growth of *mnn4*Δ(Clp10) in MEB. Cell density was measured every 30 min over a 540 min period; n = 3 mean ± 2 SD.

Chapter 3

3. Effect of alterations in the cell wall composition of *Candida albicans* on susceptibility to several cationic antimicrobial peptides.

3.1 Introduction

The *Candida* cell wall consists of an outer layer of mannoproteins and inner layers of various carbohydrate polymers such as glucans, chitin and galactomannan (Figure 3.1) (Latge *et al*, 2005; Ruiz-Herrera *et al*, 2006). These are essential components and even minor modifications can reduce viability *in vitro*, so maintenance of its integrity is essential. The glucans and chitin polymers give the wall structure and rigidity (Ruiz-Herrera *et al*, 1994) whilst the mannosyl content mediates adhesion to host cells, enhancing virulence (Netea *et al*, 2008). In *C. albicans* the inner layer is predominantly 1,3-β glucan and 1,3-α glucan with lesser amounts of 1,6-β glucan and chitin. The cell wall of *C. albicans* also contains a mannosylphosphate-containing fraction with N-linked regions structured with an 1,6-α linked polymannose backbone with 1,2-α and 1,3-α-linked oligomannosides and one to fourteen 1,2-β mannose residues attached via mannosylphosphate and anchored by phosphodiester linkages (Figure 3.2). Loss of mannosylphosphate from the cell wall in *S. cerevisiae* causes a reduction in negative charge while changes in the outer layer of mannoproteins influence cell wall porosity (Ballou, 1990; de Nobel *et al*, 1990).
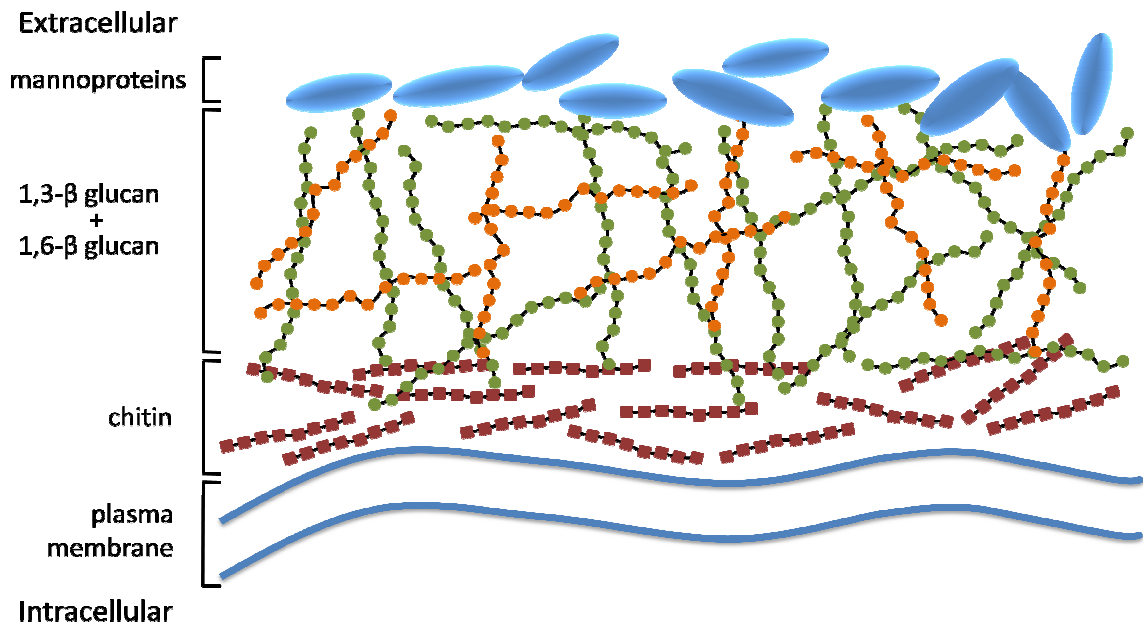
Figure 3.1. Schematic diagram of the *Candida* cell wall.

Several studies have highlighted the importance of the cell wall in mediating antimicrobial peptide action, however, most studies have focused on bacteria (Pooley *et al*, 1994; Peschel *et al*, 2001). In one study, *S. aureus* mutants with an increased negative charge (mutant teichoic acids lacking D-alanine) were more susceptible to growth inhibition by mag 2 and human defensins (Peschel *et al*, 1999). One of the few studies investigating the role of the cell wall in yeast showed that sensitivity of *S. cerevisiae* to the action of nisin was dependent on the levels of a protein found in the cell wall (Cwp2p) (Dielbandhoesing *et al*, 1998). Cells with high levels of Cwp2p were more resistant to the action of nisin, whilst cells lacking Cwp2p were significantly more susceptible probably due to thinner cell walls. Morton[b] *et al* (2007), using *S. cerevisiae*, showed that disruption of genes involved in cell wall organisation and biogenesis, such as *LDB7*, confer sensitivity to DsS3(1-16) and mag 2.
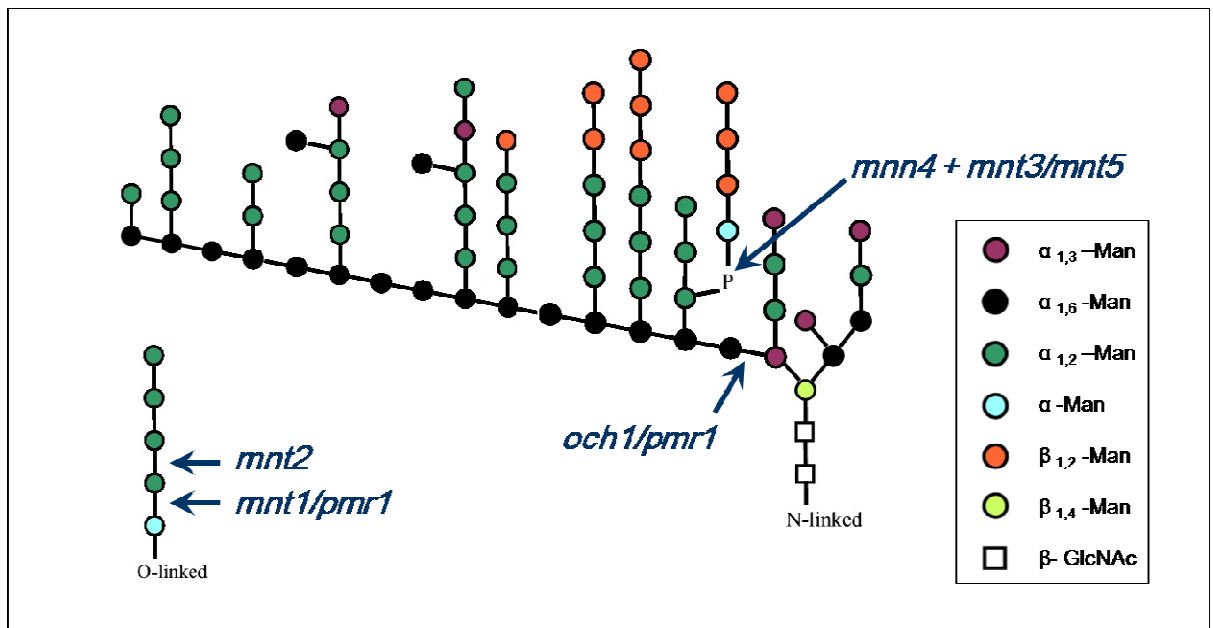
Figure 3.2. Morphology of the *C. albicans* cell wall showing the structure of the N- and O-linked glycans. The areas of effect resulting from each gene deletion are also highlighted. Man: mannosyl, β-GlcNAc: β *N*-acetylglucosamine.

As the action of AMPs in yeast has not been studied with respect to cell wall structure, a group of well characterised *C. albicans* cell wall mutants were acquired to test their susceptibility towards cationic antimicrobial peptides. Genes under investigation were: *MNN4, MNT1, MNT2, MNT3, MNT5, OCH1* and *PMR1* which all lack specific, well-characterised cell wall components (Figure 3.2). *MNN4* is required for mannosylphosphorylation. This is necessary for mannosyl phosphate transfer which in turn is required for the attachment of 1,2-β mannose to the N-mannan side chains (Hobson *et al*, 2004). *MNT3* and *MNT5* are also required for mannosylphosphorylation, encoding functionally redundant phosphomannosyltransferases, which also function in the modification of the N-linked fraction. *MNT1* and *MNT2* are mannosyltransferases that add the second and third mannose residues to the O-linked glycan fraction. They play a role in adherence of *C. albicans* to host cells. The double null mutant *mnt1-mnt2Δ* has reduced Man_2-Man_5 residues, displays a large increase in Man_1 O-linked glycans and

is hypersensitive to the cell wall perturbation agent Calcofluor White (Munro *et al*, 2005). *OCH1* encodes a 1,6-α mannosyltransferase that is responsible for outer-chain branching of N-glycans, null-mutants lack the 1,6-α linked polymannose fraction (Bates *et al*, 2006). The final gene mutated is *PMR1.* The *C. albicans* homolog of *PMR1* in *S. cerevisiae* encodes a P-type ATPase which supplies the Golgi with calcium and magnesium ions (Rudolph *et al*, 1989). In *C. albicans* the null mutant displays severe glycosylation defects with an 80 % reduction in mannose content and is hypersensitive to Calcofluor white. As these mutants display varying changes in cell wall architecture they may influence the action of cationic antimicrobial peptides either in their interaction with the cell wall or the membrane beneath. The following investigation aimed to explore whether changes to cell wall structure influenced the action of three cationic peptides: DsS3(1-16), mag 2 and rana.

3.2 Results

3.2.1 MIC determination

MICs were determined for the three peptides (DsS3(1-16), mag 2 and rana) against the parent strain (CAI-4) and each of the cell wall mutant strains (Table 3.1). The wild type strain, CAI-4, had a MIC for DsS3(1-16) of 5 µg/ml. The *mnt1Δ* and *mnt2Δ* strains had MICs similar to CAI-4 (6 µg/ml and 5 µg/ml respectively). The *mnt1-mnt2Δ* double deletion was more sensitive to DsS3(1-16) than the parent, with growth inhibited at 4 µg/ml. The *mnt3/mnt5Δ* double deletion and the *och1Δ* were intermediately sensitive to the peptide with MICs of 7 µg/ml. Least sensitivity to DsS3(1-16) was seen with *pmr1Δ* and *mnn4Δ* which had MICs of 11 µg/ml and 14 µg/ml respectively which are more than double the MIC of the parent strain and nearly triple the MIC for *mnn4Δ*.

The mag 2 plate shows a similar trend but with greater concentrations of peptide required to inhibit growth. CAI-4, *mnt1Δ* and the double deletion *mnt1-mnt2Δ* had MICs of 22 µg/ml. *mnt2Δ* again showed a slight decrease in susceptibility as well as *mnt3/mnt5Δ* and *och1Δ*, with 24 µg/ml of mag 2 needed for complete visual growth inhibition. Peptide efficacy was noticeably reduced in the *pmr1Δ* and *mnn4Δ* mutants with MICs of 28 µg/ml and 32 µg/ml respectively. This shows a 1.5x increase in peptide needed to inhibit the growth of the *mnn4Δ* mutant.

When the cell wall mutants were exposed to rana they showed similar patterns to those observed with mag 2 and DsS3(1-16), with MICs ranging from 4 µg/ml to 24 µg/ml. The

CAI-4 control and *mnt1Δ-mnt2Δ* double deletion mutants had MICs of 12 μg/ml, whilst *mnt1Δ*, *mnt2Δ* and *och1Δ*, all had MICs of 14 μg/ml. *mnt3/mnt5Δ* growth was inhibited at 16 μg/ml. The lowest levels of susceptibility were displayed by *pmr1Δ* and *mnn4Δ*. Peptide action against *pmr1Δ* appears to be the least effective with a MIC of 22 μg/ml, almost double that of the wild type strain. The *mnn4Δ* mutant does not show the least susceptibility here, but the MIC of 18 μg/ml is still substantially higher than the parent strain.

Table 3.1. MIC determination for three AMPs (DsS3(1-16), mag 2 and rana) against CAI-4 (the parent *C. albicans* strain) and various cell wall mutants; n = 3, std. dev. in brackets. Representative plates are shown in Appendix II.

	MIC (mean μg/ml)		
	DsS3(1-16)	Magainin 2	Ranalexin
CAI-4 (Clp10)	5 (0.58)	22 (1.15)	12 (0)
mnt1Δ (Clp10)	6 (0.58)	22 (0)	14 (0)
mnt2Δ (Clp10)	5 (0)	24 (2)	14 (2.31)
mnt1-mnt2Δ (Clp10)	4 (0)	22 (2.31)	12 (1.15)
mnt3/mnt5Δ (Clp10)	7 (1.15)	24 (0)	16 (1.15)
pmr1Δ (Clp10)	11 (1)	28 (3.06)	22 (0)
och1Δ (Clp10)	7 (0.58)	24 (2.31)	14 (1.15)
mnn4Δ (Clp10)	14 (1.15)	32 (3.06)	18 (2.31)

Reintegration strains for each deletion were also tested against each peptide and displayed levels of peptide susceptibility equal to that of the CAI-4 parent strain.

3.2.2 Growth of cell wall mutants
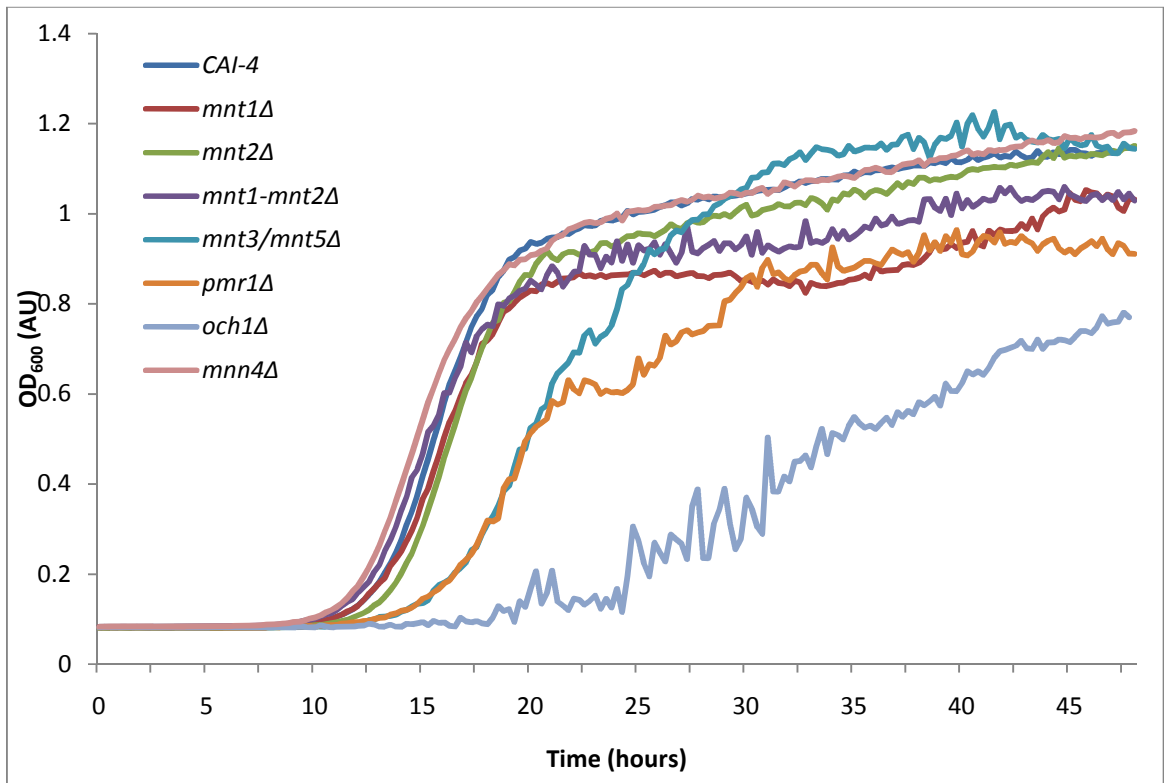
Figure 3.3. Growth of CAI-4 and all deletion strains. Graph displays the differences in population density between mutant strains; n = 2.

Growth of the parent and each mutant strain was monitored during 48 h (Figure 3.3). For the CAI-4 strain the lag phase lasted ~10 h followed by a period of exponential growth (11-18 h). Growth then slowed as the culture approached stationary phase. The final reading was taken at 48 h with an OD_{600} of 1.15. *mnt1Δ, mnt2Δ, mnt1-mnt2Δ* and *mnn4Δ* all grew similarly to the parent strain. The *pmr1Δ* and *mnt3/mnt5Δ* double deletion had a longer lag phase compared to CAI-4 and grew more slowly during exponential phase. Exponential phase lasted for approximately 12 h for *mnt3/mnt5Δ* and 9 h with the *pmr1Δ* strain. The *och1Δ* mutant had a long lag phase (~18 h) followed by slow growth and at 48 h the OD_{600} was 0.77 AU. The apparent erratic nature of the readings recorded, especially between 24 and 30 h incubation, was probably due to cell clumping, a commonly encountered phenotype in this strain (Bates *et al*, 2005).

3.2.3 Growth inhibition on exposure to peptide

The growth of the parent strain and each of the cell wall mutants was monitored in the presence of DsS3(1-16), mag 2 or rana.
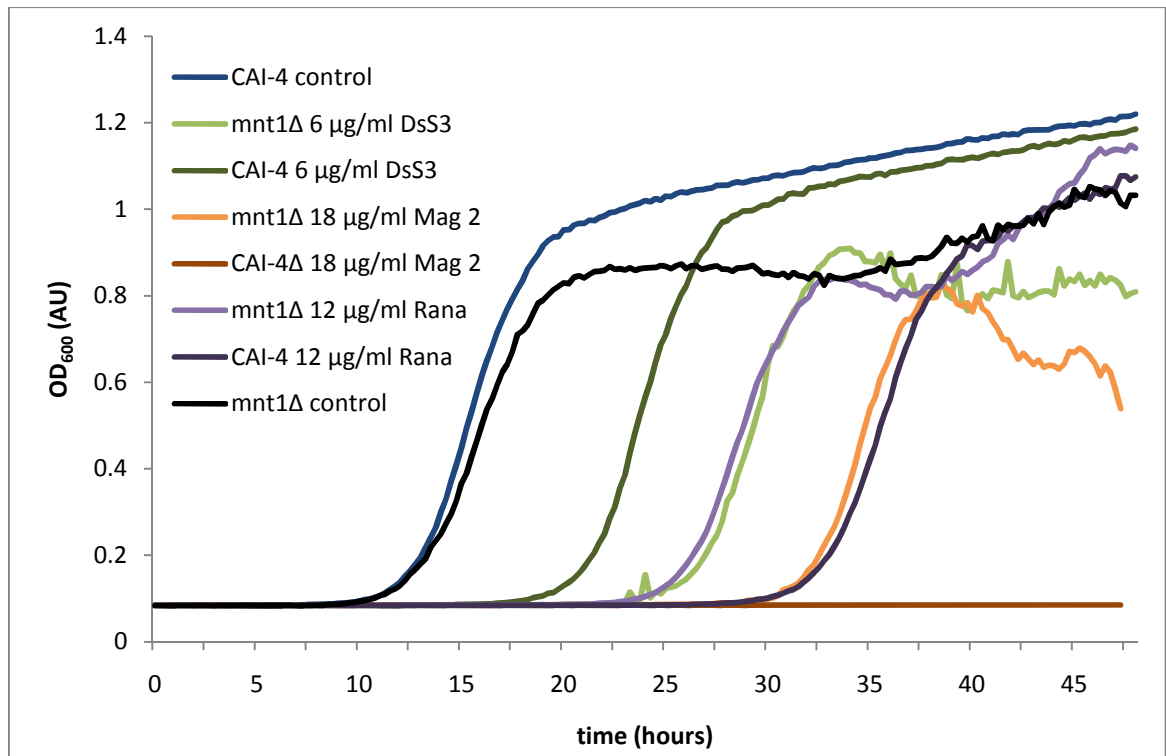
Figure 3.4. Growth of *mnt1Δ* and CAI-4 when exposed to DsS3(1-16), mag 2 or rana. Cell density was measured every 15 min over a 48 h period; n = 3.

mnt1Δ: With the addition of 6 µg/ml DsS3(1-16), both the *mnt1Δ* and CAI-4 showed initial inhibition then displayed similar levels of growth. *mnt1Δ* appeared to be slightly more inhibited. When 18 µg/ml of mag 2 was added, growth of the *mnt1Δ* strain was observed after an extended lag phase of 18 h while growth of the parent strain was completely inhibited. In the presence of 12 µg/ml rana, both strains displayed growth after initial inhibition. All *mnt1Δ* cultures recorded a drop in population density after exponential growth.
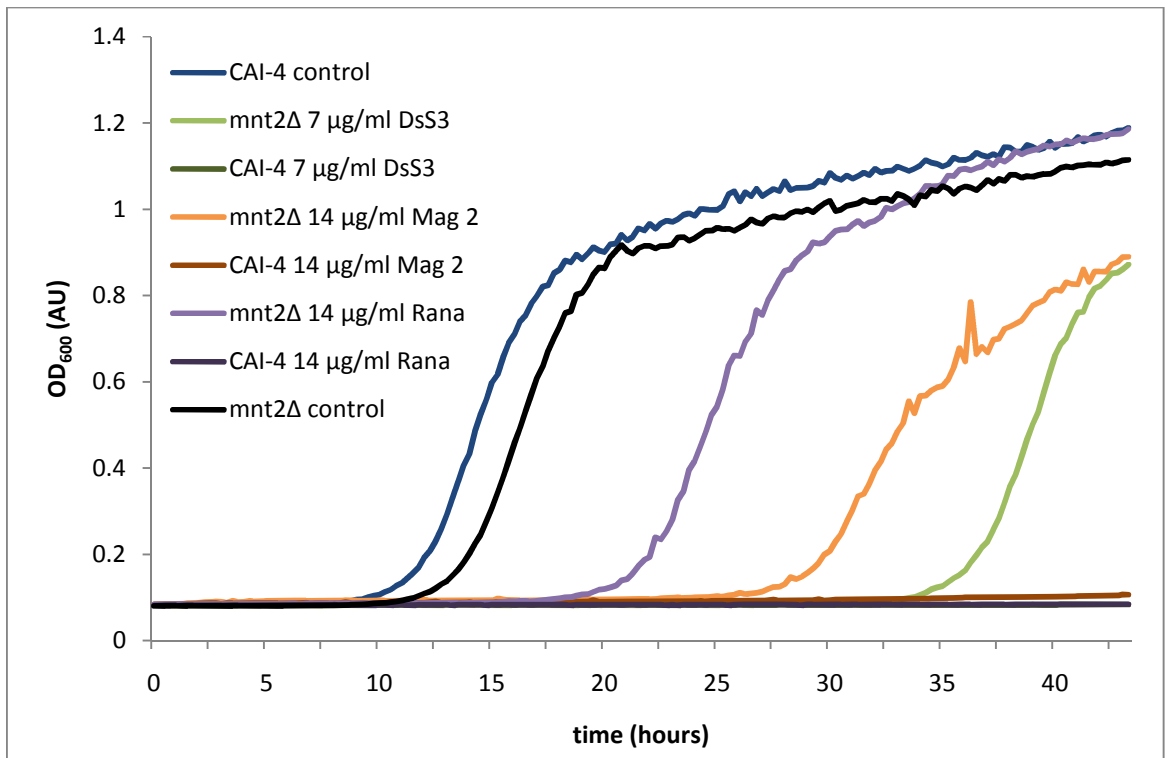
Figure 3.5. Growth of *mnt2Δ* and CAI-4 when exposed to DsS3(1-16), mag 2 or rana. Cell density was measured every 15 min over a 48 h period; n = 3.

mnt2Δ: At a concentration of 7 µg/ml DsS3(1-16) the *mnt2Δ* mutant showed growth after an extended lag phase lasting 34 h. CAI-4 displayed no growth at the same level indicating decreased susceptibility in the mutant strain. When 14 µg/ml mag 2 was present, similar results were obtained with *mnt2Δ* entering exponential growth, while CAI-4 displayed no change in population density. *mnt2Δ* was also less susceptible to rana displaying exponential growth with 14 µg/ml, while the parent strain did not grow at the same concentration.
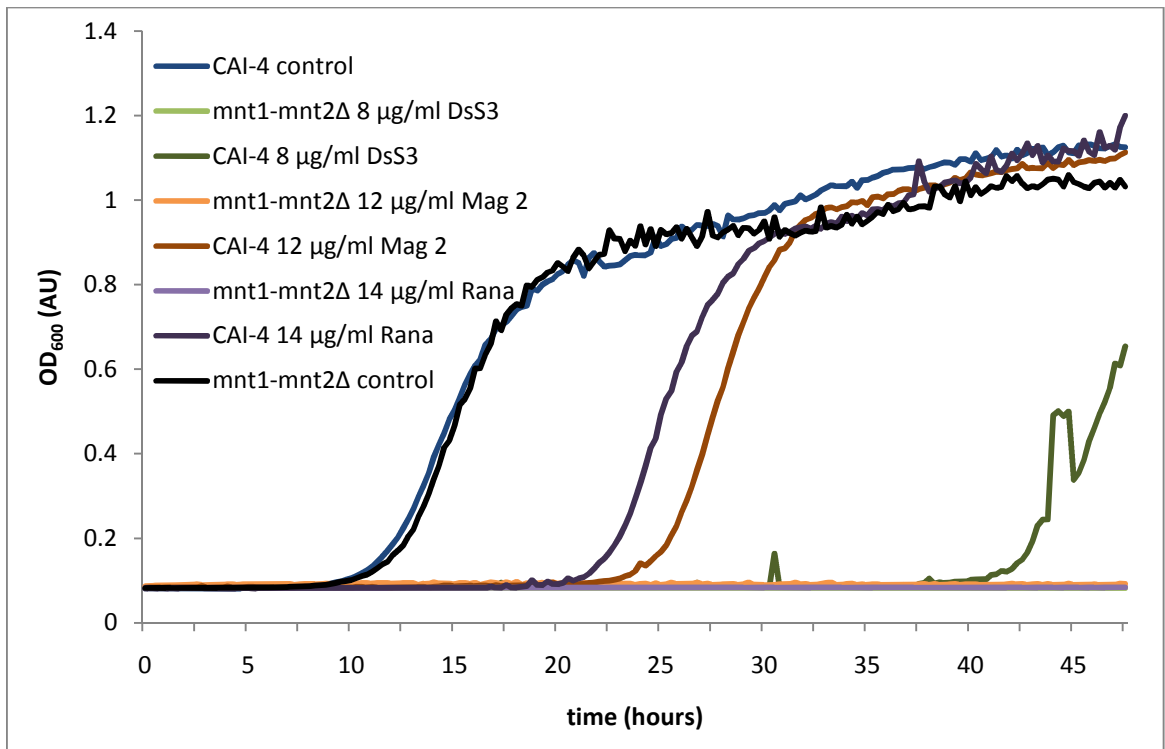
Figure 3.6. Growth of *mnt1-mnt2Δ* and CAI-4 when exposed to DsS3(1-16), mag 2 or rana. Cell density was measured every 15 min over a 48 h period; n = 3.

mnt1-mnt2Δ: With 8 µg/ml of DsS3(1-16) the double deletion showed significant growth inhibition, however, at the same concentration no CAI-4 growth was recorded. In the presence of mag 2 the *mnt1-mnt2Δ* strain displayed no growth at 12 µg/ml. The CAI-4 strain entered exponential growth at the same concentration. The presence of rana generated similar results, with growth of the parent strain but no *mnt1-mnt2Δ* growth. This data reaffirms the slight increase in sensitivity seen with this mutant. This mutant did show a reduction in CFU/ml compared to the parent strain that could account for the increased sensitivity (Table 2.6).
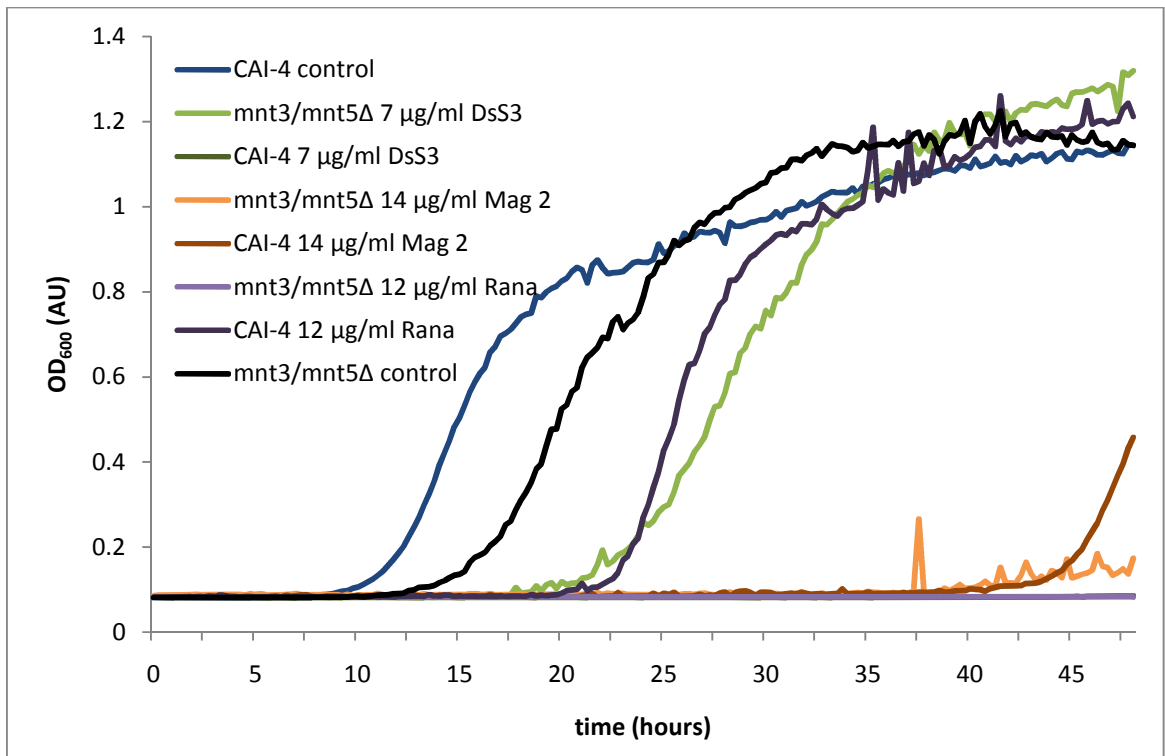
Figure 3.7. Growth of *mnt3/mnt5Δ* and CAI-4 when exposed to DsS3(1-16), mag 2 or rana. Cell density was measured every 15 min over a 48 h period; n = 3.

mnt3/mnt5Δ: With the addition of 7 μg/ml of DsS3(1-16) the parent strain did not grow, while the *mnt3/mnt5Δ* mutant was relatively unaffected with a slight increase in lag phase. At 14 μg/ml of mag 2, growth of *mnt3/mnt5Δ* was inhibited. Results were similar with the parent strain. When rana was present, the CAI-4 strain displayed less susceptibility, growing at 12 μg/ml while *mnt3/mnt5Δ* growth did not occur.
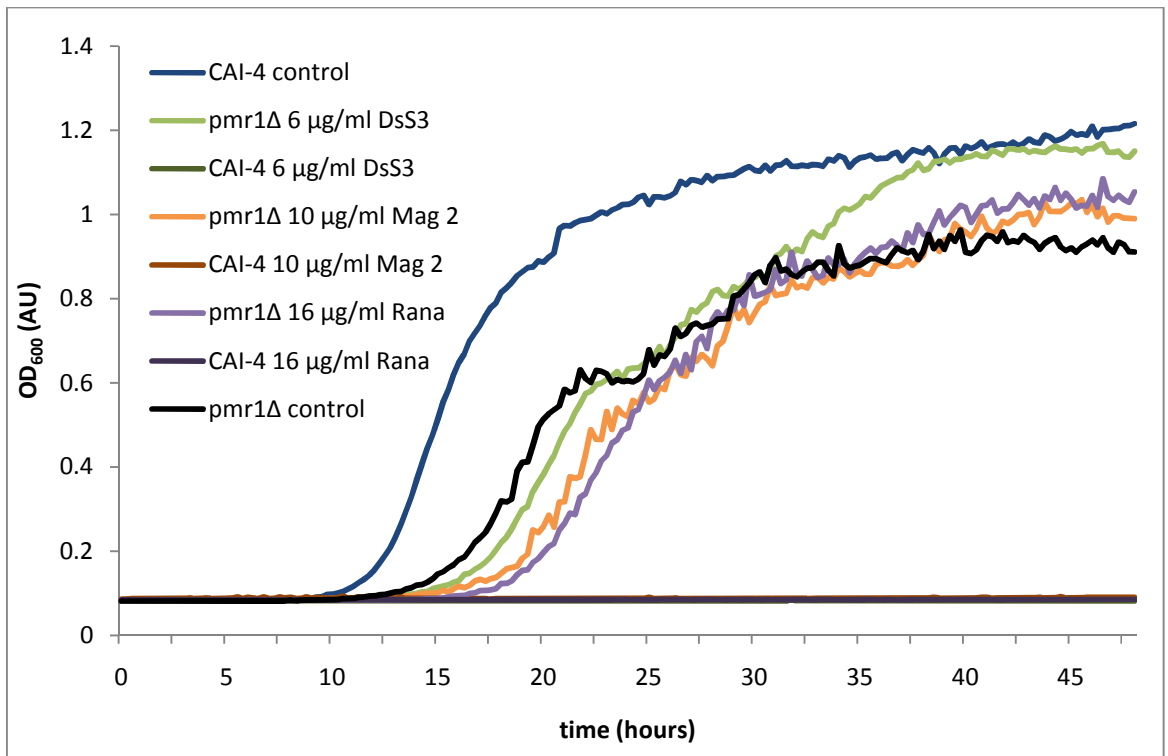
Figure 3.8. Growth of *pmr1Δ* and CAI-4 when exposed to DsS3(1-16), mag 2 or rana. Cell density was measured every 15 min over a 48 h period; n = 3.

pmr1Δ: The *pmr1Δ* growth curve data displayed decreased susceptibility to all three of the peptides. Concentrations that prevented growth in the parent strain did not inhibit growth of the deletion strain when compared to the growth observed with the *pmr1Δ* control.
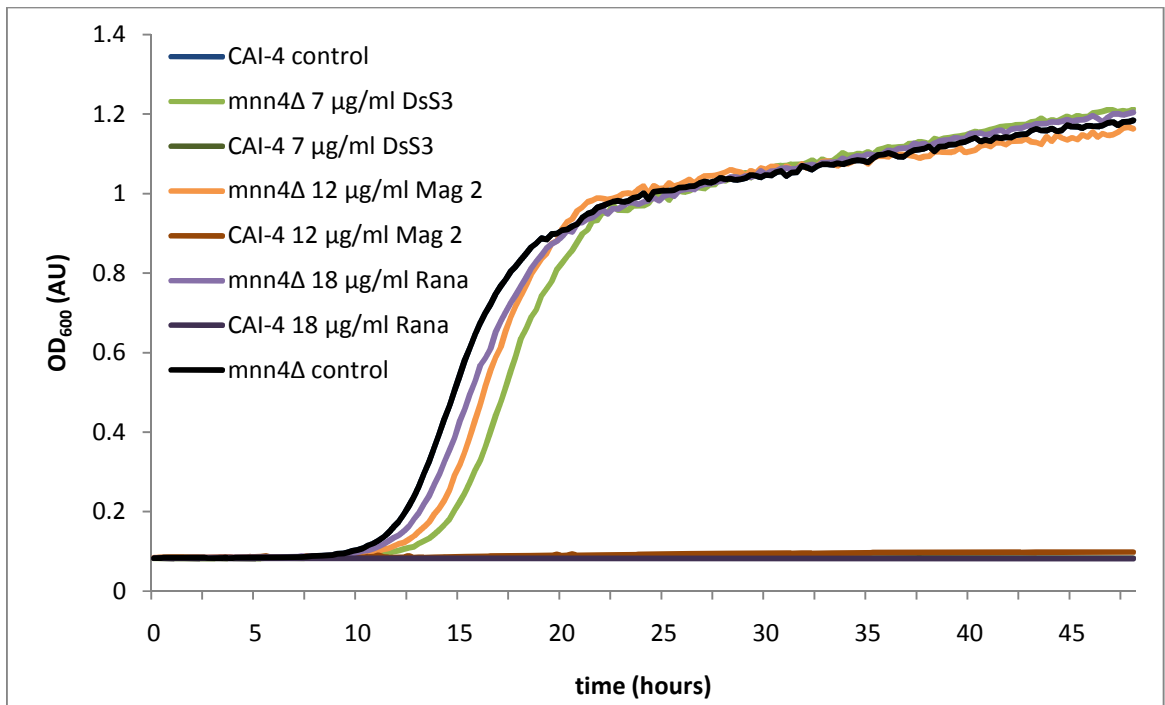
Figure 3.9. Growth of *mnn4Δ* and CAI-4 when exposed to DsS3(1-16), mag 2 or rana. Cell density was measured every 15 min over a 48 h period n = 3.

mnn4Δ: The *mnn4Δ* mutant displayed the least susceptibility to peptide action. With no growth recorded in the parent strain, these same concentrations have little effect on *mnn4Δ* growth, which closely mirrors that of the CAI-4 control.

It was not possible to gather data for *och1Δ* as the cell clumping phenotype was observed and this increased with increasing peptide concentration, thus interfering with the optical density readings.

3.2.4 Population viability using fluorescence microscopy

Fluorescence microscopy was employed to observe viability of the *C. albicans* cell wall mutants in the presence of increasing concentrations of DsS3(1-16). For all strains in the

absence of peptide, as expected, most cells (>97 %) were viable as they stained with CTG (Figure 3.10). As the concentration of Flu-DsS3(1-16) was increased to 5, 10 and 15 µg/ml, so the proportion of PI stained cells concomitantly increased e.g. for CAI-4 the proportion of PI fluorescent cells in the population increased from 0.2 % (no peptide) to 94.9 % (15 µg/ml peptide). Again, considerable differences in peptide efficacy were observed when comparing CAI-4 with the *pmr1Δ* and *mnn4Δ* mutants. For example, at 5 µg/ml, 50.8 % of the parent strain population was stained with PI compared to 3.8 % and 6.9 % PI stained cells in the *mnn4Δ* and *pmr1Δ* populations respectively. The *mnt1-mnt2Δ*, *och1Δ* and *mnt3/mnt5Δ* populations all displayed intermediate proportions of PI stained cells; less than the parent strain but greater than the *pmr1Δ/mnn4Δ* strains.
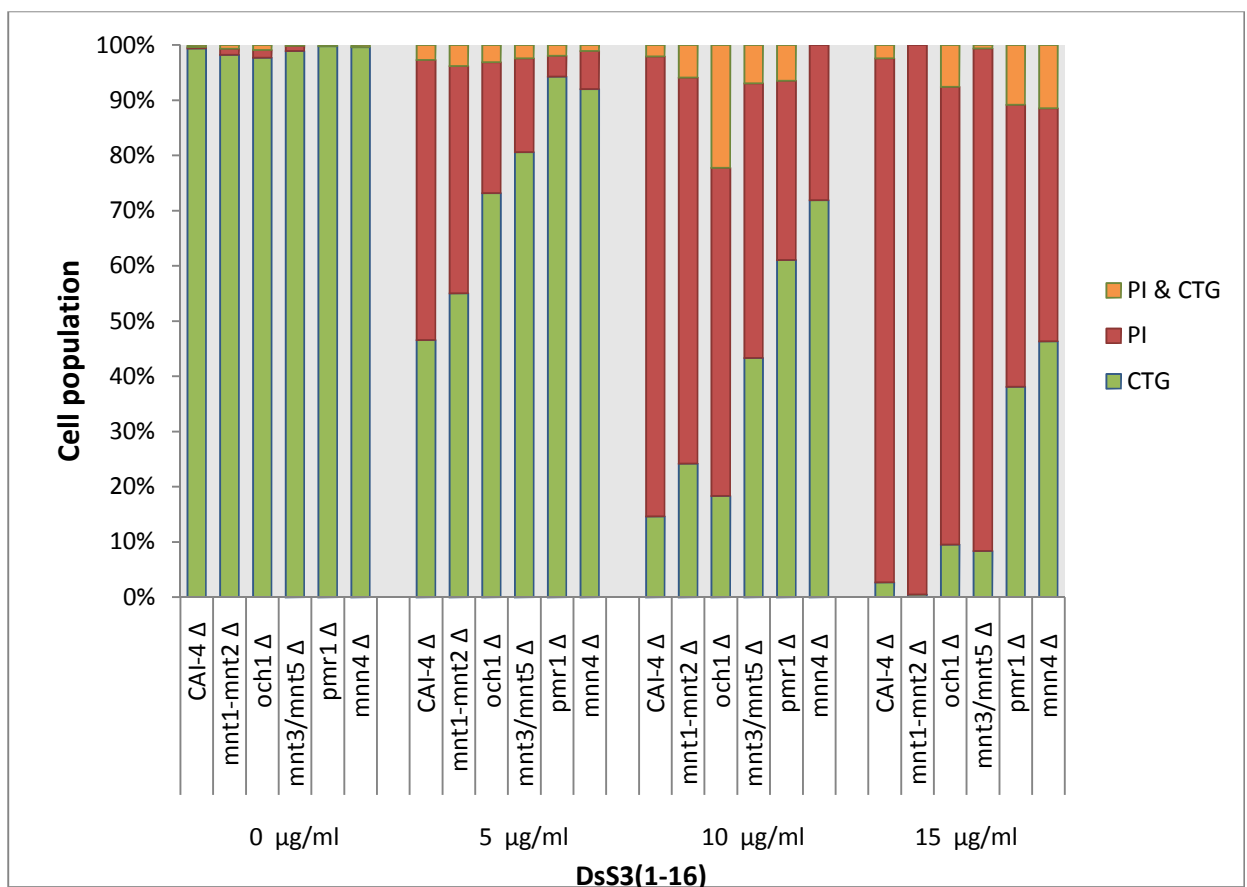
Figure 3.10. Percentage of each cell population fluorescing with CellTracker™ green, propidium iodide or dual staining when exposed to DsS3(1-16) . For each assay a minimum of 300 cells were counted and quantified into a percentage of the sampled population; n = 2.

Viability counts were performed simultaneously to confirm the microscope data (Figure 3.11). The *mnt1-mnt2Δ* double deletion showed similar viability to the parent strain, with both displaying a one log reduction in CFU/ml at 15 µg/ml peptide compared to the untreated control. *pmr1Δ*, *mnn4Δ* and *mnt3/mnt5Δ* were less susceptible to the peptide with only a 0.22 log reduction at 15 µg/ml. The colony count data corroborated the microscopy data in terms of the susceptibility of each strain to the peptide with the *pmr1Δ* and *mnn4Δ* strains displaying the smallest reduction in cell numbers and the highest proportion of metabolically active cells as demonstrated through CTG staining.
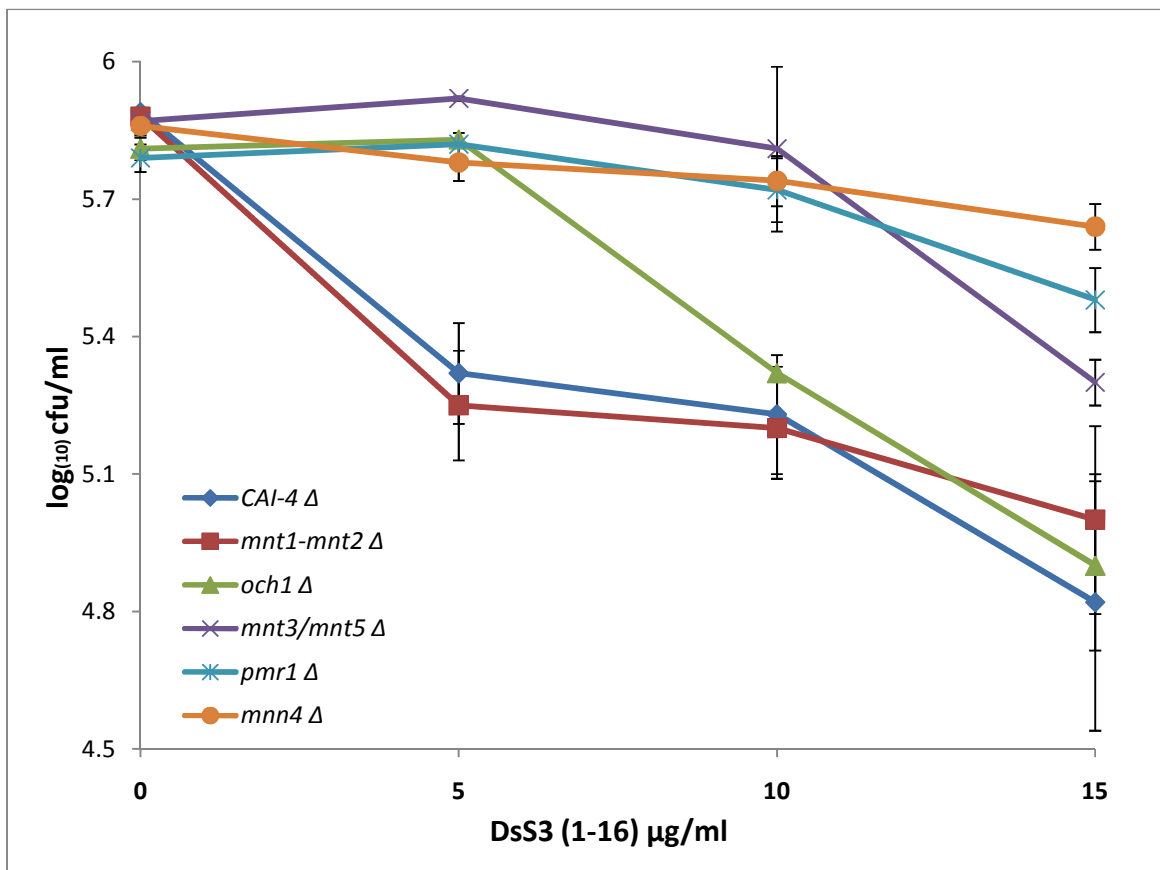
Figure 3.11. Cell viability count after exposure to DsS3(1-16). The results are plotted as colony forming units (CFU) per ml in log scale; n = 2 ± 1 SD.

3.2.5 Flu-DsS3(1-16) sequestration

To further understand the phenotypes recorded with the glycosylation mutants, an assay was designed to measure the sequestration of Flu-DsS3(1-16) by yeast cells. The MIC of Flu-DsS3(1-16) against CAI-4 was 30 μg/ml which was higher than the untagged peptide (MIC 5 μg/ml) (Appendix III). The cell wall mutants that expressed the greatest variation in peptide susceptibility (*mnt3/mnt5Δ*, *och1Δ*, *pmr1Δ*, *mnn4Δ*) were incubated in the presence of Flu-DsS3(1-16) (5 , 10 , 15 and 20 μg/ml), separated from the media and the fluorescence of the supernatant was measured.

Results show that as peptide concentration increased, the total mass of peptide sequestered decreased (Figure 3.12). With 5 μg/ml, cells of the parent strain sequestered 83.2% of available peptide. At 20 μg/ml the same strain bound 49.2% of the Flu-DsS3(1-16). There were also noteworthy strain differences: CAI-4 sequestered the greatest percentage of peptide (83.2 %) followed by *mnt3/mnt5Δ* (66.6 %), *och1Δ* (64.4 %), *pmr1Δ* (57.8 %) and lastly *mnn4Δ* (46 %). Differences were most apparent between CAI-4 and the *mnn4Δ* mutant e.g. at 5 μg/ml, CAI-4 was responsible for removing 83.2% of Flu-DsS3(1-16), whereas *mnn4Δ* cells removed 46%. This data set correlates with the previous studies on visible growth inhibition, microscope fluorescence levels and CFU counts showing the lowest levels of peptide susceptibility in *mnn4Δ*, followed by *pmr1Δ*, *mnt3/mnt5Δ*, *och1Δ* and lastly the *mnt1Δ* and *mnt2Δ* mutants.
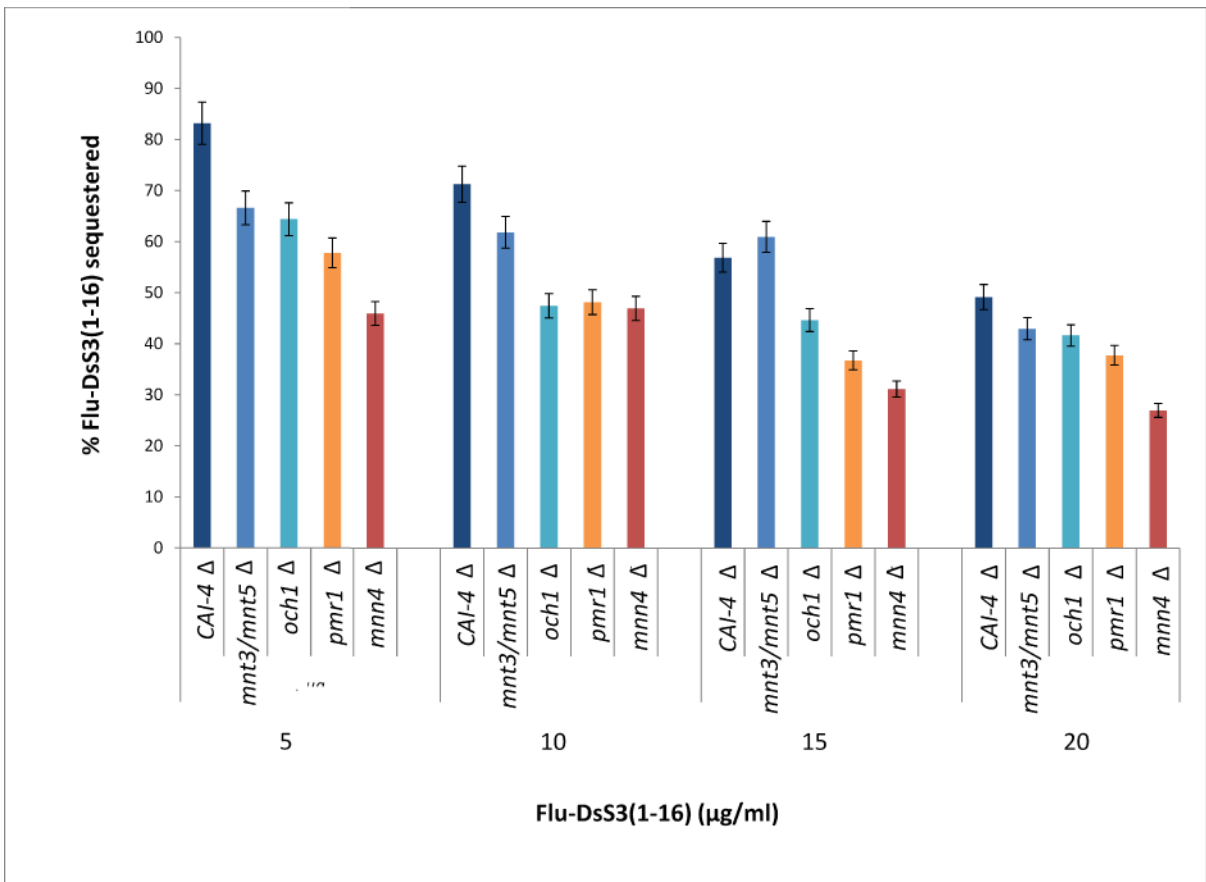
Figure 3.12. Cell wall mutant Flu-DsS3(1-16) sequestration. Flu-DsS3(1-16) was added at 5, 10, 15 or 20 µg/ml to an equal number of cells from each deletion strain (with the exception of *mnt1Δ* and *mnt2Δ*). Fluorescent intensity of the media was measured. From this, the percentage of Flu-DsS3(1-16) sequestered by each cell population was calculated and plotted; n = 3 mean ± 2 SD.

3.2.6 Peptide action in the presence of exogenous phosphate

Regarding previous data, it appears that in the mutants whose walls are deficient in phosphomannan, namely *pmr1Δ* and *mnn4Δ*, show decreased susceptibility towards DsS3(1-16), mag 2 and rana. Thus, it could be postulated that, in order for cationic antimicrobial peptides to exert their full effect, it is important that they bind to the negatively-charged phosphomannan component of the cell wall. Therefore, the effect of adding exogenous phosphate (that could compete with phosphate on the cell wall) on the action of DsS3(1-16) was determined against CAI-4, *pmr1Δ* and *mnn4Δ*. Glucosamine

6-phosphate (G-6-P) was selected as a phosphate source, with glucosamine hydrochloride (GHCl) as a negative control. Glucosamine itself is an abundant monosaccharide that functions as a precursor for the production of chitin and was considered a suitable molecule from which to study the effects of attached phosphate on peptide action.

Plate reader assays monitored growth of the CAI-4 strain in the presence or absence of GHCl or G-6-P (Figure 3.13). The GHCl incubated cultures had a reduced exponential growth rate (doubling time = 120 min) compared to the control (doubling time = 105 min), however, the population density after 48 h was similar (OD_{600} = 1.3 in the GHCl, OD_{600} = ~1.24 in the control). G-6-P treated cultures had a reduced OD_{600} of ~0.85 compared to the control at ~0.97 after 48 h. The subsequent stationary phase displayed reduced growth compared to the control. The G-6-P cultures finished with an OD_{600} of 0.99 AU.
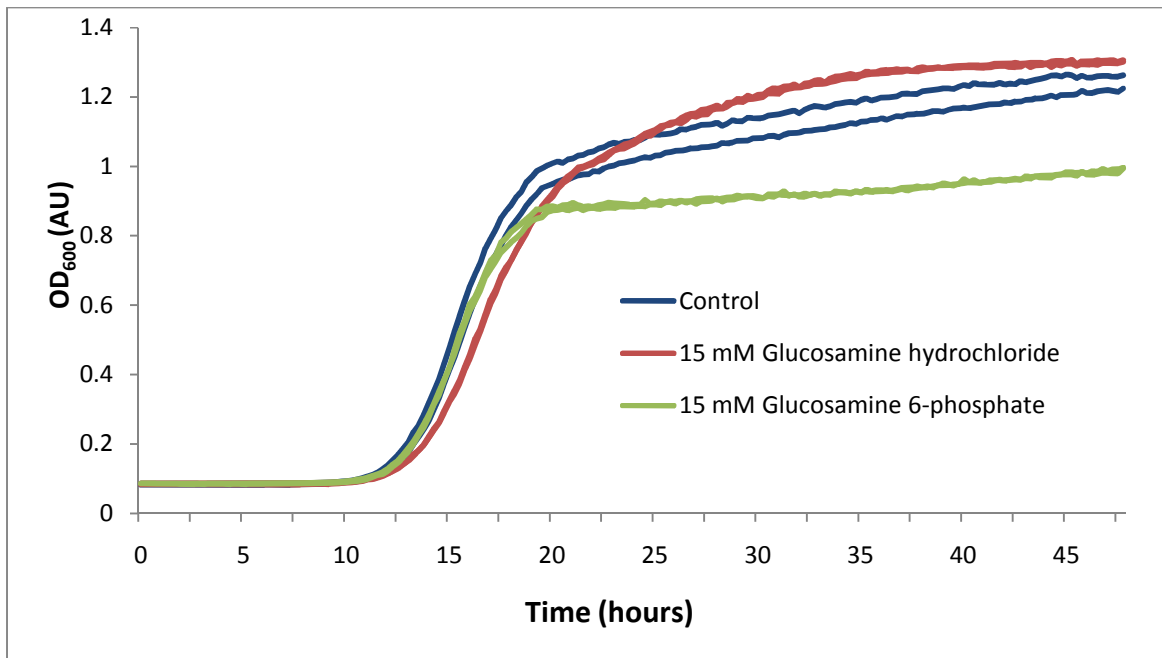
Figure 3.13. Growth of CAI-4 with and without the presence of 15 mM Glucosamine hydrochloride or 15 mM Glucosamine 6-phosphate. Readings were taken every 15 min for 48 h. The experiment was carried out in duplicate and both versions are plotted above.

CAI-4 growth was monitored in the presence of absence of GHCl and G-6-P in media containing 6 or 9 µg/ml of DsS3(1-16) (Figure 3.14). The addition of 6 µg/ml of peptide, prevented growth in the GHCl and control cultures. Growth of the G-6-P treated cultures was inhibited with an increased lag phase. The initial growth readings were erratic suggesting possible clumping of the cells. With the addition of 9 µg/ml DsS3(1-16), the lag phase was extended to 19 h suggesting inhibition. Growth inhibition by DsS3(1-16) was diminished in the presence of G-6-P.
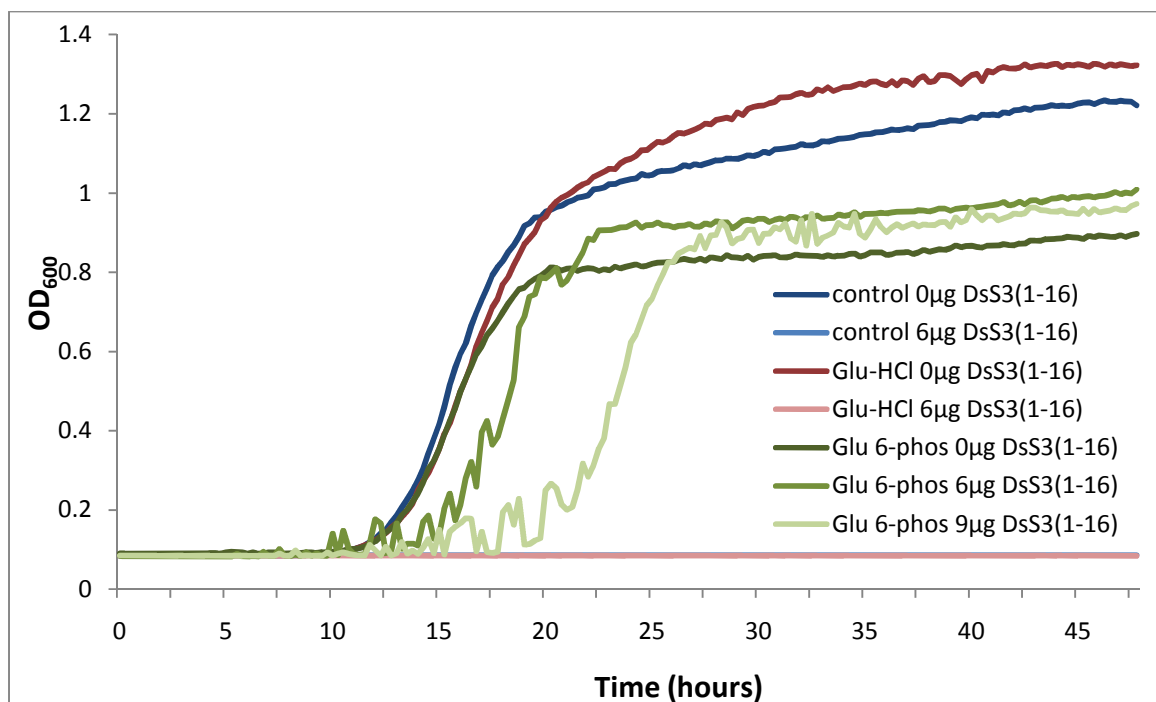
Figure 3.14. Growth of CAI-4 with and without the presence of 15 mM Glucosamine hydrochloride or 15 mM Glucosamine 6-phosphate and DsS3(1-16). Readings were taken every 15 min over 48h.

The glycosylation mutants were cultured with 5, 10 or 15 mM of either G-6-P or GHCl and incubated in the presence of increasing concentrations of DsS3(1-16) (Table 3.2, plate scans in Appendix II). GHCl had a slight effect on peptide action in the CAI-4 and *pmr1Δ* strains, increasing the MIC by 1 µg/ml and 2 µg/ml respectively. Greatest variation was observed in the G-6-P treated media and as the G-6-P concentration increased, the peptide activity reduced. This trend was apparent in the three strains tested. For CAI-4 and *pmr1Δ* approximately twice the concentration of peptide was needed to prevent visible growth at 15 mM G-6-P when compared to the negative control. Notably, this may be even higher for CAI-4 as there was visible growth at the greatest peptide concentration (13 µg/ml). *mnn4Δ* also displayed reduced growth inhibition with the MIC increasing from 16 µg/ml in the GHCl media to 22 µg/ml in the presence of G-6-P.

Table 3.2. MIC determination for CAI-4, *pmr1Δ and mnn4Δ* strains. Wells contained increasing concentrations of DsS3(1-16) with 5, 10 or 15 mM of either Glucosamine hydrochloride or Glucosamine 6-phosphate; n = 3, ± 1 SD in brackets.

		MIC (mean µg/ml)		
		CAI-4	*pmr1Δ*	*mnn4Δ*
control	0	6 (0.82)	10 (1.47)	16 (1.60)
Glucosamine hydrochloride (mM)	5	7 (0)	12 (0.82)	16 (0.41)
	10	7 (0)	12 (1.10)	16 (0)
	15	7 (0.84)	12 (0.75)	16 (2.35)
Glucosamine 6-phosphate (mM)	5	8 (1.17)	14 (1.75)	18 (2.34)
	10	10 (1.86)	18 (3.67)	18 (2.23)
	15	>13 (0)	22 (2.31)	22 (2.31)

For each strain, viability cell counts were also performed in the presence of GHCl or G-6-P with various concentrations of DsS3(1-16). G-6-P treated cells were less susceptible to the killing effects of DsS3(1-16) (Figure 3.15) e.g. 30 min after CAI-4 was exposed to 20 µl DsS3(1-16) there was a 0.3 log reduction in viable count for the control compared to a 0.4 log reduction in the G-6-P treatment. For the *pmr1Δ*, at 60 min there was a 0.4 log reduction in viable cell count and after 90 min the *mnn4Δ* viable count reduced by 0.86 log. The three strains tested show a clear reduction in viable cell number in the control cultures when compared to the G-6-P treatment.
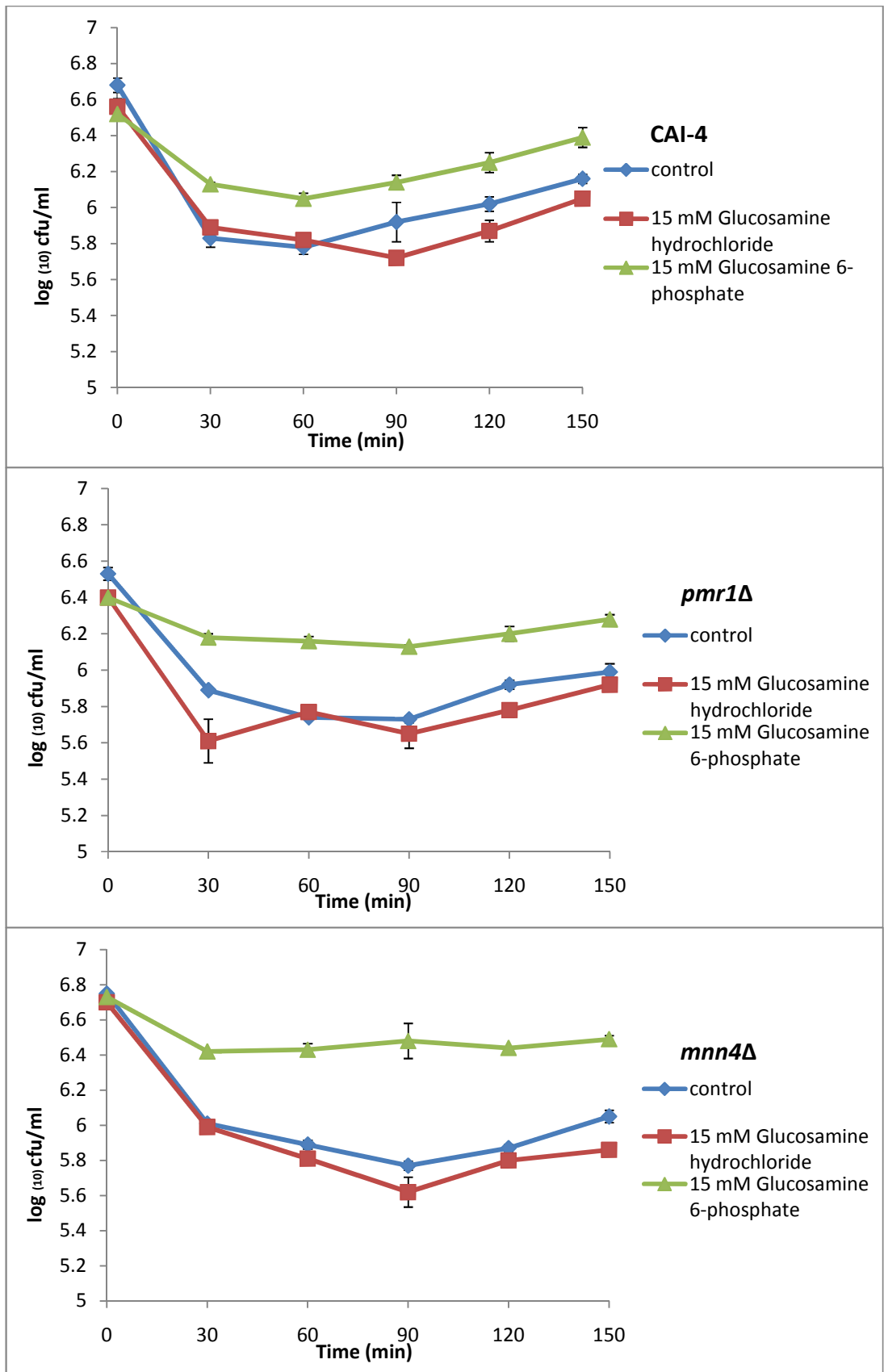
Figure 3.15. Peptide action against CAI-4, *pmr1Δ* and *mnn4Δ* strains with exogenous phosphate. Initial readings were taken prior to DsS3(1-16) addition. To CAI-4, 20 µg/ml DsS3(1-16) was added, 30 µg/ml was added to *pmr1Δ* and 40 µg/ml was added to *mnn4Δ* cultures. Three assays were performed for each strain; the first with peptide only, the second with peptide and 15 mM Glucosamine hydrochloride and the third with peptide and 15 mM Glucosamine 6-phosphate; n = 3 mean ± 2 SD.

3.2.7 Visualisation and quantification of Flu-DsS3(1-16) with CAI-4, *pmr1Δ* and *mnn4Δ*.

Flu-DsS3(1-16) uptake by CAI-4, *pmr1Δ* and *mnn4Δ* cultures was observed with a DeltaVision microscope. Three distinct phases of peptide interaction with *C. albicans* cells were observed. First the peptide was taken up into vacuoles, as confirmed by the presence of the vacuolar stain CellTracker™ Blue (Figure 3.16-A). Next the peptide localised throughout the cytosol (Figure 3.16-B). Finally the peptide appeared to be bound to the cell surface though this was observed infrequently and so was not quantified in the following assays (Figure 3.16-C).
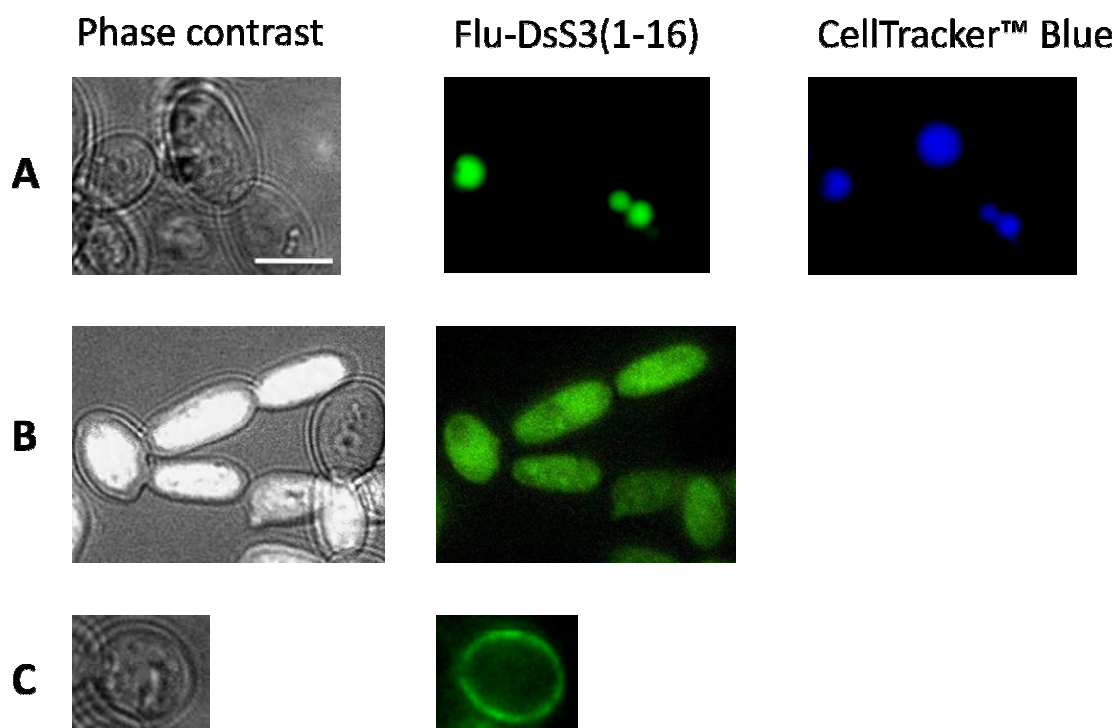
Figure 3.16. Differential peptide localisation using fluorescent microscopy. Cells captured are of the parent strain, CAI-4, and show peptide localisation after incubation with 20 μg/ml Flu-DsS3(1-16); scale bar = 5 μM. Row A shows DsS3(1-16) internalised in the vacuole, as confirmed by the presence of CellTracker™ Blue (CTB). Row B shows Flu-DsS3(1-16) occupying the cytosol. Row C shows a cell that has bound peptide around the periphery of the cell. This may be bound to the cell wall and/or membrane.

Cells from each strain treated with GHCl or G-6-P were grouped into those that showed no fluorescence, those with vacuolar fluorescence, and those with whole cell cytosolic fluorescence (Figure 3.17). The majority of cells in all assays showed no fluorescence, with the highest proportion of vacuolar/whole cell fluorescence at 46.4 % in the CAI-4 strain and lower proportions of 14 % in *pmr1Δ* and 19.1 % in *mnn4Δ*. With the addition of G-6-P, total fluorescence decreased in CAI-4, *mnn4Δ* and *pmr1Δ* by 26.8 %, 14.5 % and 11.9 % respectively. Again, the addition of G-6-P had a negative effect on peptide efficacy. However, the GHCl also appears to have affected Flu-DsS3(1-16) action e.g. there was a 0.6 % difference between GHCl and G-6-P treatments with *mnn4Δ*. In all strains, the proportion of cells displaying whole cell fluorescence dropped on exposure to G-6-P (1 - 2 %) and similar decreases were observed in vacuolar staining with *mnn4Δ* (11.9% - 4.3 %) and *pmr1Δ* (5.7 % - 2 %). Vacuolar staining in CAI-4 remained at similar levels through the treatments.
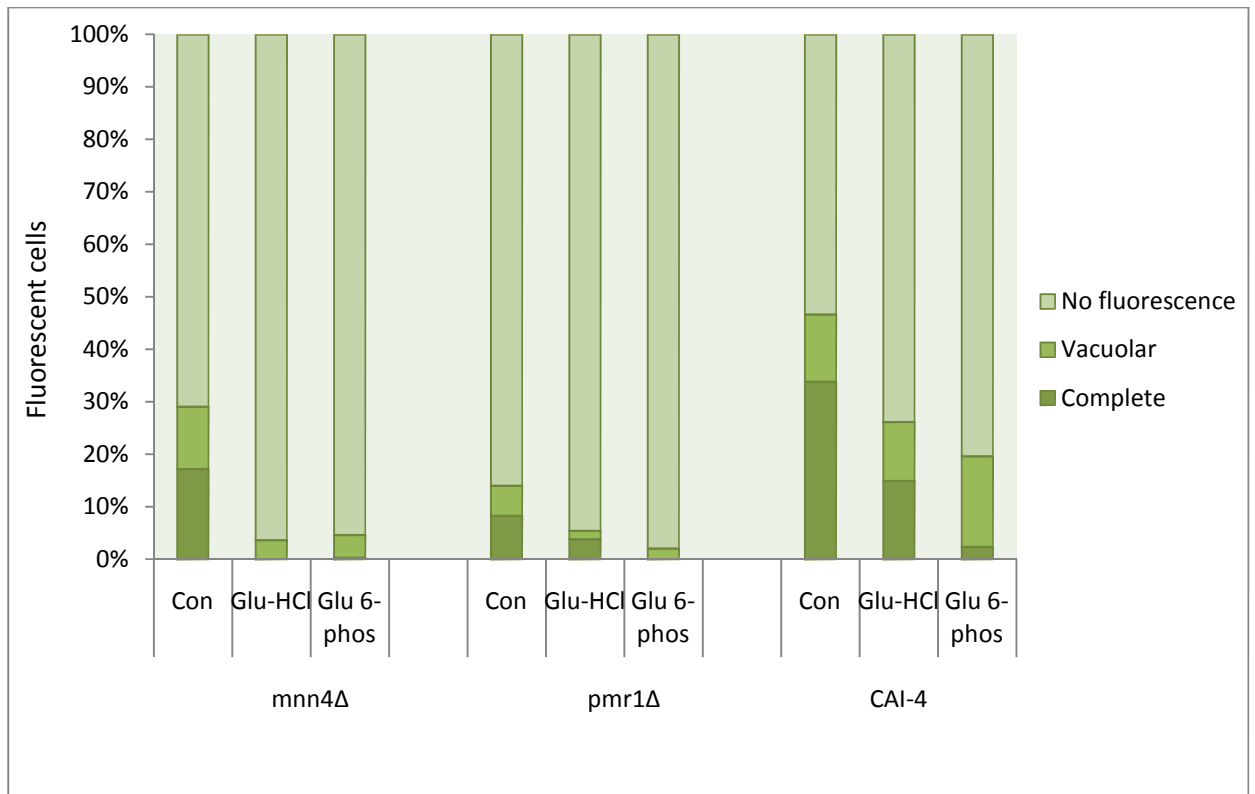
Figure 3.17. Percentage of cell population showing no fluorescence, vacuolar fluorescence or cytoplasmic fluorescence after DsS3(1-16) treatment. Cells from *mnn4Δ*, *pmr1Δ* or the parent CAI-4 were incubated with 20 µg/ml Flu-DsS3(1-16) and 15 mM Glucosamine hydrochloride or 15 mM Glucosamine 6-phosphate. A minimum of 200 cells (generally ~300) from each assay were quantified to give the final result; n = 2.

With CAI-4, in the presence of peptide only, the majority of cells displaying peptide staining had cytosolic Flu-DsS3(1-16) localisation. However in the presence of GHCl there was a mixture of both complete and cytosolic fluorescence, while the cells in the G-6-P treated culture only showed vacuolar fluorescence (Figure 3.18).
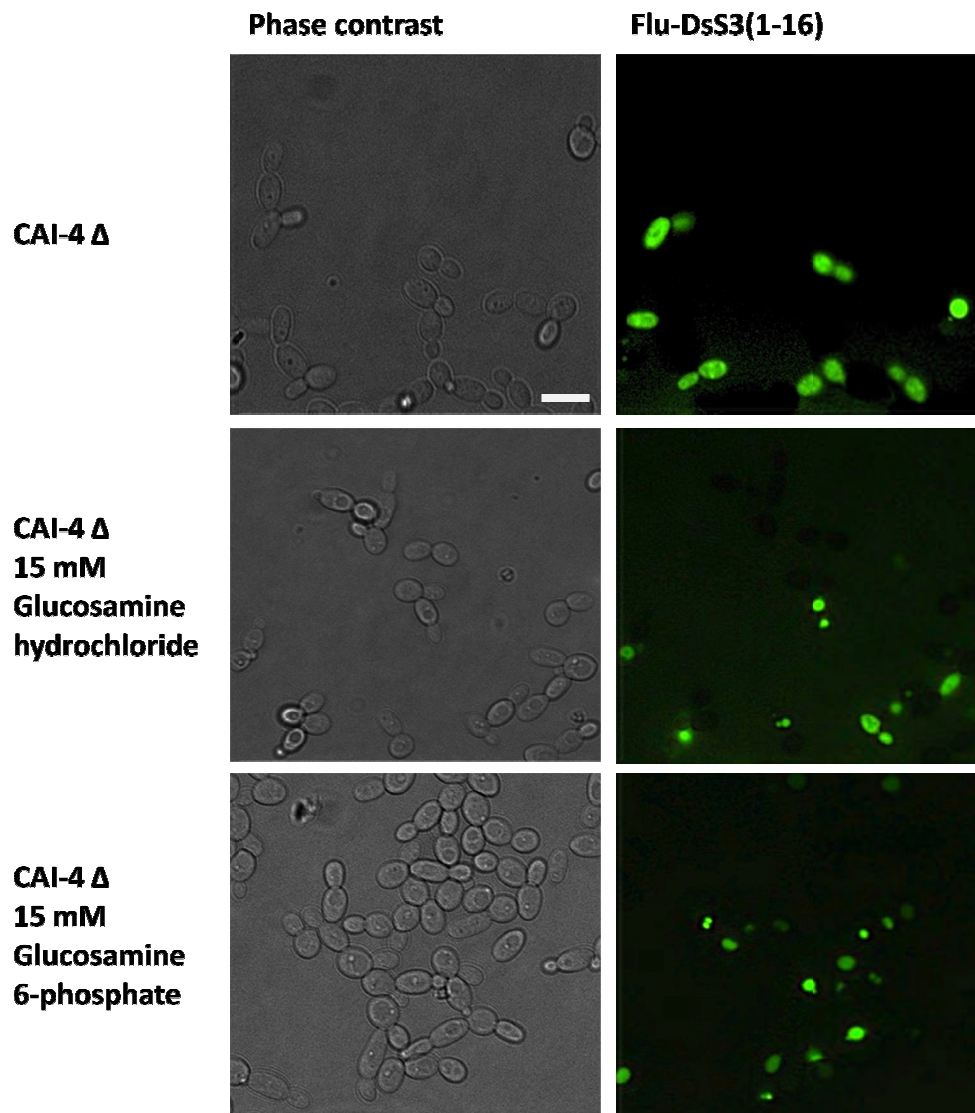
Figure 3.18. Image series representative of the changing Flu-DsS3(1-16) localisation in CAI-4 with 15 mM glucosamine hydrochloride or 15 mM glucosamine 6-phosphate; scale bar = 10 µM.

3.3. Discussion

C. albicans cell wall mutants were variably susceptible to the action of three cationic AMPs; DsS3(1-16), mag 2 and rana. Visual growth, viability assays and microscope observations showed that the *mnn4Δ* and *prm1Δ* mutants were less susceptible to peptide action. *pmr1Δ* is defective in up to 80 % of mannose content and lacks the phosphomannan fraction while *mnn4Δ* is also phosphomannan deficient (Bates *et al*, 2005; Hobson *et al*, 2004). These data indicate that decreased peptide susceptibility is conferred with a reduction in the cell wall phosphate content. It is likely that to exert their full antimicrobial potential, cationic AMPs must first bind to negatively charged phosphate on the cell wall. This is supported by Alcian blue binding affinity in these mutants. With this cationic dye, loss of negatively charged phosphomannan is directly comparable to the extent of Alcian blue binding. Mannosylphosphate loss correlates with a decrease in dye binding (Friis *et al*, 1970). Several studies have quantified the mutants ability to bind this cationic dye and its link to loss of cell wall negative charge: when compared to the parent strain, the *mnt1-mnt2Δ* mutant displayed a 10% reduction in binding (Mora-Montes and Gow, unpublished results), *mnt3/mnt5Δ* displayed 50% reduced binding (Mora-Montes and Gow, unpublished results), *och1Δ* displayed 83% reduced binding (Netea *et al*, 2006), *pmr1Δ* displayed 95% reduced binding and lastly, the *mnn4Δ* strain lacked any ability to bind Alcian blue (Bates *et al*, 2005).

The extent of Alcian blue binding correlates with the degree of peptide susceptibility found in these mutants. As *och1Δ* displays a significant reduction in binding, it would be expected that this would show lower levels of susceptibility than *mnt3/mnt5Δ*, however,

results are fairly similar when comparing both, especially in terms of MIC values perhaps in part due to the slow growth of *och1Δ*. The *mnn4Δ* mutant displayed the least susceptibility to peptide, lower than *pmr1Δ* levels even with the extensive loss of mannan in this mutant. However, *pmr1Δ* still retains a small proportion of phosphomannan that may account for this while *mnn4Δ* has no detectable levels of phosphomannan. The phosphomannan fraction of the cell wall is acid-labile and composed of a chain of 1,2-β mannose residues. These are attached to 1,2-α mannan chains by phosphodiester linkages. It is reduction in these negatively charged residues that confers decreased susceptibility, presumably through reduced peptide binding affinity.

The ability of the *mnn4Δ* mutant to bind Alcian blue would suggest that the wall was completely devoid of phosphate. This however may not be the case: in a separate study, detectable levels were found when mannan was purified from this deletion strain (Singleton *et al*, 2005). Similar results were gathered when studying the *MNN4* ortholog in *S. cerevisiae* (Friis *et al*, 1970) where it was speculated that phosphate was still present in the cell wall but in deeper, less exposed areas. These are likely to be inaccessible to Alcian blue and possibly attached to N-linked glycans in the core portion of the cell wall (Odani *et al*, 1996) or may be from other sources such as the phospholipomannan fraction thought to play a role in cell wall adhesion (Dalle *et al*, 2003). This would perhaps explain the continued action of AMPs on this mutant as a fraction of the phosphate content is still present in less exposed areas of the cell wall

that may facilitate peptide binding, especially in truncated peptides such as DsS3(1-16) with its relatively small 16 a.a. composition.

The severe reduction in the mannan levels of *pmr1Δ* reduces cell wall thickness in this strain (Figure 3.19) (Netea *et al*, 2006). It was expected that the cells with thinner cell walls would show increased susceptibility to peptide action due to increased membrane accessibility allowing greater accumulation of peptide; however, this is not the case. The parent strain CAI-4 has a wall thickness of approximately 140 nm, *mnn4Δ* has a similar thickness of 135 nm, while *pmr1Δ* is greatly reduced at only 65 nm. The severe wall disruption in *pmr1Δ* causes increased sensitivity to known cell wall perturbing agents such as Calcofluor White and Congo Red (Bates *et al*, 2006). The *och1Δ*, *mnt1-mnt2Δ* and *mnt3/mnt5Δ* strains also show this increase indicating all are more sensitive to cell wall stress (Bates *et al*, 2005; Munro *et al*, 2005; Mora-Montes and Gow, unpublished data). Conversely, *mnn4Δ* displays no such decrease in cell wall integrity (Hobson *et al*, 2004). Even with *mnn4Δ* and *pmr1Δ* displaying similar levels of peptide susceptibility, in terms of cell wall integrity and thickness, there seems to be no correlation between this and the decreased peptide susceptibility found in both mutants. This data indicates that changes to cell wall integrity and thickness caused by glycosylation defects do not seem to affect the action of DsS3(1-16) in *C. albicans*.
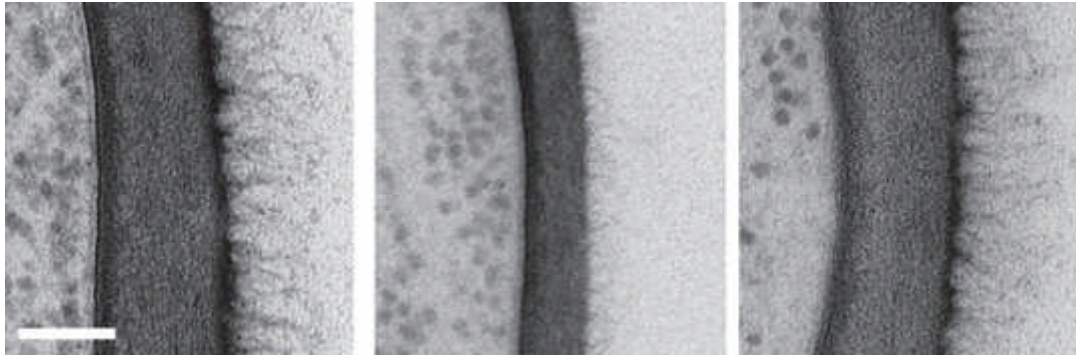
Figure 3.19. TEM micrographs of cell wall morphology of, from left to right, CAI-4, *pmr1Δ* and *mnn4Δ* showing changes in cell wall thickness (Netea *et al*, 2006). Bar represents 100 nm.

Several other studies have reported binding of antimicrobial compounds to the phosphomannan component of the yeast cell wall (Ibeas *et al*, 2000; Monk *et al*, 2005). A decrease in the cationic protein osmotin resulted when *MNN4* was disrupted while disruption of *MNN6* also conferred similar levels of susceptibility. *MNN4* and *MNN6* are both directly implicated in the transfer of mannosylphosphate to N- and O-linked glycans in *S. cerevisiae* (Odani *et al*, 1996). Only 10 % of normal phosphate levels are retained in these mutants. These mutants again showed greatly reduced Alcian blue binding.

In the fluorescent microscopy study, there was a percentage of cells in each population that displayed both CTG and PI staining. This was surprising as these markers are designed to label very different cell states. PI is a measure of membrane integrity, entering cells whose membranes have been compromised and binding to DNA and RNA, so staining non-viable cells. CTG freely permeabilises through the membrane of viable cells, is cleaved by esterases, and subsequently fluoresces. The dual staining may be explained by initial fluorescence from the CTG in metabolically active cells followed by increasing peptide action that leads to loss of viability and resulting PI staining prior to

microscope image acquisition. The double staining may also have occurred in cells with CTG staining that, as a result of peptide action, have destabilised membranes allowing moderate entry of PI into the cell while still remaining viable. This increased membrane permeability to PI has been documented in other studies on exposure to the cationic AMP Histatin-5: at 1 µM Histatin-5, ~27 % of *C. albicans* cells were labelled with PI while only ~9 % were non-viable (Helmerhorst[a] *et al*, 1999). This indicates that viable cells are internalising PI due to an increase in membrane porosity.

Images acquired during the examination of Flu-DsS3(1-16) and its interaction with *Candida* cells show three distinct patterns of localisation. Firstly, peptide was observed binding round the periphery of the cell, possibly causing phospholipid disruption (Shai, 2001). This was only observed on a few occasions possibly due to the transient nature of this stage. If image acquisition was possible directly after peptide exposure it is likely that a greater proportion of the population would have displayed this binding. It is probable that this phase leads to the other phase observed, where peptide was observed uniformly throughout the cytoplasm. This peptide translocation may also lead to intracellular targeting, resulting in programmed cell death possibly via DNA damage (Morton[a] *et al*, 2007). When peptide binding is not so prolific, it is proposed that peptide is sequestered from the plasma membrane into the vacuole via endocytosis; this could be an effective means of quarantining toxic peptide from the cytosol preventing DNA damage. Indeed, it has been demonstrated that genes involved in vacuolar transport are vital for decreasing susceptibility to DsS3(1-16) (Morton[a] *et al*, 2007). A study using Histatin-5, also an α-helical cationic peptide, found similar distinct vacuolar and

cytoplasmic populations (Mochon *et al*, 2008). The increase in MIC observed when fluorescein is attached to the peptide (5 μg/ml untagged, 30 μg/ml tagged), could be due to fluorescein interfering with peptide binding affinity. As the mode of action of DsS3(1-16) is proposed to resemble the carpet model (Netea *et al*, 2006), the overall clustering of peptide may be reduced. If the monomers cannot cluster sufficiently, this would affect the extent of membrane destabilisation causing a reduction in antimicrobial efficacy.

At lower concentrations of Flu-DsS3(1-16), and indeed in the presence of G-6-P, the proportion of the population showing vacuolar localisation was increased while those displaying cytoplasmic localisation were diminished. Conversely, at higher peptide concentrations or in the absence of G-6-P, the proportion of the cell population showing cytoplasmic peptide localisation was much greater, indicating that endocytosis of DsS3(1-16) occurs when lower levels have bound to the membrane. CAI-4 parent strain, *pmr1Δ* and *mnn4Δ* all displayed decreased susceptibility to peptide with G-6-P. Exogenous phosphate from G-6-P may have sequestered a fraction of the DsS3(1-16) limiting its binding to the phosphomannan on the cell wall and the plasma membrane. When bound, this peptide is then translocated to the vacuole where the concentration builds but may not be sufficient to cause cell death. If the concentration increases sufficiently in the vacuole, peptide may leak into the cytoplasm and cause cell lysis. Vacuolar peptide may also destabilise the vacuolar membrane causing it to burst. At elevated DsS3(1-16) concentrations, more peptide binds to the plasma membrane causing rapid destabilisation, cytoplasmic internalisation and killing. This is possibly to

prevent the relatively slow process of endocytosis and subsequent removal of peptide from the membrane, lessening the likelihood of phospholipid disintegration. Hence, these differential internalisation pathways probably give rise to the two distinct cell populations recorded in this investigation.

Using growth curves, cell viability counts, fluorescent cell labelling and quantification with fluorescein tagged peptide to compare cell wall compromised mutants, it is clear that *C. albicans* cell wall N-linked mannosylphosphate is required for optimum antimicrobial action of DsS3(1-16). Additional data indicates that this is also the case for the linear cationic antimicrobial peptides mag 2 and rana. Exogenous negatively charged phosphate was shown to interfere with peptide action, possibly by binding DsS3(1-16), hence the mode of action of these peptides seems enhanced by binding to negatively charged phosphate in the cell wall. Fluorescently labelled DsS3(1-16) has also been visualised with differential localisation on the surface of the cell, sequestration to the vacuole and diffuse localisation throughout the cytoplasm and it has been concluded that localisation within the cell is related to the extent of peptide bound to the cell membrane.

Chapter 4

4. The inhibitory effects of the echinocandins in combination with several structurally diverse antimicrobial peptides.

4.1. Introduction

The clinically available echinocandins are synthetically modified papulacandins originally derived from *Papularia sphaerosperma* and consist of cyclic hexapeptides linked to a long chain fatty acid. Due to the large molecular size (MW = 1093.31 g-1270.28 g) they are only administered intravenously due to poor oral absorption. Effective dosages for candidiasis lie in the range of 70 mg per day for caspofungin and 100 mg per day for micafungin and anidulafungin (www.pbm.va.gov). Echinocandins show reduced toxicity towards *C. neoformans* (Dannaoui *et al*, 2008), however, relatively high concentrations of caspofungin have been shown to reduce the number of 1,3-β glucan linkages leaving other linkages intact (Feldmesser *et al*, 2000). Reduced susceptibility may be due to a resistance of 1,3-β glucan synthase to the inhibitory effects of caspofungin in *C. neoformans*. Within the last few years there have been several cases of caspofungin resistant strains of *Candida* where mutations in the subunits of 1,3-β glucan synthase have caused highly elevated MICs (Balashov *et al*, 2006). These are still relatively rare, possibly due to the short clinical usage of this drug class (Baixench *et al*, 2007). Hospital isolate strains of *C. neoformans*, *C. glabrata* and *C. albicans* were acquired to test their susceptibility towards echinocandin and AMP combination treatments. Studies were initially carried out against *S. cerevisiae*.

The strains used in this study have varying levels of susceptibility to conventionally used antifungal agents. Levels of resistance are likely to increase against all major classes of drug due to the development of drug-resistant strains in patients undergoing treatment. Testing for potentially increased drug action with combination treatment is essential to combat this and prolong the shelf life of existing antifungal agents. Synergistic interactions help to slow down the emergence of resistance and allow lower dosages to be given while still retaining their effectiveness, reducing both toxicity and cost (Lupetti *et al*, 2003).

Several antimicrobial peptides under investigation in this study have previously been shown to work in synergy with other antimicrobial agents. For example, mag 2 was demonstrated to work in synergy with the antimicrobial peptide PGLa (Hoffman *et al*., 1983) and in combination displayed a marked increase in effectiveness against bacteria, tumour cells and artificial membranes (Matsuzaki *et al*., 1998). The combination had a marked increase in potency against *C. albicans* but was ineffective against *C. glabrata* (Helmerhorst[b] *et al*, 1999; Helmerhorst *et al*, 2005). Synergy was also shown with the dermaseptins. One study looked at the effects of combining dermaseptin s1, s2, s3, s4 and s5. The effects were observed on various microorganisms including *C. albicans*. In some cases a 100-fold increase in activity was recorded. DsS3(1-16) was especially potent when combined with others; against *C. albicans* it showed a drop in MIC from 10 μM to 3 μM (Mor† *et al*., 1994). There have been no reports of rana synergy in yeasts, however, synergy versus other species was observed including the gram positive bacteria *S. aureus* (Giacometti *et al*., 2000; Graham *et al*, 2007). As the echinocandins

inhibit the synthesis of 1,3-β glucan linkages it was reasoned that disruption of this cell wall component would increase the access of AMPs to the cell membrane. Combinations of various echinocandins and a range of structurally diverse antimicrobial peptides were tested in combination in the following study.

4.2 Results

4.2.1 Initial studies using *S. cerevisiae* and caspofungin

Checkerboard assay of yeast growth inhibition

To investigate the inhibitory effects of the echinocandins and AMPs, initial studies were carried out using *S. cerevisiae*. Checkerboard growth assays (Section 2.6) were prepared in 96-well plates to which increasing concentrations of caspofungin were added to each column and increasing concentrations of DsS3(1-16), mag 2, rana or gomesin were added to each row. Initial plate scans indicated synergy was present between the linear peptides and caspofungin (Figure 4.1). Data from all checkerboard work was gathered to calculate the corresponding FICs displayed by each combination of echinocandin and AMP. Against *S. cerevisiae*, rana and mag 2 in combination with caspofungin produce values of 0.516 and 0.529 respectively, slightly above the synergy range (Table 4.1). DsS3(1-16) gives a higher value of 0.667, indicating the combination is additive. The compounds in MEB against *C. neoformans* were also tested but display no synergy, with FICs ranging from 1.09 - 1.36.

Table 4.1. FICI for *C. neoformans* and *S. cerevisiae* in combination with caspofungin and DsS3(1-16), mag 2 or rana. Values were determined from 96-well plate growth assays. FIC ≤ 0.5; synergy, FIC > 4.0; no interaction, FIC > 0.5 – 4.0; antagonism.

	Caspofungin	
Peptide	*C. neoformans*	*S. cerevisiae*
DsS3(1-16)	1.36	0.667
Ranalexin	1.14	0.516
Magainin 2	1.09	0.529
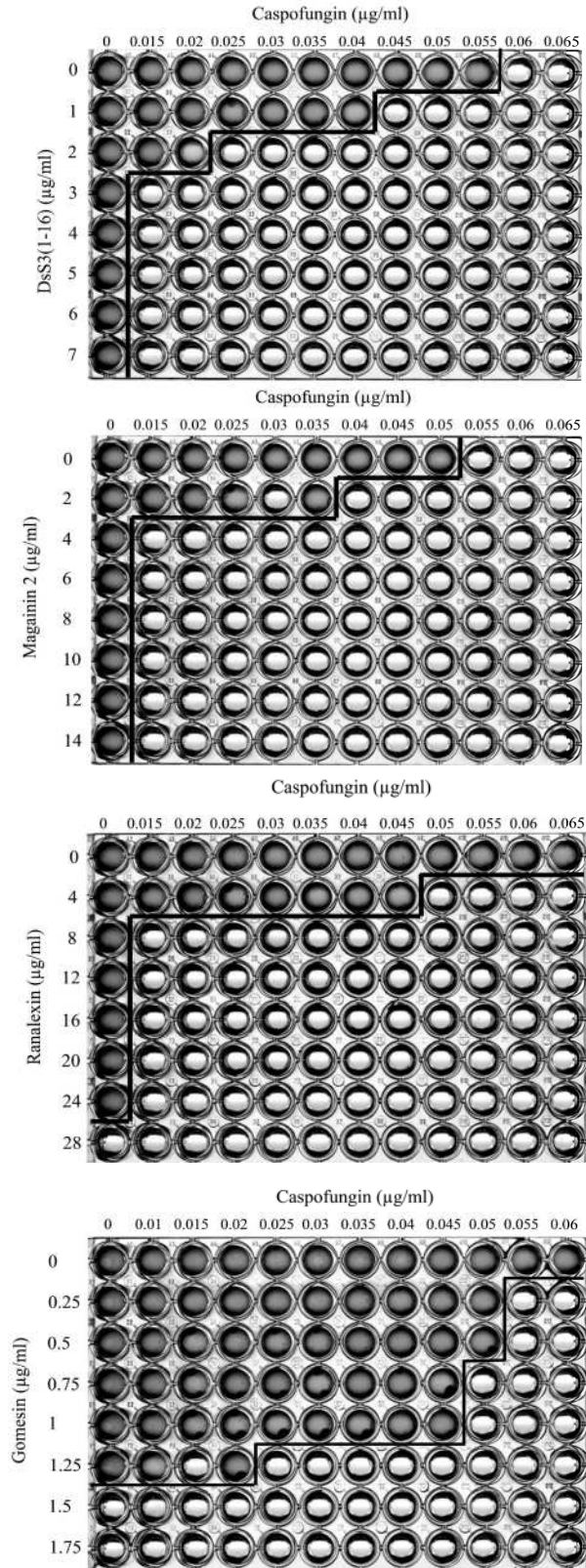
Figure 4.1. Representative checkerboard assays used to determine FICs with *S. cerevisiae*. Each well of a 96-well plate was inoculated to give 1.0 x 10³ cells per well. Experiments were carried out in triplicate and representative images for each are shown. Lines separate wells where growth was present from wells where growth was absent.

Growth of *S. cerevisiae*

After the initial plate scans, growth was monitored over a 48 h period at OD_{600} using similar combination treatments (Figure 4.2). DsS3(1-16), mag 2 and rana were selected as they displayed patterns of synergistic growth inhibition. In the DsS3(1-16) treatment, addition of 1.5 µg/ml caused little growth inhibition with exponential growth after 14 h. When 0.035 µg/ml caspofungin was present there was inhibition of growth with an extended lag phase lasting an additional 11 h compared to the control. The culture reached stationary phase with a reduced population density (OD_{600} = 0.771). When a combination of DsS3(1-16) and caspofungin was present no growth was recorded. In the mag 2 / caspofungin growth analysis similar results were obtained. In the presence of 2 µg/ml mag 2, growth closely mirrored that of the control. In combination, no growth was recorded over the 48 h period. The rana / caspofungin results were similar: with 0.025 µg/ml caspofungin there was an extended lag phase of 3 h, a reduced exponential growth rate and stationary phase population density. When both agents were present no growth was recorded. There results show that with caspofungin alone there was slight growth inhibition, while in combination no growth was recorded.
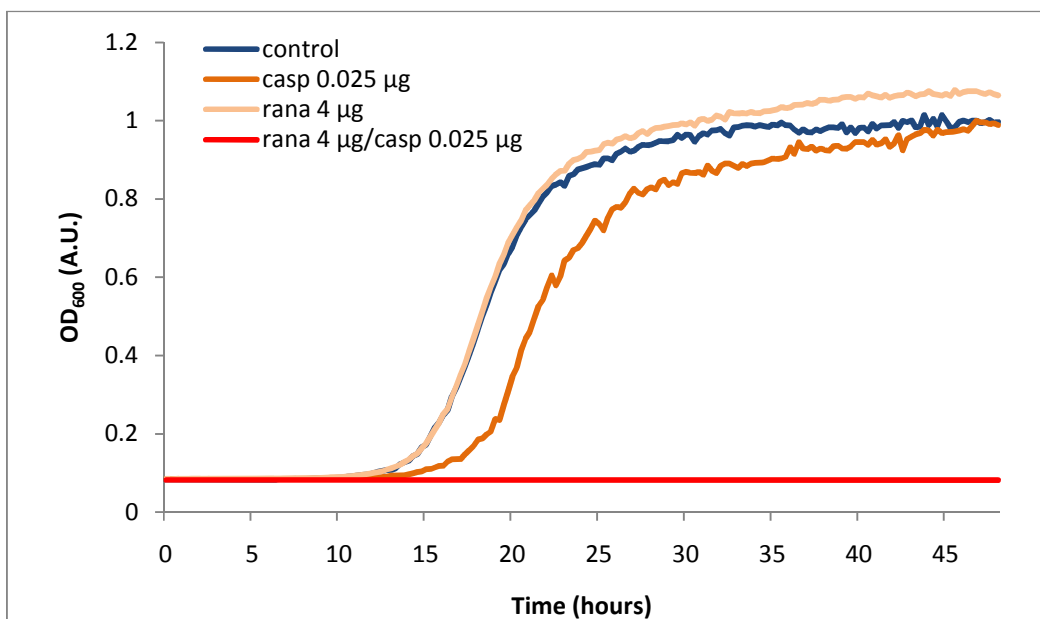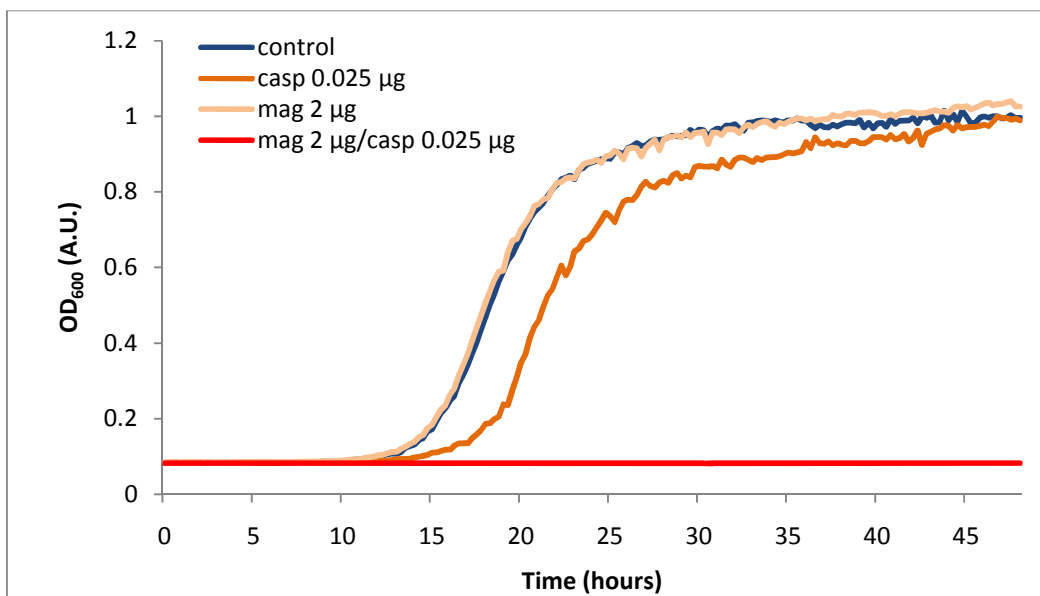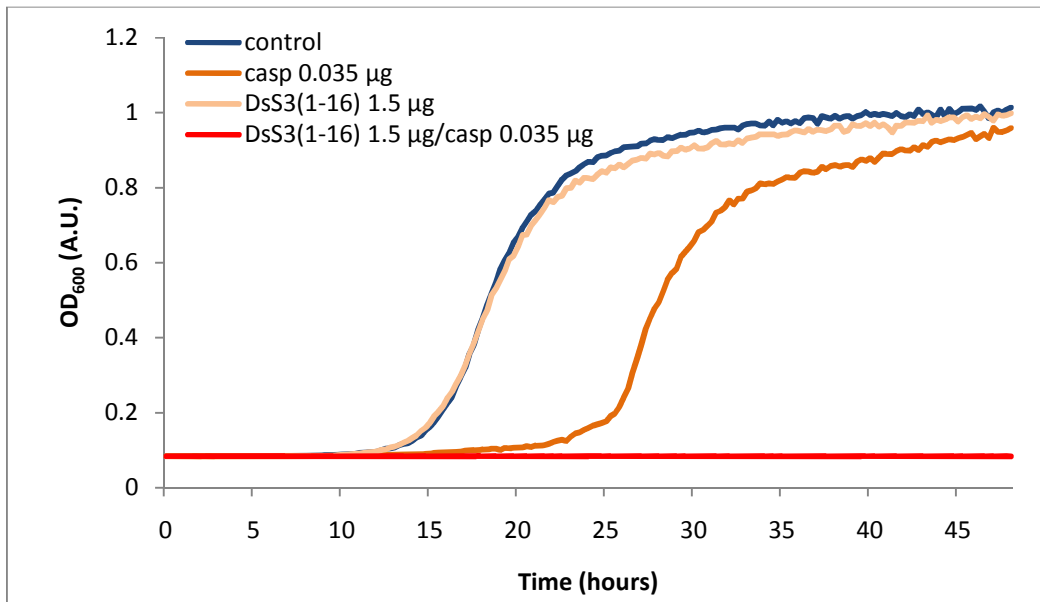
Figure 4.2. Growth of *S. cerevisiae* when exposed to DsS3(1-16), mag 2 or rana alone or in combination with caspofungin. Cell density was measured every 15 min over a 48 h period in MEB at 30 °C. Each experiment was carried out in triplicate and representative graphs for each are show.

Cell viability

To determine if the synergistic inhibition of the combinations enhanced the fungicidal activity of the AMPs and caspofungin, the combined effect on viability of *S. cerevisiae* cultures was monitored. Caspofungin and AMP were added at mid-exponential phase and readings were taken every 15 min (Figure 4.3).

With the DsS3(1-16) treatment, peptide and caspofungin were added to the cultures after 360 min, prior to the initial CFU/ml reading. Compared to the control, the caspofungin treated cells showed a reduction in growth. This reduction was also reflected in terms of CFU/ml. Changes in cell number were apparent directly after compound addition. At the final time point, caspofungin treated cells were similar to the control at 6.32 log CFU/ml and 6.36 log CFU/ml respectively. Cell viability was reduced in the DsS3(1-16) treatment dropping to 5.77 CFU/ml. The dual treatment displayed the greatest decrease in cell number ending at 5.15 log CFU/ml. This is a 0.62 log reduction when compared to the DsS3(1-16) treatment alone.

The mag 2 with caspofungin data set displayed differences between the various treatments. Changes to population density became apparent 3 h after treatment. The control culture continued to increase in cell density to OD_{600} = 0.47 while the treated cultures all show reduced growth. Again, the dual treatment resulted in the greatest decrease in population density. This was also observed in terms of CFU/ml with the control ending with a reading of 6.51 log CFU/ml followed by a slight reduction in the caspofungin and mag 2 treatments at 6.31 and 6.13 CFU/ml respectively and then a

decrease in cell number on combination to 5.2 log CFU/ml; a reduction of 0.93 log CFU/ml on combination when compared to mag 2 on its own.

The rana and caspofungin assays also show variance in cell viability. The control culture displays continuous growth until the final reading and ends on an OD_{600} of 0.45. The rana, caspofungin and dual treatments all displayed reduced growth 2 h after addition. This was reflected in terms of cell number, with final readings of 6.51 log CFU/ml for the control, 6.22 for the rana treatment, 6.32 for the caspofungin treatment and 5.63 in combination. This represents a decrease in cell number of 0.59 log CFU/ml when compared to rana alone. The AMPs in combination with caspofungin all result in a decrease in both population density and cell viability indicating synergistic fungicidal killing.
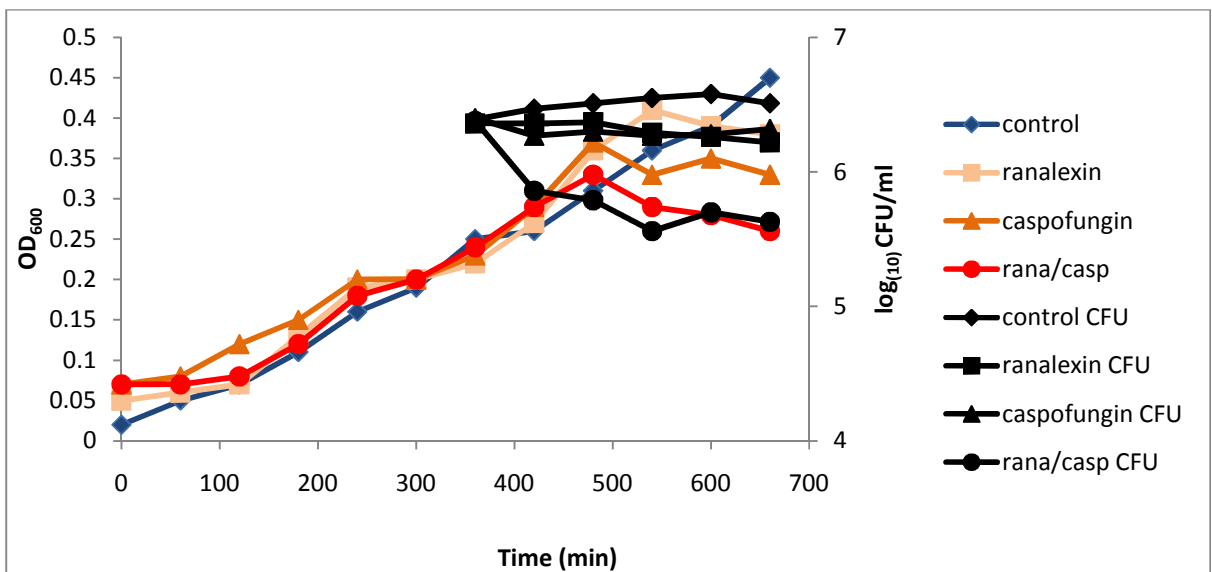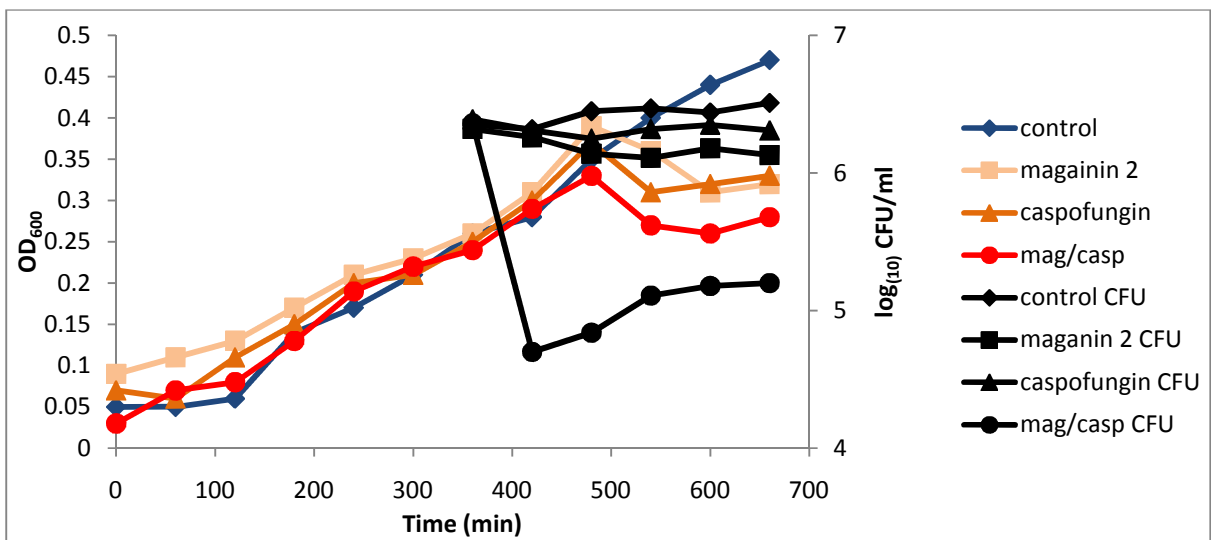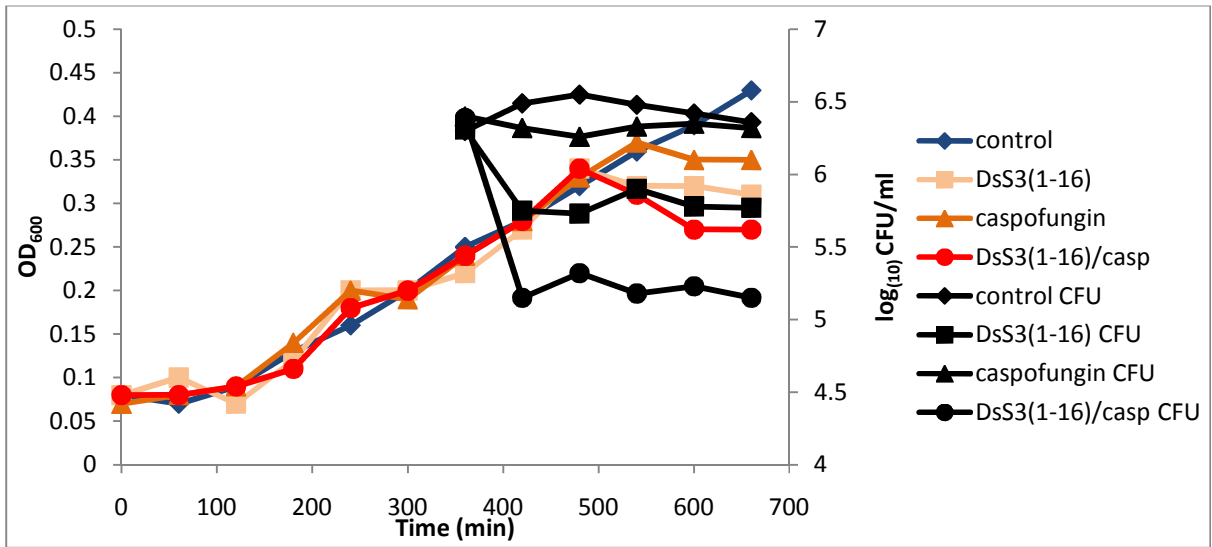
Figure 4.3. Optical density versus viable cell number assays of *S. cerevisiae* with AMP and caspofungin. Viability was recorded over 5 h at 60 min time intervals. Initial viability readings were taken prior to peptide addition. Concentrations of 2 μg/ml DsS3(1-16), 4 μg/ml of mag 2 and 5 μg/ml of rana and 0.04 μg/ml of caspofungin were used.

Disc diffusion assay of yeast inhibition

The increase in antifungal action observed on combination with caspofungin was visualised in terms of area of growth inhibition over a solid medium (Figure 4.4). With caspofungin alone there was no inhibition of growth up to 0.03 µg and a small ring around the disc where no growth was apparent at 0.035 µg. With DsS3(1-16) there was also no growth inhibition. When DsS3(1-16) and caspofungin were combined, clear zones of inhibition were formed even at the lowest concentrations of both compounds. The zone progressively increased as the concentrations were increased until a zone of approximately 3 mm formed around the disc. Mag 2 acting alone displayed inhibition at 6 µg, 8 µg and 10 µg, with a 1 - 2 mm zone forming at the later concentration. In combination with caspofungin there were clear zones of inhibition formed around all discs even at the lowest concentration. With 10 µg mag 2 and 0.035 µg caspofungin there was a 5 - 6 mm zone where no growth was apparent. On exposure to rana alone, there were no visual signs of growth inhibition around the discs. In combination there was a zone at 6 µg of rana and 0.02 µg caspofungin that increased in size up to the greatest concentration of each, where a zone of 4 - 5 mm was measured from the disc.

S. cerevisiae MEB 48h

Caspofungin (µg)

| 0.015 | 0.02 | 0.025 | 0.03 | 0.035 |

DsS3(1-16) (µg)

| 0.5 | 1 | 2 | 3 | 4 |

DsS3(1-16)/Caspofungin (µg)

| 0.5/0.015 | 1/0.02 | 2/0.025 | 3/0.03 | 4/0.035 |

Magainin 2 (µg)

| 2 | 4 | 6 | 8 | 10 |

Magainin 2/Caspofungin (µg)

| 2/0.015 | 4/0.02 | 6/0.025 | 8/0.03 | 10/0.035 |

Ranalexin (µg)

| 3 | 6 | 9 | 12 | 15 |

Ranalexin/Caspofungin (µg)

| 3/0.015 | 6/0.02 | 9/0.025 | 12/0.03 | 15/0.035 |
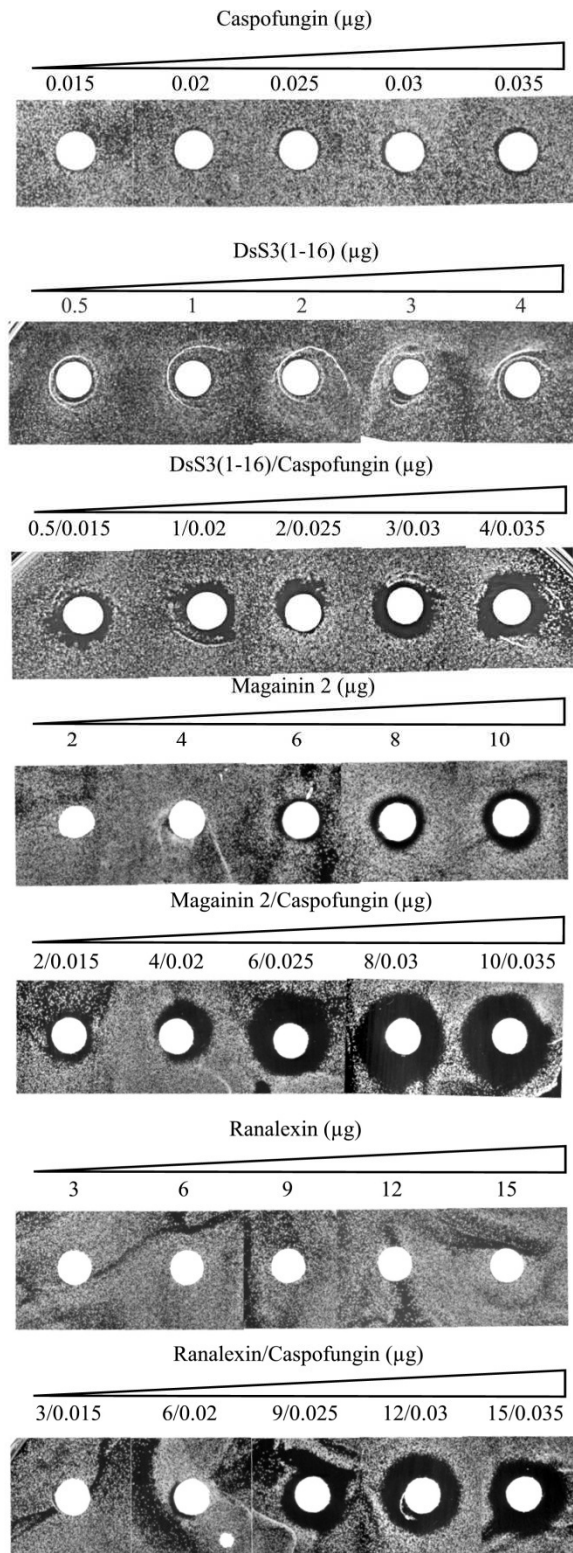
Figure 4.4. Disc diffusion assays monitoring inhibition of *S. cerevisiae* with AMP and caspofungin. Discs were impregnated with increasing concentrations of peptide in the presence or absence of caspofungin. Plates were spread with mid-exponential phase *S. cerevisiae* culture. The assay was carried out in duplicate.

There appeared to be no increase in antifungal action on combination with peptide or caspofungin against *C. neoformans* indicating additive rather than synergistic killing (Appendix IV).

4.2.2 Growth of *C. glabrata*, *C. albicans* hospital isolate and SC5314 strains in the presence of caspofungin with DsS3(1-16), magainin 2, ranalexin, 6752 or GS14K4.

This section investigates the action of caspofungin with the three linear AMPs used previously and two cyclic peptides. The cyclic peptides, 6752 and GS14K4, were employed to test varying peptide structures and their effect on combination with caspofungin. The strains tested with these peptides were *C. albicans* and *C. glabrata* hospital isolates and *C. albicans* SC5314 commonly used for *in vivo* studies. Additionally, all strains were cultured in RPMI 1640 media or MEB. The MEB data set is presented in Appendix IV. An RPMI 1640 data set was obtained as this is the standard medium for echinocandin *in vitro* susceptibility testing (Odds *et al*, 2004). This additional data set would provide useful standardised data for any future studies progressing to *in vivo* work. The growth of each strain in RPMI 1640 media was initially monitored over a 48 h period (Figure 4.5). *S. cerevisiae* did not grow in RPMI 1640 media. Both strains of *C. albicans* began exponential growth after 13 h incubation and approached stationary phase at a density of $OD_{600} = 0.2$. *C. glabrata* also began exponential growth after 13 h, the population density increased at a greater rate and cells entered stationary phase at an OD_{600} of 0.25.
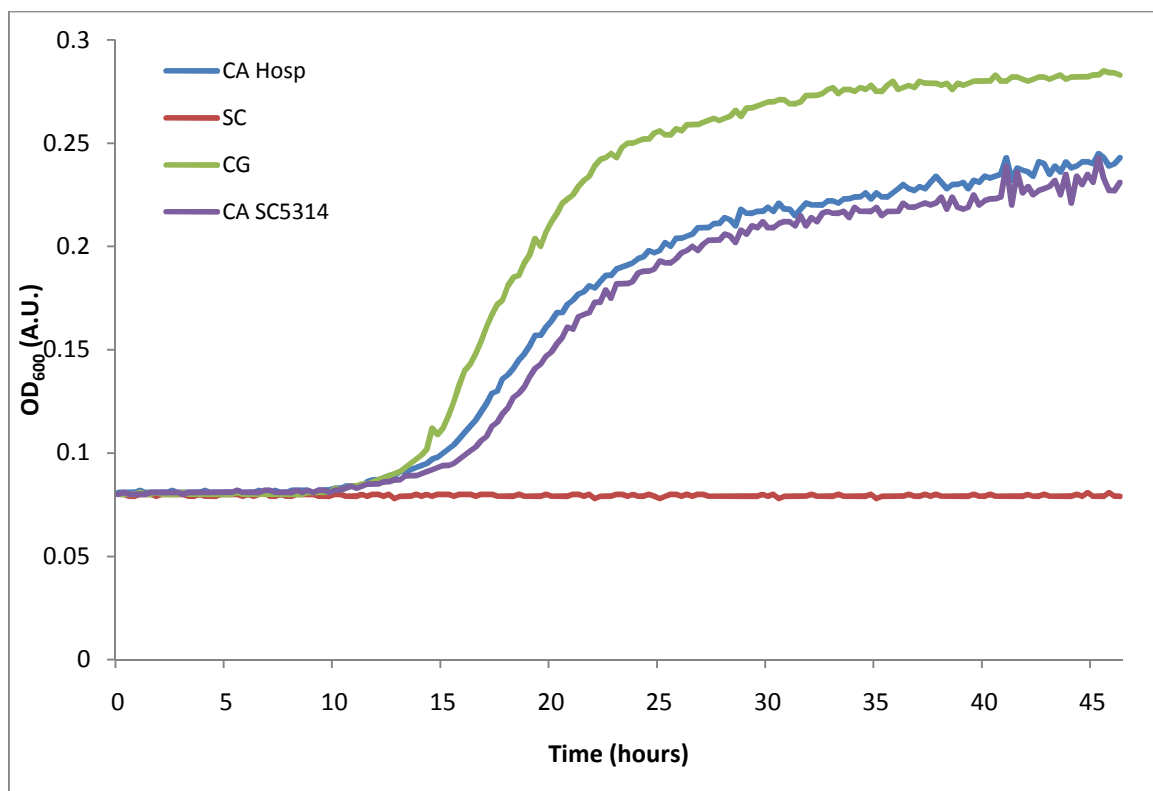
Figure 4.5. Growth of *S. cerevisiae*, *C. glabrata* and *C. albicans* in RPMI 1640. Cell density was recorded every 15 min over a 48 h period. Each experiment was carried out in triplicate and representative graphs for each are shown.

Checkerboard assays of yeast growth inhibition

Growth of the *C. albicans* SC5314 strain in RPMI is shown in Figure 4.6. In RPMI media the required concentration of caspofungin in order to prevent visible growth was increased, generating an elevated MIC of between 0.15 µg/ml and 0.2 µg/ml compared to the MEB data set. The five peptides tested appear to lose antifungal action in this media. In each plate, concentrations of peptide ranged from 5 µg/ml to 35 µg/ml. This was not sufficient to produce a MIC, however, in order to conserve peptide this concentration range was selected. MICs for each peptide were calculated (Table 4.3). The concentration of caspofungin required for inhibition of *C. glabrata* in RPMI 1640 was reduced when compared to MEB with MICs ranging from 0.11 - 0.12 µg/ml (Figure 4.6). Strains of *C. albicans* clinical isolate, CASC5314 and *C. glabrata* were tested in this way

with combinations of AMPs and caspofungin, micafungin or anidulafungin (Appendix IV).

FIC values of the *C. albicans* and *C. glabrata* strains in MEB and RPMI with caspofungin were calculated next (Table 4.2). Focusing initially on the SC5314 strain, DsS3(1-16) displays synergy with a value of 0.486, while mag 2 and rana have values of 0.553 and 0.508 respectively in MEB. The cyclic peptides have elevated values of up to 1.125 for GS14K4, indicative of an additive effect. In RPMI media, all peptides in combination with caspofungin displayed reduced FICs when compared to MEB values. These all group in the synergy range with values of 0.144 to 0.267. The values obtained while monitoring the *C. albicans* hospital isolate strain in MEB show values above 0.5, mag 2 is fractionally above at 0.507. The remaining peptides give values of 0.671 - 0.844 displaying additive killing. In RPMI there was up to a 5.2 x reduction in FIC values. All peptides again fall below the synergy value, indicative of synergistic killing in combination with caspofungin. When *C. glabrata* was cultured in MEB in combination, DsS3(1-16) and GS14K4 produce values of 0.499 and 0.479 respectively, demonstrating synergistic killing. Mag 2 falls just outside the range, with an FIC of 0.55. Rana and 6752 have elevated FICs in comparison, indicating limited interaction. Values from the RPMI media data set are all between 0.186 and 0.347, well below the 0.5 indicative of synergy.

Table 4.2. FICI for *C. albicans* and *C. glabrata* in combination with caspofungin and DsS3(1-16), mag 2, rana, 6752 or GS14K4. Values were determined from 96-well plate growth assays. FIC ≤ 0.5; synergy, FIC > 4.0; no interaction, FIC > 0.5 – 4.0; antagonism.

	Caspofungin					
	***C. albicans* SC5314**		***C. albicans* (Hospital isolate)**		***C. glabrata***	
Peptide	MEB	RPMI 1640	MEB	RPMI 1640	MEB	RPMI 1640
DsS3(1-16)	0.486	0.164	0.844	0.164	0.499	0.282
Ranalexin	0.508	0.221	0.673	0.164	0.761	0.186
Magainin 2	0.553	0.144	0.507	0.135	0.55	0.278
6752	0.619	0.15	0.671	0.289	1.94	0.347
GS24K4	1.125	0.267	0.725	0.139	0.479	0.269

Table 4.3. MIC values for all peptides in RPMI 1640 against *C. albicans* strains and *C. glabrata*. Scans of the 96-well plates used in determining these values can be found in Appendix III. Each well of a 96-well plate, containing RPMI 1640 was inoculated to give 1.0 x 10^3 cells per well. The experiment was carried out in duplicate producing identical MIC values.

Peptide	***C. albicans* SC5314** MIC (µg/ml)	***C. albicans* (hospital isolate)** MIC (µg/ml)	***C. glabrata*** MIC (µg/ml)
DsS3(1-16)	256	128	>512
Ranalexin	128	128	256
Magainin 2	512	512	>512
6752	256	256	>512
GS14K4	64	128	256
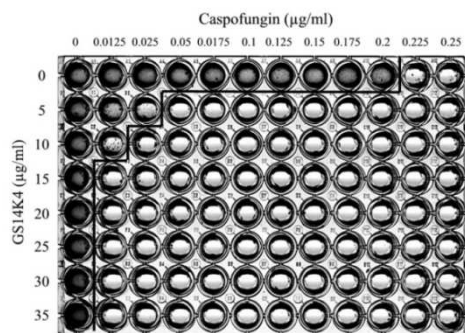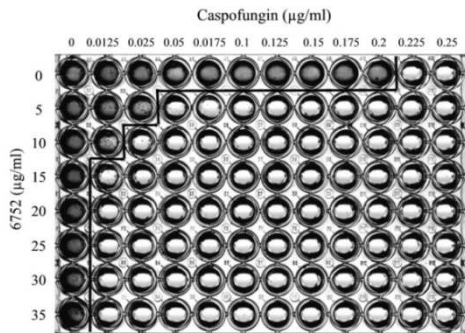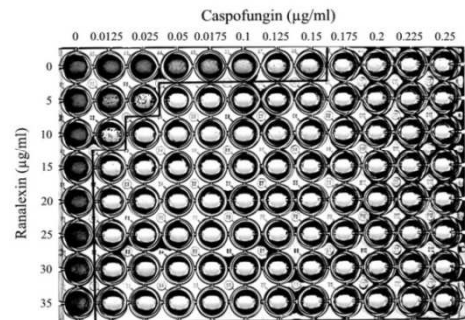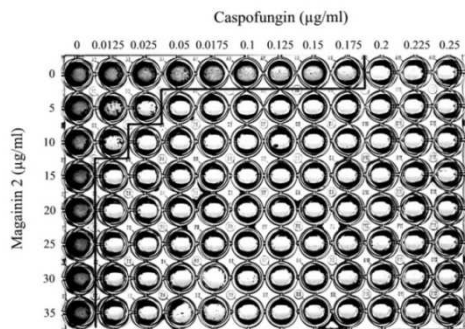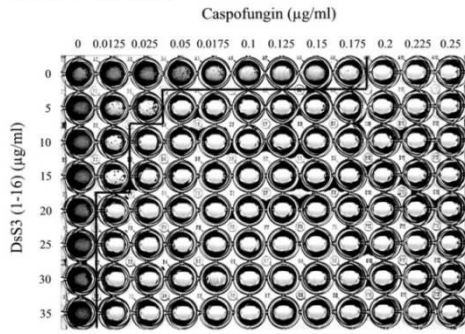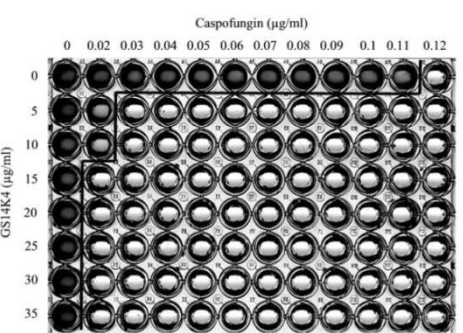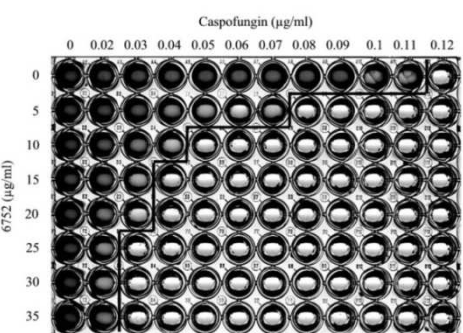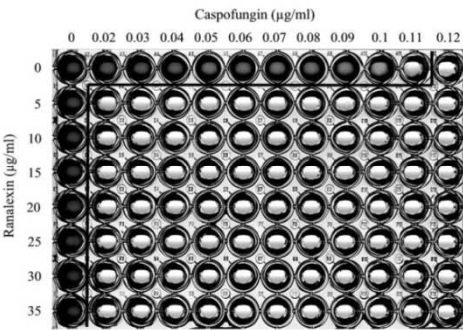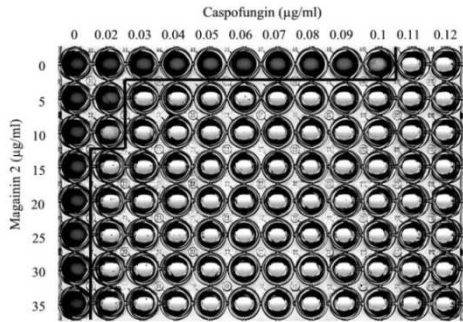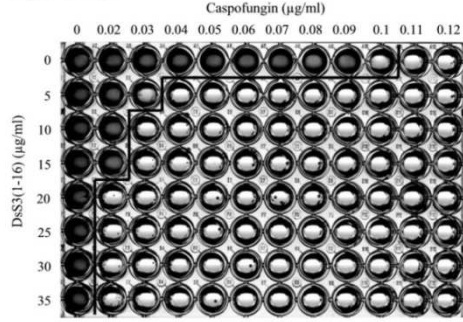
Figure 4.6. Representative checkerboard assays used to determine FICs with SC5314 and *C. glabrata*. Each experiment was carried out in triplicate and representative images for each are shown. Lines separate wells where growth was present from wells where growth was absent.

Disc diffusion assays of yeast growth inhibition

As with *S. cerevisiae*, disc diffusion assays were prepared using *C. albicans* and *C. glabrata* to determine the inhibitory effects of caspofungin with DsS3(1-16), mag 2 and rana on a solid porous surface (Figure 4.7; *C. glabrata* and *C. albicans* hospital isolate Appendix V). At caspofungin concentrations greater than 0.025 μg there were areas of inhibition of up to 1.5 mm round the discs. With all three peptides, as with the previous strain, there were no signs of growth inhibition up to 25 μg. However, when discs were impregnated with the combination of AMP and caspofungin there were clear zones of inhibition. The lowest combination treatments produced areas where no growth was apparent that increased in size as the concentrations were increased. At the greatest concentration clear areas round each disc of 5.5 mm, 5 mm and 7 mm were produced for DsS3(1-16), mag 2 and rana respectively. *C. glabrata* was tested only using MEB agarose plates as growth was not visible on RPMI agarose after 48 h resulting in similar inhibited areas. These disc diffusion experiments demonstrate the increased fungicidal action of DsS3(1-16), mag 2 and rana when combined with caspofungin on a solid surface, producing at least a two to three fold increase in the zone of inhibition surrounding these treatment areas for *C. glabrata* and both *C. albicans* strains.
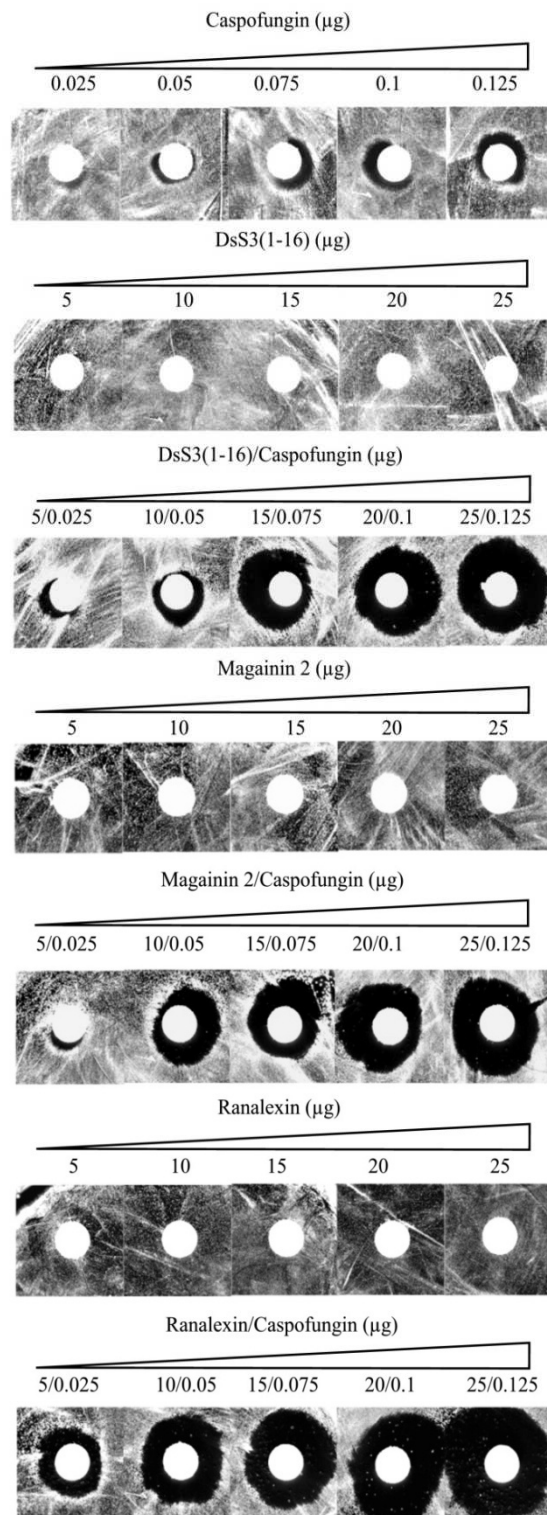
**Figure 4.7. Disc diffusion assays monitoring inhibition of SC5314 with AMP and caspofungin. Discs were impregnated with increasing concentrations of peptide in the presence or absence of caspofungin.** *C. albicans* **SC5314 mid-exponential phase cells were spread onto plates. The experiment was carried out in duplicate and representative images are displayed.**

Yeast cell viability

Regarding previous experiments, it appears that caspofungin in combination with various AMPs causes increased inhibition of growth in *C. albicans*. To quantify this in terms of cell viability, growth curves and cell survival were calculated on exposure to caspofungin, AMP or in combination (Figure 4.8). In the DsS3(1-16) and caspofungin growth curve, the antifungal agents were added after 240 min of growth. At 4 μg/ml, DsS3(1-16) had little effect on growth which closely mirrored that of the control. With the addition of 0.01 μg/ml caspofungin and dual treatments, growth was reduced. These readings were reflected in terms of cell number, with the control and DsS3(1-16) treated cultures finishing with counts of 7.33 log CFU/ml and 7.28 log CFU/ml respectively. Inhibition of growth was recorded on addition of 0.01 μg/ml caspofungin finishing with a count of 7.15 log CFU/ml. When DsS3(1-16) and caspofungin were present, cell number was reduced at each time point with a final reading of 6.7 log CFU/ml giving a reduction of 0.63 log CFU/ml on combination.

The mag 2 and caspofungin treated cells displayed a marked effect upon exposure. When 10 μg/ml mag 2 was added to cultures, there was a slight reduction in growth. When both agents were present there was increased inhibition with cell number continuously reduced after exposure, reaching 6.38 log CFU/ml for the final reading. This gives a 0.82 log reduction compared to caspofungin alone and a 1.18 log reduction compared to the control population at 7.56 log CFU/ml.

Rana data displayed a similar trend, with the control and peptide only treatment at similar levels in both growth and cell number. On treatment with 0.01 μg/ml caspofungin there was reduced growth and cell number reducing to 7.35 log CFU/ml. On combination, growth reduction was observed 60 min after exposure and continued to decrease to OD_{600} = 0.51 (6.43 CFU/ml). This was a 0.87 log reduction compared to the caspofungin only treatment and a 1.17 log reduction compared to the control.

This data would further indicate that a synergistic interaction was present causing increased loss of cell viability through an increase in the fungicidal action of the antimicrobial peptides, caspofungin or both. In the following section the action of anidulafungin and micafungin is investigated.
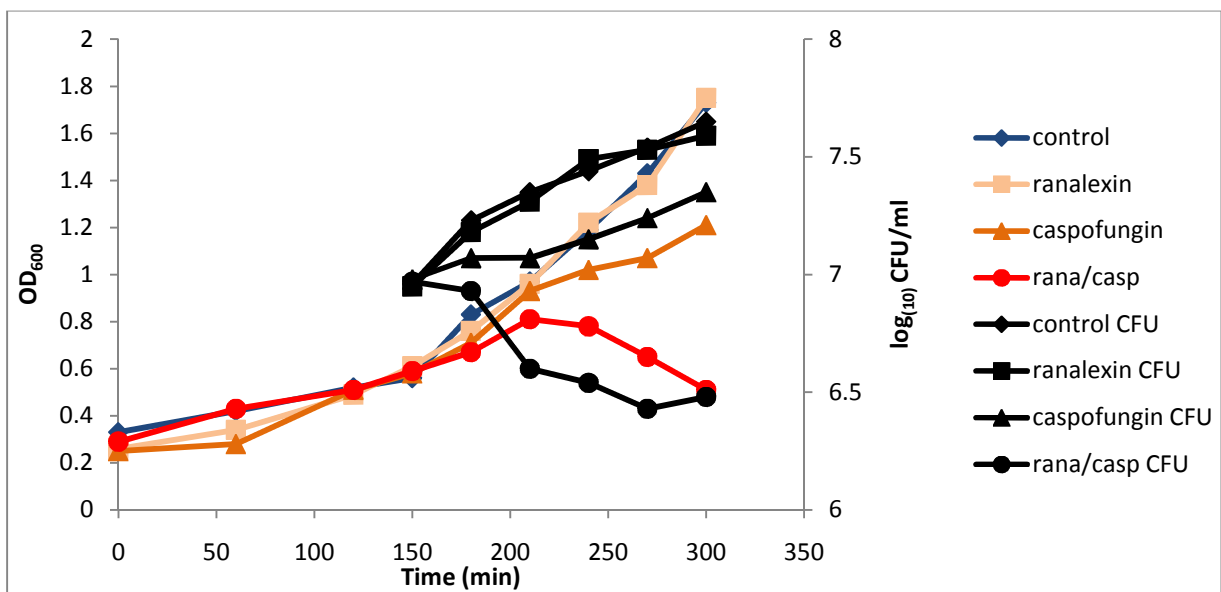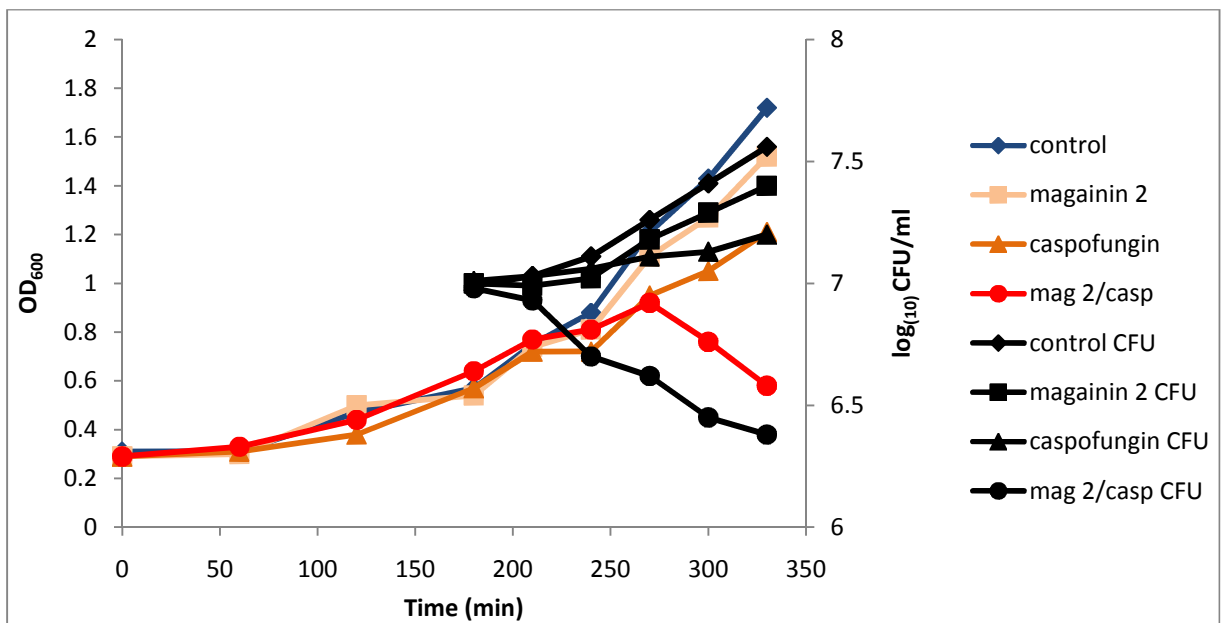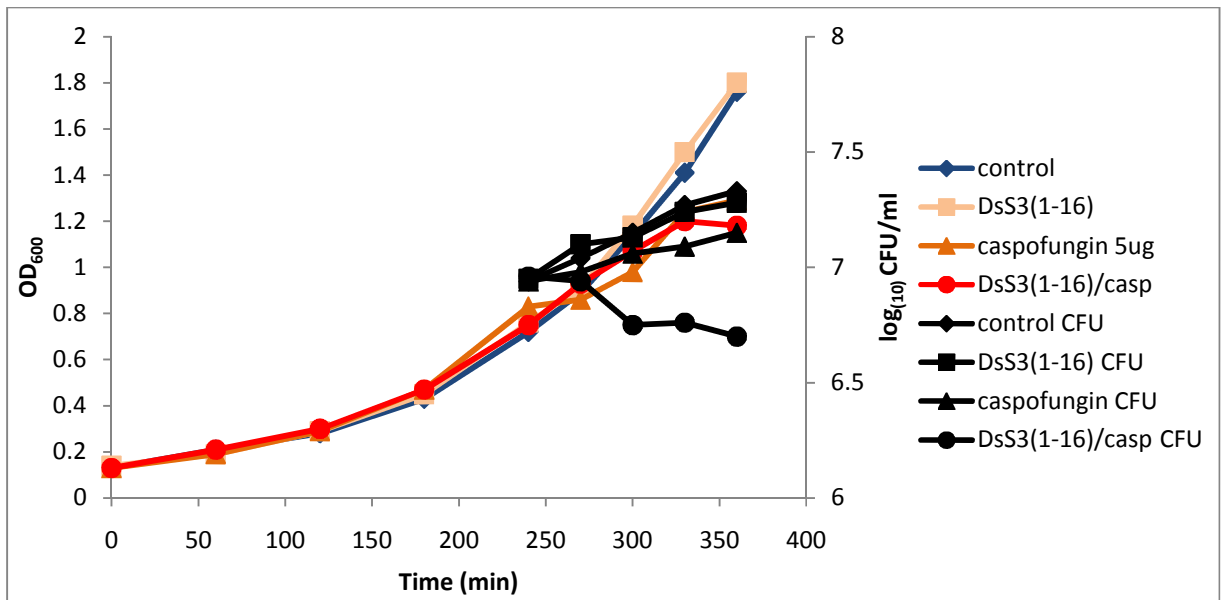
Figure 4.8. Optical density versus viable cell number assays monitoring inhibition of *C. albicans* SC5314 with AMP and caspofungin. Viability was recorded over 5 h (4 h with DsS3(1-16)). Initial viability readings were taken prior to peptide addition. These were carried out in MEB due to the reduced growth in RPMI 1640 media. Concentrations of 20 µg/ml DsS3(1-16), 10 µg/ml mag 2 or 9 µg/ml rana were added with 0.01 µg/ml of caspofungin.

4.2.3 Growth of *C. glabrata*, *C. albicans* hospital isolate and SC5314 strains in the presence of anidulafungin and micafungin with DsS3(1-16), magainin 2, ranalexin, 6752 or GS14K4.

Checkerboard assays of yeast growth inhibition

Micafungin FIC values in MEB for all strains were similar, ranging from 1.08 - 1.48, strongly indicating that no interaction was taking place (Table 4.4). Combinations in RPMI display reduced FICs that were still outside the synergy range. Only DsS3(1-16) and micafungin against SC5314 was below 0.5 at 0.487. All other FIC values with micafungin indicate a purely additive effect on growth inhibition.

With anidulafungin and the SC5314 strain, only the rana combination has a FIC ≤0.5, falling into the synergy range (Table 4.5). DsS3(1-16), mag 2 and GS14K4 have values ranging from 0.619 - 0.917, indicating no interaction was present. The cyclic peptide, 6752, displayed antagonism when combined with anidulafungin, with a highly elevated FIC of 5.04. The value in RPMI was also increased at 0.773, higher than all other peptides. DsS3(1-16), rana, mag 2 and GS14K4 displayed low synergistic values, ranging from 0.095 to 0.142. The FIC values calculated using the *C. albicans* hospital isolate in MEB indicate synergy was occurring with Dss3(1-16), rana and possibly GS14K4, which falls slightly outside the synergy cut-off at 0.531. The mag 2 treatment produced a value of 0.667, so an additive effect is probable. 6752 again displayed an elevated FIC of 3.19, approaching a value at which antagonism would be indicated. In RPMI media all peptides had values indicative of synergy, ranging from 0.111 with DsS3(1-16) and rana to 0.287 with GS14K4. The 6752 peptide again displayed a substantial reduction in FIC to

0.563 in RPMI media, just outside the synergy range. FICs in MEB using *C. glabrata* displayed increased inhibition upon combination with values of 0.490 and 0.282 for DsS3(1-16) and GS14K4 respectively. Rana and mag 2 fall outside the synergy range at 0.75 and 0.622 respectively. 6752, as with the other strains, had a relatively high FIC at 3.03, approaching a value that would be considered antagonistic. Results for *C. glabrata* in RPMI media would indicate an increase in fungicidal action in combination, with values in the range of 0.287 with DsS3(1-16) and 0.443 with rana. 6752 with a value of 0.737 indicates no interaction with anidulafungin against *C. glabrata*. In summary, all peptides (with the exception of 6752) in combination with anidulafungin generate FIC values that demonstrate the strong synergistic interactions against *C. albicans* and *C. glabrata* in RPMI media.

Table 4.4. FICI for *C. albicans* and *C. glabrata* in combination with micafungin and DsS3(1-16), mag 2 or rana. Values were determined from 96-well plate growth assays. FIC ≤ 0.5; synergy, FIC > 4.0; no interaction, FIC > 0.5 – 4.0; antagonism.

| | Micafungin | | | | | |
| | *C. albicans* SC5314 | | *C. albicans* (Hospital isolate) | | *C. glabrata* | |
Peptide	MEB	RPMI 1640	MEB	RPMI 1640	MEB	RPMI 1640
DsS3(1-16)	1.43	0.487	1.08	0.687	1.45	0.589
Ranalexin	1.31	0.677	1.48	0.715	1.33	0.581
Magainin 2	0.93	0.706	1.4	0.656	1.34	0.686

Table 4.5. FICI for *C. albicans* and *C. glabrata* in combination with anidulafungin and DsS3(1-16), mag 2, rana, 6752 or GS14K4. Values were determined from 96-well plate growth assays. FIC ≤ 0.5; synergy, FIC > 4.0; no interaction, FIC > 0.5 – 4.0; antagonism.

| | Anidulafungin | | | | | |
| | *C. albicans* SC5314 | | *C. albicans* (Hospital isolate) | | *C. glabrata* | |
Peptide	MEB	RPMI 1640	MEB	RPMI 1640	MEB	RPMI 1640
DsS3(1-16)	0.619	0.107	0.361	0.111	0.49	0.287
Ranalexin	0.452	0.106	0.291	0.111	0.75	0.443
Magainin 2	0.917	0.095	0.667	0.087	0.622	0.376
6752	5.04	0.773	3.19	0.563	NA	0.737
GS24K4	0.633	0.142	0.531	0.287	0.282	0.341

Disc diffusion assays of yeast growth inhibition

Disc diffusion assays were undertaken with both *C. albicans* strains on RPMI 1640 agarose. For SC5314, with anidulafungin alone there were no areas of inhibition observed up to 0.02 µg (Figure 4.9). At 0.025 µg there was a small area of 0.5 mm round one section of the disk. With DsS3(1-16) and mag 2, up to concentrations of 25 µg, there were no inhibited areas while in the rana treatment there was no inhibition up to 20 µg. DsS3(1-16) on combination with anidulafungin produced zones of inhibition at 10 - 25 µg of peptide. At 25 µg DsS3(1-16) and 0.025 µg of anidulafungin, a clear area was observed that extended between 3 mm and 5 mm round the circumference of the disc. The dual treatment using mag 2 produced inhibition at 15 - 25 µg of peptide in combination with increasing concentrations of anidulafungin. At the greatest concentration, a zone of 4 mm was visible from the disc. On exposure to the combination with rana, zones of inhibition were observable from 10 µg of peptide and 0.012 µg of anidulafungin giving a 3 mm inhibited zone at 25 µg. Results were similar when monitoring inhibition of the *C. albicans* hospital isolate (Appendix V).

These results demonstrate the increased inhibition of growth on a solid medium and possible killing of both strains of *C. albicans* with a combination of AMP and anidulafungin. In general, no inhibition was observed at the greatest concentrations of each compound alone, however, when in combination growth was inhibited with clear areas radiating up to 5 mm from the discs.
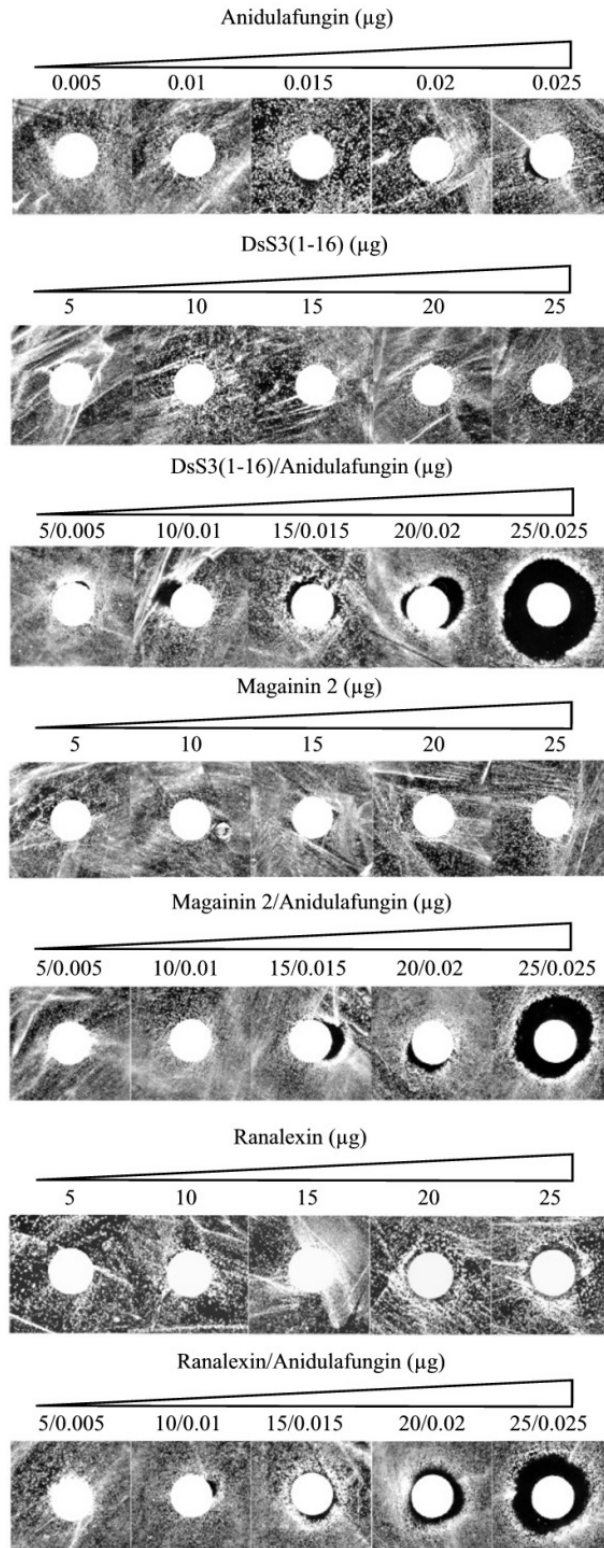
Figure 4.9. Disc diffusion assays monitoring inhibition of SC5314 with AMP and anidulafungin. Discs were impregnated with increasing concentrations of peptide and anidulafungin. Mid-exponential *C. albicans* SC5314 culture was spread onto RPMI 1640 agarose plates. The experiment was carried out in duplicate and representative images are displayed.

4.2.4 Intracellular localisation of Flu-DsS3(1-16) using fluorescence microscopy.

To understand the basis of the increased antimicrobial action of AMPs in combination with caspofungin and anidulafungin, Flu-DsS3(1-16) was employed in a microscope study. This aimed to investigate the uptake of Flu-DsS3(1-16) in *C. albicans* SC5314 cells and monitor changes to localisation in the presence of echinocandin. PI was also used to correlate stages of peptide uptake with loss of viability. Cells displaying whole cell fluorescence with Flu-DsS3(1-16) also stained with P.I. so were grouped together. Flu-DsS3(1-16) in combination with caspofungin produced a FIC value of 0.175, demonstrating synergy was present at levels observed with native DsS3(1-16) (Appendix IV). Three distinct groups of cells were visible and quantified as such in the following graphs (Figure 4.10).

In MEB with 20 µg/ml of Flu-DsS3(1-16), 64.3 % of cells displayed no fluorescence, 4.8 % displayed vacuolar localisation, while 30.9 % displayed disseminated fluorescence (Figure 4.10, top). Exposure to 0.001 µg/ml caspofungin resulted in ~5 % of cell staining with PI. On exposure to a combination of caspofungin and Flu-DsS3(1-16) ~27 % of the population stained with PI and Flu-DsS3(1-16). Exposure to 0.01 µg/ml caspofungin resulted in 57.6 % PI staining while a combination of Flu-DsS3(1-16) and caspofungin caused 72.3 % of the population to stain with PI and Flu-DsS3(1-16). This increase in PI staining and Flu-DsS3(1-16) internalisation in combination was also observed upon exposure to 0.05 - 1 µg/ml caspofungin. Paradoxically, at these concentrations the

proportion of cells that were PI-positive decreased when compared to the decreased concentrations of 0.001 µg/ml and 0.01 µg/ml caspofungin.

When the assay was performed in RPMI media, 20 µg/ml of Flu-DsS3(1-16) had a reduced effect, with only 3.7 % of cells displaying whole cell peptide incorporation and P.I staining (Figure 4.10, centre). Exposure to 0.001 µg/ml caspofungin resulted in ~16 % of cells staining with PI. Upon combination treatment the PI-positive and Flu-DsS3(1-16) stained fraction increased to ~35 %. Exposure to 0.01 and 0.05 µg/ml caspofungin resulted in ~24 and ~26 % staining with PI. The combination of Flu-DsS3(1-16) and 0.01 – 0.05 µg/ml caspofungin increased the PI-positive proportion to 32 and 37 % respectively. Exposure to 0.1 and 1 µg/ml caspofungin resulted in a reduction in PI-positive cells to ~18 % in both treatments. In combination with Flu-DsS3(1-16) there was an increase in PI-positive cells and Flu-DsS3(1-16) staining at 24 – 26 %. Additionally, as the proportion of cells displaying dissemination of Flu-DsS3(1-16) increased, so the proportion displaying vacuolar localisation decreased.

In the anidulafungin experiment, 20 µg/ml Flu-DsS3(1-16) produced 1.6 % whole cell fluorescence and 17.8 % vacuolar fluorescence (Figure 4.10, bottom). Results with anidulafungin in RPMI were similar with increases in PI-positive cells and Flu-DsS3(1-16) staining when used in combination. This was most noticeable on exposure to 0.005 µg/ml anidulafungin. Individually anidulafungin caused ~5 % PI staining while in combination with Flu-DsS3(1-16) the proportion increased to ~ 35 % PI-positive and Flu-

DsS3(1-16) staining. As with caspofungin, vacuolar localisation decreased as the proportion of cells displaying disseminated peptide localisation increased.
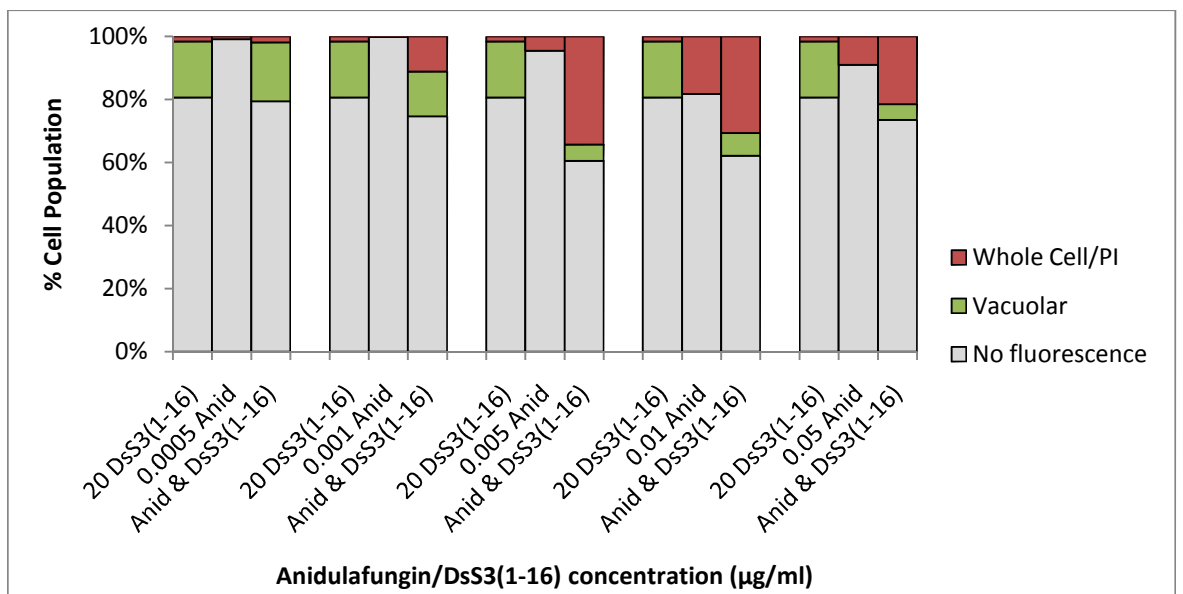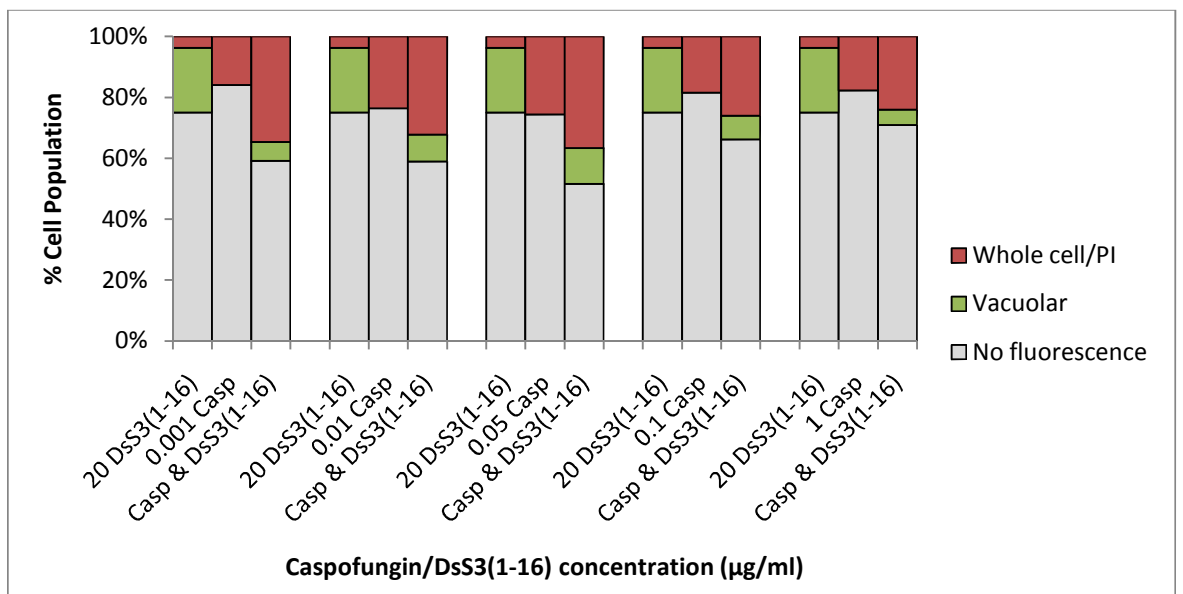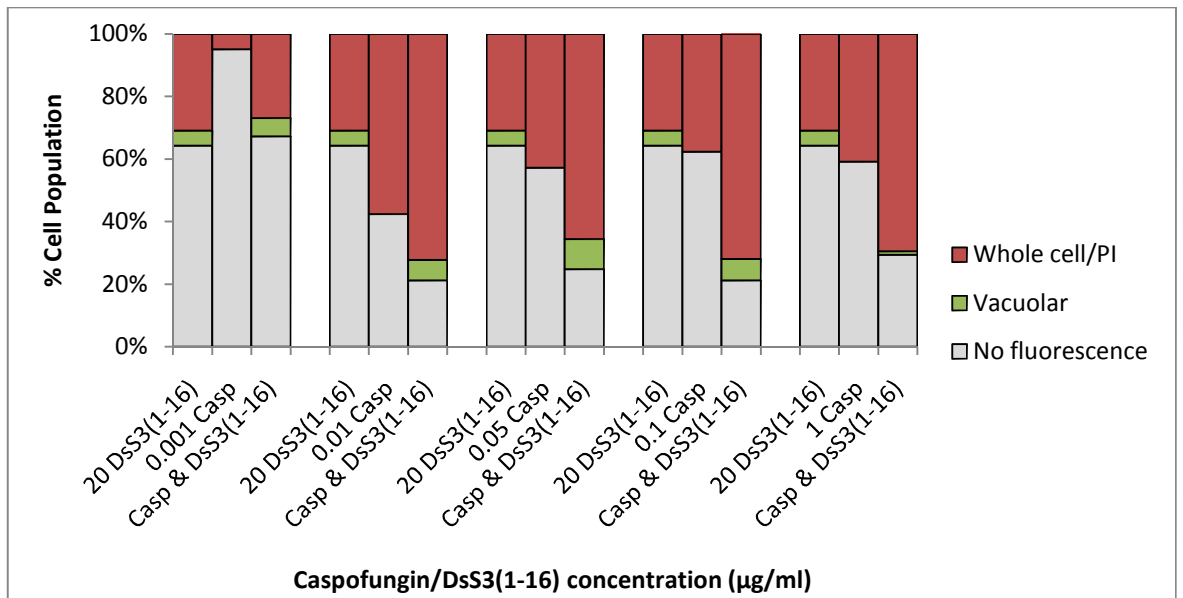
Figure 4.10. Fluorescent microscopy study quantifying cell viability and peptide sequestration in *C. albicans* SC5314. Cultures were incubated with Flu-DsS3(1-16) and echinocandin with P.I. A minimum of 200 cells (generally 300) from each assay were quantified to give the final results. Percent of cell population displaying whole cell/P.I. or vacuolar fluorescence in MEB with caspofungin (top), RPMI with caspofungin (middle) and RPMI with anidulafungin (bottom) are displayed; n = 2.

Representative images acquired from the microscope are presented (Figure 4.11). The initial set of three images (top) shows the fluorescence from Flu-(DsS3(1-16), from P.I. and a composite image of both. The three cells staining with P.I. were also seen to fluoresce throughout with Flu-DsS3(1-16). The two remaining cells have concentrated peptide present in their vacuoles and are absent of any P.I. staining. This demonstrates that cells with vacuolar localisation were viable while cells with fluorescence occurring throughout were non-viable. Representative images captured during an experiment using anidulafungin are also presented (Figure 4.11). Few cells were P.I. positive at concentrations of 0.0005 µg/ml and 0.001 µg/ml. At 0.005 µg/ml proportionally more cells display P.I. staining in the dual treatment. This also occurs at greater concentrations, although in reduced numbers. With 20 µg/ml, peptide vacuolarisation was observed up to 0.001 µg/ml of anidulafungin. These three data sets show that upon exposure to caspofungin or anidulafungin, the number of cells that show peptide internalisation and whole cell localisation was greatly increased.
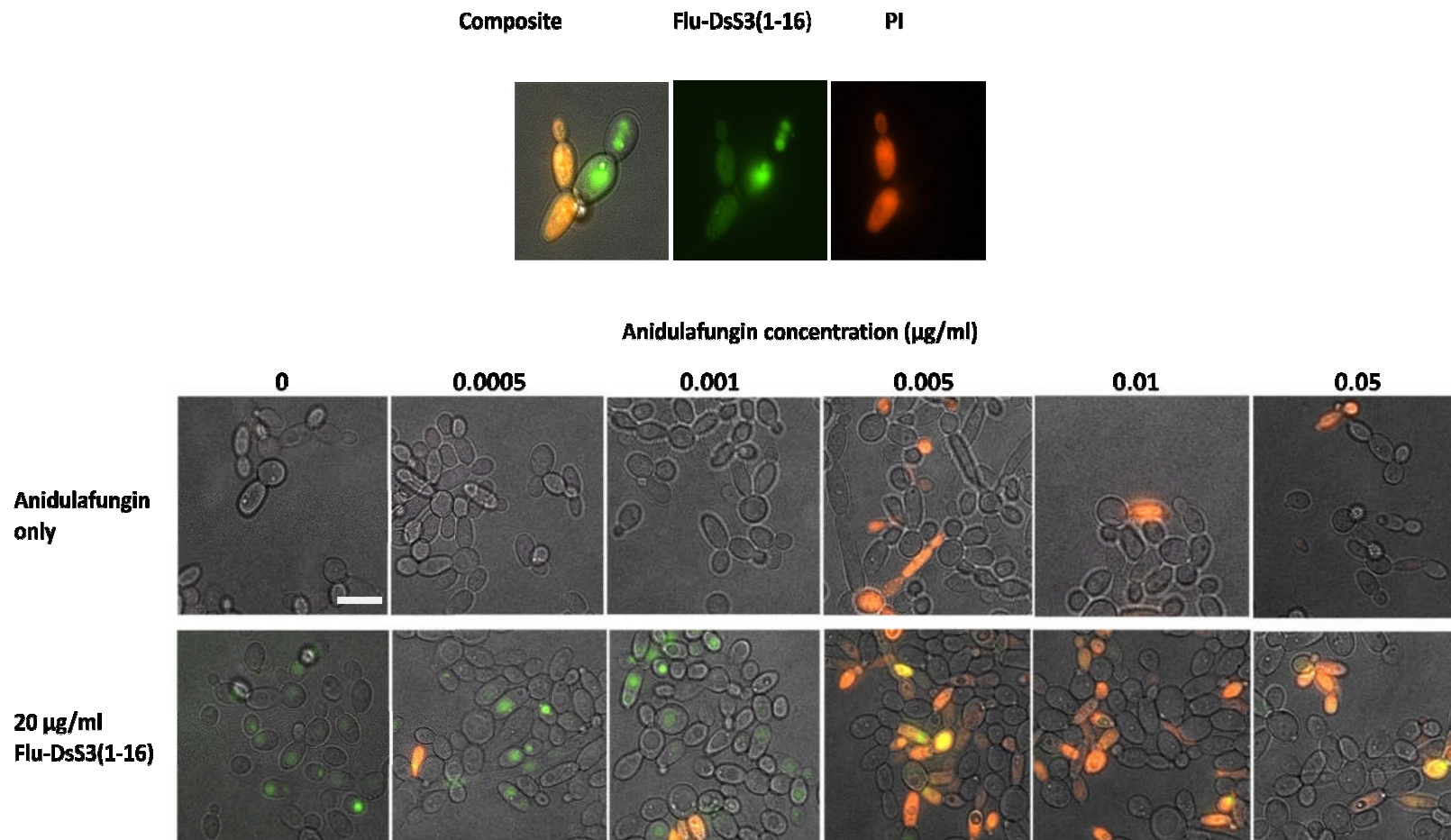
Figure 4.11. Image series representative of Flu-DsS3(1-16) localisation and PI staining. Initial three images (top) demonstrating P.I. staining when peptide has localised throughout the SC5314 cells leading to loss of cell viability. Flu-DsS3(1-16) that has localised to the vacuole display no P.I. staining indicating these cells remained viable. Below is a series of representative images from the anidulafungin assay displaying peptide vacuolarisation at low anidulafungin concentrations and increased P.I. and peptide incorporation at intermediate concentrations of 0.005 μg/ml and 0.01 μg/ml in combination; scale bar = 10 μM.

4.3 Discussion

The echinocandins are a relatively new class of antifungals that are active against *Candida* and *Aspergillus* species. They act by damaging the cell wall, inhibiting the synthesis of 1,3-β glucan. There are currently no reports of synergy between the echinocandins and antimicrobial peptides. As AMPs have to traverse the cell wall to access the plasma membrane it was postulated that the lack of 1,3-β glucan would increase peptide binding, leading to increased fungicidal killing. The results gathered in this chapter reveal the increased action of these antimicrobial agents when combined. The use of growth assays, disc diffusion assays, cell viability assays and fluorescent microscopy demonstrate the synergistic action of caspofungin and anidulafungin when combined with DsS3(1-16), mag 2, rana or GS14K4. Loss of viability was observed in *S. cerevisiae*, *C. albicans* SC5314 and clinical isolates of *C. albicans* and *C. glabrata*. This was further elucidated when FICs were calculated for each combination with the majority recording values of ≤0.5. In general, FICs with *C. glabrata* were higher than for the *C. albicans* clinical isolates. *C. glabrata* is genetically quite dissimilar from other *Candida* sp. and many conventional drugs are ineffective (Kurtzman *et al*, 1997) e.g. resistant to the azoles (Rex *et al*, 1995). They also display decreased susceptibility to the peptides used in this study.

The cyclic peptide gomesin, containing cysteine with two disulphide bonds, did not display synergistic characteristics against *S. cerevisiae* in initial studies with an additive growth pattern in combination with caspofungin. The cyclic synthetic peptide 6752 displayed no synergy in MEB with caspofungin while in combination with anidulafungin

the FIC values were increased further, approaching values that would indicate antagonism. The presence of 6752 substantially increased the anidulafungin MIC indicating peptide interference with anidulafungin activity on 1,3-β glucan synthase while retaining its antimicrobial activity (MICs for 6752 remained constant). As GS14K4 displayed strong synergistic killing in identical assays it is unlikely that this lack of action by 6752 was solely due to the cyclic structure. The action of 6752 against bacteria has been demonstrated (Dartois *et al*, 2005); however, its action against fungi was unknown. In this study the antifungal action of this peptide has been demonstrated. In terms of efficacy, levels of antifungal activity are comparable to mag 2 and rana. The antimicrobial activity of GS14K4 was previously determined (Kondejewski *et al*, 2002) and has now been demonstrated to kill *C. glabrata* and *S. cerevisiae* cells with levels similar to those observed with DsS3(1-16), which is effective at 3.45 µg/ml (Coote *et al*, 1998). These peptides are both short chains and so will be relatively inexpensive to synthesize and are effective at killing infectious strains of *Candida* so have the potential to be used as clinical antifungals. Their haemolytic and cytotoxic effects are analysed in Chapter 5.

All strains displayed severely inhibited growth in combinations of echinocandin and AMP with the exception of *C. neoformans*, where no interaction was observed, producing FIC values of 1.09 - 1.36. As the echinocandins are relatively ineffective against *C. neoformans*, with MICs ranging from 8 - 16 µg/ml (Dannaoui *et al*, 2008), this was not surprising. This resistance is not yet understood as it has been demonstrated that 1,3-β glucan synthase in *C. neoformans* is very sensitive to caspofungin. Other possible

mechanisms of resistance are currently under investigation including multidrug resistance pumps and degradation pathways (Maligie *et al*, 2005).

Both caspofungin and anidulafungin displayed potent synergistic killing, this however was not observed with micafungin. As demonstrated in the visible growth assays and disc diffusion assay (Section 4.2.4 and Appendix V), there was no observable increase in fungicidal action with micafungin on combination with DsS3(1-16), mag 2 or rana in RPMI media or MEB. FIC values in MEB (0.93 - 1.48) strongly indicated an additive rather than synergistic inhibitory effect. Values in RPMI ranged from 0.581 - 0.715 (with the exception of DsS3(1-16) against SC5314), again indicating no interaction was present. As the echinocandins differ in chemical structure there may be specific differences in peptide interaction (Denning, 2003). Micafungin contains a sulphate moiety, which increases its water solubility, that is absent in both caspofungin and anidulafungin (Figure 1.5). However, it is unlikely that this would be responsible for the lack of synergy. As the mode of action of all echinocandins is to inhibit 1,3-β glucan synthase, potentially allowing greater access to the plasma membrane, it is puzzling that similar results were not observed with micafungin.

The experiments performed in RPMI media generated consistently increased FIC values when compared to MEB media. Peptide action was also diminished with elevated MICs observed for all peptides. Cation interference for binding sites is unlikely as pH levels were maintained with MOPS. This decrease in activity may result from peptide binding

to proteins in the bovine calf serum. It is also likely that the salt content in this media was interfering with the peptides as RPMI 1640 contains 0.4 g/L KCL and 6 g/L NaCl. Salt leads to increased compaction of the membrane, increasing its structural integrity and reducing the destabilisation effect of AMPs (Kandasamy *et al*, 2006). For example, the activity of magainin was significantly reduced in the presence of 100 mM NaCl (Lee *et al*, 1997). However, on combination with caspofungin or anidulafungin, mag 2 is again more effective (inhibition at 5 μg/ml). This is a substantial decrease, proportionally far greater than levels displayed in MEB. The synergistic effects of this combination could be due to the reduced growth rate and diminished population densities of each strain when cultured in RPMI when compared to MEB. Cells may display increased inhibition and susceptibility if their growth rates and final population densities are reduced.

Data from the fluorescent microscopy study using Flu-DsS3(1-16) indicates that with peptide alone, few cells displayed peptide internalisation, especially in RPMI media. In the presence of caspofungin and anidulafungin the internalisation of peptide greatly increased. It is likely that the action of these echinocandins was increasing the peptide bound to the membrane by inhibiting the synthesis of 1,3-β glucan, thereby increasing the access of peptide to the membrane. This in turn may result in increased peptide internalisation. The images acquired during the study also demonstrate that cells that have sequestered peptide into their vacuoles (possibly via endocytosis) retain their viability as no P.I. staining occurred. Cells that display diffuse cytoplasmic localisation however have lost their viability as P.I. staining was present. This work also highlighted the reduced susceptibility of *C. albicans* cells at higher concentrations of echinocandin.

This phenomenon has been documented in several papers and is known as the paradoxical effect (Wiederhold *et al*, 2005; Stevens *et al*, 2006; Fleischhacker *et al*, 2008). One study observed this effect in 40 % of *C. albicans* strains tested when exposed to caspofungin and anidulafungin (Chamilos *et al*, 2007). The cause of the reduced efficacy is not clear, however, some studies suggest the involvement of the protein kinase C cell wall integrity pathway (Reinoso-Martin *et al*, 2003). An increase in chitin production (898 %) in *Candida* cells undergoing the paradoxical effect has also been proposed to compensate for the decrease in 1,3-β glucan and 1,6-β glucan following caspofungin treatment (Smits *et al*, 2001; Stevens *et al*, 2006).

It has been demonstrated in this chapter that combinations of cationic linear or cyclic AMPs with caspofungin or anidulafungin act synergistically to kill *S. cerevisiae*, *C. albicans* and *C. glabrata* strains. Cationic peptides have yet to be successfully developed into clinical antimicrobial drugs due to sensitivity to proteolytic degradation, toxicity levels and high cost of synthesis. Several have been developed for topical use only, including the protegrins and defensins (Chen *et al*, 2000; Cole *et al*, 2005). Combinations of drugs that act synergistically may be a route to clinical approval and application resulting in reduced dosages and toxicity, while still retaining their antimicrobial efficacy. It has also been demonstrated that these combinations result in effective killing of clinical infectious strains cultured on a porous solid surface resulting in large areas of inhibition around the treatment area. This combination treatment may have potential use as a topical treatment for invasive medical devices or for mucosal infection. The use

of caspofungin or anidulafungin with cationic antimicrobial peptides is patent pending as

of 8th September 2009 (No. GB0817121.7).

Chapter 5

5. The cytotoxic, haemolytic and antifungal activity of cationic antimicrobial peptides.

5.1 Introduction

Antimicrobial peptides are found throughout nature and constitute the first line of defence against infection from pathogenic microbes (Hancock *et al*, 1998). Many cationic AMPs have now been discovered that are potent killers of bacteria, fungi and viruses (Giuliani *et al*, 2008). Due to their potency they are of interest in the development of potential new antimicrobial therapeutics. Ideally these peptides should have potent antimicrobial activity with minimal cytotoxicity towards host cells. The effects of salt, ionic strength, temperature and exposure to proteins and macromolecules encountered in the changing microenvironments found in the human body must also be considered. Peptides may lose their antimicrobial action in biological fluids such as human serum where proteases may degrade AMPs (Tanaka *et al*, 2000). Components of human serum are also present in the mouth during inflammation, potentially affecting AMPs used in the treatment of oral fungal infections. This chapter aims to study the antimicrobial potency of several AMPs from various structural classes under different conditions *in vitro* against *S. cerevisiae* and assess their cytotoxic and haemolytic effects. The AMPs under investigation are the cationic α-helical peptides DsS3(1-16) and mag 2, the cationic peptides containing cysteine with one or two disulphide bonds (rana and gomesin respectively) and the synthetic cyclic peptides GS14K4 and 6752.

5.2 Results

5.2.1 Effects of salt, pH, temperature and human serum on AMP antifungal activity.

Growth of *S. cerevisiae* cultures was monitored in the presence of AMPs and the effects of NaCl, pH, temperature and human serum were analysed. MICs were obtained for each AMP against *S. cerevisiae* in MEB. Gomesin displayed potent antifungal action with an MIC of 1.5 µg/ml followed by GS14K4 (2 µg/ml), DsS3(1-16) (5 µg/ml), 6752 (8 µg/ml), rana (11 µg/ml) and finally mag 2 (13 µg/ml) (Table 5.1). The presence of NaCl decreased the antifungal potency of each AMP. The MICs increased as salt concentration increased and were >100 µg/ml (the highest concentration tested) for DsS3(1-16), mag 2 and 6752 at 200 mM NaCl. Gomesin's MIC increased to 30 µg/ml, GS14K4's MIC increased to 50 µg/ml and rana's MIC increased to 50 µg/ml at 200 mM NaCl.

For each AMP, greatest antifungal activity was observed at pH 7 (Table 5.2). As the media pH increased or decreased away from neutrality there was a concomitant decrease in antifungal efficacy e.g. 6752 had a MIC of 8 µg/ml at pH 7 but at pH 9 this increased to 11 µg/ml whilst at pH 5 the MIC was 14 µg/ml. All AMPs with the exception of mag 2 were more affected by increased acidity compared to increased basicity.

After incubation of AMP at temperatures up to 100 °C, all peptides retained antifungal activity with only a slight increase in MIC for DsS3(1-16) (1 µg/ml), mag 2 (3 µg/ml), 6752 (2 µg/ml) and GS14K4 (2 µg/ml) (Table 5.3). There was no change in the potency of rana

and there was a slight increase in the MIC of gomesin (0.25 µg/ml). There was no change in MIC values comparing the 80 °C and 100 °C incubated peptide aliquots.

At concentrations above 6 % human serum (HS; active or inactive), growth of *S. cerevisiae* was inhibited, as such, concentrations of up to 5 % were used at which no inhibition was observed (Tables 5.4 and 5.5). As the concentration of active HS in the media increased so the MIC values for each peptide also increased. This was most noticeable for 6752, which had a MIC of 8 µg/ml in the absence of HS, but in 1 % HS the MIC increased to 25 µg/ml. MICs were even higher for 6752 in 3 – 5 % HS (50 µg/ml). Rana and mag 2 generated MICs above 50 µg/ml (the greatest concentration used). Gomesin was least affected by HS with no increase in MIC at 1 % and a slight increase (to 4 µg/ml) at 3 – 5 %. The results with inactivated HS showed similar trends of inhibition of action but the AMPs were affected to a reduced degree.

Table 5.1. MIC determination for each AMP against *S. cerevisiae* exposed to various concentrations of NaCl; n = 2, ± 1 SD in brackets.

NaCl	DsS3(1-16)		Ranalexin		Magainin 2		Gomesin		6752		GS14K4	
control	5	(0)	11	(0.58)	13	(1.15)	1.5	(0.14)	8	(0)	2	(0)
50 mM	20	(2.89)	15	(0)	15	(2.89)	2	(0)	30	(2.89)	2	(0.29)
100 mM	50	(0)	50	(11.5)	100	(28.9)	4	(0)	50	(0)	10	(1.15)
150 mM	100	(0)	50	(0)	>100	(0)	8	(1.15)	100	(28.9)	30	(11.5)
200 mM	>100	(0)	50	(0)	>100	(0)	30	(2.89)	>100	(0)	50	(0)

Table 5.2. MIC determination for each AMP against *S. cerevisiae* at various pH values; n = 2, ± 1 SD in brackets.

pH	DsS3(1-16)		Ranalexin		Magainin 2		Gomesin		6752		GS14K4	
5	12	(1)	22	(2.31)	25	(2.31)	2	(0.14)	14	(1.15)	7	(1.53)
6	6	(0)	20	(1.53)	15	(1)	1.25	(0.14)	10	(1.15)	2	(0.25)
7	5	(0)	11	(0)	13	(0.58)	1	(0)	8	(0.58)	2	(0.14)
8	5	(0)	18	(0.58)	17	(1.15)	1	(0)	9	(1.73)	3	(0)
9	7	(0.58)	20	(0.58)	25	(0.73)	1.25	(0.25)	14	(1.53)	6	(0.58)

Table 5.3. MIC determination for each AMP exposed to various temperatures (prior to peptide addition) against *S. cerevisiae*; n = 2, ± 1 SD in brackets.

temp. (°C)	DsS3(1-16)		Ranalexin		Magainin 2		Gomesin		6752		GS14K4	
30	5	(0)	11	(0)	13	(0)	1.5	(0)	8	(0)	2	(0)
80	6	(0.58)	11	(0)	15	(0)	1.25	(0)	10	(0)	3	(0.29)
100	6	(0)	11	(0)	15	(0)	1.25	(0.14)	10	(1.15)	4	(0.29)

Table 5.4. MIC determination for each AMP against *S. cerevisiae* exposed to various concentrations of active HS; n = 2, ± 1 SD in brackets.

% HS (Active)	DsS3(1-16)		Ranalexin		Magainin 2		Gomesin		6752		GS14K4	
0	5	(0)	12	(0.58)	14	(0.58)	1.5	(0)	8	(0)	2	(0)
1	22	(1.15)	25	(2.31)	30	(0)	1.5	(0.25)	25	(0)	8	(1.15)
2	25	(2.31)	50	(0)	50	(0)	2	(0.14)	30	(11.5)	15	(1.73)
3	30	(2.31)	>50	(0)	>50	(11.5)	4	(0)	50	(0)	25	(0)
5	30	(0)	>50	(0)	>50	(0)	4	(0.58)	50	(0)	25	(2.89)

Table 5.5. MIC determination for each AMP against *S. cerevisiae* exposed to various concentrations of heat-inactivated HS; n = 2, ± 1 SD in brackets.

% HS (Inactive)	DsS3(1-16)		Ranalexin		Magainin 2		Gomesin		6752		GS14K4	
0	5	(0)	12	(0.58)	14	(0.58)	1.5	(0)	8	(0)	2	(0)
1	20	(1.15)	30	(2.89)	30	(0)	2	(0.29)	25	(0)	8	(1.15)
2	22	(2)	30	(2.89)	50	(14.4)	4	(1.15)	25	(2.89)	20	(0)
3	25	(0)	50	(11.5)	50	(0)	4	(1)	30	(11.5)	25	(2.89)
5	25	(0)	50	(0)	50	(0)	5	(0.58)	30	(0)	25	(0)

5.2.2 *In vitro* haemolytic assay of echinocandins and AMPs

The lytic activities of the AMPs and echinocandins (anidulafungin and caspofungin) were assessed against horse erythrocytes. (Tables 5.6 – 5.7). AMPs were not lytic at 2 µg/ml (Table 5.6), but at 5 µg/ml, rana, 6752 and GS14K4 caused low level haemolysis (0.5 – 4.1 %). Haemolytic activity of these peptides increased in a concentration dependent manner. DsS3(1-16) and gomesin were not lytic even at 50 µg/ml followed by mag 2 (5.2 %), 6752 (5.3 %), GS14K4 (8.3 %) and rana (19.1 %). Caspofungin was non-haemolytic up to 30 µg/ml (10 %) while increasing to 50 µg/ml caused 32 % lysis. Anidulafungin was haemolytic at 1 µg/ml (6.7 %) through 50 µg/ml (47.5 %). As anidulafungin was solubilised in 20 % (v/v) ethanol this was used as an additional control and generated no haemolytic activity.

Combinations of echinocandin and peptide were subsequently monitored (Table 5.7). In the presence of caspofungin there was no lysis recorded up to 10 µg/ml of caspofungin and 30 µg/ml of AMP. At the highest concentration tested there was no lysis with gomesin followed by DsS3(1-16) (3.1 %), 6752 (3.5 %), mag 2 (5 %), GS14K4 (10 %) and rana (14.6 %). The combination of anidulafungin and AMP caused increased lysis with up to 16.7 % at 1 µg/ml anidulafungin and 10 µg/ml of peptide. At the greatest concentration, lysis was increased to 31.9 – 34.9 % for all AMPs with the exception of 6752 recording 76.6 % haemolysis.

In summary, DsS3(1-16) and gomesin displayed no toxicity towards erythrocytes. A combination of caspofungin and AMP produced low levels of toxicity while combinations of anidulafungin and AMP displayed lysis at the lowest concentrations tested.

Table 5.6. Erythrocytes exposed to various concentrations of AMP or echinocandin. Lytic activity was determined at OD$_{570}$. Results are displayed as percentage haemolysis compared to the control. Water was used as a positive control and reference point for complete lysis; n = 3, ± 1 SD in brackets.

	Concentration (µg/ml)						
	1	**2**	**5**	**10**	**20**	**30**	**50**
DsS3(1-16)	0 (0)	0 (0)	0 (0)	0 (0)	0 (0)	0 (0)	0 (0)
Ranalexin	0 (0)	0 (0)	4.1 (3.4)	6.2 (2.1)	4.7 (1.3)	6.8 (5.1)	19.1 (4.9)
Magainin 2	0 (0)	0 (0)	0 (0)	0 (0)	0 (0)	0 (0)	5.2 (3.2)
Gomesin	0 (0)	0 (0)	0 (0)	0 (0)	0 (0)	0 (0)	0 (0)
6752	0 (0)	0 (0)	0.7 (0.5)	0.7 (0.5)	0 (0)	0 (0)	5.3 (1.7)
GS14K4	0 (0)	0 (0)	0.5 (0.5)	0 (0)	9.1 (4.5)	7.9 (5.1)	8.3 (5)
Caspofungin	0 (0)	0 (0)	0 (0)	0 (0)	0 (0)	10 (2.6)	32 (7.9)
Anidulafungin	6.7 (3.2)	6.9 (5.5)	23 (13.5)	38.8 (23.3)	36.8 (18.2)	36.1 (17.9)	47.5 (18.4)

Table 5.7. Erythrocytes exposed to various concentrations of AMP with echinocandin. Lytic activity was determined at OD$_{570}$. Results are displayed as percentage haemolysis compared to the control. Water was used as a positive control and reference point for complete lysis; n = 3, ± 1 SD in brackets.

	Concentration (µg/ml)			
	1 & 10	**5 & 20**	**10 & 30**	**15 & 50**
Caspofungin & DsS3(1-16)	0 (0)	0 (0)	0 (0)	3.1 (1.1)
Caspofungin & Ranalexin	0 (0)	0 (0)	0 (0)	14.6 (4.6)
Caspofungin & Magainin 2	0 (0)	0 (0)	0 (0)	5 (0.3)
Caspofungin & Gomesin	0 (0)	0 (0)	0 (0)	0 (0)
Caspofungin & 6752	0 (0)	0 (0)	0 (0)	3.5 (2.7)
Caspofungin & GS14K4	0 (0)	0 (0)	0 (0)	10 (3.1)
Anidulafungin & DsS3(1-16)	11.9 (2.9)	14.5 (5.8)	23.7 (4.2)	34.9 (4.9)
Anidulafungin & Ranalexin	16.1 (5)	18.7 (4.6)	22.8 (6.3)	33.1 (6.6)
Anidulafungin & Magainin 2	11.3 (2.8)	22.7 (7)	25.8 (4)	26.9 (7)
Anidulafungin & Gomesin	8.6 (0.7)	10.7 (1.2)	18.3 (1.9)	31.9 (5.4)
Anidulafungin & 6752	0 (0)	18.7 (1.1)	19.1 (6.4)	76.6 (9.9)
Anidulafungin & GS14K4	16.7 (2.5)	15.3 (2.6)	24.7 (2.5)	33.9 (5.2)

5.2.3 *In vitro* mammalian cell cytotoxicity assay of echinocandins and AMPs

Cytotoxicity assays were performed using *Vero* cells with a fibroblast morphology, the most common cell type in connective tissue. This lineage can be replicated through many cycles of division without senescence so was selected (Yasamura *et al*, 1963). Viability was measured after exposure to AMP and echinocandin using the neutral red procedure (Borenfreund *et al*, 1985). Cell viability was unaffected by caspofungin up to 50 μg/ml (Figure 5.1). Anidulafungin at 10 μg/ml reduced cell viability to 89 % but similar viability reductions were seen up to 50 μg/ml (87 % viability). *Vero* cell viability after exposure to AMPs remained unchanged up to 50 μg/ml (97.3 – 100 %) (Figure 5.2). As AMP concentration increased to 100 μg/ml, cytotoxicity was apparent with rana (79.2 %), gomesin (64.5 %) and GS14K4 (33.9 %). Exposure to DsS3(1-16), mag 2 and 6752 resulted in only slight reductions in viability (95.1 – 99.8 %).

Vero cell viability was assessed with combinations of echinocandin with AMPs (Figures 5.3 – 5.4). At low concentrations there was no cytotoxicity with caspofungin and AMP. At 15 μg/ml caspofungin and 50 μg/ml AMP there was reduced viability with rana (85.5 %) and gomesin (96 %). At 100 μg/ml caspofungin and AMP further reductions were observed: GS14K4 (51.1 % viable), rana (72 %), DsS3(1-16) (82.7 %), gomesin (83.4 %), 6752 (94.9 %) and mag 2 (97.3 %). With 10 μg/ml anidulafungin, cytotoxicity was apparent with DsS3(1-16) (11.2 %) and gomesin (10.7 %). At 100 μg/ml anidulafungin and AMP, viability was reduced further: GS14K4 (16.5 % viable), gomesin (36 %), mag 2 (42.4 %), 6752 (65.7 %), DsS3(1-16) (67.4 %) and rana (78.6 %). As a positive control, CCCP was added at 0.15 μg/ml and rendered 76.7 % of cells non-viable.

In summary, DsS3(1-16), mag 2 and 6752 displayed no cytotoxicity against *Vero* cells when used individually up to 100 μg/ml. In combination with caspofungin, cytotoxicity was observed only at the highest concentrations. In combination with anidulafungin, cytotoxicity was increased and observed with all AMPs at reduced concentrations compared to caspofungin. However, these concentrations are much greater than those required to inhibit growth of *C. albicans in vitro.*
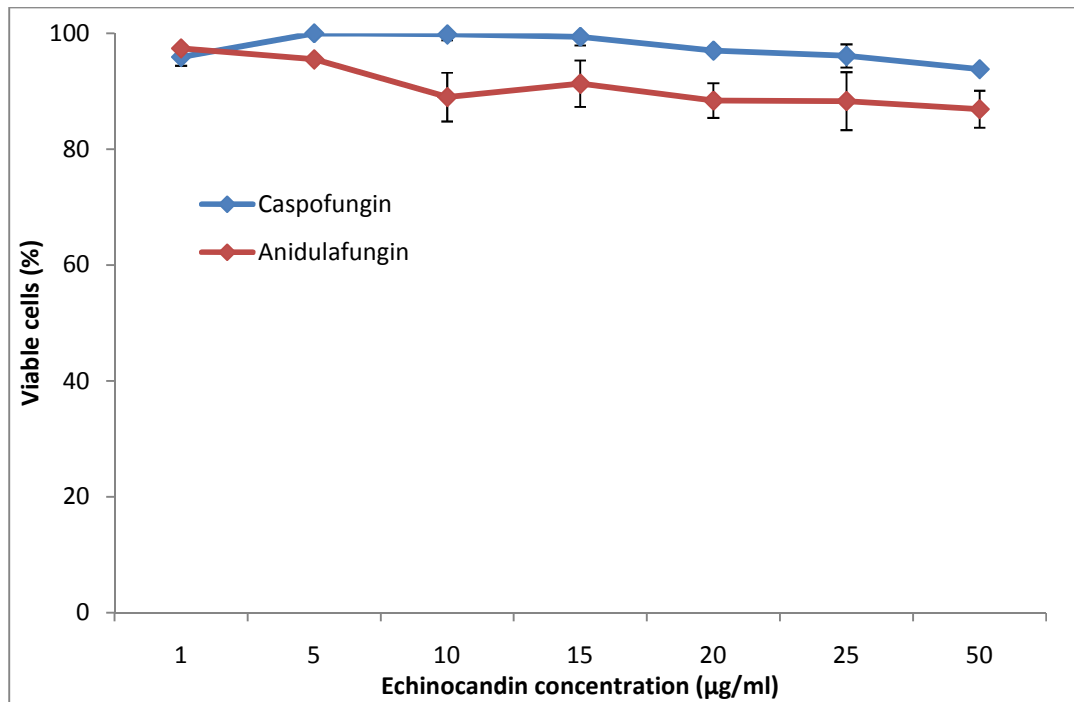
Figure 5.1. Mammalian cell cytotoxicity assay with echinocandins. *Vero* cells were exposed to echinocandins and cytotoxicity was determined via the neutral red assay. Viability was determined by percentage of control value; n = 2 ± 1 SD.
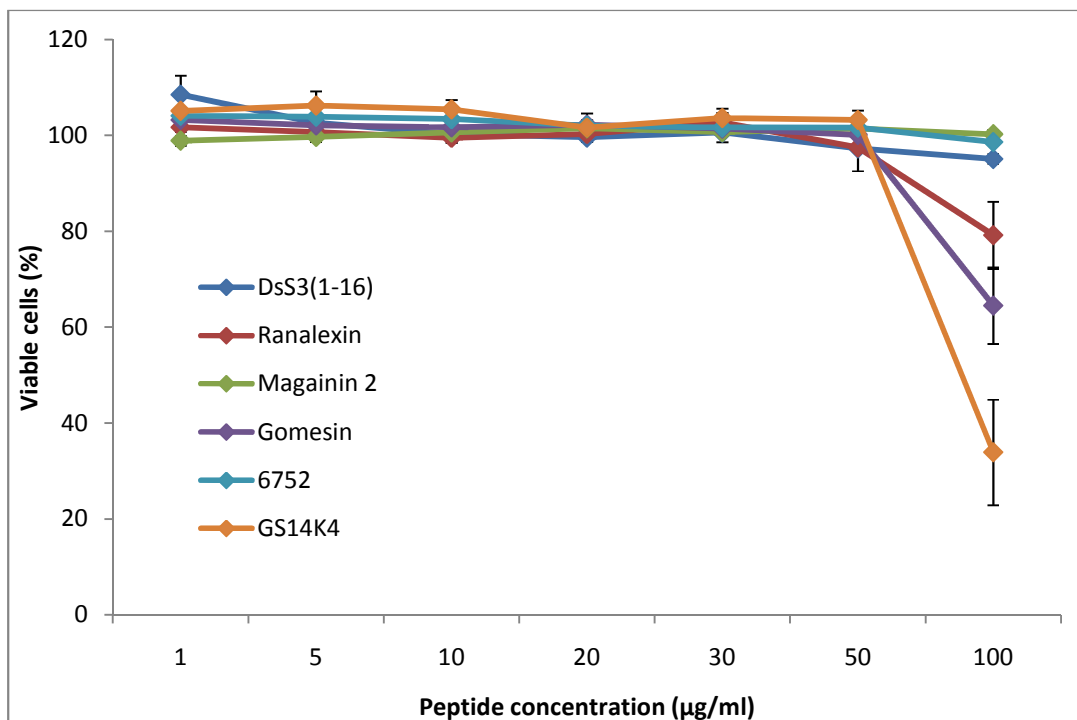
Figure 5.2. Mammalian cell cytotoxicity assay with AMPs. *Vero* cells were exposed to AMPs and cytotoxicity was determined via the neutral red assay. Viability was determined by percentage of control value; n = 2 ± 1 SD.
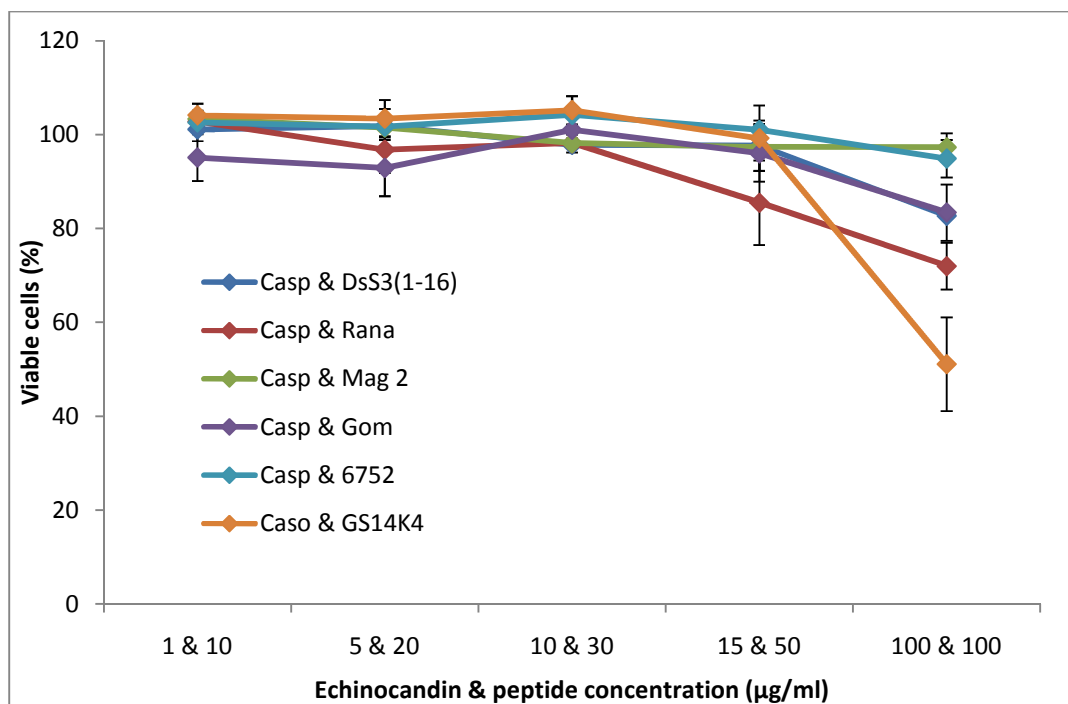
Figure 5.3. Mammalian cell cytotoxicity assay with combinations of AMP and caspofungin. *Vero* cells were exposed to AMPs with caspofungin and cytotoxicity was determined via the neutral red assay. Viability was determined by percentage of control value; n = 2 ± 1 SD.
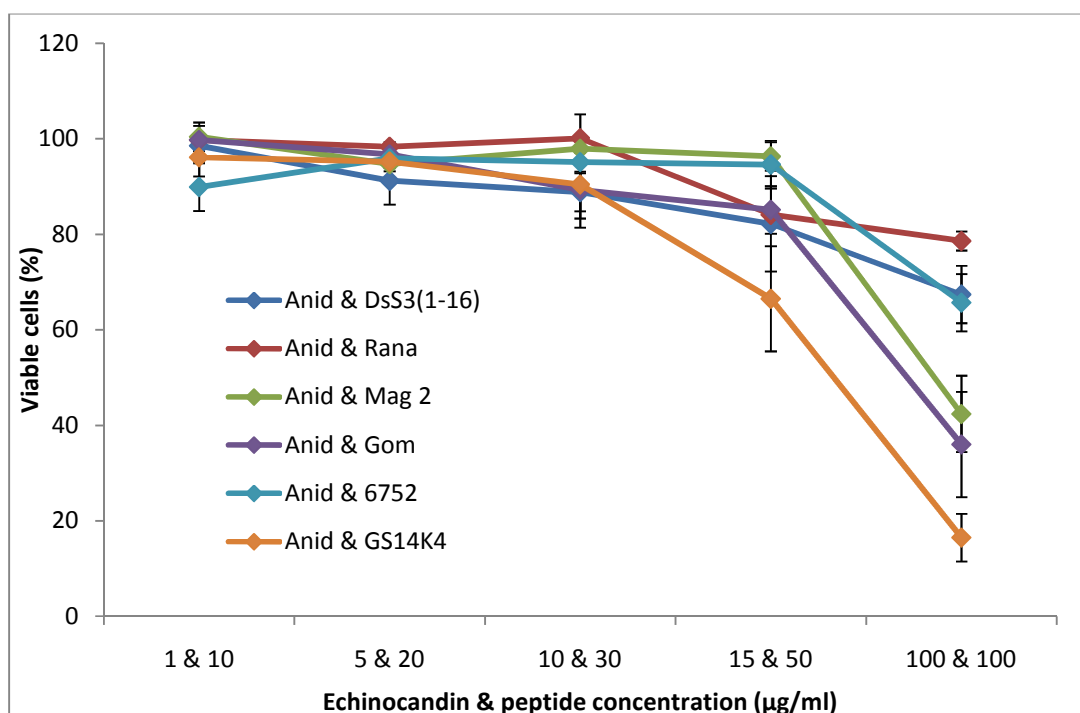
Figure 5.4. Mammalian cell cytotoxicity assay with combinations of AMP and anidulafungin. *Vero* cells were exposed to AMPs with anidulafungin and cytotoxicity was determined via the neutral red assay. Viability was determined by percentage of control value; n = 2 ± 1 SD.

5.2.4 Efficacy *in vivo* of the combination of caspofungin with ranalexin in a murine model of disseminated Candidiasis

This work was performed by Prof. Frank Odds group, School of Medical Sciences, University of Aberdeen. In the first experiment, with caspofungin given IP at 0.01 mg/kg, the 72 h kidney burden was reduced significantly below placebo (p<0.05) in mice given the caspofungin/ranalexin combination: however, the extent of the effect was less than a 1-log burden reduction (Table 5.8). No significant reduction in weight loss relative to placebo-treated mice was seen for any of the test agents. In the second experiment, with a greater caspofungin dose of 0.05 mg/kg, IV dosing of both test agents, and BID dosing of ranalexin, highly significant (p<0.01) reductions in kidney burdens and 3-day weight loss were seen for groups of animals receiving treatments that included caspofungin. Disappointingly, the combination treatment did not result in enhanced efficacy compared to the single treatments.

Table 5.8. The effect of combination treatment with caspofungin and ranalexin compared to the individual treatments alone on kidney burden of *C. albicans* SC5314 and animal weight in a mouse model of disseminal Candidiasis. Mean ± 1 SD.

treatment	kidney $\log_{10}$ CFU/g mean	weight change (%) day 0 - day 3 mean
saline IP/saline IV	4.1 (0.6)	0.3 (3.5)
caspofungin (0.01 mg/kg) IP/saline IV	3.4 (0.4)	1.4 (2.5)
saline IP/ranalexin IV	3.8 (0.6)	-1.0 (2.4)
caspofungin IP/ranalexin IV	3.4 (0.3)	-1.1 (1.9)
saline IV	4.0 (0.3)	-5.8 (0.9)
caspofungin (0.05 mg/kg) IV	2.5 (0.3)	-2.2 (1.4)
ranalexin (10 mg/kg) IV	4.5 (0.7)	-5.0 (3.3)
caspofungin & ranalexin IV	3.2 (0.2)	-1.5 (1.6)

***p<0.05** and ***p<0.01** relative to placebo-treated group (Mann-Whitney *U* test).

5.3 Discussion

Resistance to conventional antimicrobials is increasingly prevalent and treatment with drugs can be complicated by toxicity and the emergence of drug-resistant strains (Pfaller *et al*, 2007). To combat drug resistant pathogens new antimicrobial treatments must be considered. As antimicrobial peptides have a wide spectrum of activity against many pathogenic microorganisms and resistance events are extremely rare due to their mode of action they are of interest for the development of new treatments (van't Hof *et al*, 2001). Therefore, it is important that new drugs have low toxicity, long half-life in the body and retain antimicrobial activity *in vivo*. In this chapter the efficacy of several AMPs has been determined against *S. cerevisiae* in the presence of various salt, pH, temperature and human serum conditions. AMPs had reduced efficacy in salt conditions, at pH values deviating from neutral and with HS, but were not affected by exposure to high temperature. The haemolytic and cytotoxic properties of these peptides have also been investigated with no increase in lytic activity when echinocandins and AMPs were combined.

All AMPs were inhibited by NaCl with a 25-fold increase in MIC with one peptide. This will be problematic for future treatment considering that physiological NaCl concentrations are in the range of 150 mM (Maeda *et al*, 1990) and also for topical treatments given the salt content of sweat which contains ~ 0.9 g/L sodium (Montain *et al*, 2007). NaCl resistance is important for the activity of AMPs *in vivo*. For example, an increase in NaCl concentration in the lungs to 120 mM decreased the activity of AMPs produced on the mucosal surface (Goldman *et al*, 1997). The presence of divalent

cations such as $CaCl_2$ and $MgCl_2$ also resulted in decreased activity of several mammalian AMPs (Lehrer *et al*, 1988). The ability of AMPs to resist high salt concentrations is important for the development of future therapeutic applications.

The pH also influenced the efficacy of AMPs with increased MICs in acidic or basic conditions. The action of all peptides was greatest at neutral pH values. As the pH is decreased this would result in neutralisation of the negative charges found on the membrane surface (Dychala *et al*, 1991) which, in turn, would reduce the binding affinity of cationic AMPs, probably reducing their activity. This is problematic for future topical applications given the acidic conditions on the skin surface (~pH 5.6) and in the stomach. If used intravenously, the blood has a closely regulated pH of 7.35 - 7.45 so ionic interference would be less problematic. However HS substantially increased the MIC of each peptide probably due to the presence of inhibiting proteins, peptidases or other macromolecules or salts which competitively bind peptide monomers. The serum may also contain molecules that could obscure the sites of peptide action on the yeast cell wall or membrane. Active HS had the greatest effect on peptide action, however, both decreased antifungal action suggesting the proteins and peptidases contribute but are not wholly responsible to loss of efficacy (Panyutich *et al*, 1991). In order to reduce HS interference, derivatives of these AMPs may have to be developed with reduced affinity from interfering components that would increase therapeutic potential.

All peptides displayed low-level haemolytic activity at concentrations in excess of those required for *S. cerevisiae* inhibition with the exception of rana. Similar results were obtained for caspofungin. With combinations of AMP and caspofungin there was no increase in haemolytic activity when comparing individual results to combined, while on combination with anidulafungin a slight increase in haemolysis was observed.

All peptides displayed no cytotoxicity towards mammalian *Vero* cells up to 50 µg/ml. In combination with caspofungin there was no increase in cytotoxicity. In combination with anidulafungin there was only a slight increase in cytotoxicity. *C. albicans* cultures were rendered non-viable at concentrations >100 µg/ml in RPMI (Chapter 4), at similar concentrations cytotoxicity against *Vero* cells was observed with rana, gomesin and GS14K4 indicating these AMPs are cytotoxic to mammalian cells at fungicidal concentrations. However, DsS3(1-16), mag 2 and 6752 did not display cytotoxic activity either individually or in combination with caspofungin so may warrant further investigation. Additionally, gomesin displayed no haemolytic activity so should also be considered. The mode of action of mag 2 against mammalian cells is different from that of microbes. Instead of forming toroidal pores (Tachi *et al*, 2002) it caused membrane deformation including budding on mammalian membranes displaying a 'carpet-like' action (Imura *et al*, 2008). Mag 2 has previously been shown to cause haemolysis but at far greater concentrations than bactericidal and fungicidal levels (Imura *et al*, 2008). Importantly, the study revealed that concentrations of the antifungals in combination that are much greater than concentrations necessary to completely inhibit growth of *C. albicans in vitro* did not induce cytotoxicity *in vitro*.

The combination treatment was further investigated using a murine model for preliminary *in vivo* studies. Effectiveness was monitored using fungal kidney burden and animal weight. A single combination of caspofungin and rana was tested at one concentration and selected as previous work using this peptide had generated appropriate *in vivo* dosages that were non-toxic. Disappointingly, there was no indication of enhanced efficacy of these antifungal agents in the murine models, some of which demonstrated rana toxicity. As only one combination was tested due to limited resources there is still scope for further investigation using antimicrobial peptides that show reduced toxicity *in vivo.*

The dermaseptins show very low levels of haemolytic activity at levels far above their antimicrobial concentrations (Helmerhorst[b] *et al*, 1999; Brand *et al*, 2002). A truncated 16 a.a. derivative of Dermaseptin S4 displayed good antimicrobial activity in a murine model with no toxicity (Navon-Venezia *et al*, 2002). Recently Dermaseptin 01 has been shown to have no significant lytic effect on mammalian erythrocytes or tissues *in vivo* (Leite *et al*, 2008). DsS3(1-16) displays similar characteristics *in vitro* and is a truncated version of the native form increasing its suitability for peptide synthesis. Future work will be beneficial in establishing its therapeutic index. Gomesin displayed levels of cytotoxicity towards mammalian cells which have been reported previously (Fazio *et al*, 2006). Several gomesin analogues have been developed that retain the same antimicrobial activity and reduce the cytotoxic effects increasing its therapeutic index (Fazio *et al*, 2007). These results indicate that derivatives of gomesin are of increased

interest in terms of their therapeutic potential even with the lack of synergy on combination with echinocandins (Chapter 4).

Chapter 6

6. Deletion of *HAL5, LDB7* and *IMP2'* in *S. cerevisiae* results in increased susceptibility to several cationic antimicrobial peptides.

6.1. Introduction

Most studies suggest that AMPs exert their antifungal action by interacting with the plasma membrane, however, AMPs may also affect intracellular targets (Morton[a] *et al*, 2007; Hale *et al*, 2007). These alternative modes of action may function as complementary mechanisms that are required to kill certain pathogens. For example, thrombin-induced platelet microbicidal protein (tPMP) acts to permeabilise the membrane of *S. aureus* cells. After this membrane action, cells were found to remain viable long after exposure. It was discovered that tPMP acts to inhibit DNA and RNA synthesis some 30 min after membrane permeabilisation (Xiong *et al*, 2002). Furthermore, cells were exposed to antibiotics immediately prior to peptide addition that inhibited DNA or protein synthesis and prevented tPMP killing. Thus an additional mode of action of certain cationic peptides may be to bind negatively charged nucleic acids, causing or further increasing their antimicrobial action. AMPs have also been discovered that inhibit intracellular organelles. For example, the cationic peptide histatin-5 was found to perturb the membrane and inhibit mitochondrial transmembrane potential (Helmerhorst[a] *et al*, 1999).

A study comparing the inhibitory effects of mag 2 and DsS3(1-16) on the model fungus *S. cerevisiae* employed global deletion mutant library phenotypic screening and expression analysis. This involved the screening of 4,847 nonessential gene deletions in *S. cerevisiae* BY4741 *MAT*a. Of these genes, it was found that 0.7 % showed sensitivity to both peptides, 1.7 % showed DsS3(1-16) sensitivity only and 0.4 % showed mag 2 sensitivity only (Morton[b] *et al*, 2007). Three such genes that confer sensitivity upon deletion to both peptides were *LDB7*, *IMP2'* and *HAL5*. Moreover, *HAL5* was the only gene found to become up-regulated upon treatment with mag 2 and DsS3(1-16).

The low-dye-binding (*LDB*) genes are involved in the RSC (Remodelling the Structure of Chromatin) chromatin remodelling complex that is implicated in nuclear protein transport and chromatin structure. Ldb7 encodes the protein Rsc14 that is a subunit forming the RSC complex (Wilson *et al*, 2006) and is involved in the transfer of mannosylphosphate groups into the N-linked oligosaccharides on the cell wall (Corbacho *et al*, 2004). This complex is also required to maintain cell wall integrity as *rsc14Δ* mutants displayed cell wall defects. Additionally, RSC is involved in DNA damage response; it was shown that deletion of *RSC7* confers more sensitivity to DNA damaging agents (Wilson *et al*, 2006). This complex has also been implicated in double-strand break repair (Chai *et al*, 2005).

IMP2' encodes a transcription factor and is involved in glucose signalling. It also indirectly regulates GAL gene expression, which is involved in galactose metabolism

(Alberti *et al*, 2003). The role of *IMP2'* may be more extensive, as *IMP2'* mutants are hypersensitive to temperature, oxidative damage and osmotic stress. *IMP2'* encodes a protein that protects the cell against DNA-damage from oxidative agents as imp2' mutants display an increase in genetic recombination (Masson *et al*, 1996).

HAL5 acts with *HAL4* to regulate the Trk1-Trk2 potassium transporter. It acts by increasing the influx of potassium and decreasing the electrical membrane potential and is activated by low potassium levels and sodium stress (Ramos *et al*, 1990). This is achieved via the regulation of the potassium transporter, Trk1-Trk2. Over expression of both *HAL4* and *HAL5* increase sodium and lithium tolerance by reducing accumulation and increasing intracellular potassium while deletion confers sensitivity (Mulet *et al*, 1999). It has since been discovered that Hal4 and Hal5 kinases are involved in the stability of the Trk1 transporter. These potassium transporters are degraded on deletion of these genes while over-expression results in an increased build up of Trk1 in the plasma membrane (Perez-Valle *et al*, 2007). *HAL5* is an indirect regulator of membrane potential and therefore may influence the susceptibility of the cell to cationic antimicrobial agents. Deletion of *HAL4* and *HAL5* also confers increased sensitivity to several chemotherapeutic agents due to loss of selectivity of plasma membrane transporters resulting in increased drug transport (Thornton *et al*, 2005). As *LDB7*, *IMP2'* and *HAL5* confer changes in sensitivity to both DsS3(1-16) and mag 2 and phenotype screening shows their change in regulation upon exposure, these genes were selected for additional studies to elucidate their involvement in response to AMP action.

6.2 Results

6.2.1 MIC determination

MICs with DsS3(1-16), mag 2 and rana were determined with deletion strains and performed as described previously (Section 3.2.1). The BY4741a wt strain had a MIC of 20 µg/ml for rana, 8 µg/ml for DsS3(1-16) and 14 µg/ml for mag 2 (Table 6.1). The mutant strains were more sensitive to the action of all the peptides. The *ldb7Δ* strain was more susceptible to rana (MIC of 18 µg/ml), DsS3(1-16) (MIC of 6 µg/ml) and mag 2 (MIC of 12 µg/ml). Similarly, the *hal5Δ* mutant had reduced MICs compared to the parent strain against rana, DsS3(1-16) and mag 2 with MICs of 18, 4 and 10 µg/ml respectively. Moreover, with the *imp2'Δ* deletion strain MICs for rana, DsS3(1-16) and mag2 were 18, 6 and 12 µg/ml respectively. All deletion mutants selected here displayed increased sensitivity when exposed to DsS3(1-16), mag 2 and rana.

Table 6.1. MIC values of wt, *hal5Δ*, *ldb7Δ* and *imp2'Δ* when exposed to DsS3(1-16), mag 2 and rana. Plate scans in appendix II; n = 3.

	MIC (µg/ml)		
	DsS3(1-16)	Magainin 2	Ranalexin
wt	8	14	20
hal5Δ	4	10	18
ldb7Δ	6	12	18
imp2'Δ	6	12	18

6.2.2 Growth of deletion mutants

To further study the increased susceptibility of *S. cerevisiae* cells on deletion of *HAL5*, *LDB7* and *IMP2'* to the action of AMPs, growth curves were produced (Figures 6.1 – 6.3). All deletion strains had reduced growth compared to the parent strain in the absence of

peptide. Compared to the wt, the *ldb7Δ* strain showed reduced growth after 48 h (Figure 6.1). At 5 µg/ml DsS3(1-16), growth of the wt was inhibited with an increased lag phase (31.25 h) compared to the control (13.5 h). At the same DsS3(1-16) concentration, there was no growth of the *ldb7Δ* mutant. At 10 µg/ml of mag 2, inhibition was apparent in both the wt and *ldb7Δ* strains with increased lag phases of 2.5 h. With 12 µg/ml mag 2 growth was inhibited in the wt strain and absent in the *ldb7Δ* mutant. On exposure to rana, similar results were observed. Growth at 16 µg/ml was inhibited in both strains with increased lag phases of 1 h (wt) and 9.5 h (*ldb7Δ*). With 22 µg/ml rana, growth of the wt strain was inhibited further, with an increased lag phase and reduced growth. In comparison, the *ldb7Δ* strain displayed no growth after 48 h.

Results with *imp2'Δ* were similar (Figure 6.2). On exposure to 4 µg/ml DsS3(1-16), both strains displayed inhibited growth. With 5 µg/ml, the wt was inhibited with an increase in lag phase of 15.25 h while the *imp2'Δ* strain displayed no growth. At 10 µg/ml of mag 2, growth of the wt strain was inhibited while no growth with *imp2'Δ* was recorded. With 16 µg/ml of rana the *imp2'Δ* strain displayed no growth.

Compared to the wt strain, the *hal5Δ* mutant had an extended lag phase lasting an additional 4.5 h (Figure 6.3). Growth with 3 µg/ml DsS3(1-16) was inhibitory to *hal5Δ*, with an increase in lag phase of 6.5 h. At 5 µg/ml DsS3(1-16), inhibition of the wt strain was observed with a doubling in lag phase (27 h) while there was no growth of *hal5Δ*. At 10 µg/ml mag 2 the wt displayed an increase in lag phase of 11.75 h while the deletion

strain failed to grow. With 18 μg/ml rana, the wt strain was inhibited with a doubling in lag phase (26 h) while the *hal5Δ* deletion strain displayed no growth. These results indicate that in the presence of DsS3(1-16), mag 2 and ranalexin there was increased inhibition upon deletion of *HAL5*, *LDB7* and *IMP2'*. However, all three mutants appear to have a reduced growth phenotype in the absence of peptide compared to the parent strain. Studies with rana also highlight the increase in population density observed when sub-lethal concentrations of peptide were present after 48 h of incubation.
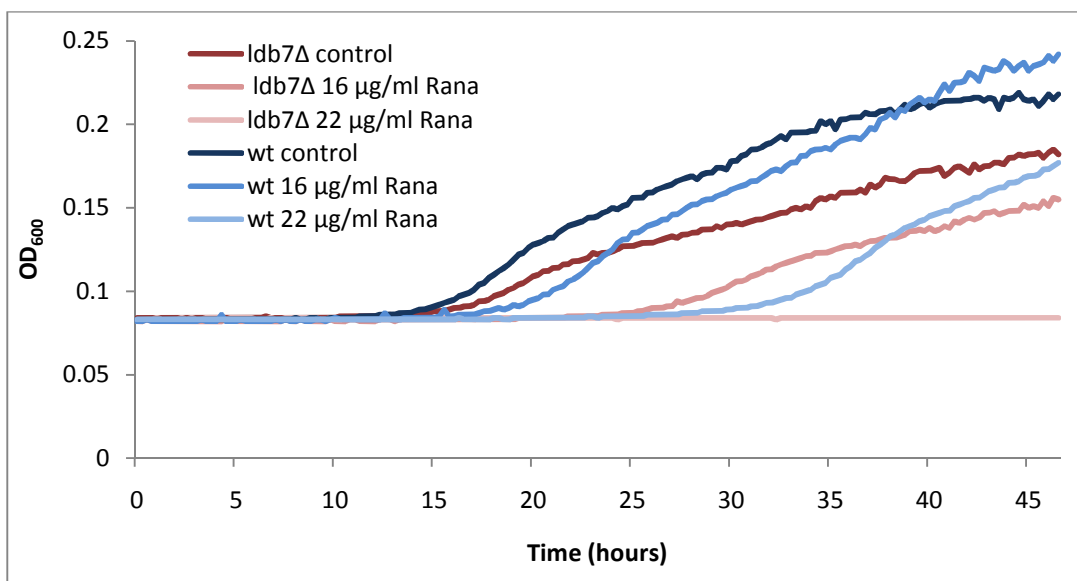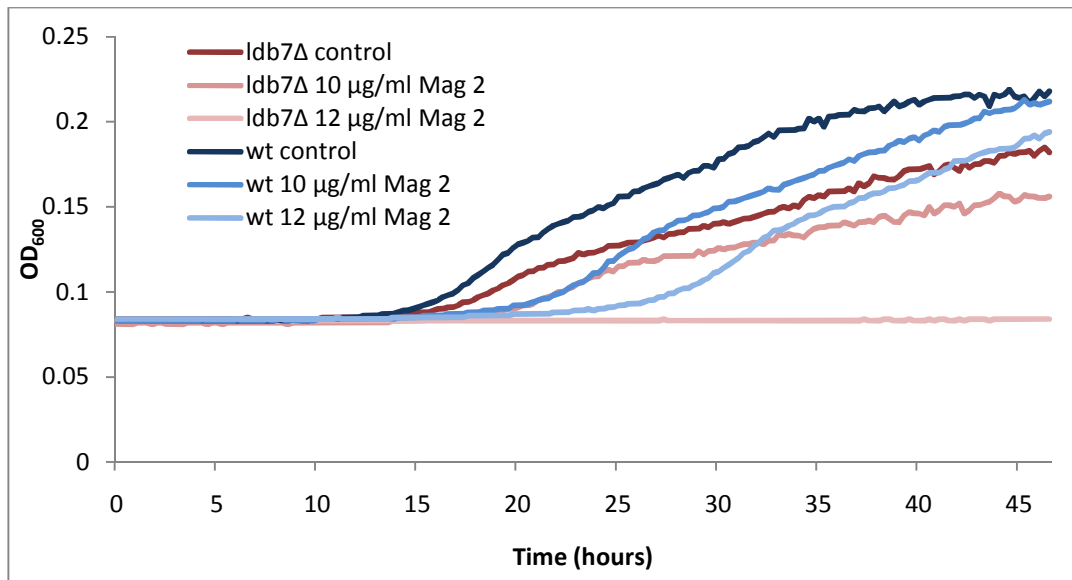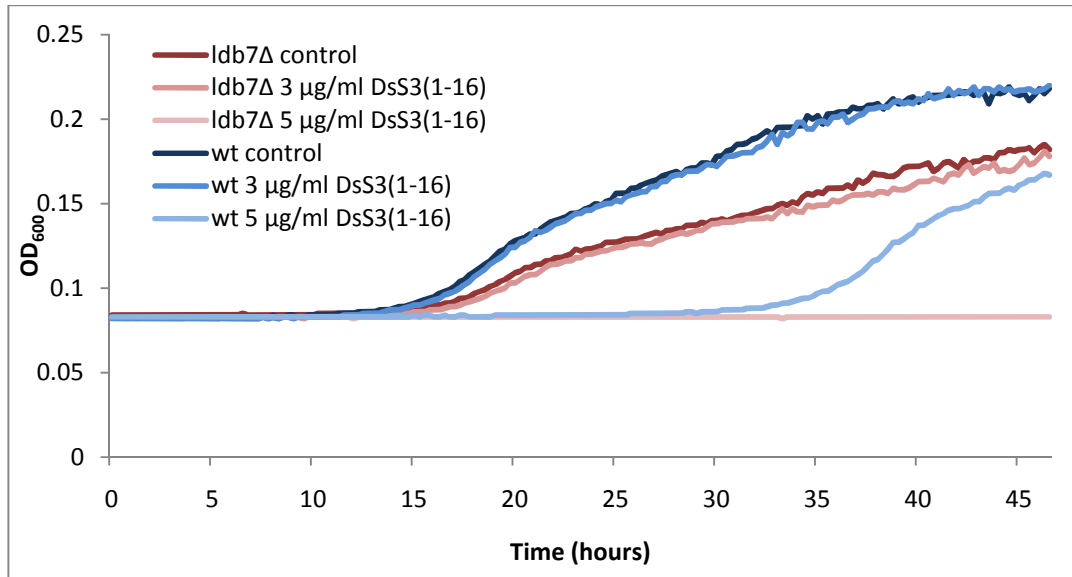
Figure 6.1. Growth of *ldb7Δ* and wt strains when exposed to various concentrations of DsS3(1-16), mag 2 or rana. Cell density (OD_{600}) was measured every 15 min over a 48 h period. Each experiment was carried out in duplicate and representative graphs for each are shown.
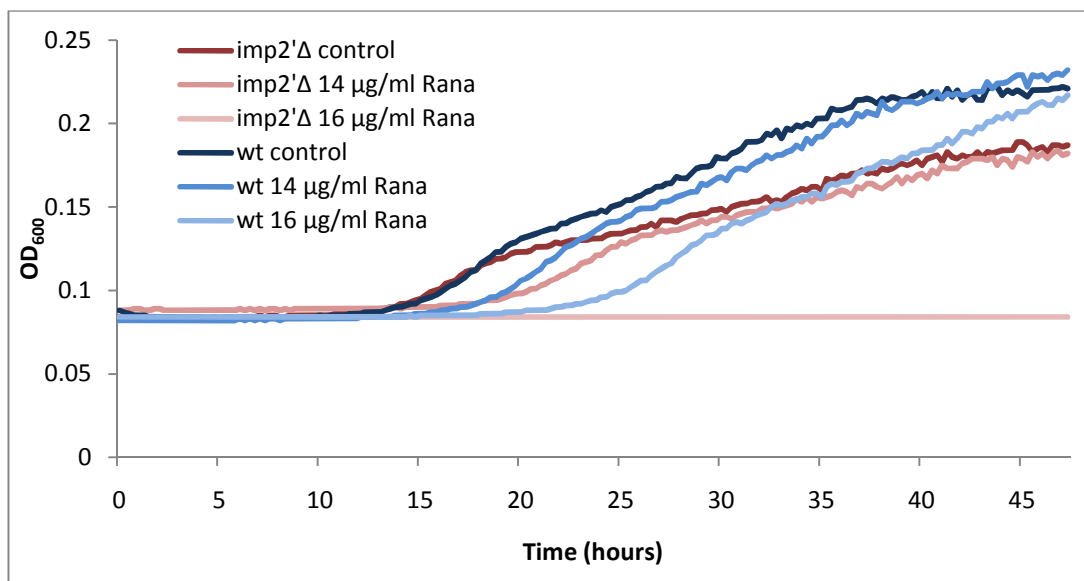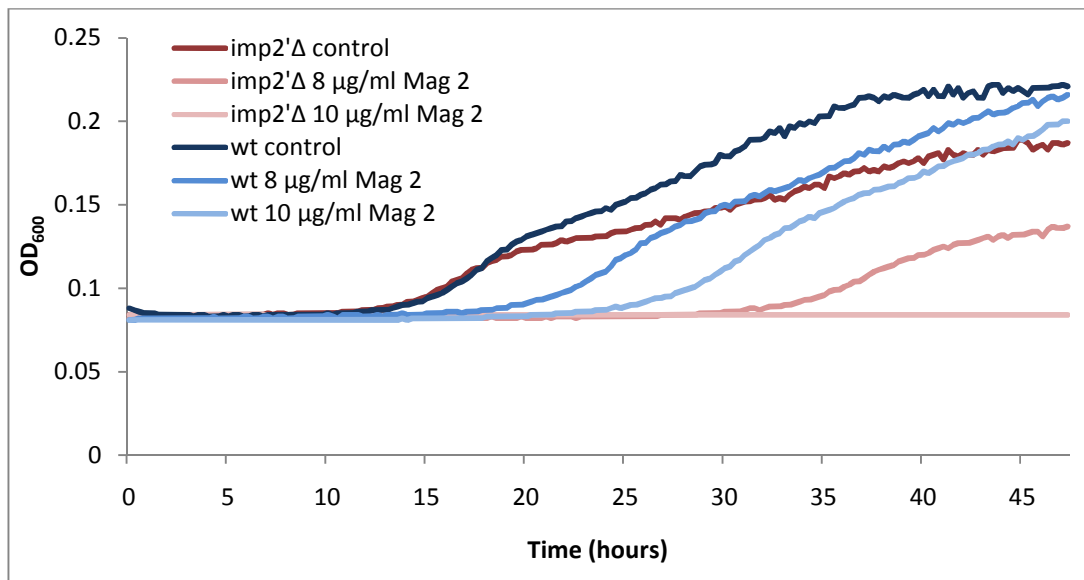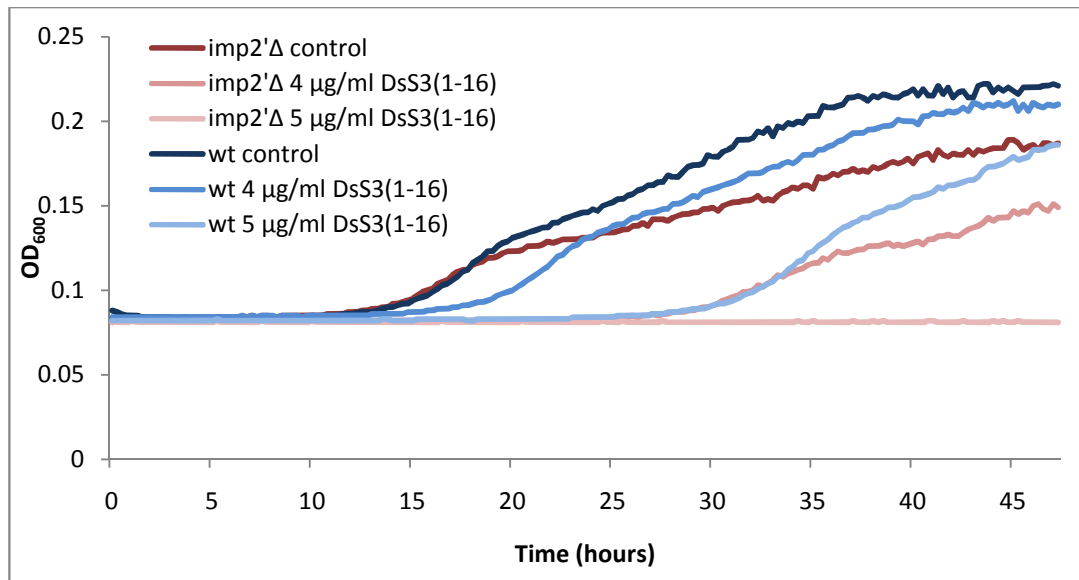
Figure 6.2. Growth of *imp2'Δ* and wt strains when exposed to various concentrations of DsS3(1-16), mag 2 or rana. Cell density (OD$_{600}$) was measured every 15 min over a 48 h period. Each experiment was carried out in duplicate and representative graphs for each are shown.
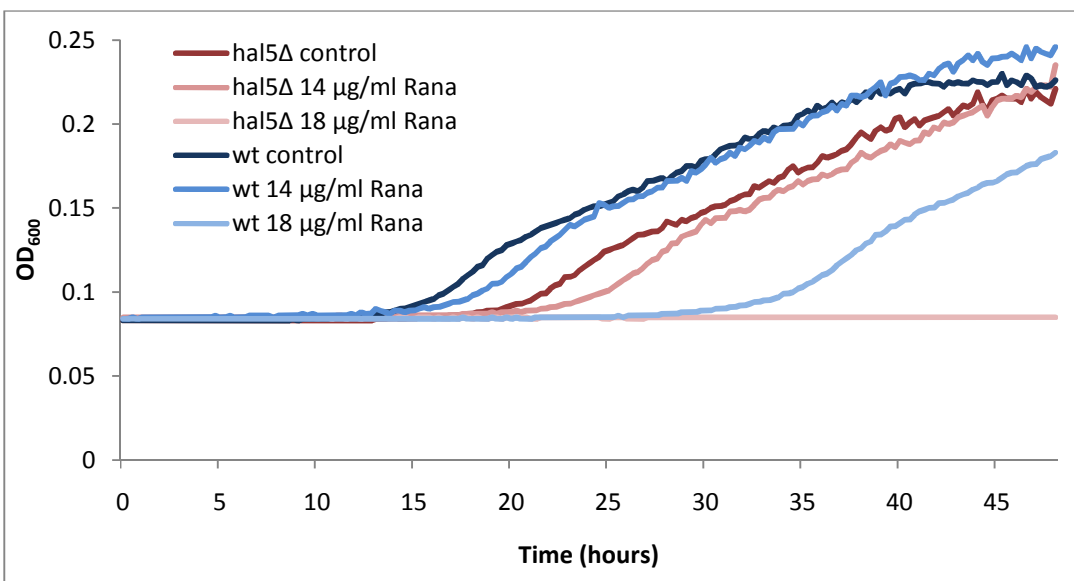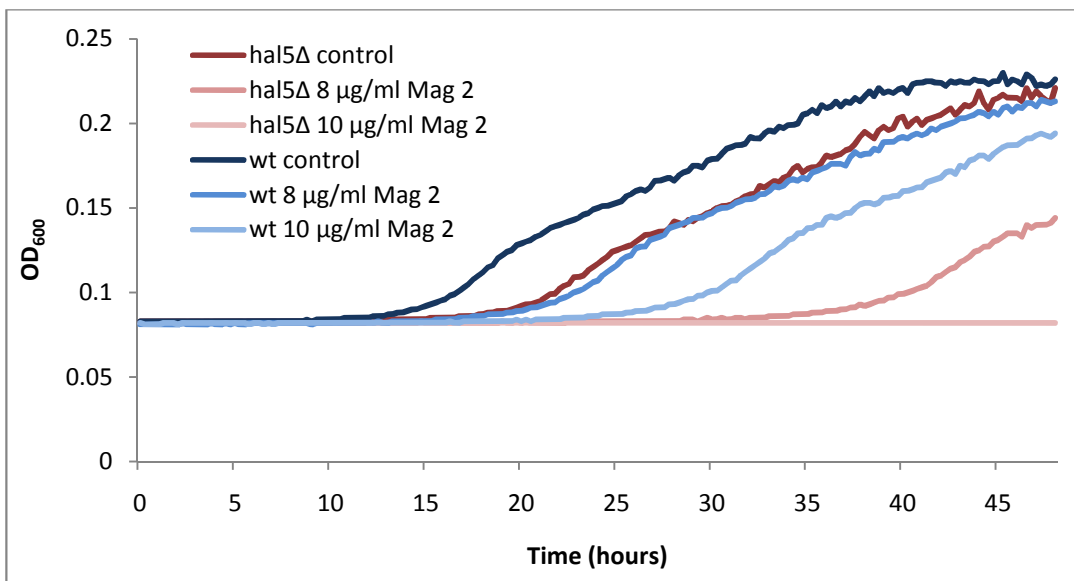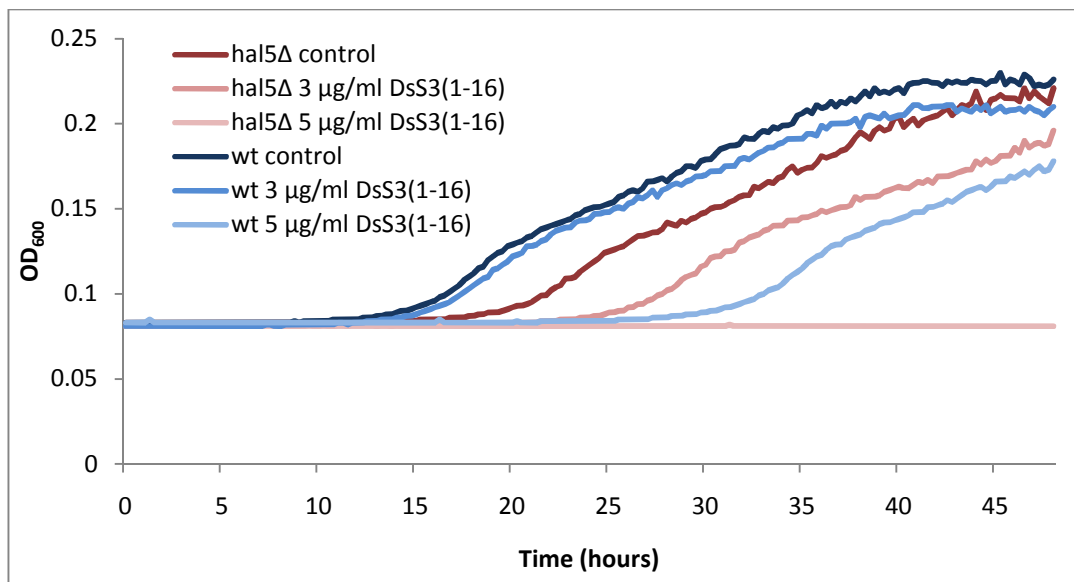
Figure 6.3. Growth of *hal5Δ* and wt strains when exposed to various concentrations of DsS3(1-16), mag 2 or rana. Cell density (OD$_{600}$) was measured every 15 min over a 48 h period. Each experiment was carried out in duplicate and representative graphs for each are shown.

6.2.3 Quantification of Flu-DsS3(1-16) binding and internalisation by *S. cerevisiae* cells.

Deletion of *HAL5*, *LDB7* and *IMP2'* caused increased susceptibility of *S. cerevisiae* cells to several cationic AMPs. It is possible that this increased peptide action is the result of an increase in peptide binding and internalisation. Peptide sequestration was monitored using Flu-DsS3(1-16) as before (Section 3.2.5).

There was increased Flu-DsS3(1-16) sequestration by the deletion strains compared to the wt at lower concentrations of peptide (Figure 6.4). However, at the greatest concentration used (20 µg/ml), the differences were less obvious as may be expected due to cell saturation with peptide (Section 3.2.5). At 5 µg/ml, after 30 min, the wt population sequestered 41 % of the available peptide, *hal5Δ* sequestered 45.6 %, *imp2Δ* sequestered 49 % and *ldb7Δ* sequestered 51 %. At 10 and 15 µg/ml the wt sequestered 35.6 % and 39.55 % of the available peptide respectively, whilst the *hal5Δ* and *ldb7Δ* strains sequestered more peptide (43.5 - 45.9 %). The *imp2'Δ* mutant strain sequestered the greatest percentage of available peptide at 10 µg/ml (51.7 %) and 15 µg/ml (50.23 %). This data indicates that these strains show increased peptide binding and internalisation on deletion with differences of up to 16.1 % increased peptide sequestration compared to the wt *S. cerevisiae* strain. Consequently there is a correlation between degree of peptide binding and sensitivity to the inhibitory action of the peptides.
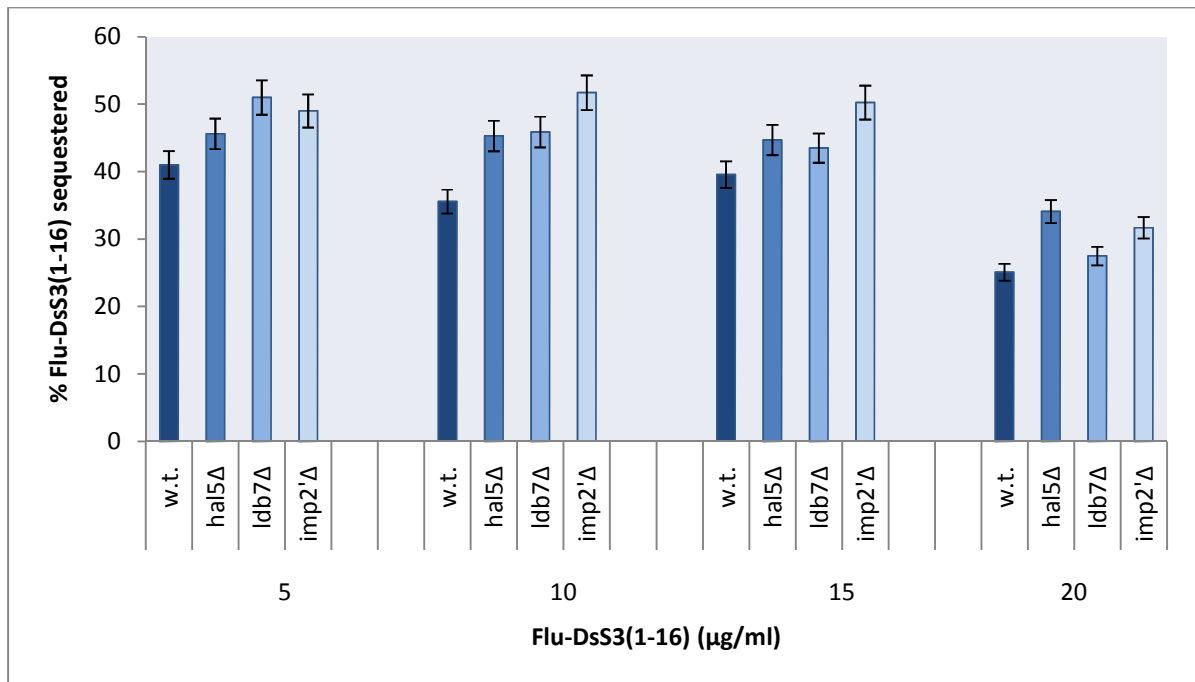
Figure 6.4. Peptide sequestration by wt, *hal5Δ*, *ldb7Δ* and *imp2'Δ*. Flu-DsS3(1-16) was added at 5, 10, 15 or 20 μg/ml to an equal number of cells from each deletion strain. The percentage of Flu-DsS3(1-16) sequestered by each cell population was calculated and plotted; n = 3 mean ± 1 SD.

6.2.4 Population viability using fluorescence microscopy

To quantify cell viability, cells were stained with PI or CTG after exposure to DsS3(1-16) (Figure 6.5). A group of cells in each assay stained with both PI and CTG so were labelled as 'dual staining'. In the absence of Flu-DsS3(1-16) 90.1 - 94.4 % of the cells in the wt, *hal5Δ* and *imp2'Δ* populations stained with CTG, whilst only 79.1 % of the *ldb7Δ* population staining with CTG. As the concentration of DsS3(1-16) was increased, so the proportion of cells with CTG staining decreased indicating reduced viability in the cell populations. At all concentrations of peptide, the wt strain had the lowest susceptibility to the peptide compared to the deletion strains. This was most apparent at 4 μg/ml of DsS3(1-16) where 81.3 % of wt cells stained with CTG compared to 43.7 %, 44.9 % and 38.4 % in the *hal5Δ, ldb7Δ* and *imp2'Δ* deletion strains respectively. At 2 μg/ml, *ldb7Δ*

was most sensitive to peptide action, however, as the concentration was increased it was the *imp2'Δ* mutant that showed more sensitivity.
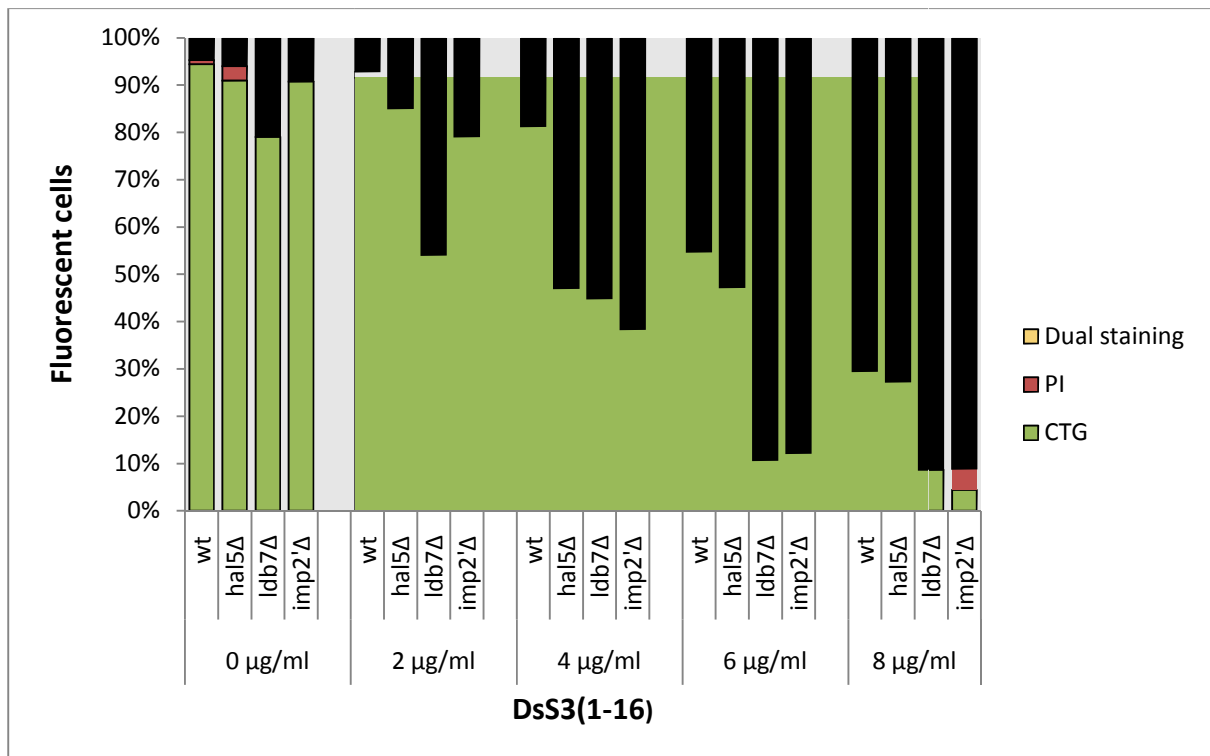
Figure 6.5. Percentage of each cell population fluorescing with CTG, PI or dual staining when exposed to DsS3(1-16). For each assay a minimum of 300 cells were counted and quantified into a percentage of the sampled population; n = 2.

Concomitantly, cell viability was assessed by dilution and plating (Figure 6.6). The wt strain had the smallest decrease in viability over the concentration range, with 40.2 % survivors at 8 µg/ml of DsS3(1-16). The *ldb7Δ* mutant's viability reduced gradually from 57.1 % at 2 µg/ml DsS3(1-16) to 17.3 % at 8 µg/ml of DsS3(1-16). Cell survival with *imp2'Δ* decreased to 5.6 % at 8 µg/ml of DsS3(1-16). The strain that had the greatest reduction in viability was *hal5Δ* with 3.1 % survivorship at 8 µg/ml. In terms of peptide action, the wt strain was least susceptible followed by *ldb7Δ*, *imp2'Δ* with *hal5Δ* being the most susceptible. The extent of killing in this viability assay would indicate that cells

which had stained with both CTG and PI were non-viable e.g. the wt strain decreased to 40.2 % survivorship at 8 µg/ml DsS3(1-16)) and displayed an increase in dual staining of 66 % compared to the no peptide control.
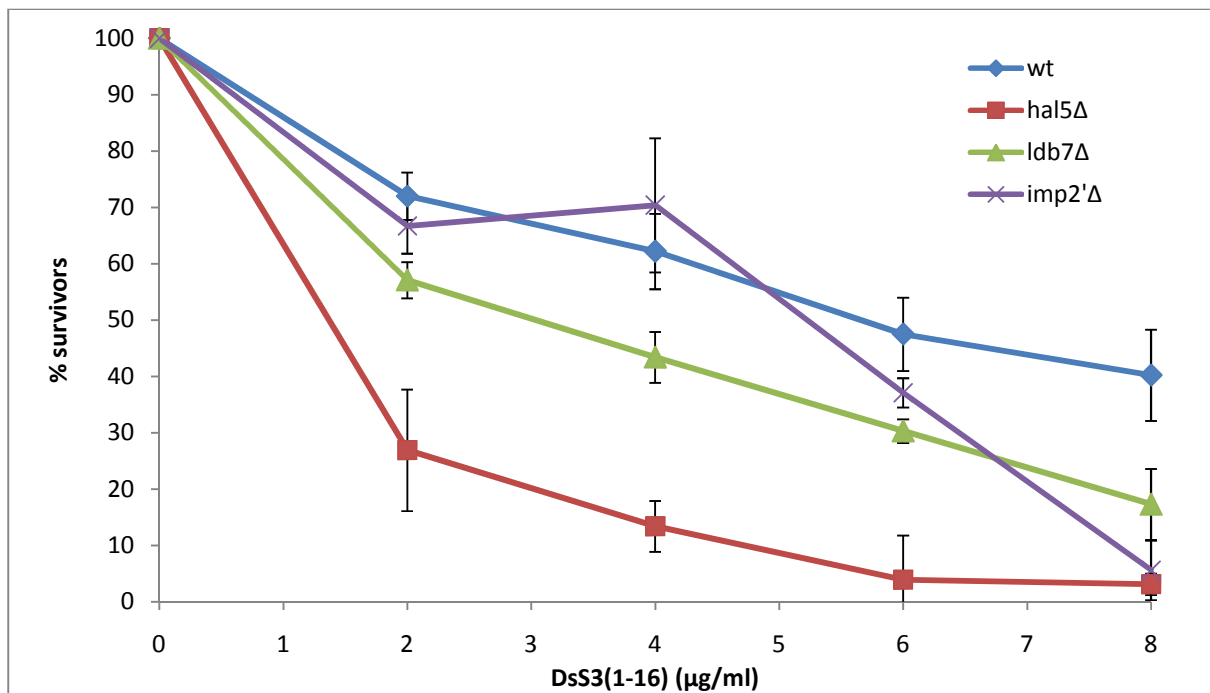
Figure 6.6. Cell viability count after exposure to DsS3(1-16). The results are plotted as percent survivors; n = 3 mean ±2SD.

6.2.5 GFP-tagging of *HAL5*, *LDB7* and *IMP2'*

GFP constructs were created to monitor changes in protein expression and localisation upon peptide exposure. In the absence of peptide, *LDB7-GFP* localised at the nucleus corresponding with fluorescence from the DAPI staining (Figure 6.7). As *LDB7* encodes Rsc14 that is involved in chromatin remodelling, this localisation at the nucleus would be expected (Wilson *et al*, 2006). With the addition of 6 µg/ml DsS3(1-16) there were no observable differences in localisation and expression 60 min after peptide exposure. When observing the *HAL5-GFP* population in the absence of peptide, diffuse expression

occurred throughout the cell. *HAL5* encodes Trk1 and Trk2 which regulate potassium transport and are found in the membrane, as a result whole cell expression would be expected. With the addition of 6 µg/ml of DsS3(1-16) no observable expression or localisation changes were observed when comparing the two populations. Culturing of the *IMP2'-GFP* revealed little fluorescence in the absence of DsS3(1-16). Levels were low throughout the population, as a result, localisation patterns were not observable. Upon exposure to 6 µg/ml of DsS3(1-16) there was an increase in fluorescing cells throughout the population.
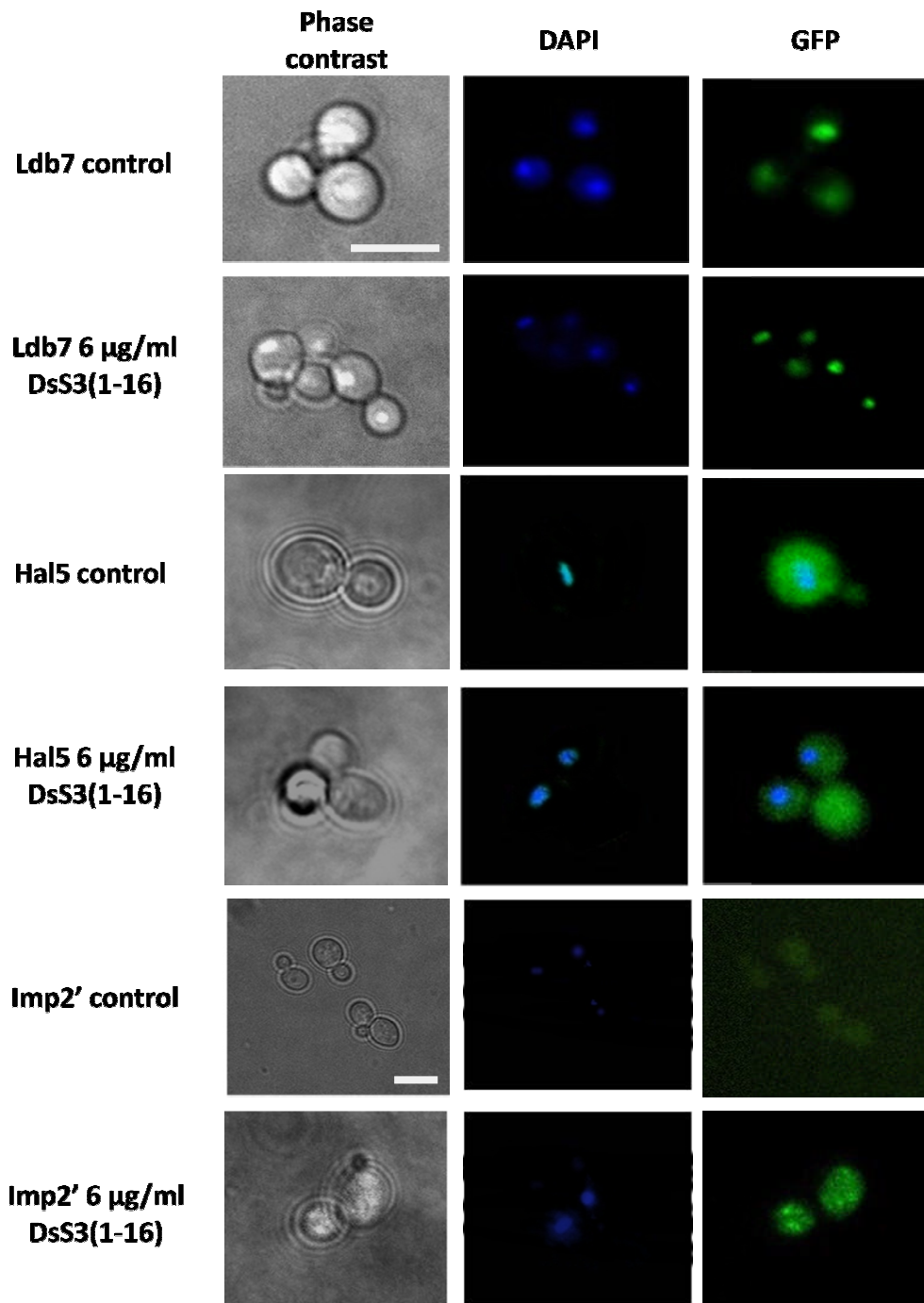
Figure 6.7. Representative images acquired from fluorescent microscopy of GFP-labelled proteins. Cells were incubated in the presence or absence of DsS3(1-16) for 60 min prior to image acquisition. Localisation and expression of Hal5 and Ldb7 remained unchanged in the presence of DsS3(1-16), however, upregulation of Imp2' was observed; scale bar = 5 µM.

6.2.6 Cytometric analysis of membrane potential

Changes to membrane potential in wt and mutant strains on exposure to DsS3(1-16) were recorded. As the proposed initial interaction of DsS3(1-16) is with the membrane surface, a resulting shift in membrane potential may occur. *HAL5* is of particular interest as it encodes a protein kinase that acts to stabilise potassium transporters found in the plasma membrane so may produce more pronounced changes in membrane potential upon peptide exposure. To monitor membrane potential changes a fluorescent redistribution probe (diS-C$_3$(3)) was used. *Hal5Δ*, *ldb7Δ*, *imp2'Δ* and wt strains were incubated with diS-C$_3$(3) and DsS3(1-16). A representative data set is presented (Table 6.2) and corresponding diS-C$_3$(3) log fluorescent histograms were generated (Figures 6.8 and 6.9). These graphs display the relative fluorescence plotted against the number of events. Sections A (all events), B (low level fluorescence) and C (high level fluorescence) in the table correspond to sections A, B and C in each graph. A bimodal distribution was generated by all strains.

When exposed to 10 μg/ml or 20 μg/ml of DsS3(1-16), the wt population displayed a slight increase in fluorescence with the median increasing from 5.8 to 6.5 in both treatments. Fluorescence in the two sub-populations (B and C) also increased with a concurrent increase in gated cells to 26.2 % (B) and 57.2 % (C). The culture treated with 6.5 μM of amphotericin B displayed a marked decrease in median fluorescence, reducing from 5.8 to 3.4. There was also an increase in the population of cells displaying low fluorescence (B), from 26.2 % in the negative control to 31.7 % in the amphotericin B positive control. This data demonstrates the depolarising effects of amphotericin B and

subsequent efflux of dS-C$_3$(3) producing a decrease in fluorescence. However, with the addition of DsS3(1-16) no such decrease was observed indicating no change in membrane potential 20 min after peptide exposure.

The *ldb7Δ* strain displayed decreased levels of probe uptake compared to the wt strain, with medians of 2.3 and 5.8 respectively. There was also a higher proportion of cells in section B (60.2 %) compared to the wt (26.2 %). As with the wt, there was an increase in fluorescence upon exposure to DsS3(1-16), with the median increasing to 2.8 at 10 µg/ml and 2.7 at 20 µg/ml. The percentage of gated cells remained unchanged on peptide addition between populations B and C.

The *imp2'Δ* cells generated decreased fluorescence levels when compared to the wt, with 45.2 % gated in the lower fluorescent population (B) compared to 26.2 % of wt cells. The medians generated were also reduced. On peptide addition there was a gradual increase in the percentage of gated cells in population B, from 45.2 % in the control to 46.5 % at 10 µg/ml and 48.7 % at 20 µg/ml. This change was very minor so it is difficult to attribute this with increased depolarisation.

The *hal5Δ* mutant control data was similar to the wt strain with gating levels at 25.2 % (B) and 58.1 % (C). Median values were also comparable to the wt control (6). When cultures were exposed to peptide there was little change in median value (6.3 at 10 µg/ml). However, the percentage of cells observed in section B (reduced fluorescence) increased as the DsS3(1-16) concentration increased. At 10 µg/ml this increased by 1.15 %, while at 20 µg/ml there was an increase of 35.1 % giving 60.2 % gated in section B.

This was indicative of depolarisation and diS-C$_3$(3) efflux from cells in the population. This fluorescent reduction may be linked to peptide concentration as the highest percentage of cells gated occurred at the highest AMP concentration.

The data from the cytometer experiments show strain variation in terms of initial probe uptake. These strain distribution differences could result from differential activity of MDR efflux pumps that are responsible for diS-C$_3$(3) distribution and equilibrium within the cell or from differences in resting membrane potential between the mutants (Malac *et al*, 2005). The wt, *ldb7Δ* and *imp2'Δ* strains display minor changes in fluorescence levels as peptide was added without a considerable increase in depolarisation at 20 µg/ml Dss3(1-16). However, the wt strain displayed depolarisation in the presence of amphotericin B indicating the assay was sensitive to changes in membrane potential. The *hal5Δ* strain showed overall decreases in fluorescence when monitoring the percentage of gated cells displaying low fluorescence (section B). This indicates that Hal5 may protect cells from peptide action by inhibiting membrane depolarisation and increasing stability while Ldb7 and Imp2' have different protective mechanisms.

Table 6.2. Changes in dS-C$_3$(3) fluorescence in *S. cerevisiae* mutants upon exposure to DsS3(1-16) or amphotericin B (AMP). 'A' records all events, 'B' records the cells displaying reduced fluorescence, 'C' records the percentage of cells with increased diS-C$_3$(3) fluorescence. At least 98.5 % of events were gated in section A.

	Section	% Gated	x-Median
wt control	**A**	**99.08**	**5.8**
	B	26.16	1.7
	C	57.17	8.3
wt 10 μg/ml DsS3(1-16)	**A**	**99.39**	**6.5**
	B	28.57	2.2
	C	59.55	8.6
wt 20 μg/ml DsS3(1-16)	**A**	**99.5**	**6.5**
	B	28.01	2.2
	C	58.65	8.8
wt AMP control 6.5 μM	**A**	**99.79**	**3.4**
	B	31.7	0.6
	C	50.47	7
***ldb7*Δ control**	**A**	**98.58**	**2.3**
	B	60.22	1.2
	C	33.67	11.7
***ldb7*Δ 10 μg/ml DsS3(1-16)**	**A**	**99.22**	**2.8**
	B	61.7	1.5
	C	33.55	13.7
***ldb7*Δ 20 μg/ml DsS3(1-16)**	**A**	**98.87**	**2.7**
	B	60.59	1.4
	C	33.94	13.8
***imp2'*Δ control**	**A**	**98.96**	**4.7**
	B	45.22	1.7
	C	37.33	11.5
***imp2'*Δ 10 μg/ml DsS3(1-16)**	**A**	**99.47**	**5**
	B	46.49	1.9
	C	38.2	11.9
***imp2'*Δ 20 μg/ml DsS3(1-16)**	**A**	**99.44**	**4.4**
	B	48.7	1.8
	C	37.01	11.7
***hal5*Δ control**	**A**	**98.78**	**6**
	B	25.16	1.4
	C	58.1	8.5
***hal5*Δ 10 μg/ml DsS3(1-16)**	**A**	**98.5**	**6.3**
	B	26.31	1.5
	C	56.74	9.2
***hal5*Δ 20 μg/ml DsS3(1-16)**	**A**	**98.93**	**5.8**
	B	60.22	1.2
	C	33.67	11.7
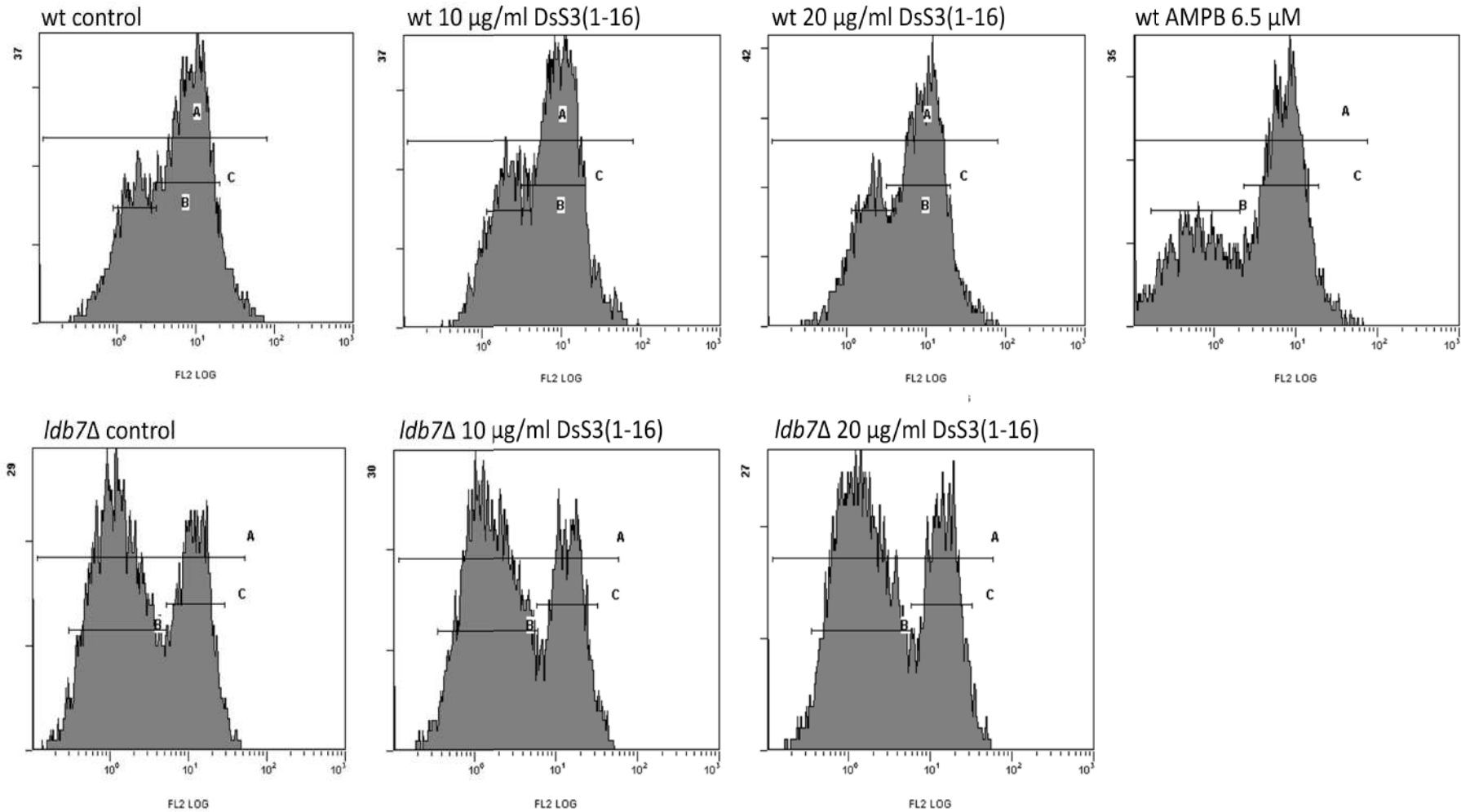
Figure 6.8. Fluorescent histograms displaying log fluorescence (FL2) against number of events recorded with wt and *ldb7Δ*. The sections quantified in table 6.2 correspond to sections A, B and C displayed in each graph. Top: wt strain, bottom: *ldb7Δ*. Results are displayed with increasing concentrations of DsS3(1-16) and the positive control, amphotericin B (AMPB). The experiment was carried out in triplicate and a representative run is presented.
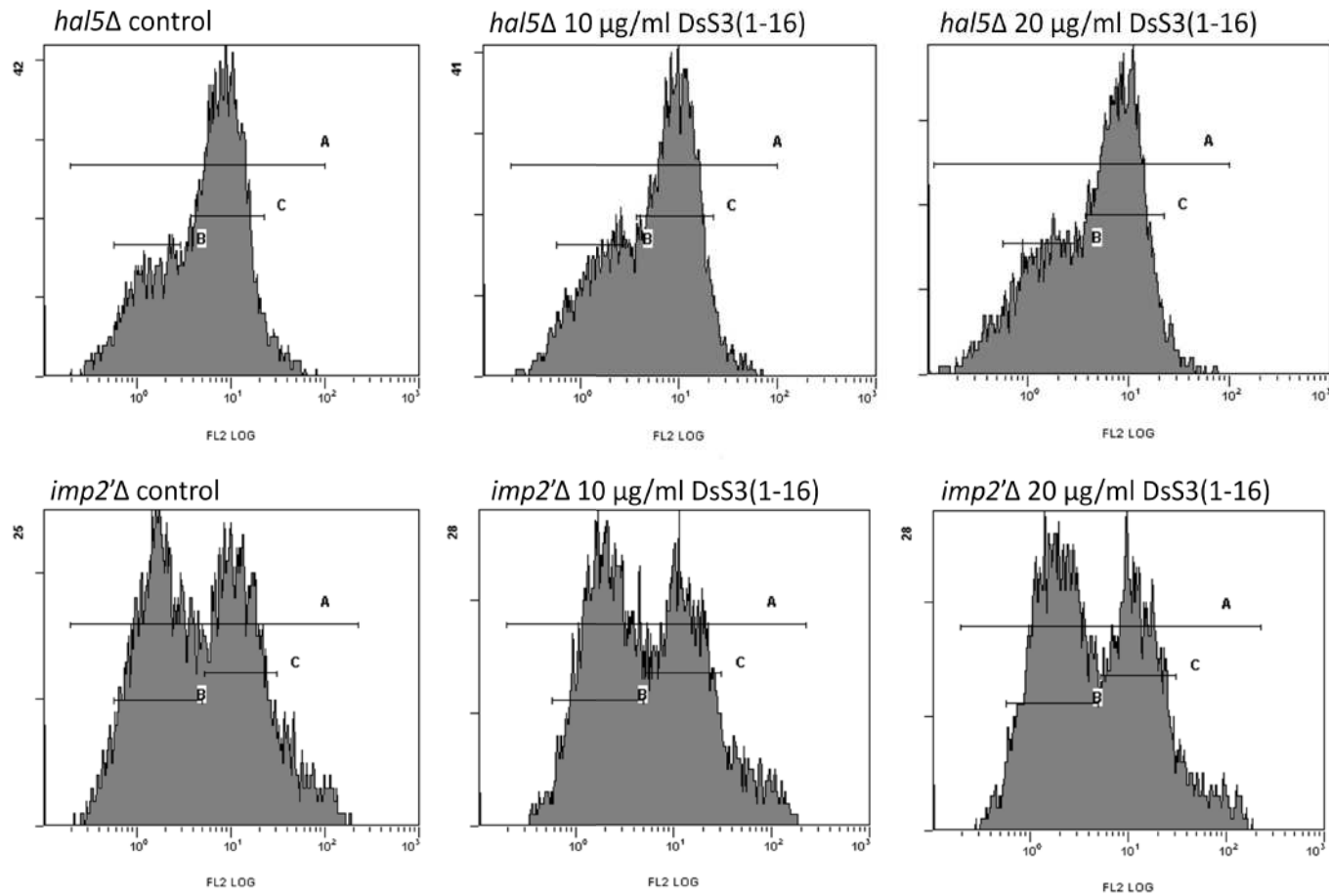
Figure 6.9. Fluorescent histograms displaying log fluorescence (FL2) against number of events recorded with *hal5Δ* and *imp2'Δ*. The sections quantified in table 6.2 correspond to sections A, B and C displayed in each graph. Top: *hal5Δ*, bottom: *imp2'Δ*. Results are displayed with increasing concentrations of DsS3(1-16). The experiment was carried out in triplicate and a representative run is presented.

6.3 Discussion

In a previous investigation a genetic screen of all non-essential genes in *S. cerevisiae* demonstrated that upon deletion 1.7 % showed DsS3(1-16) sensitivity, 0.4 % showed mag 2 sensitivity and 0.7 % showed sensitivity to both peptides (Morton[b] *et al*, 2007). Of the genes conferring dual sensitivity, *HAL5, LDB7* and *IMP2'* were selected for further analysis. The results from this present chapter confirm a previous report that *HAL5, LDB7* and *IMP2'* mutants have increased sensitivity to AMPs. Additionally, mutants sequestered an increased amount of available peptide, membrane depolarisation was recorded upon deletion of *HAL5* and Imp2' was up regulated on exposure to peptide.

The *ldb7Δ* mutant displayed a reduction in MIC when exposed to DsS3(1-16), mag 2 and rana and also showed no growth at concentrations that were only partially inhibitory to the wt strain. The deletion strain displayed an increase in peptide sequestration and showed greater loss of cell viability when exposed to increasing concentrations of DsS3(1-16) in a cell labelling assay. This data demonstrates the increase in susceptibility of *S. cerevisiae* cells that lack the *LDB7* gene. Ldb7 is involved in chromatin remodelling and its localisation has been shown around the nucleus in the GFP tagging study. The gene encodes Rsc14 that forms the RSC chromatin remodelling complex. Rsc14 is also required for the association of other RSC components. This complex has been linked to cell wall integrity as mutations in subunits confer cell wall defects such as reduced oligosaccharide branching and mannosylphosphate attachment (Wilson *et al*, 2006). If cell wall integrity is reduced this could perpetuate peptide binding to the membrane and increase disruption leading to enhanced killing. As reduced mannosylphosphate

attachment is a phenotype of several mutations to *ldb* genes, a decrease in the phosphate component of the cell wall would be expected. However, a study of Alcian blue binding found only a marginal decrease in binding affinity with *ldb7Δ* when compared to the wt strain suggesting phosphate levels were conserved (Corbacho *et al*, 2004).

The RSC has also been implicated in double-strand break repair via homologous recombination. Mutations to the RSC rendered cells hypersensitive to the DNA damaging agents bleomycin, hydroxyurea, methyl methanesulfonate and ultraviolet radiation (Chai *et al*, 2005). Mag 2 and DsS3(1-16) bind to DNA and may induce strand breaks *in vitro* (Morton[b] *et al*, 2007). DsS3(1-16) can also induce programmed cell death by indirectly damaging DNA and interfering with DNA replication (Morton[a] *et al*, 2007). As double-strand break repair is compromised in the *ldb7Δ* mutant, the DNA damage induced by DsS3(1-16) and mag 2 may lead to a decrease in viability through programmed cell death.

The *imp2'Δ* mutant also displayed an increase in peptide sensitivity with a decrease in MIC against DsS3(1-16), mag 2 and rana, an increase in peptide sequestration and a decrease in cell viability. The role of *IMP2'* is poorly understood; however, it encodes a transcription factor and has been implicated in DNA-damage protection as *IMP2'* mutants display increased levels of genetic recombination (Masson *et al*, 1996). It has been proposed that Imp2' activates the expression of several proteins involved in the protection of DNA against oxidative damage (Masson *et al*, 1996). Similar to *ldb7Δ*, the

increased sensitivity observed in this mutant may be due to an increase in DNA damage from peptide interference. Similarly, *IMP2'* protects cells from the glycopeptide bleomycin and *imp2'Δ* mutants are hypersensitive to the drug (Masson *et al*, 1996). Bleomycin is a peptide used in cancer therapy that induces DNA strand breaks (Povirk *et al*, 1977). This resistance is conferred by *IMP2'* through DNA damage repair or detoxification of the drug (Alberti *et al*, 2003). The GFP-tagged Imp2' also displayed an increase in expression levels upon DsS3(1-16) exposure. If the peptide causes DNA damage, this may promote Imp2' transcription, in turn activating the proteins involved in DNA protection. The expression of Imp2' was observed throughout the cell with increased expression in several localised patches on exposure to DsS3(1-16).

As with the previous deletion strains, *hal5Δ* displayed increased sensitivity to DsS3(1-16), mag 2 and rana. *HAL5* encodes a protein kinase that acts to stabilise the potassium transporters Trk1 and Trk2 that are found in the plasma membrane. *Hal5Δ* displayed a reduction in growth when compared to the wt strain (Figure 6.3) that is probably due to K^+ levels in the media, limiting growth in this mutant (Ramos *et al*, 1994). Membrane depolarisation was also recorded after exposure to DsS3(1-16) (Table 6.2, Figure 6.9). On deletion of *HAL5*, there is mislocalisation and destabilisation of the Trk1 potassium transporter which would result in decreased K^+ uptake (Pérez-Valle *et al*, 2007). This may increase the probability of membrane depolarisation: there would be reduced intracellular K^+ due to the lack of Trk1-Trk2 functionality, as a result there would not be sufficient K^+ efflux required for inhibition of membrane depolarisation. This would cause an increased occurrence of depolarisation with the concomitant reduction in diS-C$_3$(3) fluorescence observed in the cytometer work. Pore-forming peptides, including the

dermaseptins, have been shown to cause membrane depolarisation followed by cell death (Papo *et al*, 2003; Duclohier, 2006). This mode of action would cause leakage of K^+ through the membrane as a result of increased membrane porosity. As there is insufficient K^+ sequestering by Trk1-Trk2 this increases the probability of depolarisation and cell death facilitated by ion leakage.

In this chapter it has been demonstrated that deletion of *LDB7*, *IMP2'* and *HAL5* confers sensitivity to the antimicrobial peptides DsS3(1-16), mag 2 and rana. This increase in susceptibility is likely to be due to the protection against DNA damage conferred by *IMP2'* and *LDB7* which is diminished upon deletion. Loss of *HAL5* may increase the sensitivity resulting from the reduction in intracellular K^+, increasing the probability of membrane depolarisation. This subsequently may lead to cell death, facilitated by loss of ions through peptide pore formation.

Chapter 7

7. Discussion

7.1 Final discussion

Antimicrobial peptides have the potential to function as a new class of antifungal drugs to combat increasingly resistant pathogenic fungi. Infections by *C. albicans* account for 1.1 – 2.4 per 100,000 cases with a mortality rate of 30 % while infections from *C. glabrata* have increased within the last few years with mortality rates of up to 100 % for bone marrow transplant patients (Gudlaugsson *et al*, 2003; Wisplinghoff *et al* 2004). Therefore, it is important to investigate antifungal peptides and their actions against infectious fungi to understand in greater detail their individual modes of action, to identify genes that confer changes to fungal susceptibility and to evaluate these AMPs for their potential use in future therapeutic applications.

The effect of the *Candida* cell wall in mediating AMP action was examined on mutants devoid of specific cell wall components. It was discovered that mutants lacking or deficient in the phosphomannan fraction of the cell wall were less susceptible to the action of several cationic AMPs. Additional data in which exogenous phosphate was present confirmed these findings and it is proposed that in order for AMPs to exert their full antifungal action they must first bind to the negatively charged phosphate component of the cell wall. This then facilitates binding to the plasma membrane; increasing antimicrobial efficacy. Other studies have also reported AMP binding to phosphomannan (Ibeas *et al*, 2000; Monk *et al*, 2005). The use of Flu-DsS3(1-16) confirmed this, with increased cellular sequestration of peptide by the parent strain compared to the phosphomannan deficient mutants. Analysis with Flu-DsS3(1-16)

highlighted the differential localisation patterns of DsS3(1-16); it was observed on the periphery of cells, localised to the vacuole or found diffusely through the cytoplasm. As DsS3(1-16) is proposed to cause lysis via a 'carpet-like' mechanism (Netea *et al*, 2006) it is proposed that at low concentrations, peptide binds to the cell wall or membrane and is internalised and transported to the vacuole via endocytosis. At greater concentrations the peptide binds, causing pore formation and internalisation of peptide with interference to cellular processes such as DNA replication (Morton[a] *et al*, 2007).

Drug combinations examining the antifungal activity of AMPs with echinocandins was subsequently monitored. The efficacy of AMPs when combined with caspofungin or anidulafungin was seen to increase in a synergistic manner against clinical isolates of *C. albicans* and *C. glabrata* as well as *S. cerevisiae*. All peptides (ex. 6752) produced FICs in RPMI media and several in MEB that were in the synergy range. Experiments using Flu-DsS3(1-16) revealed that the presence of caspofungin or anidulafungin increased the proportion of cells displaying peptide internalisation. The use of PI in these experiments also demonstrated that when peptide was localised to the vacuole cells remained viable, while peptide localisation to the cytoplasm was cytotoxic.

Subsequent murine studies monitored the effectiveness of rana with caspofungin using fungal kidney burden and weight in a mouse model of systemic Candidiasis. Unfortunately there was no increase in inhibition on combination with several displaying rana toxicity. Rana generated the greatest levels of haemolysis and also displayed high levels of cytotoxicity against *Vero* cells relative to the other AMPs tested. Moreover,

DsS3(1-16) showed low level haemolytic and cytotoxic activity so could function as a viable alternative. Importantly, with all AMPs there was no increase in toxicity on combination with caspofungin.

Topical applications may also be considered as an alternative route for clinical application. In chapter 4, synergy was observed on a solid porous medium with various combinations. Recent advances in topical applications for AMPs include pexiganan: against diabetic foot ulcer infection it had similar eradication rates to oral antibiotic treatment but without the emergence of resistance (Lipsky *et al*, 2008). Topical treatment against *Pseudomonas aeruginosa* with D2A2L in rat models was also more effective than standard therapy (Chalekson *et al*, 2003). Recent AMP *in vivo* trials have also been encouraging: indolicodin was effective in preventing the lethality of polymicrobial peritonitis in two rat models and when combined with antibiotics the effectiveness was increased further (Ghiselli *et al*, 2008). The peptide IB-367 was assessed against catheter infections of *S. aureus* and *E. faecalis* in a rat model and when used in combination with an antibiotic its activity was observed to 'strongly increase' when combating infection (Ghiselli *et al*, 2007). The peptide heliomicin is also under development for systemic infections (Andres *et al*, 2007). These studies highlight the viability of AMPs for the treatment of infectious diseases in various topical applications or when used in combination with current clinically available drugs. Due to technical difficulties and the high production costs associated with peptide antibiotic treatment there has been limited interest from the pharmaceutical industry in the development of new peptide derived drugs. The capacity to manufacture AMPs in a cost effective manner is required. One of the challenges in developing these peptides for therapeutic

use will be to overcome their short half life due to proteolytic degradation and interaction with other molecules. This study has demonstrated the potential for AMP integration with conventional treatments that could provide benefits such as: increased antimicrobial action, lower doses, reduced toxicity and decreased resistance events.

It was previously reported that changes to gene expression may influence *S. cerevisiae* susceptibility toward several AMPs. More specifically, deletion of *HAL5*, *LDB7* and *IMP2'* was found to confer sensitivity to DsS3(1-16) and mag2. In chapter 6 it was demonstrated that these mutants were more sensitive to rana. Moreover, deletion strains were shown to sequester more DsS3(1-16) and have reduced viability. Increased expression of Imp2' was also observed with concentrated patches visible upon peptide exposure. No such change was observed with Hal5 or Ldb7. However, *HAL5* mutants did display changes in membrane potential. The increase in depolarisation may be due to insufficient K^+ efflux required to inhibit depolarisation leading to ion leakage and cell death. *Ldb7Δ* sensitivity may result from increased DNA damage, as double-strand break repair is compromised in the mutant (Chai *et al*, 2005). DNA damage may also account for the increased susceptibility *of imp2'Δ* as expression has been implicated in the activation of proteins involved in DNA protection (Masson *et al*, 1996). These data further highlights the inhibitory action of AMPs not just in membrane disruption but also the transcriptional response of the cell to the inhibitory action of cellular functions. The main findings of this thesis are summarised in the following diagram (Figure 7.1).
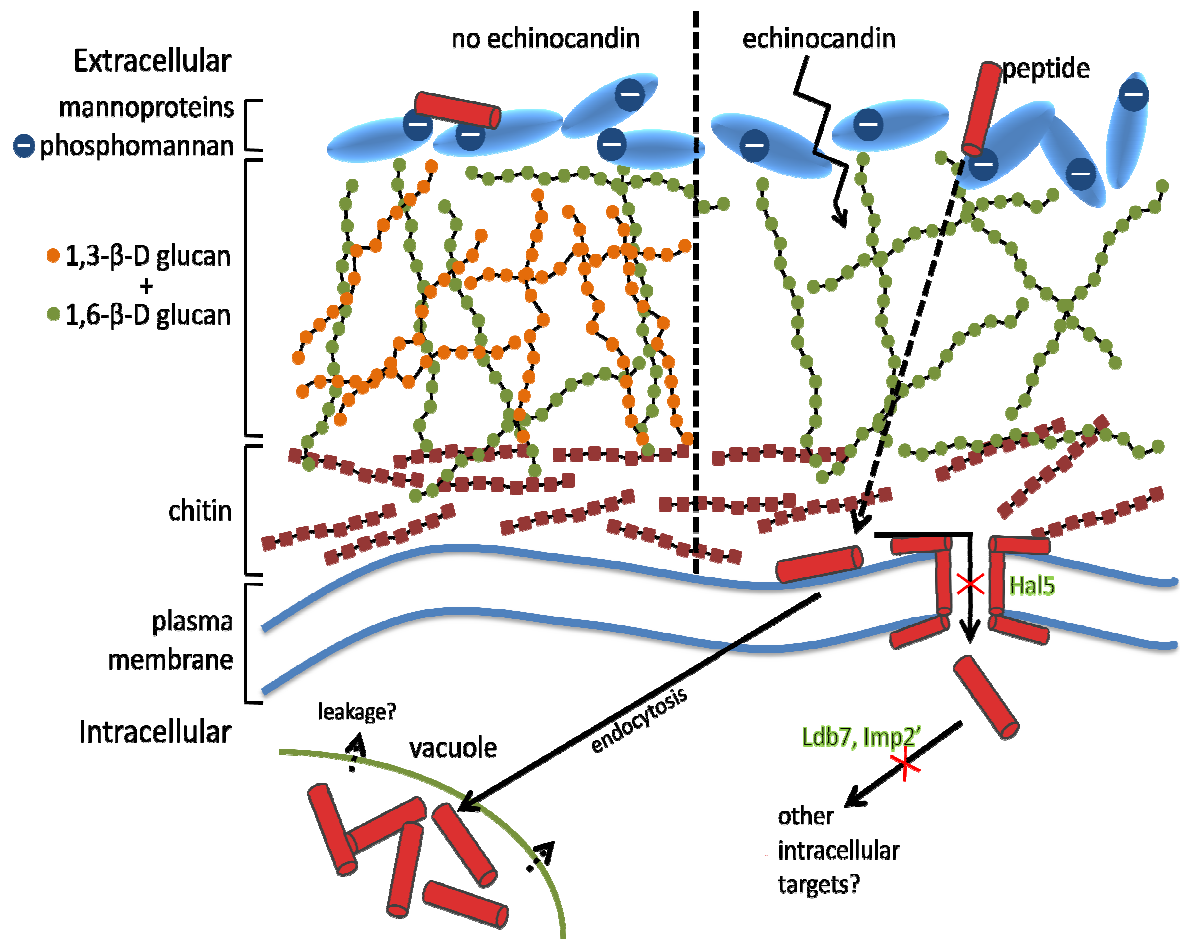
Figure 7.1 Summary of proposed AMP mechanisms of action and fungal susceptibility. The AMPs used in this study are thought to function predominantly via the barrel-stave or carpet models. Cationic peptides bind to the phospholipid head groups of the plasma membrane until a critical concentration is attained, resulting in lipid destabilisation, pore formation (toroidal or barrel-stave) and peptide internalisation. This binding is facilitated by negatively charged phosphate expressed on the cell wall. Additionally, peptide action can be enhanced upon inhibition of 1,3-β glucan synthase, reducing 1,3-β glucan levels in the cell wall thus increasing peptide binding to the membrane. After binding, DsS3(1-16) has been shown to then localise to the vacuole (non-cytotoxic) or cytoplasm (cytotoxic) in a concentration dependent manner. Increased peptide concentration in the vacuole may lead to leakage into the cytoplasm. It is also proposed that yeast genes such as Hal5 confer decreased susceptibility by inhibiting peptide mediated depolarisation while Ldb7 and Imp2' decrease susceptibility via maintenance of DNA integrity directly or indirectly.

7.2 Future work

To further evaluate the internalisation events of DsS3(1-16), time-lapse confocal microscopy could be used where Flu-DsS3(1-16) localisation is monitored directly after addition. This would allow visualisation of peptide from the membrane to the vacuole or cytoplasm and the time periods over which these events occur. A group of cells would be selected and images acquired every few seconds for a defined period of time, as many peptides bind to the membrane several seconds after addition (Hancock *et al*, 1999). The mode of action of histatin-5 has been elucidated using similar methodology (Mochon *et al*, 2008). Purification of the cell wall would allow the quantification of peptide bound to the wall and plasma membrane and the contribution of the various cell wall components in determining cell susceptibility to AMP. In order to further quantify cells, cytometric analysis could be employed, increasing the sample population and generating additional data such as cell size while still retaining the ability to separate cells with vacuolar or whole cell localisations. Fluorescent markers could also be attached to other peptides in this study to investigate their mode of action and compare localisation patterns and sequestration levels. Preliminary microscope experiments were undertaken with fluorescein tagged rana, however, the majority of the peptide monomers clumped together. This may have occurred during initial solubilisation to stock concentrations or when added to growth media.

The results obtained with *in vitro* work were not observed with the *in vivo* trial thus additional tests may have been beneficial in predicting the need for *in vivo* studies. *C. albicans* and *C. glabrata* can both undergo phenotypic switching within the host. This

hyphal transformation contributes to pathogenicity, allowing colonies to rapidly adapt in response to antifungal treatment or the host immune response (Lachke *et al*, 2000). Therefore, to better mimic *in vivo* conditions a series of experiments to monitor and compare the susceptibility of various morphogenic states to AMP would be beneficial before subsequent studies. Candidiasis is frequently associated with invasive medical devices that often promote the formation of biofilms. Conventionally available antifungal drugs show reduced efficacy against biofilms and infections are often persistent (Chandra *et al*, 2001). The effect of biofilms formation on AMP susceptibility is likely to contribute to the success of *in vivo* testing and should also be investigated. The cytotoxicity data indicates that selection of an AMP with reduced toxicity may produce favourable results from *in vivo* work, such as DsS3(1-16), which displayed strong synergy *in vitro* with low level cytotoxicity and haemolysis. Additional studies are required to determine if echinocandin and AMP combinations will be viable clinical alternatives for the treatment of invasive fungal infections. Several studies have already reported little or no cytotoxicity *in vivo* with mag 2 and members of the dermaseptin family (Helmerhorst[b] *et al*, 1999; Navon-Venezia *et al*, 2002; Leite *et al*, 2008). Studies with additional peptide/echinocandin combinations are ongoing with the aim of finding more potent combinations.

To further study the effects of AMP action on cellular responses preliminary data was gathered using iTRAQ (data not shown). This is a method employed to monitor changes in protein expression which allows the comparison of different conditions (Aggarwal *et al*, 2006). Future work would aim to monitor expression levels in cells exposed to sub-lethal concentrations of AMP. Changes in protein expression could provide clues to the

inhibitory action of the peptide on yeast, highlighting additional cellular responses and pathways that are affected by peptide action. Furthermore, one of the mutant strains displaying increased sensitivity could be compared to investigate differential expression thus providing additional evidence as to why these strains display increased sensitivity.

The work presented in this thesis has furthered our understanding of the interactions that underlie the mode of action of AMPs and the potential for synergistic interactions of peptides with clinically used antifungals. These interactions highlight the potential of AMP usage in the pursuit of alternative treatments that will help to combat microbial resistance. Increasing our understanding of AMPs and their mode or action will also facilitate the development of new peptide derivatives with increased antimicrobial action which display reduced toxicity for host cells.

References & Appendices

References

Antimicrobial peptide database website. Retrieved 16/07/09, from http://aps.unmc.edu/AP/main.php.

Aggarwal, K., Choe, L.H., Lee, K.H. (2006) "Shotgun proteomics using iTRAQ isobaric tags." *Briefings in Functional Genomics and Proteomics*. **5** (2): 112-120.

Alberti, A., Lodi, T., Ferrero, I., Donnini, C. (2003). "MIG1-dependent and MIG1-independent regulation of GAL gene expression in *Saccharomyces cerevisiae*: role of Imp2p." *Yeast*. **20** (13): 1085-1096.

Andrès, E., Dimarcq, J.L. (2007). "Cationic antimicrobial peptides: from innate immunity study to drug development. Update." *Medecine et Maladies Infectieuses*. **37** (4): 194-199.

Arathoon, E. G., Gotuzzo, E., Noriega, L.M., Berman, R.S., DiNubile, M.J., Sable, C.A. (2002). "Randomized, double-blind, multicenter study of caspofungin versus amphotericin B for treatment of oropharyngeal and esophageal candidiases." *Antimicrobial Agents and Chemotherapy.* **46**: 451-457.

Arnusch, C., Branderhorst, H., de Kruijff, B., Liskamp, R., Breukink, E., Pieters, R. (2007) "Enhanced membrane pore formation by multimeric/oligomeric antimicrobial peptides." *Biochemistry*. **46** (46): 13437-13442.

Ashrafuzzaman, M., Andersen, O., McElhaney, R. (2008). "The antimicrobial peptide gramicidin S permeabilises phospholipid bilayer membranes without forming discrete ion channels." *Biochimica et Biophysica Acta*. **1778** (12): 2814-2822.

Bachmann, S., VandeWalle, K., Ramage, G., Patterson, T., Wickes, B., Graybill, J., Lopez-Ribot, J. (2002). "*In vitro* activity of caspofungin against *Candida albicans* biofilms." *Antimicrobial Agents and Chemotherapy*. **46** (11): 3591-3596.

Baginski, M., Sternal, K., Czub, J., Borowski, E. (2005) "Molecular modelling of membrane activity of amphotericin B, a polyene macrolide antifungal antibiotic. *Acta Biochimica Polonica.* **52** (3): 655-658.

Baixench, M. T., Aoun, N., Desnos-Ollivier, M., Garcia-Hermoso, D., Bretagne, S., Ramires, S., Piketty, C., Dannaoui, E. (2007). "Acquired resistance to echinocandins in *Candida albicans*: case report and review." *The Journal of Antimicrobial Chemotherapy.* **59** (6): 1076-1083.

Balashov, S. V., Park, S., Perlin, D.S. (2006). "Assessing resistance to the echinocandin antifungal drug caspofungin in *Candida albicans* by profiling mutations in FKS1." *Antimicrobial Agents and Chemotherapy.* **50** (6): 2058-2063.

Ballou, C. E. (1990). "Isolation, characterization, and properties of *Saccharomyces cerevisiae* mnn mutants with nonconditional protein glycosylation defects." *Methods in enzymology*. **185**: 440-470.

Bates, S., MacCallum, D.M., Bertram, G., Munro, C.A., Hughes, H.B., Buurman, E.T., Brown, A.J., Odds, F.C., Gow, N.A. (2005). "*Candida albicans* Pmr1p, a secretory pathway P-type Ca2+/Mn2+-ATPase, is required for glycosylation and virulence." *The Journal of Biological Chemistry.* **280** (24): 23408-23415.

Bates, S., Hughes, H.B., Munro, C.A., Thomas, W.P., MacCallum, D.M., Bertram, G., Atrih, A., Ferguson, M.A., Brown, A.J., Odds, F.C., Gow, N.A. (2006). "Outer chain N-glycans are required for cell wall integrity and virulence of *Candida albicans*." *The Journal of Biological Chemistry.* **281** (1): 90-98.

Bechinger, B., Lohner, K. (2006) "Detergent-like actions of linear amphipathic cationic antimicrobial peptides." *Biochimica et Biophysica Acta*. **1758** (9): 1529-1539.

Bechinger, B., Zasloff, M., Opella, S.J. (1993). "Structure and orientation of the antibiotic peptide magainin in membranes by solid-state nuclear magnetic resonance spectroscopy." *Protein Science*. **2** (12): 2077-2084.

Bechinger, B. (1997). "Structure and functions of channel-forming peptides: magainins, cecropins, melittin and alamethicin." *Journal of Membrane Biology*. **156** (3): 197-211.

Ben-Efraim, I., Bach, D., Shai, Y. (1993). "Spectroscopic and functional characterization of the putative transmembrane segment of the minK potassium channel." *Biochemistry.* **32** (9): 2371-2377.

Ben-Efraim, I., Shai, Y. (1997). "The structure and organization of synthetic putative membranous segments of ROMK1 channel in phospholipid membranes." *Biophysical Journal*. **72** (1): 85-96.

Bodhe, P. V., Kotwani, R.N., Kirodian, B.G., Kshirsagar, N.A., Pandya, S.K. (2002). "Open label, randomised, comparative phase III safety and efficacy study with conventional amphotericin B and liposomal amphotericin B in patients with systemic fungal infection." *The Journal of the Association of Physicians of India.* **50** (5): 662-670.

Boman, H. G., Agerberth, B., Boman, A. (1993). "Mechanisms of action on *Escherichia coli* of cecropin P1 and PR-39, two antibacterial peptides from pig intestine." *Infection and Immunity*. **61** (7): 2978-2984.

Borenfreund, E., Puerner, J.A. (1985). "Toxicity determined in vitro by morphological alterations and neutral red absorption." *Toxicology Letters*. **24** (2-3): 119-124.

Bouvrais, H., Meleard, P., Pott, T., Jensen, K., Brask, J., Ipsen, J. (2008) "Softening of POPC membranes by magainin." *Biophysical Chemistry*. **137** (1): 7-12.

Brand, G. D., Leite, J.R., Silva, L.P., Albuquerque, S., Prates, M.V., Azevedo, R.B., Carregaro, V., Silva, J.S., Sá, V.C., Brandão, R.A., Bloch, C. Jr. (2002). "Dermaseptins from *Phyllomedusa oreades* and *Phyllomedusa distincta*. Anti-Trypanosoma cruzi activity without cytotoxicity to mammalian cells." *The Journal of Biological Chemistry*. **277** (51): 49332-49340.

Brown, S., Campbell, L., Lodge, J. (2007). "*Cryptococcus neoformans*, a fungus under stress." *Current Opinion in Microbiology*. **10** (4): 320-325.

Cabiaux, V., Agerberth, B., Johansson, J., Homblé, F., Goormaghtigh, E., Ruysschaert, J.M. (1994). "Secondary structure and membrane interaction of PR-39, a Pro+Arg-rich antibacterial peptide." *European Journal of Biochemistry*. **224** (3): 1019-1027.

Calderone, R. A. (2002). "*Candida* and Candidiasis." Washington, D.C.: ASM Press.

Cannon, R. D., Lamping, E., Holmes, A.R., Niimi, K., Tanabe, K., Niimi, M., Monk, B.C. (2007). "*Candida albicans* drug resistance another way to cope with stress." *Microbiology*. **153** (Pt 10): 3211-3217.

Cappelletty, D., Eiselstein-McKitrick, K. (2007). "The echinocandins." *Pharmacotherapy*. **27** (3):369-388.

Casadevall, A. (1998). *Cryptococcus neoformans*. Washington, D.C., ASM Press.

Cassone, M., Serra, P., Mondello, F., Girolamo, A., Scafetti, S., Pistella, E., Venditti, M. (2003). "Outbreak of *Saccharomyces cerevisiae* subtype *boulardii* fungemia in patients neighboring those treated with a probiotic preparation of the organism." *Journal of Clinical Microbiology.* **41** (11): 5340-5343.

Chai, B., Huang, J., Cairns, B.R., Laurent, B.C. (2005). "Distinct roles for the RSC and Swi/Snf ATP-dependent chromatin remodelers in DNA double-strand break repair." *Genes & Development*. **19** (14): 1656-1661.

Chalekson, C. P., Neumeister, M.W., Jaynes, J. (2003). "Treatment of infected wounds with the antimicrobial peptide D2A21." *The Journal of Trauma*. **54** (4): 770-774.

Chamilos, G., Lewis, R.E., Albert, N., Kontoyiannis, D.P. (2007). "Paradoxical effect of Echinocandins across *Candida* species in vitro: evidence for echinocandin-specific and *candida* species-related differences." *Antimicrobial Agents and Chemotherapy.* **51** (6): 2257-2259.

Chandra, J., Kuhn, D., Mukherjee, P., Hoyer, L., McCormick, T., Ghannoum, M. (2001). "Biofilm formation by the fungal pathogen Candida albicans: development, architecture, and drug resistance." *Journal of Bacteriology.* **183** (18): 5385-5394.

Chen, A., Sobel, J.D. (2005). "Emerging azole antifungals." *Expert Opinion on Emerging Drugs.* **10** (1): 21-33

Chen, J., Falla, T.J., Liu, H., Hurst, M.A., Fujii, C.A., Mosca, D.A., Embree, J.R., Loury, D.J., Radel, P.A., Cheng Chang, C., Gu, L., Fiddes, J.C. (2000). "Development of protegrins for the treatment and prevention of oral mucositis: structure-activity relationships of synthetic protegrin analogues." *Biopolymers.* **55** (1): 88-98.

Chen, S.C., Sorrell, T.C. (2007) "Antifungal agents." *The Medical Journal of Australia*. **187** (7): 404-409.

Clark, D. P., Durell, S., Maloy, W.L., Zasloff, M. (1994). "Ranalexin. A novel antimicrobial peptide from bullfrog (*Rana catesbeiana*) skin, structurally related to the bacterial antibiotic, polymyxin." *The Journal of Biological Chemistry*. 269(14): 10849-10855.

Cole, A. M. (2005). "Antimicrobial peptide microbicides targeting HIV." *Protein and Peptide Letters.* **12** (1): 41-47.

Conlon, J. M., Kolodziejek, J., Nowotny, N. (2004). "Antimicrobial peptides from *ranid* frogs: taxonomic and phylogenetic markers and a potential source of new therapeutic agents." *Biochimica et Biophysica Acta*. **1696** (1): 1-14.

Coote, P. J., Holyoak, C.D., Bracey, D., Ferdinando, D.P., Pearce, J.A. (1998). "Inhibitory action of a truncated derivative of the amphibian skin peptide dermaseptin s3 on *Saccharomyces cerevisiae*." *Antimicrobial Agents and Chemotherapy*. **42** (9): 2160-2170.

Corbacho, I., Olivero, I., Hernández, L.M. (2004). "Identification of low-dye-binding (ldb) mutants of *Saccharomyces cerevisiae*." *FEMS Yeast Research*. **4** (4-5): 437-444.

D'Abramo, M., Rinaldi, A., Bozzi, A., Amadei, A., Mignogna, G., Di Nola, A., Aschi, M. (2006). "Conformational behaviour of temporin A and temporin L in aqueous solution: a computational/experimental study." *Biopolymers*. **81** (3): 215-224.

Dalle, F., Jouault, T., Trinel, P.A., Esnault, J., Mallet, J.M., d'Athis, P., Poulain, D., Bonnin, A. (2003). "Beta-1,2- and alpha-1,2-linked oligomannosides mediate adherence of *Candida albicans* blastospores to human enterocytes in vitro." *Infection and Immunity.* **71** (12): 7061-7068.

Dannaoui, E., Lortholary, O., Raoux, D., Bougnoux, M.E., Galeazzi, G., Lawrence, C., Moissenet, D., Poilane, I., Hoinard, D., Dromer, F. (2008). "Comparative *in vitro* activities of caspofungin and micafungin, determined using the method of the European Committee on Antimicrobial Susceptibility Testing, against yeast isolates obtained in France in 2005-2006." *Antimicrobial Agents and Chemotherapy*. **52** (2): 778-781.

Dartois, V., Sanchez-Quesada, J., Cabezas, E., Chi, E., Dubbelde, C., Dunn, C., Granja, J., Gritzen, C., Weinberger, D., Ghadiri, M.R., Parr, T.R. Jr. (2005). "Systemic antibacterial activity of novel synthetic cyclic peptides." *Antimicrobial Agents and Chemotherapy*. **49** (8): 3302-3310.

Dathe, M., Nikolenko, H., Meyer, J., Beyermann, M., Bienert, M. (2001). "Optimization of the antimicrobial activity of magainin peptides by modification of charge." *FEBS Letters*. **501** (2-3): 146-150.

de Nobel, J. G., Klis, F.M., Priem, J., Munnik, T., van den Ende, H. (1990). "The glucanase-soluble mannoproteins limit cell wall porosity in *Saccharomyces cerevisiae*." *Yeast*. **6** (6): 491-499.

Denning, D.W. (2003). "Echinocandin antifungal drugs." *Lancet*. **362** (9390): 1142-1151.

Dick, J., Merz, W., Saral, R. (1980). "Incidence of polyene-resistant yeasts recovered from clinical specimens." *Antimicrobial Agents and Chemotherapy*. **18** (1): 158-163.

Dielbandhoesing, S. K., Zhang, H., Caro, L.H., van der Vaart, J.M., Klis, F.M., Verrips, C.T., Brul, S. (1998). "Specific cell wall proteins confer resistance to nisin upon yeast cells." *Applied and Environmental Microbiology*. **64** (10): 4047-4052.

Douglas, C.M. (2001) "Fungal beta(1,3)-D-glucan synthesis." *Medical Mycology.* **39** (Suppl 1): 55-66.

Douglas, C.M. (2006). "Understanding the microbiology of the *Aspergillus* cell wall and the efficacy of caspofungin." *Medical Mycology*. **44** (Suppl.): 95-99.

Duclohier, H. (2006). "Bilayer lipid composition modulates the activity of dermaseptins, polycationic antimicrobial peptides." *European Biophysics Journal*. **35** (5): 401-409.

Duellman, W., Trueb, L. (1994). "Biology of Amphibians." Johns Hopkins Univ. Press. Baltimore.

Dychala, G. R., and Lopes, J. A. (1991). "Disinfection, sterilization and preservation." Lea and Febiger, Philadelphia, Pa.

Fahrner, R., Dieckmann, T., Harwig, S., Lehrer, R., Eisenberg, D., and Feigon, J. (1996). "Solution structure of protegrin-1, a broad-spectrum antimicrobial peptide from porcine leukocytes." *Chemistry and Biology*. **3**: 543-550.

Fázio, M. A., Oliveira, V.X. Jr, Bulet, P., Miranda, M.T., Daffre, S., Miranda, A. (2006). "Structure-activity relationship studies of gomesin: importance of the disulfide bridges for conformation, bioactivities, and serum stability." *Biopolymers*. **84** (2): 205-218.

Fázio, M. A., Jouvensal, L., Vovelle, F., Bulet, P., Miranda, M.T., Daffre, S., Miranda, A. (2007). "Biological and structural characterization of new linear gomesin analogues with improved therapeutic indices." *Biopolymers*. **88** (3): 386-400.

Feldmesser, M., Kress, Y., Mednick, A., Casadevall, A. (2000). "The effect of the echinocandin analogue caspofungin on cell wall glucan synthesis by *Cryptococcus neoformans*." *The Journal of Infectious Diseases*. **182** (6): 1791-1795.

Feng, Z., Jiang, B., Chandra, J., Ghannoum, M., Nelson, S., Weinberg, A. (2005). "Human beta-defensins: differential activity against candidal species and regulation by *Candida albicans*." *Journal of Dental Research.* **84** (5): 445-450.

Fernandez-Lopez, S., Kim, H., Choi, E., Delgado, M., Granja, J., Khasanov, A., Kraehenbuehl, K., Long, G., Weinberger, D., Wilcoxen, K., Ghadiri, M. (2001). "Antimicrobial agents based on the cyclic D,L-alpha-peptide architecture." *Nature*. **412** (6845): 452-455.

Fleischhacker, M., Radecke, C., Schulz, B., Ruhnke, M. (2008). "Paradoxical growth effects of the echinocandins caspofungin and micafungin, but not of anidulafungin, on clinical isolates of *Candida*

albicans and *C. dubiniensis*." *European Journal of Clinical Microbiology and Clinical Infectious Diseases*. **27** (2): 127-131.

Friis, J., Ottolenghi, P. (1970). "The genetically determined binding of alcian blue by a minor fraction of yeast cell walls." *Comptes-Rendus des Travaux du Laboratoire Carlsberg*. **37** (15): 327-341.

Ganz, T., Selsted, M., Szklarek, D., Harwig, S., Daher, K., Bainton, D., Lehrer, R. (1985). "Defensins. Natural peptide antibiotics of human neutrophils." *The Journal of Clinical Investigation.* **76** (4): 1427-1435.

Gaskova, D., Brodska, B., Herman, P., Vecer, J., Malinsky, J., Sigler, K., Benada, O., Plasek, J. (1998). "Fluorescent probing of membrane potential in walled cells: diS-C3(3) assay in *Saccharomyces cerevisiae*." *Yeast*. **14** (13): 1189-1197.

Gazit, E., Boman, A., Boman, H.G., Shai, Y. (1995). "Interaction of the mammalian antibacterial peptide cecropin P1 with phospholipid vesicles." *Biochemistry*. **34** (36): 11479-11488.

Ghiselli, R., Giacometti, A., Cirioni, O., Mocchegiani, F., Orlando, F., Silvestri, C., Di Matteo, F., Abbruzzetti, A., Scalise, G., Saba, V. (2008). "Efficacy of the bovine antimicrobial peptide indolicidin combined with piperacillin/tazobactam in experimental rat models of polymicrobial peritonitis." *Critical Care Medicine*. **36** (1): 240-245.

Ghiselli, R., Giacometti, A., Cirioni, O., Mocchegiani, F., Silvestri, C., Orlando, F., Kamysz, W., Licci, A., Nadolski, P., Della Vittoria, A., Łukasiak, J., Scalise, G., Saba, V. (2007). "Pretreatment with the protegrin IB-367 affects Gram-positive biofilm and enhances the therapeutic efficacy of linezolid in animal models of central venous catheter infection." *Journal of Parenteral and Enteral Nutrition*. **31** (6): 463-468.

Ghiselli, R., Giacometti, A., Cirioni, O., Orlando, F., Mocchegiani, F., Pacci, A.M., Scalise, G., Saba, V. (2001). "Therapeutic efficacy of the polymyxin-like peptide ranalexin in an experimental model of endotoxemia." *The Journal of Surgical Research*. **100** (2): 183-188.

Giacometti, A., Cirioni, O., Barchiesi, F., Scalise, G. (2000). "*In-vitro* activity and killing effect of polycationic peptides on methicillin-resistant *Staphylococcus aureus* and interactions with clinically used antibiotics." *Diagnostic Microbiology and Infectious Disease.* **38** (2): 115-118.

Giacometti, A., Cirioni, O., Greganti, G., Quarta, M., Scalise, G. (1998). "In vitro activities of membrane-active peptides against gram-positive and gram-negative aerobic bacteria." *Antimicrobial Agents and Chemotherapy*. **42** (12): 3320-3324.

Gietz, R. D., Schiestl, R.H., Willems, A.R., Woods, R.A. (1995). "Studies on the transformation of intact yeast cells by the LiAc/SS-DNA/PEG procedure." *Yeast*. **11** (4): 355-360.

Giuliani, A., Pirri, G., Bozzi, A., Di Giulio, A., Aschi, M., Rinaldi, A.C. (2008). "Antimicrobial peptides: natural templates for synthetic membrane-active compounds." *Cellular and Molecular Life Sciences*. (16): 2450-2460.

Goffeau, A., Barrell, B.G., Bussey, H., Davis, R.W., Dujon, B., Feldmann, H., Galibert, F., Hoheisel, J.D., Jacq, C., Johnston, M., Louis, E.J., Mewes, H.W., Murakami, Y., Philippsen, P., Tettelin, H., Oliver, S.G. (1996). "Life with 6000 genes." *Science*. **274** (5287): 563-567.

Goldman, M. J., Anderson, G.M., Stolzenberg, E.D., Kari, U.P., Zasloff, M., Wilson, J.M. (1997). "Human beta-defensin-1 is a salt-sensitive antibiotic in lung that is inactivated in cystic fibrosis." *Cell*. **88** (4): 553-560.

Graf, C., Gavazzi, G. (2007). "*Saccharomyces cerevisiae* fungemia in an immunocompromised patient not treated with *Saccharomyces boulardii* preparation." *The Journal of Infection*. **54** (3): 310-311.

Graham, S., Coote, P.J. (2007). "Potent, synergistic inhibition of *Staphylococcus aureus* upon exposure to a combination of the endopeptidase lysostaphin and the cationic peptide ranalexin." *The Journal of Antimicrobial Chemotherapy*. **59** (4): 759-762.

Gubbins, P., Amsden, J. (2005). "Drug-drug interactions of antifungal agents and implications for patient care." *Expert Opinion in Pharmacotherapy*. **6** (13): 2231-2243.

Gudlaugsson, O., Gillespie, S., Lee, K., Vande Berg, J., Hu, J., Messer, S., Herwaldt, L., Pfaller, M., Diekema, D. (2003) "Attributable mortality of nosocomial candidemia revisited." *Clinical Infectious Diseases.* **37** (9): 1172-1177.

Hale, J. D., and Hancock, R.E.W. (2007). "Alternative mechanisms of action of cationic antimicrobial peptides on bacteria." *Expert Review of Anti-Infective Therapy*. **5**: 951-959.

Hancock, R. E., Chapple, D.S. (1999). "Peptide antibiotics." *Antimicrobial Agents and Chemotherapy.* **43** (6): 1317-1323.

Hancock, R. E., Lehrer, R. (1998). "Cationic peptides: a new source of antibiotics." *Trends in Biotechnology*. **16**: 82.

Haney, E., Hnter, H., Matsuzaki, K., Vogel, H. (2009). "Solution NMR studies of amphibian antimicrobial peptides: linking structure to function?" *Biochimica et Biophysica Acta.* **1788** (8): 1639-1655.

Haukland, H. H., Ulvatne, H., Sandvik, K., Vorland, L.H. (2001). "The antimicrobial peptides lactoferricin B and magainin 2 cross over the bacterial cytoplasmic membrane and reside in the cytoplasm." *FEBS Letters*. **508** (3): 389-393.

Helmerhorst, E. J., Breeuwer, P., van't Hof, W., Walgreen-Weterings, E., Oomen, L.C., Veerman, E.C., Amerongen, A.V., Abee, T. (1999). "The cellular target of histatin 5 on *Candida albicans* is the energized mitochondrion." *The Journal of Biological Chemistry*. **274** (11): 7286-7291.

Helmerhorst[b], E. J., Reijnders, I.M., van 't Hof W, Veerman, E.C., Nieuw Amerongen, A.V. (1999). "A critical comparison of the hemolytic and fungicidal activities of cationic antimicrobial peptides." *FEBS Letters*. **449** (2-3): 105-110.

Helmerhorst, E. J., Van't Hof, W., Veerman, E., Simoons-Smit, I., Nieuw Amerongen, A. (1997). "Synthetic histatin analogues with broad-spectrum antimicrobial activity." *The Biochemical Journal.* **326** (Pt1): 39-45.

Helmerhorst, E.J., Venuleo, C., Beri, A., Oppenheim, F. (2005). "*Candida glabrata* is unusual with respect to its resistance to cationic antifungal proteins." *Yeast*. **22** (9): 705-714.

Henry-Toulmé, N., Sarthou, P., Seman, M., Bolard, J. (1989). "Membrane effects of the polyene antibiotic amphotericin B and of some of its derivatives on lymphocytes." *Molecular and Cellular Biochemistry*. **91** (1-2): 39-44.

Hobson, R. P., Munro, C.A., Bates, S., MacCallum, D.M., Cutler, J.E., Heinsbroek, S.E., Brown, G.D., Odds, F.C., Gow, N.A. (2004). "Loss of cell wall mannosylphosphate in *Candida albicans* does not influence macrophage recognition." *The Journal of Biological Chemistry.* **279** (38): 39628-39635.

Hoffmann, W., Richter, K., Kreil, G. (1983). " A novel peptide designated PYLa and its precursor as predicted from cloned mRNA of *Xenopus laevis* skin." *The EMBO Journal*. **2** (5): 711-714.

Hugosson, M. A., D. Boman, H.G. Glaser, E. (1994). "Antibacterial peptides and mitochondrial coupling, respiration and protein import." *European Journal of Biochemistry*. **223**: 1027-1033.

Ibeas, J. I., Lee, H., Damsz, B., Prasad, D.T., Pardo, J.M., Hasegawa, P.M., Bressan, R.A., Narasimhan, M.L. (2000). "Fungal cell wall phosphomannans facilitate the toxic activity of a plant PR-5 protein." *The Plant Journal for Cell and Molecular Biology*. **23** (3).

Imura, Y., Choda, N., Matsuzaki, K. (2008). "Magainin 2 in action: distinct modes of membrane permeabilization in living bacterial and mammalian cells." *Biophysical Journal.* **95** (12): 5757-5765.

Jacob, L., Zasloff, M. (1994). "Potential therapeutic applications of magainins and other antimicrobial agents of animal origin." *Ciba Foundation Symposium*. **186**: 197-216.

Johansson, J., Gudmundsson, G., Rottenberg, M., Berndt, K., Agerberth, B. (1998). "Conformation-dependent antimicrobial activity of the naturally occurring human peptide LL-37." *The Journal of Biological Chemistry.* **273** (6): 3718-3724.

Kagan, B., Selsted, M., Ganz, T., Lehrer, R. (1990) "Antimicrobial defensins peptides from voltage-dependent ion-permeable channels in planar lipid bilayer membranes." *PNAS*. **87** (1): 210-214.

Kanafani, Z., Perfect, J. (2008). "Antimicrobial resistance: resistance to antifungal agents: mechanisms and clinical impact." *Clinical Infectious Diseases*. **46** (1): 120-128.

Kandasamy, S. K., Larson, R.G. (2004). "Binding and insertion of alpha-helical anti-microbial peptides in POPC bilayers studied by molecular dynamics simulations." *Chemistry and Physics of Lipids*. **132** (1): 113-132.

Kandasamy, S. K., Larson, R.G. (2006). "Effect of salt on the interactions of antimicrobial peptides with zwitterionic lipid bilayers." *Biochimica et Biophysica Acta*. **1758** (9): 1274-1284.

Katiyar, S., Pfaller, M., Edlind, T. (2006). "*Candida albicans* and *Candida glabrata* clinical isolates exhibiting reduced echinocandin susceptibility." *Antimicrobial Agents and Chemotherapy.* **50** (8): 2892-2894.

Kauffman, C., Carver, P. (1997). "Use of azoles for systemic antifungal therapy." *Advances in Pharmacology*. **39**: 143-189.

Kleinberg, M. (2006). "What is the current and future status of conventional amphotericin B?" *International Journal of Antimicrobial Agents*. **27** (Suppl 1): 12-16.

Khot, P., Suci, P., Miller, L., Nelson, R., Tyler, B. (2006). "A small subpopulation of blastospores in *Candida albicans* biofilms exhibit resistance to amphotericin B associated with differential regulation of ergosterol and β-1,6-glucan pathway genes." *Antimicrobial Agents and Chemotherapy*. **50** (11): 3708-3716.

Kondejewski, L. H., Lee, D.L., Jelokhani-Niaraki, M., Farmer, S.W., Hancock, R.E., Hodges, R.S. (2002). "Optimization of microbial specificity in cyclic peptides by modulation of hydrophobicity within a defined structural framework." *The Journal of Biological Chemistry.* **277** (1): 67-74.

Kurihara, T., Takeda, H., Ito, H. (1972) "Studies on the compounds related to colistin. V. Synthesis and pharmacological activity of colistin analogues." *Yakugaku Zasshi*. **92** (2): 129-134.

Kurtzman, C. P., Robnett, C.J. (1997). "Identification of clinically important ascomycetous yeasts based on nucleotide divergence in the 5' end of the large-subunit (26S) ribosomal DNA gene." *Journal of Clinical Microbiology*. **35** (5): 1216-1223.

Kwon-Chung, K. J., Rhodes, J.C. (1986). "Encapsulation and melanin formation as indicators of virulence in *Cryptococcus neoformans*." *Infection and Immunity.* **51** (1): 218-223.

Lachke, S., Srikantha, T., Tsai, L., Daniels, K., Soll, D. (2000). "Phenotypic switching in *Candida glabrata* involves phase-specific regulation of the metallothionein gene MT-II and the newly discovered hemolysin gene HLP." *Infection and Immunity*. **68** (2): 884-895.

La Rocca, P., Biggin, P.C., Tieleman, D.P., Sansom, M.S. (1999) "Simulation studies of the interaction of antimicrobial peptides and lipid bilayers." *Biochimica et Biophysica Acta*. **1462** (1-2): 185-200.

Latgé, J. P., Mouyna, I., Tekaia, F., Beauvais, A., Debeaupuis, J.P., Nierman, W. (2005). "Specific molecular features in the organization and biosynthesis of the cell wall of *Aspergillus fumigatus*." *Medical Mycology*: S15-22.

Lee, I. H., Cho, Y., Lehrer, R.I. (1997). "Effects of pH and salinity on the antimicrobial properties of clavanins." *Infection and Immunity*. **65** (7): 2898-2903.

Lee, D., Hodges, R. (2003). "Structure-activity relationships of de novo designed cyclic antimicrobial peptides based on gramicidin S." *Biopolymers*. **71** (1): 28-48.

Lehrer, R. I., Ganz, T., Szklarek, D., Selsted, M.E. (1988). "Modulation of the *in vitro* candidacidal activity of human neutrophil defensins by target cell metabolism and divalent cations." *The Journal of Clinical Investigation*. **81** (6): 1829-1835.

Leite, J. R., Brand, G.D., Silva, L.P., Kückelhaus, S.A., Bento, W.R., Araújo, A.L., Martins, G.R., Lazzari, A.M., Bloch, C. Jr. (2008). "Dermaseptins from *Phyllomedusa oreades* and *Phyllomedusa distincta*: Secondary structure, antimicrobial activity, and mammalian cell toxicity." *Comparative Biochemistry and Physiology*. **151** (3): 336-343.

Leontiadou, H., Mark, A., Marrink, S. (2006). "Antimicrobial peptides in action." *Journal of the American Chemical Society.* **128** (37): 12156-12161.

Lherm, T., Monet, C., Nougière, B., Soulier, M., Larbi, D., Le Gall, C., Caen, D., Malbrunot, C. (2002). "Seven cases of fungemia with *Saccharomyces boulardii* in critically ill patients." *Intensive Care Medicine*. **28** (6): 797-801.

Lipsky, B. A., Holroyd, K.J., Zasloff, M. (2008). "Topical versus systemic antimicrobial therapy for treating mildly infected diabetic foot ulcers: a randomized, controlled, double-blinded, multicenter trial of pexiganan cream." *Clinical Infectious Diseases*. **47** (12): 1537-1545.

Loftus, B., Fung, E., Roncaglia, P., Rowley, D., Amedeo, P., Bruno, D. *et al*. (2005). "The genome of the basidiomycetous yeast and human pathogen *Cryptococcus neoformans*." *Science*. **25** (307): 1321-1324.

Lorin, C., Saidi, H., Belaid, A., Zairi, A., Baleux, F., Hocini, H., Bélec, L., Hani, K., Tangy, F. (2005). "The antimicrobial peptide dermaseptin S4 inhibits HIV-1 infectivity *in vitro*." *Virology*. **334** (2): 264-275.

Lu, Y., Li, J., Yu, H., Xu, X., Liang, J., Tian, Y., Ma, D., Lin, G., Huang, G., Lai, R. "Two families of antimicrobial peptides with multiple functions from skin of rufous-spotten frog, *Amolops loloensis*." *Peptides*. **27** (12): 3085-3091.

Ludtke, S. J., He, K., Heller, W.T., Harroun, T.A., Yang, L., Huang, H.W. (1996). "Membrane pores induced by magainin." *Biochemistry*. **35** (43): 13723-13728.

Lupetti, A., Nibbering, P.H., Campa, M., Del Tacca, M., Danesi, R. (2003). "Molecular targeted treatments for fungal infections: the role of drug combinations." *Trends in Molecular Medicine*. **9** (6): 269-276.

MacCallum, D.M., Odds, F.C. (2005) "Temporal events in the intravenous challenge model for experimental Candida albicans infections in female mice." *Mycoses*. **48** (3): 151-161.

MacPherson, S., Akache, B., Weber, S., De Deken, X., Raymond, M., Turcotte, B. (2005). "*Candida albicans* zinc cluster protein Upc2p confers resistance to antifungal drugs and is an activator of ergosterol biosynthetic genes." *Antimicrobial Agents and Chemotherapy*. **49** (5): 1745-1752.

Maeda, S., Nagasawa, S. (1990). "Effect of sodium chloride concentration on fluid-phase assembly and stability of the C3 convertase of the classical pathway of the complement system." *The Biochemical Journal*. **271** (3): 749-754.

Makrantoni, V., Dennison, P., Stark, M.J., Coote, P.J. (2007). "A novel role for the yeast protein kinase Dbf2p in vacuolar H+-ATPase function and sorbic acid stress tolerance." *Microbiology*. **153**: 4016-4026.

Malac, J., Urbankova, E., Sigler, K., Gaskova, D. (2005). "Activity of yeast multidrug resistance pumps during growth is controlled by carbon source and the composition of growth-depleted medium: DiS-C$_3$(3) fluorescence assay." *The International Journal of Biochemistry and Cell Biology*. **37**: 2536-2543.

Maligie, M. A., Selitrennikoff, C.P. (2005). "*Cryptococcus neoformans* resistance to echinocandins: (1,3)beta-glucan synthase activity is sensitive to echinocandins." *Antimicrobial Agents and Chemotherapy*. **49** (7): 2851-2856.

Mandard, N., Sy, D., Manfrais, C., Boumatin, J., Bulet, P., Hetru, C., Vovelle, F. (1999). "Androctonin, a novel antimicrobial peptide from scorpion *Androctonus australis*: solution structure and molecular dynamics simulations in the presence of a lipid monolayer." *Journal of Biomolecular Structure and Dynamics*. **17**: 367-380.

Mandard, N., Bulet, P., Caille, A., Daffre, S., Vovelle, F. (2002). "The solution structure of gomesin, an antimicrobial cysteine-rich peptide from the spider." *European Journal of Biochemistry.* **269**: 1190-1198.

Mangoni, M., Rinaldi, A., Di Giulio, A., Mignogna, G., Bozzi, A., Barra, D., Dimmaco, M. (2000). "Structure-function relationships of temporins, small antimicrobial peptides from amphibian skin." *European Journal of Biochemistry*. **267** (5): 1447-1454.

Mareş, M., Mareş, M., Rusu, M. (2008). "Antifungal susceptibility of 95 yeast strains isolated from oral mycoses in HIV-negative and HIV-positive patients." *Bacteriologia, Virusologia, Parazitologia, Epidemiologia.* **53** (1): 41-42.

Masson, J. Y., Ramotar, D. (1996). "The *Saccharomyces cerevisiae* IMP2 gene encodes a transcriptional activator that mediates protection against DNA damage caused by bleomycin and other oxidants." *Molecular and Cellular Biology*. **16** (5): 2091-2100.

Matsuzaki, K., Sugishita, K., Fujii, N., Miyajima, K. (1995). "Molecular basis for membrane selectivity of an antimicrobial peptide, magainin 2." *Biochemistry*. **34** (10): 3423-3429.

Matsuzaki, K., Mitani, Y., Akada, K.Y., Murase, O., Yoneyama, S., Zasloff, M., Miyajima, K. (1998). "Mechanism of synergism between antimicrobial peptides magainin 2 and PGLa." *Biochemistry*. **37** (43): 15144-15153.

McClelland, E. E., Bernhardt, P., Casadevall, A. (2006). "Estimating the relative contributions of virulence factors for pathogenic microbes." *Infection and Immunity*. **74** (3): 1500-1504.

McCullough, M. J., Clemons, K.V., Farina, C., McCusker, J.H., Stevens, D.A. (1998). "Epidemiological investigation of vaginal *Saccharomyces cerevisiae* isolates by a genotypic method." *Journal of Clinical Microbiology*. **36** (2): 557-562.

Mochon, A. B., Liu, H. (2008). "The antimicrobial peptide histatin-5 causes a spatially restricted disruption on the *Candida albicans* surface, allowing rapid entry of the peptide into the cytoplasm." *PLoS Pathogens*. **4** (10): e1000190.

Monk, B. C., Niimi, K., Lin, S., Knight, A., Kardos, T.B., Cannon, R.D., Parshot, R., King, A., Lun, D., Harding, D.R. (2005). "Surface-active fungicidal D-peptide inhibitors of the plasma membrane proton pump that block azole resistance." *Antimicrobial Agents and Chemotherapy.* **49** (1): 57-70.

Montain, S. J., Cheuvront, S.N., Lukaski, H.C. (2007). "Sweat mineral-element responses during 7 h of exercise-heat stress." *International Journal of Sport Nutrition and Exercise Metabolism.* **17** (6): 574-582.

Mor, A., Nguyen, V.H., Delfour, A., Migliore-Samour, D., Nicolas, P. (1991). "Isolation, amino acid sequence, and synthesis of dermaseptin, a novel antimicrobial peptide of amphibian skin." *Biochemistry*. **30** (36): 8824-8830.

Mor, A., Nicolas, P. (1994). "The NH2-terminal alpha-helical domain 1-18 of dermaseptin is responsible for antimicrobial activity." *The Journal of Biological Chemistry.* **269** (3): 1934-1939.

Mor, A., Hani, K., Nicolas, P. (1994). "The vertebrate peptide antibiotics dermaseptins have overlapping structural features but target specific microorganisms." *The Journal of Biological Chemistry*. **269** (50): 31635-31641.

Mora-Duarte, J., Betts, R., Rotstein, C., Colombo, A.L., Thompson-Moya, L., Smietana, J., Lupinacci, R., Sable, C., Kartsonis, N., Perfect, J. (2002). "Comparison of caspofungin and amphotericin B for invasive candidiasis." *The New England Journal of Medicine*. **347** (25): 2020-2029.

Morton[a], C. O., Dos Santos, S.C., Coote, P. (2007). "An amphibian-derived, cationic, alpha-helical antimicrobial peptide kills yeast by caspase-independent but AIF-dependent programmed cell death." *Molecular Microbiology*. **65** (2): 494-507.

Morton[b], C. O., Hayes, A., Wilson, M., Rash, B.M., Oliver, S.G., Coote, P. (2007). "Global phenotype screening and transcript analysis outlines the inhibitory mode(s) of action of two amphibian-derived, alpha-helical, cationic peptides on *Saccharomyces cerevisiae*." *Antimicrobial Agents and Chemotherapy*. **51** (11): 3948-3959.

Mulet, J. M., Leube, M.P., Kron, S.J., Rios, G., Fink, G.R., Serrano, R. (1999). "A novel mechanism of ion homeostasis and salt tolerance in yeast: the Hal4 and Hal5 protein kinases modulate the Trk1-Trk2 potassium transporter." *Molecular and Cellular Biology.* **19** (5): 3328-3337.

Muñoz, P., Bouza, E., Cuenca-Estrella, M., Eiros, J.M., Pérez, M.J., Sánchez-Somolinos, M., Rincón, C., Hortal, J., Peláez, T. (2005). "*Saccharomyces cerevisiae* fungemia: an emerging infectious disease." *Clinical Infectious Diseases*. **40** (11): 1625-1634.

Munro, C. A., Bates, S., Buurman, E.T., Hughes, H.B., Maccallum, D.M., Bertram, G., Atrih, A., Ferguson, M.A., Bain, J.M., Brand, A., Hamilton, S., Westwater, C., Thomson, L.M., Brown, A.J., Odds, F.C., Gow, N.A. (2005). "Mnt1p and Mnt2p of *Candida albicans* are partially redundant alpha-1,2-mannosyltransferases that participate in O-linked mannosylation and are required for adhesion and virulence." *The Journal of Biological Chemistry.* **280** (2): 1051-1060.

Navarro-García, F., Alonso-Monge, R., Rico, H., Pla, J., Sentandreu, R., Nombela, C. (1998). "A role for the MAP kinase gene MKC1 in cell wall construction and morphological transitions in *Candida albicans*." *Microbiology*. **144**: 411-424.

Navon-Venezia, S., Feder, R., Gaidukov, L., Carmeli, Y., Mor, A. (2002). "Antibacterial properties of dermaseptin S4 derivatives with *in vivo* activity." *Antimicrobial Agents and Chemotherapy*. **46** (3): 689-694.

Netea, M. G., Gow, N.A., Munro, C.A., Bates, S., Collins, C., Ferwerda, G., Hobson, R.P., Bertram, G., Hughes, H.B., Jansen, T., Jacobs, L., Buurman, E.T., Gijzen, K., Williams, D.L., Torensma, R., McKinnon, A., MacCallum, D.M., Odds, F.C., Van der Meer, J.W., Brown, A.J., Kullberg, B.J. (2006). "Immune sensing of *Candida albicans* requires cooperative recognition of mannans and glucans by lectin and Toll-like receptors." *The Journal of Clinical Investigation.* **116** (6): 1642-1650.

Netea, M. G., Brown, G.D., Kullberg, B.J., Gow, N.A. (2008). "An integrated model of the recognition of *Candida albicans* by the innate immune system." *Nature Reviews: Microbiology*. **6** (1): 67-78.

Nicolas, P., El Amri, C. (2009) The dermaseptin superfamily: A gene-based combinatorial library of antimicrobial peptides. *Biochimica et Biophysica Acta*. **1788** (8): 1537-1550.

Odani, T., Shimma, Y., Tanaka, A., Jigami, Y. (1996). "Cloning and analysis of the MNN4 gene required for phosphorylation of N-linked oligosaccharides in *Saccharomyces cerevisiae*." *Glycobiology*. **6** (8): 805-810.

Odds, F. (2003). "Synergy, antagonism, and what the chequerboard puts between them." *The Journal of Antimicrobial Chemotherapy*. **52** (1): 1.

Odds, F. C., Motyl, M., Andrade, R., Bille, J., Cantón, E., Cuenca-Estrella, M., Davidson, A., Durussel, C., Ellis, D., Foraker, E., Fothergill, A.W., Ghannoum, M.A., Giacobbe, R.A., Gobernado, M., Handke, R., Laverdière, M., Lee-Yang, W., Merz, W.G., Ostrosky-Zeichner, L., Pemán, J., Perea, S., Perfect, J.R., Pfaller, M.A., Proia, L., Rex, J.H., Rinaldi, M.G., Rodriguez-Tudela, J.L., Schell, W.A., Shields, C., Sutton, D.A., Verweij, P.E., Warnock, D.W. (2004). "Interlaboratory comparison of results of susceptibility testing with caspofungin against *Candida* and *Aspergillus* species." *Journal of Clinical Microbiology*. **42** (8): 3475-3482.

Oren, Z., Shai, Y. (1997). "Selective lysis of bacteria but not mammalian cells by diastereomers of melittin: structure-function study." *Biochemistry*. **36** (7): 1826-1835.

Oren, Z., Shai, Y. (1998). "Mode of action of linear amphipathic alpha-helical antimicrobial peptides." *Biopolymers*. **47** (6): 451-463.

Oura, M., Sternberg, T.H., Wright, E.T. (1955). "A new antifungal antibiotic, amphotericin B." *Antibiotics Annual*. **3**: 566-573.

Panyutich, A., Ganz, T. (1991). "Activated alpha 2-macroglobulin is a principal defensin-binding protein." *American Journal of Respiratory Cell and Molecular Biology*. **5** (2): 101-106.

Papo, N., Shai, Y. (2003). "Can we predict biological activity of antimicrobial peptides from their interactions with model phospholipid membranes?" *Peptides*. **24** (11): 1693-1703.

Pérez-Valle, J., Jenkins, H., Merchan, S., Montiel, V., Ramos, J., Sharma, S., Serrano, R., Yenush, L. (2007). "Key role for intracellular K+ and protein kinases Sat4/Hal4 and Hal5 in the plasma membrane stabilization of yeast nutrient transporters." *Molecular and Cellular Biology*. **27** (16): 5725-5736.

Perlin, D. S. (2007). "Resistance to echinocandin-class antifungal drugs." *Drug Resistance Updates*. **10** (3): 121-130.

Peschel, A., Otto, M., Jack, R.W., Kalbacher, H., Jung, G., Götz, F. (1999). "Inactivation of the dlt operon in *Staphylococcus aureus* confers sensitivity to defensins, protegrins, and other antimicrobial peptides." *The Journal of Biological Chemistry*. **274** (13): 8405-8410.

Peschel, A., Jack, R.W., Otto, M., Collins, L.V., Staubitz, P., Nicholson, G., Kalbacher, H., Nieuwenhuizen, W.F., Jung, G., Tarkowski, A., van Kessel, K.P., van Strijp, J.A. (2001). "*Staphylococcus aureus* resistance to human defensins and evasion of neutrophil killing via the novel virulence factor MprF is based on modification of membrane lipids with l-lysine." *The Journal of Experimental Medicine*. **193** (9): 1067-1076.

Pfaller, M. A., Marco, F., Messer, S., Jones, R. (1998). "*In vitro* activity of two echinocandin derivatives, LY303366 and MK-0991 (L-743,792), against clinical isolates of *Aspergillus*, *Fusarium*, *Rhizopus*, and other filamentous fungi." *Diagnostic Microbiology and Infectious Disease*. **30** (4): 251-255.

Pfaller, M. A., Diekema, D.J. (2007). "Epidemiology of invasive candidiasis: a persistent public health problem." *Clinical Microbiology Reviews*. **20** (1): 133-163.

Pooley, H. M., Karamata, D. (1994). "Bacterial Cell Wall." Elsevier science publications, Amsterdam, The Netherlands.

Pouny, Y., Rapaport, D., Mor, A., Nicolas, P., Shai, Y. (1992). "Interaction of antimicrobial dermaseptin and its fluorescently labelled analogues with phospholipid membranes." *Biochemistry*. **31** (49): 12416-12423.

Povirk, L. F., Wübter, W., Köhnlein, W., Hutchinson, F. (1977). "DNA double-strand breaks and alkali-labile bonds produced by bleomycin." *Nucleic Acids Research*. **4** (10): 3573-3580.

Powers, J.P., Hancock, R.E. (2003) "The relationship between peptide structure and antibacterial activity." *Peptides*. **24** (11): 1681-1691.

Qi, Q. G., Hu, T., Zhou, X.D. (2005). "Frequency, species and molecular characterization of oral *Candida* in hosts of different age in China." *Journal of Oral Pathology and Medicine*. **34** (6): 352-356.

Ramos, J., Haro, R., Rodríguez-Navarro, A. (1990). "Regulation of potassium fluxes in *Saccharomyces cerevisiae*." *Biochimica et Biophysica Acta*. **1029** (2): 211-217.

Ramos, J., Alijo, R., Haro, R., Rodriguez-Navarro, A. (1994). "TRK2 is not a low-affinity potassium transporter in *Saccharomyces cerevisiae*." *Journal of Bacteriology*. **176** (1): 249-252.

Redding, S. W., Zellars, R.C., Kirkpatrick, W.R., McAtee, R.K., Caceres, M.A., Fothergill, A.W., Lopez-Ribot, J.L., Bailey, C.W., Rinaldi, M.G., Patterson, T.F. (1999). "Epidemiology of oropharyngeal *Candida* colonization and infection in patients receiving radiation for head and neck cancer." *Journal of Clinical Microbiology*. **37** (12): 3896-3900.

Redding, S. W., Kirkpatrick, W.R., Dib, O., Fothergill, A.W., Rinaldi, M.G., Patterson, T.F. (2000). "The epidemiology of non-albicans *Candida* in oropharyngeal candidiasis in HIV patients." *Special Care in Dentistry*. **20** (5): 178-781.

Redding, S. W., Kirkpatrick, W.R., Coco, B.J., Sadkowski, L., Fothergill, A.W., Rinaldi, M.G., Eng, T.Y., Patterson, T.F. (2002). "*Candida glabrata* oropharyngeal candidiasis in patients receiving radiation treatment for head and neck cancer." *Journal of Clinical Microbiology*. **40** (5): 1879-1881.

Redding, S. W., Dahiya, M.C., Kirkpatrick, W.R., Coco, B.J., Patterson, T.F., Fothergill, A.W., Rinaldi, M.G., Thomas, C.R. Jr. (2004). "*Candida glabrata* is an emerging cause of oropharyngeal candidiasis in patients receiving radiation for head and neck cancer." *Oral Surgery, Oral Medicine, Oral Pathology, Oral Radiology and Endodontics*. **97** (1): 47-52.

Reinoso-Martín, C., Schüller, C., Schuetzer-Muehlbauer, M., Kuchler, K. (2003). "The yeast protein kinase C cell integrity pathway mediates tolerance to the antifungal drug caspofungin through activation of Slt2p mitogen-activated protein kinase signalling." *Eukaryotic Cell*. **2** (6): 1200-1210.

Rex, J. H., Rinaldi, M.G., Pfaller, M.A. (1995). "Resistance of *Candida* species to fluconazole." *Antimicrobial Agents and Chemotherapy*. **39** (1): 1-8.

Rezusta, A., Aspiroz, C., Boekhout, T., Cano, J.F., Theelen, B., Guarro, J., Rubio, M.C. (2008). "Cholesterol dependent and Amphotericin B resistant isolates of a *Candida glabrata* strain from an Intensive Care Unit patient." *Medical Mycology*. **46** (3): 265-268.

Rozek, A., Friedrich, C., Hancock, R. (2000). "Structure of the bovine antimicrobial peptide indolicidin bound to dodecylphosphocholine and sodium dodecyl sulphate micelles." *Biochemistry*. **39** (51): 15765-15774.

Rudolph, H. K., Antebi, A., Fink, G.R., Buckley, C.M., Dorman, T.E., LeVitre, J., Davidow, L.S., Mao, J.I., Moir, D.T. (1989). "The yeast secretory pathway is perturbed by mutations in PMR1, a member of a Ca2+ ATPase family." *Cell*. **58** (1): 133-145.

Ruiz-Herrera, J., Mormeneo, S., Vanaclocha, P., Font-de-Mora, J., Iranzo, M., Puertes, I., Sentandreu, R. (1994). "Structural organization of the components of the cell wall from *Candida albicans*." *Microbiology*. **140** (Pt 7): 1513-1523.

Ruiz-Herrera, J., Elorza, M.V., Valentín, E., Sentandreu, R. (2006). "Molecular organization of the cell wall of *Candida albicans* and its relation to pathogenicity." *FEMS Yeast Research.* **6** (1): 14-29.

Salas, S. D., Bennett, J.E., Kwon-Chung, K.J., Perfect, J.R., Williamson, P.R. (1996). "Effect of the laccase gene CNLAC1, on virulence of *Cryptococcus neoformans*." *The Journal of Experimental Medicine*. **184** (2): 377-386.

Salonen, J. H., Richardson, M.D., Gallacher, K., Issakainen, J., Helenius, H., Lehtonen, O.P., Nikoskelainen, J. (2000). "Fungal colonization of haematological patients receiving cytotoxic chemotherapy: emergence of azole-resistant *Saccharomyces cerevisiae*." *The Journal of Hospital Infection.* **45** (4): 293-301.

Sambrook, J., Fritsch, E.F., Maniatis, T. (1989). "Molecular cloning - A laboratory manual." Cold spring harbour laboratory press, New York.

Sanglard, D., Ischer, F., Monod, M., Bille, J. (1997). "Cloning of *Candida albicans* genes conferring resistance to azole antifungal agents: characterization of CDR2, a new multidrug ABC transporter gene." *Microbiology*. **143** (Pt 2): 405-416.

Sanglard, D., Ischer, F., Parkinson, T., Falconer, D., Bille, J. (2003). "*Candida albicans* mutations in the ergosterol biosynthetic pathway and resistance to several antifungal agents." *Antimicrobial Agents and Chemotherapy*. **47** (8): 2404-2412.

Sanglard, D., Kuchler, K., Ischer, F., Pagani, J., Monod, M., Bille, J. (1995). "Mechanisms of resistance to azole antifungal agents in *Candida albicans* isolates from AIDS patients involve specific multidrug transporters." *Antimicrobial Agents and Chemotherapy*. **39** (11): 2378-2386.

Savoia, D., Guerrini, R., Marzola, E., Salvadori, S. (2008). "Synthesis and antimicrobial activity of dermaseptin S1 analogues." *Bioorganic and Medical Chemistry*. **16** (17): 8205-8209.

Schimoler-O'Rourke, R., Renault, S., Mo, W., Selitrennikoff, C. (2003). "*Neurospora crassa* FKS protein binds to the (1,3)beta-glucan synthase substrate, UDP-glucose." *Current Microbiology*. **46** (6): 408-412.

Shai, Y. (1995). "Molecular recognition between membrane spanning polypeptides." *Trends in Biochemical Sciences*. **20**: 460-464.

Shai, Y. (1999). "Mechanism of the binding, insertion and destabilisation of phospholipid bilayer membranes by alpha-helical antimicrobial and cell non-selective membrane lytic peptides." *Biochimica et Biophysica Acta.* **1462** (1-2): 55-70.

Shai, Y. (2002). "Mode of action of membrane active antimicrobial peptides." *Biopolymers*. **66** (4): 236-248.

Shai, Y., Oren, Z. (1996). "Diastereoisomers of cytolysins, a novel class of potent antibacterial peptides." *The Journal of Biological Chemistry*. **271** (13): 7305-7308.

Shai, Y., Oren, Z. (2001). "From "carpet" mechanism to de-novo designed diastereomeric cell-selective antimicrobial peptides." *Peptides*. **22** (10): 1629-1641.

Sheehan, D., Hitchcock, C., Sibley, C. (1999). "Current and emerging azole antifungal agents." *Clinical Microbiology Reviews*. **12** (1): 40-79.

Sheff, M. A., Thorn, K.S. (2004). "Optimized cassettes for fluorescent protein tagging in *Saccharomyces cerevisiae*." *Yeast*. **21** (8): 661-670.

Shepherd, C., Vogel, H., Tieleman, D. (2003). "Interactions of the designed antimicrobial peptide MB21 and truncated dermaseptin S3 with lipid bilayers: molecular-dynamics simulations." *The Biochemical Journal*. **370** (Pt 1): 233-243.

Silva, P., Daffre, S., and Buylet, P. (2000). "Isolation and characterization of gomesin, an 18-residue cysteine-rich defence peptide from the spider *Acanthoscurria gomesiana* hemocytes with sequence similarities to Horseshoe crab antimicrobial peptides of the tachyplesin family." *The Journal of Biological Chemistry*. **275**: 33464-33470.

Sikorski, R., Hieter, P. (1989). "A system of shuttle vectors and yeast host strains designed for efficient manipulation of DNA in *Saccharomyces cerevisiae*." *Genetics*. **122** (1): 19-27.

Singleton, D., Masuoka, J., Hazen, K. (2005). "Surface hydrophobicity changes of two *Candida albicans* serotype B *mnn4*delta mutants." *Eukaryotic Cell*. **4** (4):639-648.

Smits, G. J., van den Ende, H., Klis, F.M. (2001). "Differential regulation of cell wall biogenesis during growth and development in yeast." *Microbiology*. **147** (Pt. 4): 781-794.

Sokolov, Y., Mirzabekov, D., Martin, D., Lehrer, R., Kagan, B. (1999). "Membrane channel formation by antimicrobial protegrins." *Biochimica et Biophysica Acta*. **1420** (1-2): 23-29.

Staubitz, P., Peschel, A., Nieuwenhuizen, W., Otto, M., Gotz, F., Jung, G., Jack, R. (2001). "Structure-function relationships in the tryptophan-rich, antimicrobial peptide indolicidin." *Journal of Peptide Science*. **7** (10): 552-564.

Stenderup, A., Pedersen, G.T. (1962). "Yeasts of human origin." *Acta Pathologica et Microbiologica Scandinavica.* **54**: 462-472.

Stevens, D. A., Ichinomiya, M., Koshi, Y., Horiuchi, H. (2006). "Escape of *Candida* from caspofungin inhibition at concentrations above the MIC (paradoxical effect) accomplished by increased cell wall chitin; evidence for beta-1,6-glucan synthesis inhibition by caspofungin." *Antimicrobial Agents and Chemotherapy*. **50** (9): 3160-3161.

Subbalakshmi, C., Bikshapathy, E., Sitaram, N., Nagaraj, R. (2000). "Antibacterial and hemolytic activities of single tryptophan analogues of indolicidin." *Biochemical and Biophysical Research Communications*. **274** (3): 714-716.

Tachi, T., Epand, R.F., Epand, R.M., Matsuzaki, K. (2002). "Position-dependent hydrophobicity of the antimicrobial magainin peptide affects the mode of peptide-lipid interactions and selective toxicity." *Biochemistry*. **41** (34): 10723-10731.

Tamba, Y., Yamazaki, M. (2009). "Magainin 2-induced pore formation in the lipid membranes depends on its concentration in the membrane interface." *The Journal of Physical Chemistry. B.* **113** (14): 4846-4852.

Tan, K., Brayshaw, N., Tomaszewski, K., Troke, P., Wood, N. (2006). "Investigation of the potential relationships between plasma voriconazole concentrations and visual adverse events or liver function test abnormalities." *Journal of Clinical Pharmacology*. **46** (2): 235-243.

Tanaka, D., Miyasaki, K.T., Lehrer, R.I. (2000). "Sensitivity of *Actinobacillus actinomycetemcomitans* and *Capnocytophaga* spp. to the bactericidal action of LL-37: a cathelicidin found in human leukocytes and epithelium." *Oral Microbiology and Immunology*. **15** (4): 226-231.

Tang, Y., Yuan, J., Osapay, K., Tran, D., Miller, C., Ouellette, A., Selsted, M. (1999). "A cyclic antimicrobial peptide produced in primate leukocytes by the ligation of two truncated alpha-defensins." *Science*. **286** (5439): 498-502.

Thornton, G., Wilkinson, M., Toone, M., Jones, N. (2005). "A novel pathway determining multidrug sensitivity in *Schizosaccharomyces pombe*." *Genes to Cells*. **10**: 941-951.

Trabi, M., Schirra, H., Craik, D. (2001). "Three-dimensional structure of RTD-1, a cyclic antimicrobial defensins from Rhesus macaque leukocytes." *Biochemistry*. **10** (14): 4211-4221.

Tran, D., Tran, P., Roberts, K., Osapay, G., Schaal, J., Ouellette, A., Selsted, M. (2008). "Microbicidal properties and cytocidal selectivity of rhesus macaque theta defensins." *Antimicrobial Agents and Chemotherapy*. **52** (3): 944-953.

Tsai, H., Krol, A., Sarti, K., Bennett, J. (2006). "*Candida glabrata PDR1*, a transcriptional regulator of a pleitropic drug resistance network, mediates azole resistance in clinical isolates and petite mutants." *Antimicrobial Agents and Chemotherapy*. **50** (4): 1384-1392.

Tsao, S., Rahkhoodaee, F., Raymond, M. (2009). "Relative contribution of the *Candida albicans* ABC transporters Cdr1p and Cdr2p to clinical azole resistance." *Antimicrobial Agents and Chemotherapy*. **58** (4): 1344-1352.

Vandeputte, P., Tronchin, G., Berges, T., Hennequin, C., Chabasse, D., Bouchara, J. (2007). "Reduced susceptibility to polyenes associated with a missense mutation in the *ERG6* gene in a clinical isolate of *Candida glabrata* with pseudohyphal growth." *Antimicrobial Agents and Chemotherapy*. **51** (3): 982-990.

Vanhoye, D., Bruston, F., Nicolas, P., Amiche, M. (2003). "Antimicrobial peptides from hylid and ranin frogs originated from a 150-million-year-old ancestral precursor with a conserved signal peptide but a hypermutable antimicrobial domain." *European Journal of Biochemistry*. **270** (9): 2068-2081.

van 't Hof, W., Veerman, E.C., Helmerhorst, E.J., Amerongen, A.V. (2001). "Antimicrobial peptides: properties and applicability." *Biological Chemistry*. **382** (4): 597-619.

Vignal, E., Chavanieu, A., Roch, P., Chiche, L., Grassy, G., Calas, B., Aumelas, A. (1998). "Solution structure of the antimicrobial peptide ranalexin and a study of its interaction with perdeuterated dodecylphosphocholine micelles." *European Journal of Biochemistry*. **253** (1): 221-228.

Villanueva, A., Gotuzzo, E., Arathoon, E.G., Noriega, L.M., Kartsonis, N.A., Lupinacci, R.J., Smietana, J.M., DiNubile, M.J., Sable, C.A. (2002). "A randomized double-blind study of caspofungin versus fluconazole for the treatment of esophageal candidiasis." *The American Journal of Medicine*. **113**: 294-299.

Wang, Y., Casadevall, A. (1994). "Susceptibility of melanized and nonmelanized *Cryptococcus neoformans* to nitrogen- and oxygen-derived oxidants." *Infection and Immunity*. **62** (7): 3004-3007.

Wasan, K., Wasan, E., Gershkovich, P., Zhu, X., Tidwell, R., Werbovetz, K., Clement, J., Thornton, S. (2009). "Highly effective oral amphotericin B formulation against murine visceral leishmaniasis." *The Journal of Infectious Diseases*. **200** (3): 357-360.

Welling, M. M., Hiemstra, P.S., van den Barselaar, M.T., Paulusma-Annema, A., Nibbering, P.H., Pauwels, E.K., Calame, W. (1998). "Antibacterial activity of human neutrophil defensins in experimental infections in mice is accompanied by increased leukocyte accumulation." *The Journal of Clinical Investigation*. **102** (8): 1583-1590.

White, T.C. (2007). "Mechanisms of resistance to antifungal agents." *Manual of clinical microbiology*, 9th Ed. ASM Press, Washington: 1961-1971.

White, T. C., Marr, K.A., Bowden, R.A. (1998). "Clinical, cellular, and molecular factors that contribute to antifungal drug resistance." *Clinical Microbiology Reviews*. **11** (2): 382-402.

Wiederhold, N. P., Kontoyiannis, D.P., Prince, R.A., Lewis, R.E. (2005). "Attenuation of the activity of caspofungin at high concentrations against *Candida albicans*: possible role of cell wall integrity and calcineurin pathways." *Antimicrobial Agents and Chemotherapy*. **49** (12): 5146-5148.

Wilson, B., Erdjument-Bromage, H., Tempst, P., Cairns, B.R. (2006). "The RSC chromatin remodeling complex bears an essential fungal-specific protein module with broad functional roles." *Genetics*. **172** (2): 795-809.

Wimley, W.C., White, S.H. (1996) "Experimentally determined hydrophobicity scale for proteins at membrane interfaces." *Nature Structural Biology*. **3** (10): 842-848.

Wisplinghoff, H. Bischoff, T., Tallent, S.M., Seifert, H., Wenzel, R.P., Edmond, M.B. (2004). " Nosocomial bloodsteam infections in US hospitals: analysis of 24,179 cases from a prospective nationwide surveillance study." *Clinical Infectious Diseases*. **39** (3): 309-317.

Wong-Beringer, A., Jacobs, R., Guglielmo, B. (1998). "Lipid formulations of amphotericin B: clinical efficacy and toxicities." *Clinical Infectious Diseases*. **27** (3): 603-618.

Xiong, Y. Q., Bayer, A.S., Yeaman, M.R. (2002). "Inhibition of intracellular macromolecular synthesis in *Staphylococcus aureus* by thrombin-induced platelet microbicidal proteins." *The Journal of Infectious Diseases*. **185** (3): 348-356.

Yasumura, Y., Kawakita, M. (1963). "The research for the SV40 by means of tissue culture technique." *Nippon Rinsho*. **21** (6): 1209-1219.

Yang, L., Weiss, T.M., Lehrer, R.I., Huang, H.W. (2000). "Crystallization of antimicrobial pores in membranes: magainin and protegrin." *Biophysical Journal.* **79** (4): 2002-2009.

Yang, C., Zhang, Y., Javob, M., Khan, S., Zhang, Y., Li, X. (2006). "Antifungal activity of C-27 steroidal saponins." *Antimicrobial Agents and Chemotherapy*. **50** (5): 1710-1714.

Yoneyama, F., Imura, Y., Ohno, K., Zendo, T., Nakayama, J., Matsuzaki, K., Sonomoto, K. (2009). "Peptide-lipid huge toroidal pore: a new antimicrobial mechanism mediated by a lactococcal bacteriocin, lacticin Q." *Antimicrobial Agents and Chemotherapy*. **53** (8): 3211-3217.

Zairi, A., Serres, C., Tangy, F., Jouannet, P., Hani, K. (2008). "*In vitro* spermicidal activity of peptides from amphibian skin: dermaseptin S4 and derivatives." *Bioorganic and Medicinal Chemistry.* **16** (1): 266-275.

Zaoutis, T. E., Foraker, E., McGowan, K.L., Mortensen, J., Campos, J., Walsh, T.J., Klein, J.D. (2005). "Antifungal susceptibility of *Candida* spp. isolated from pediatric patients: a survey of 4 children's hospitals." *Diagnostic Microbiology and Infectious Disease*. **52** (4): 295-298.

Zasloff, M. (1987). "Magainins, a class of antimicrobial peptides from *Xenopus* skin: isolation, characterization of two active forms, and partial cDNA sequence of a precursor." *Proceedings of the National Academy of Sciences in the United States of America.* **84** (15): 5449-5453.

Appendix I: Plasmid maps

pGEM-T Easy Vector (Promega)
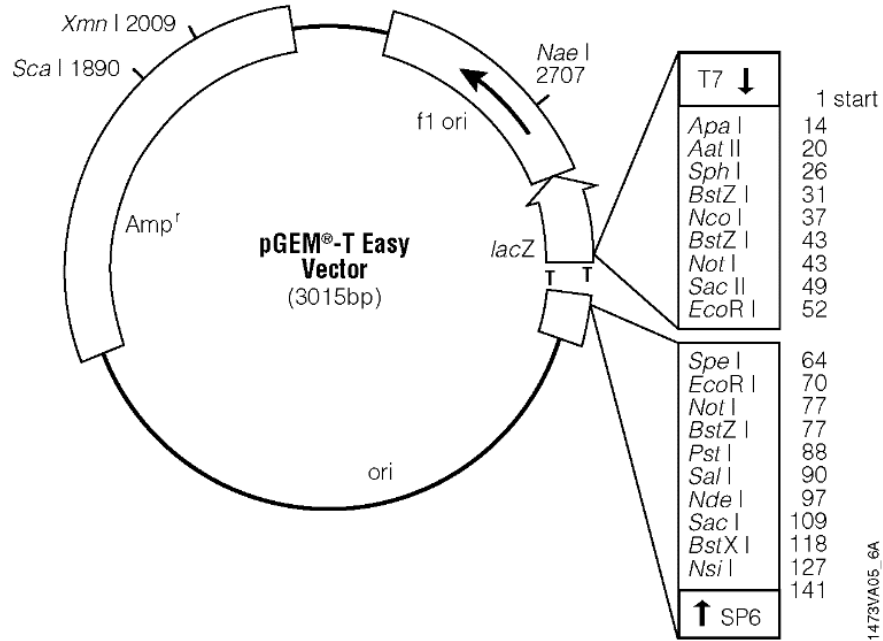
pRS313 Shuttle Vector (Sikorski, 1989)
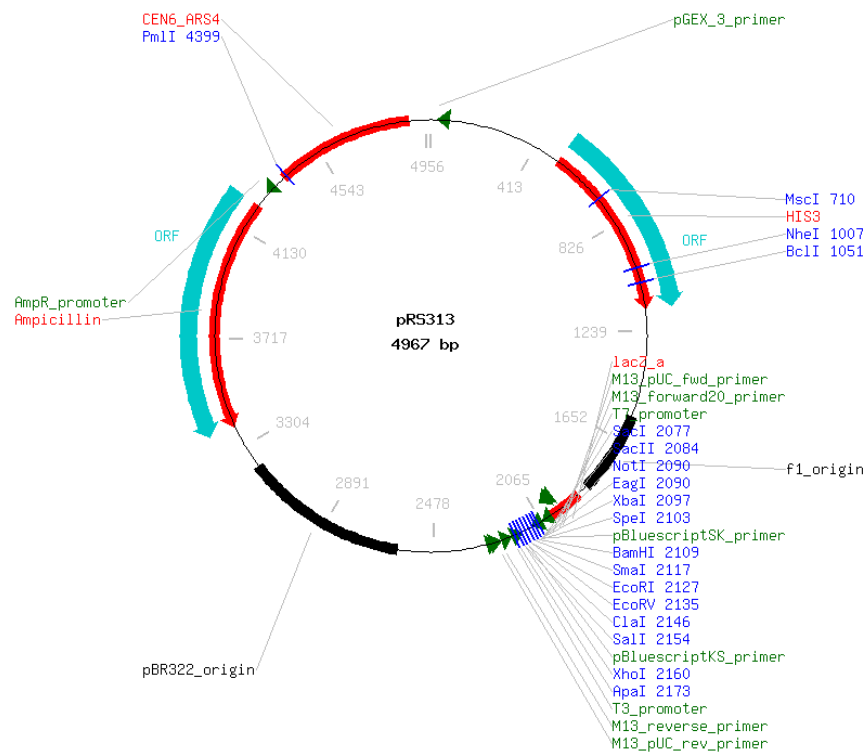
pRS423 Shuttle Vector (Sikorski, 1989)
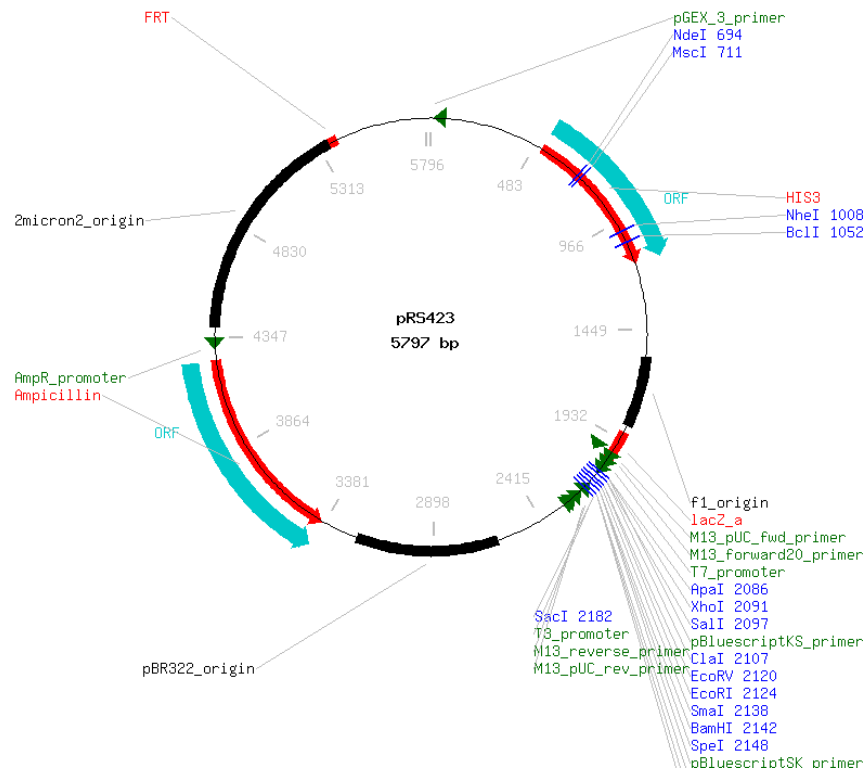
pKT209 plasmid (Sheff *et al*, 2004)
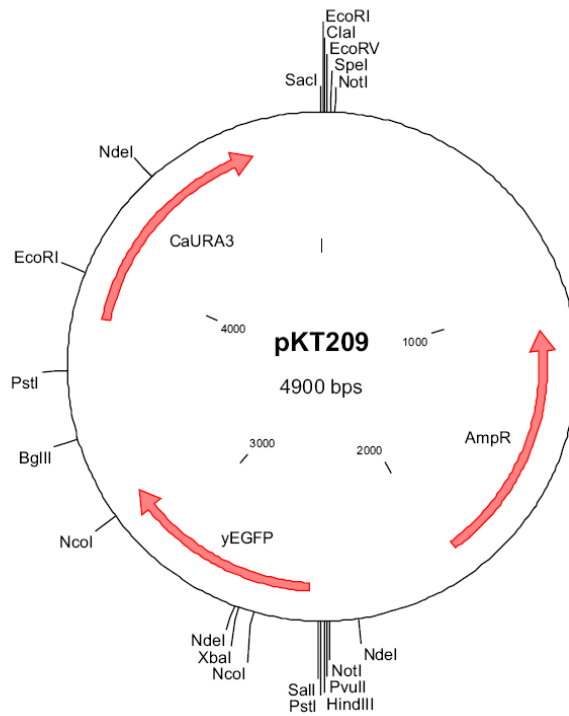
Appendix II: Growth of glycosylation mutants with AMP and in the presence or absence of exogenous phosphate
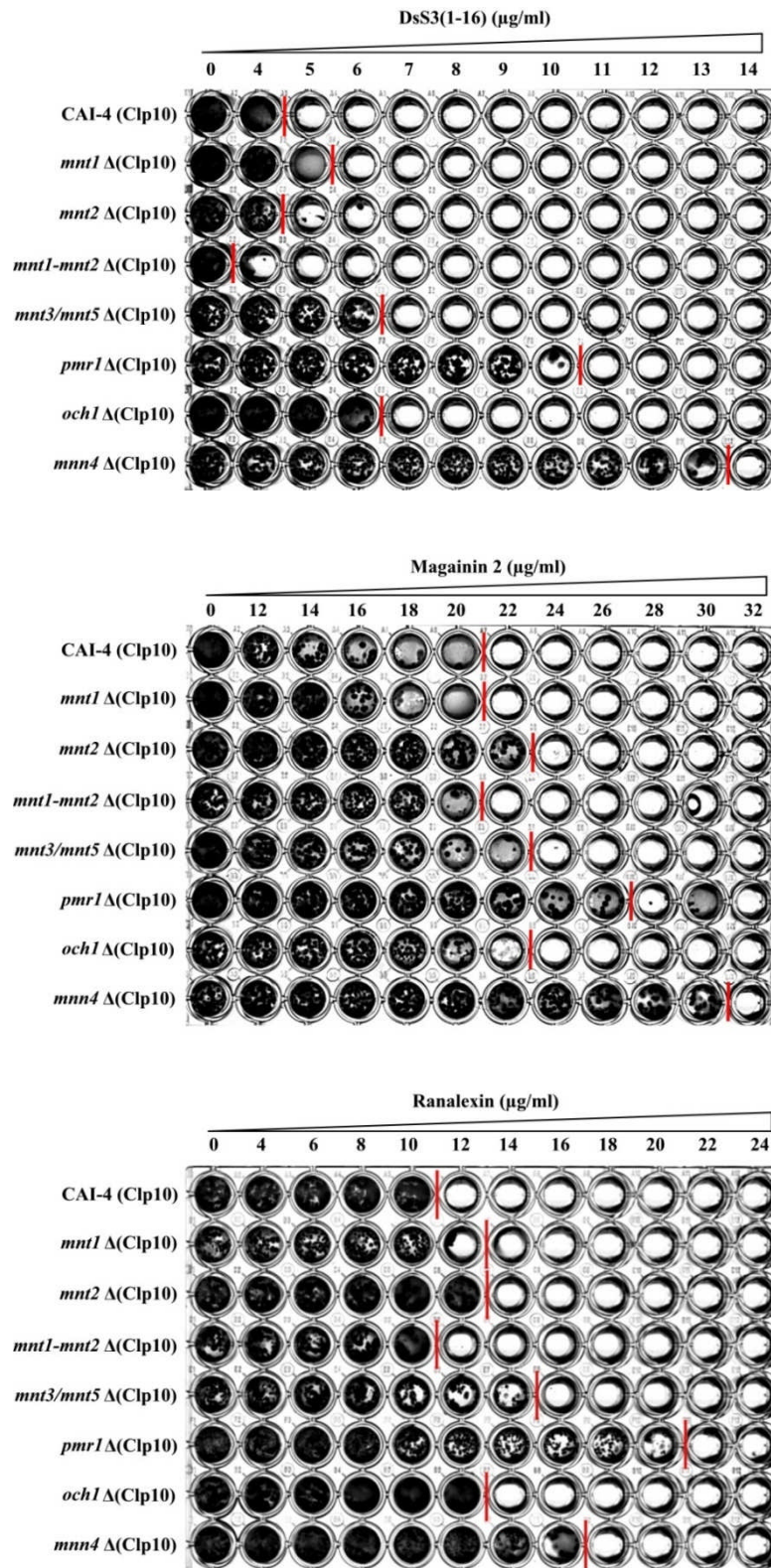
Figure 1. Representative checkerboard assays used to determine MICs with *C. albicans* glycosylation mutants in the presence of DsS3(1-16), mag 2 and rana. Experiments were carried out in triplicate and representative images for each are shown. Lines separate wells where growth was present from wells where growth was absent.
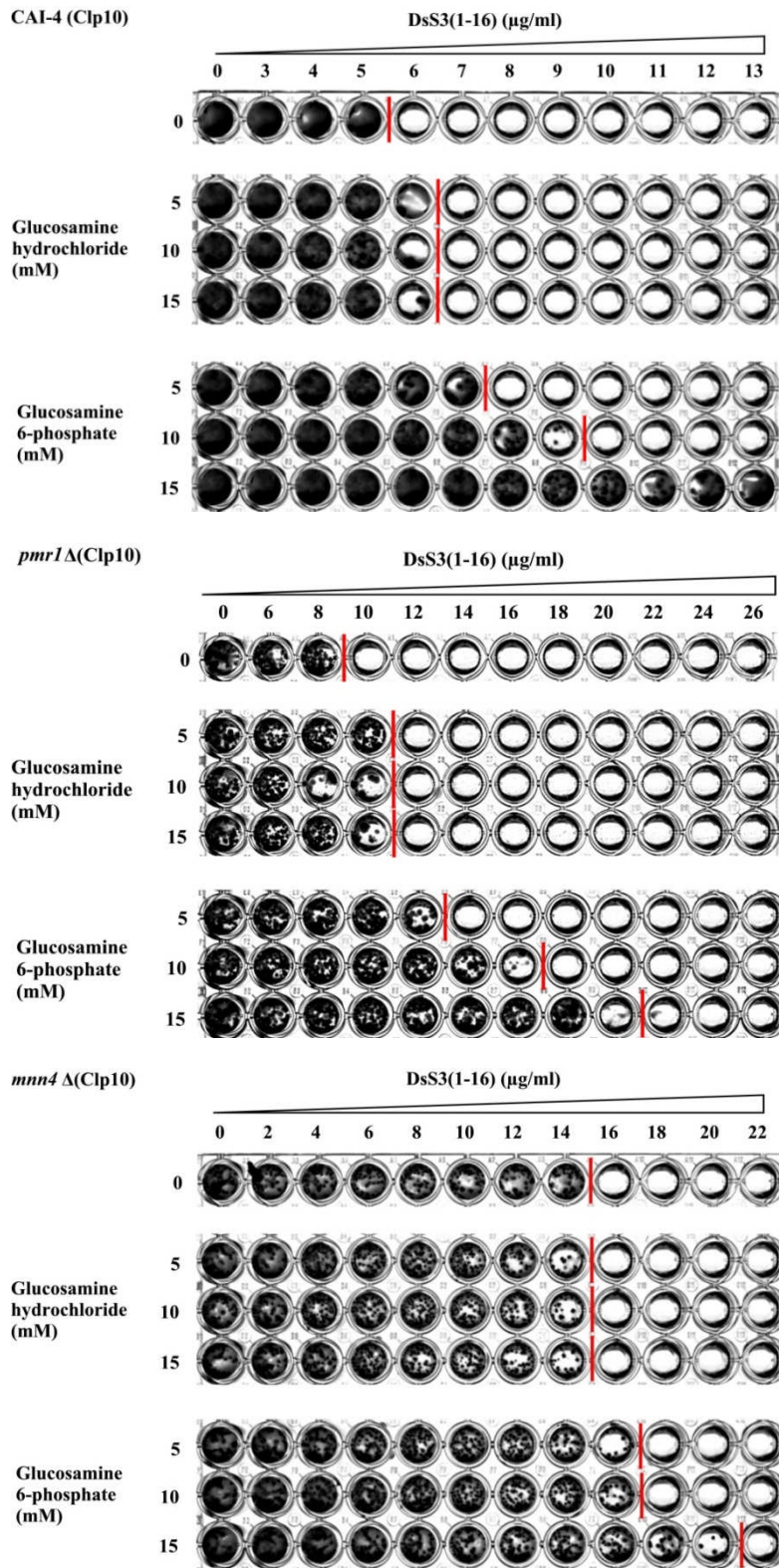
Figure 2. Representative checkerboard assays used to determine MICs with *C. albicans* glycosylation mutants in the presence or absence of exogenous phosphate and AMP. Experiments were carried out in triplicate and representative images for each are shown. Lines separate wells where growth was present from wells where growth was absent.

Appendix III: MICs of all strains exposed to each AMP in MEB or RPMI
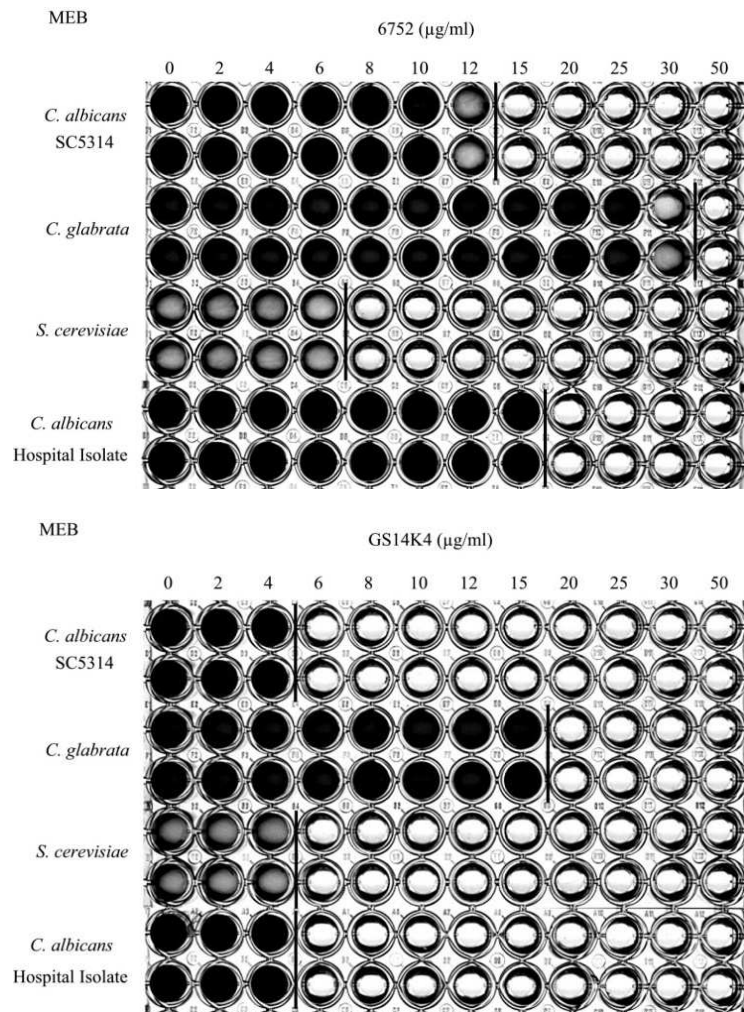
Figure 1. Representative checkerboard assays used to determine MICs for *C. albicans* hospital isolate and SC5314, *C. glabrata* and *S. cerevisiae* with 6752 and GS14K4 in MEB. Experiments were carried out in duplicate and representative images for each are shown. Lines separate wells where growth was present from wells where growth was absent.
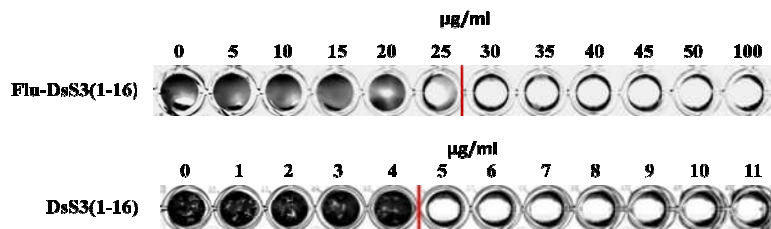

Figure 2. Representative checkerboard assays used to determine MICs for SC5314 with Flu-DsS3(1-16). Experiments were carried out in duplicate and representative images are shown. Lines separate wells where growth was present from wells where growth was absent.

RPMI Media

C. albicans Hospital Isolate

Peptide Concentration (μg/ml)

0   0.5   1   2   4   8   16   32   64   128   256   512

Ranalexin

Magainin 2

DsS3 (1-16)

GS14K4

6752

C. albicans SC5314

Peptide Concentration (μg/ml)

0   0.5   1   2   4   8   16   32   64   128   256   512

Ranalexin

Magainin 2

DsS3 (1-16)

GS14K4

6752

C. glabrata

Peptide Concentration (μg/ml)

0   0.5   1   2   4   8   16   32   64   128   256   512

Ranalexin

Magainin 2

DsS3 (1-16)

GS14K4

6752
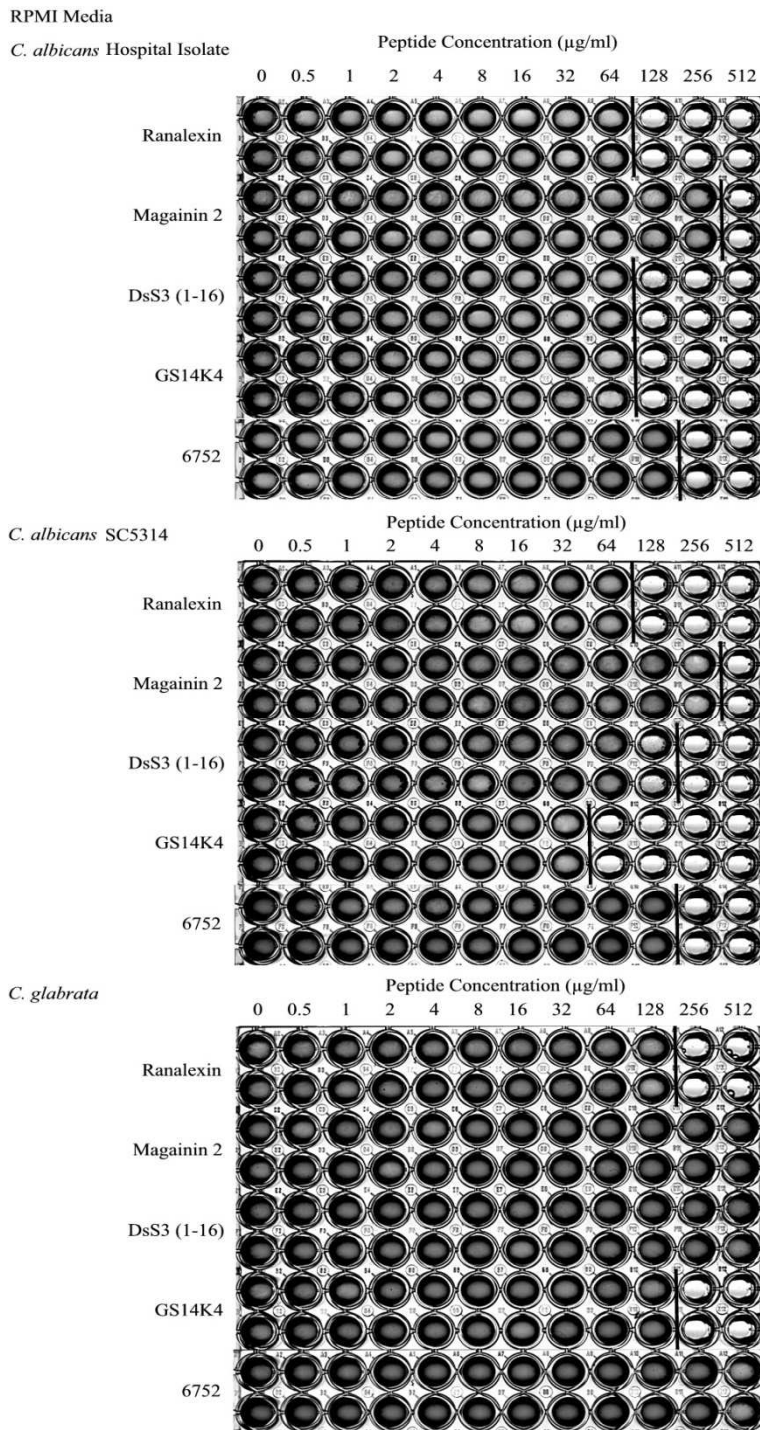
Figure 3. Representative checkerboard assays used to determine MICs for *C. glabrata*, *C. albicans* hospital isolate and SC5314 with AMP in RPMI. Experiments were carried out in duplicate and representative images for each are shown. Lines separate wells where growth was present from wells where growth was absent.

Appendix IV: Visual growth assays used for the determination of FICs
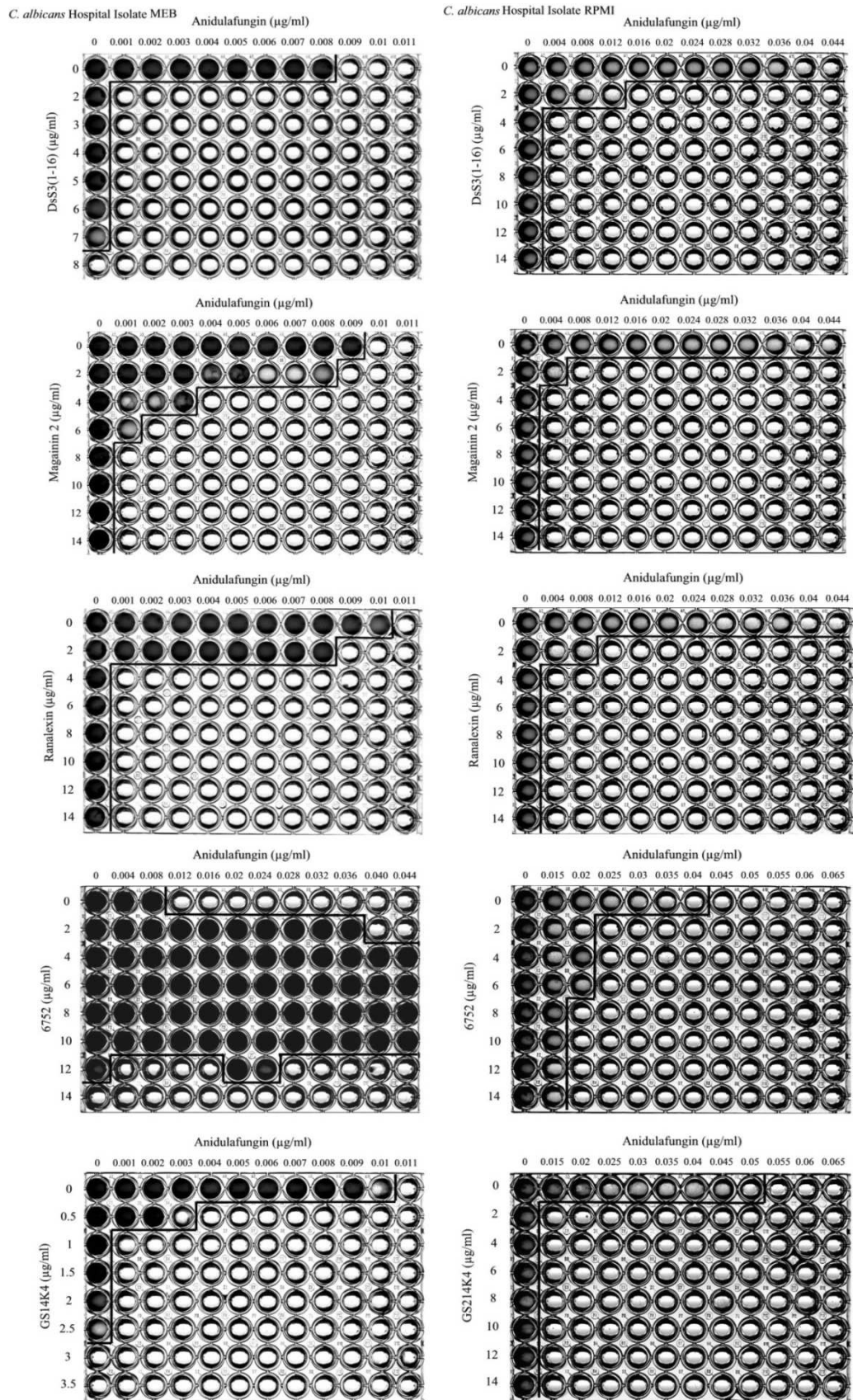
Figure 1. Representative checkerboard assays used to determine FICs with *C. albicans* hospital isolate with AMP and Anidulafungin. Each experiment was carried out in triplicate and representative images for each are shown. Lines separate wells where growth was present from wells where growth was absent.

Figure 2. Representative checkerboard assays used to determine FICs for *C. glabrata* with AMP and Anidulafungin. Each experiment was carried out in triplicate and representative images for each are shown. Lines separate wells where growth was present from wells where growth was absent.

Figure 3. Representative checkerboard assays used to determine FICs for SC5314 with AMP and Anidulafungin. Each experiment was carried out in triplicate and representative images for each are shown. Lines separate wells where growth was present from wells where growth was absent.

Figure 4. Representative checkerboard assays used to determine FICs for *C. albicans* hospital isolate with AMP and Caspofungin. Each experiment was carried out in triplicate and representative images for each are shown. Lines separate wells where growth was present from wells where growth was absent.
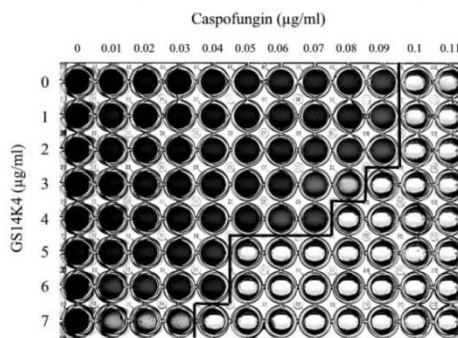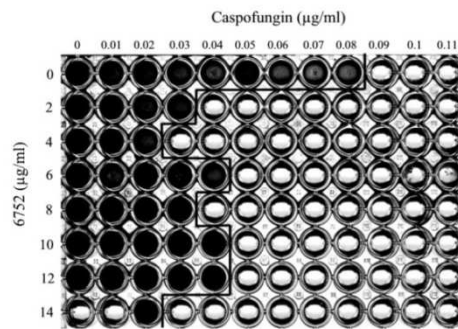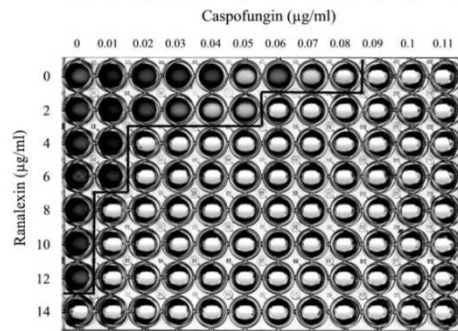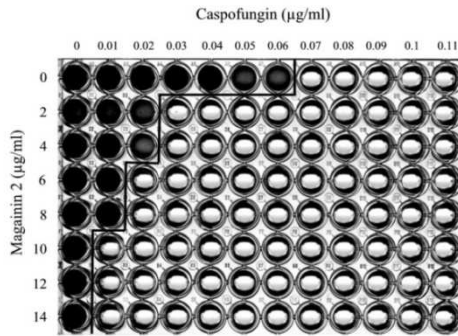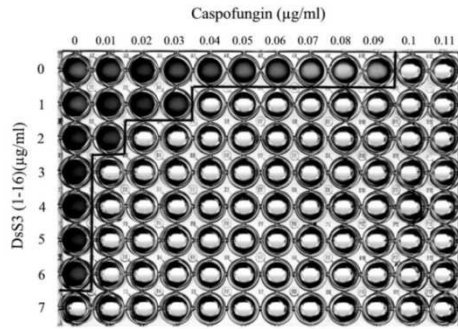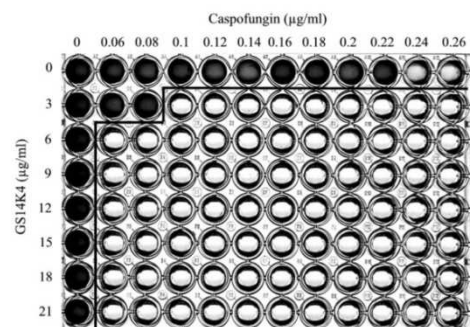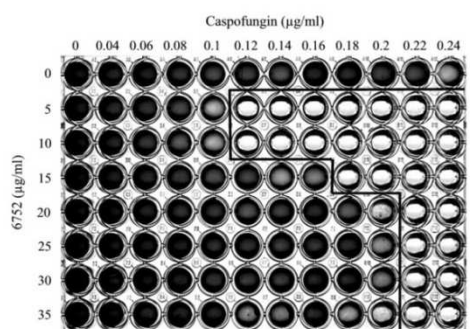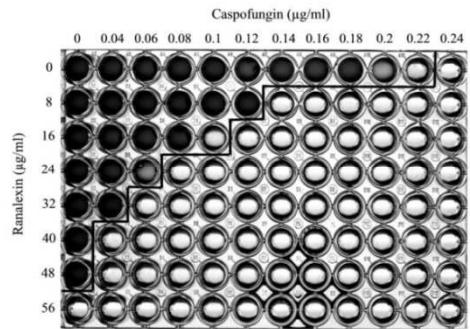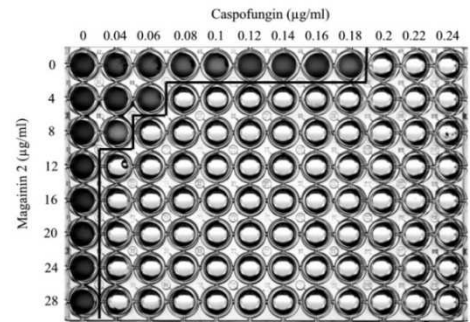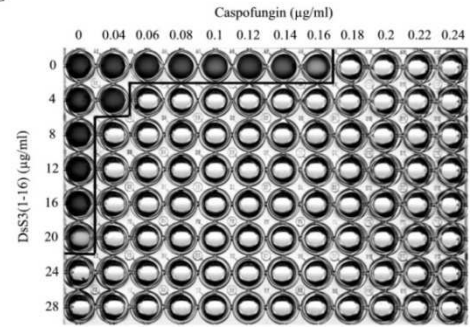
Figure 5. Representative checkerboard assays used to determine FICs for SC5314 and *C. glabrata* with AMP and Caspofungin. Each experiment was carried out in triplicate and representative images for each are shown. Lines separate wells where growth was present from wells where growth was present where growth was absent.
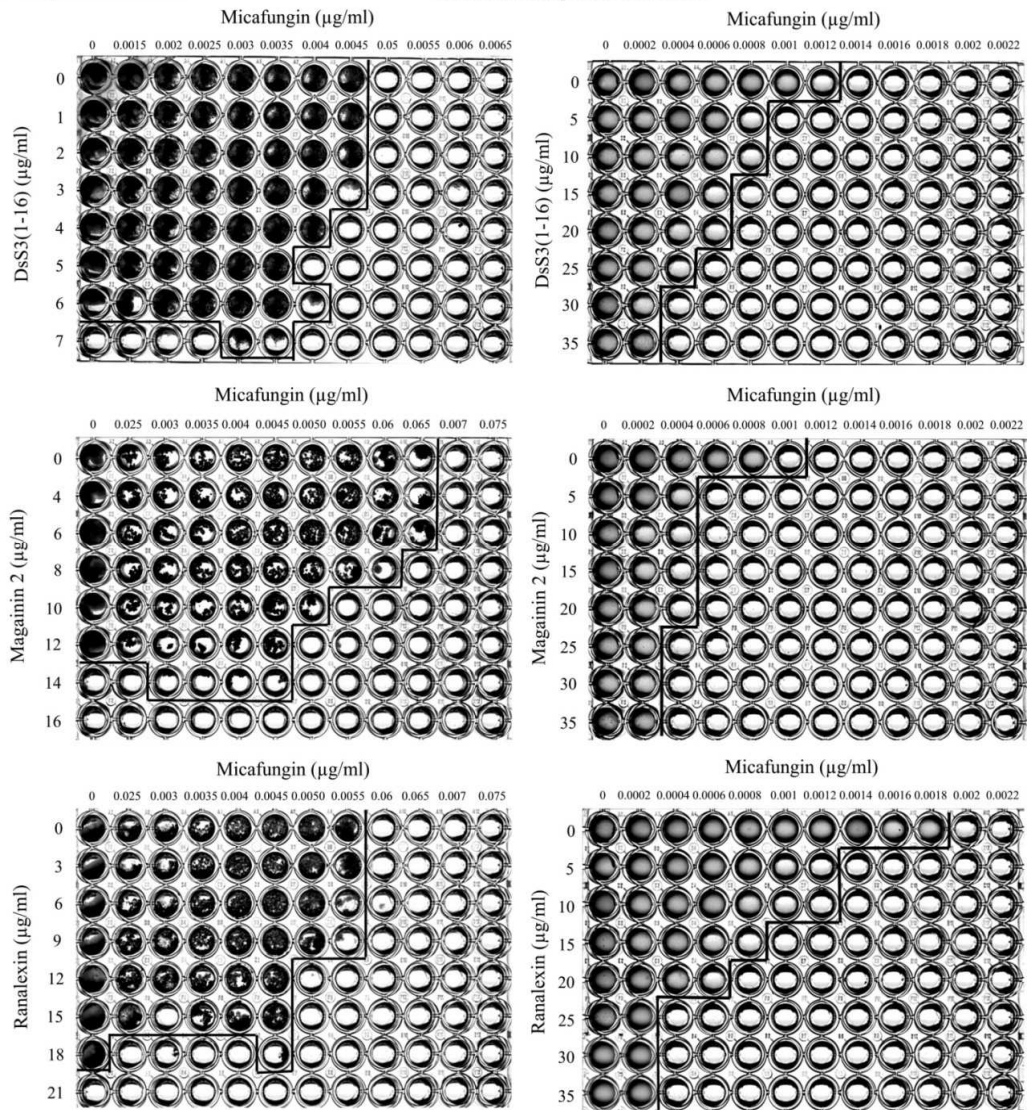
Figure 6. Representative checkerboard assays used to determine FICs for *C. albicans* hospital isolate with AMP and Micafungin. Each experiment was carried out in triplicate and representative images for each are shown. Lines separate wells where growth was present from wells where growth was absent.
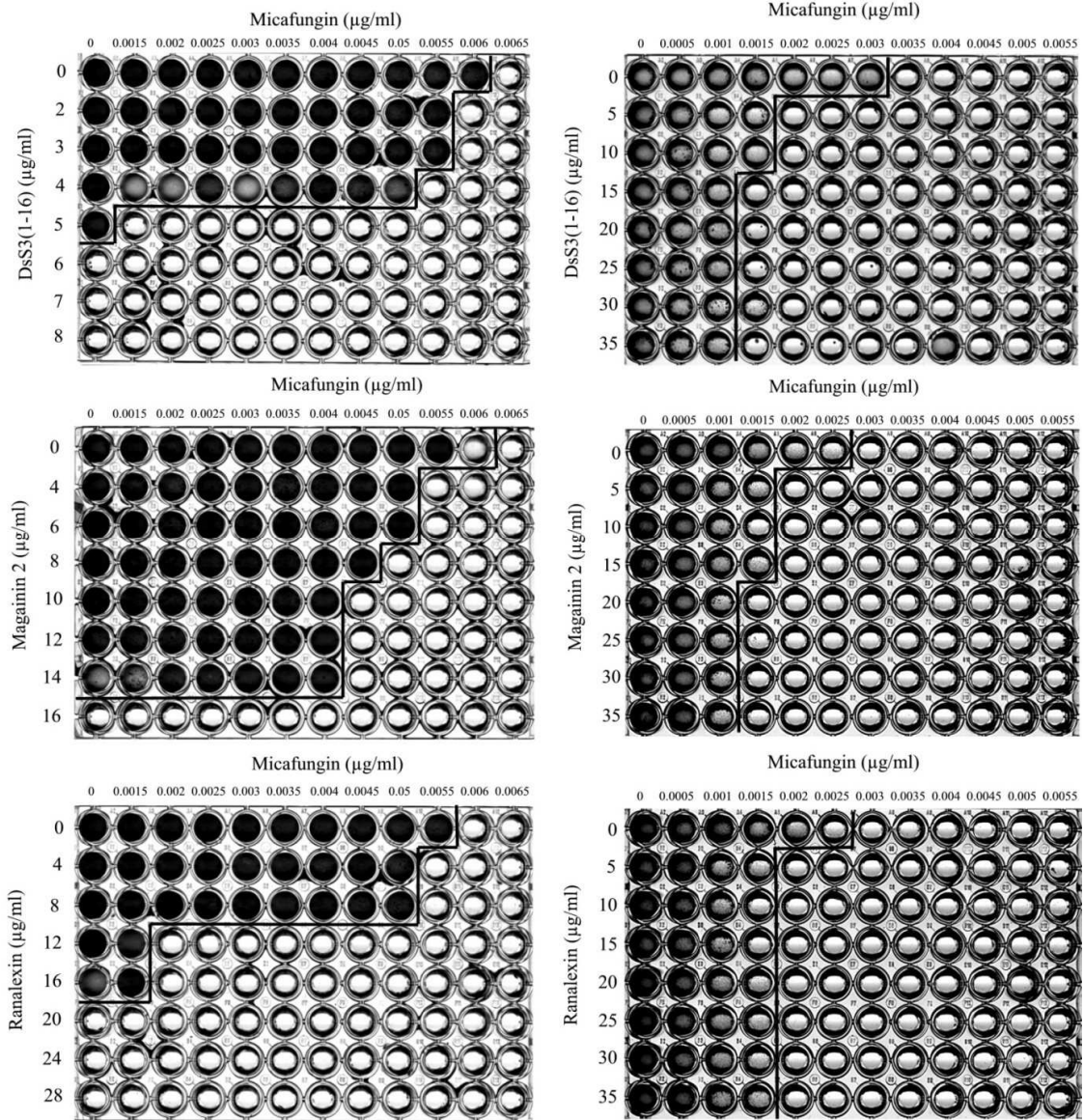
Figure 7. Representative checkerboard assays used to determine FICs for SC5314 with AMP and Micafungin. Each experiment was carried out in triplicate and representative images for each are shown. Lines separate wells where growth was present from wells where growth was absent.
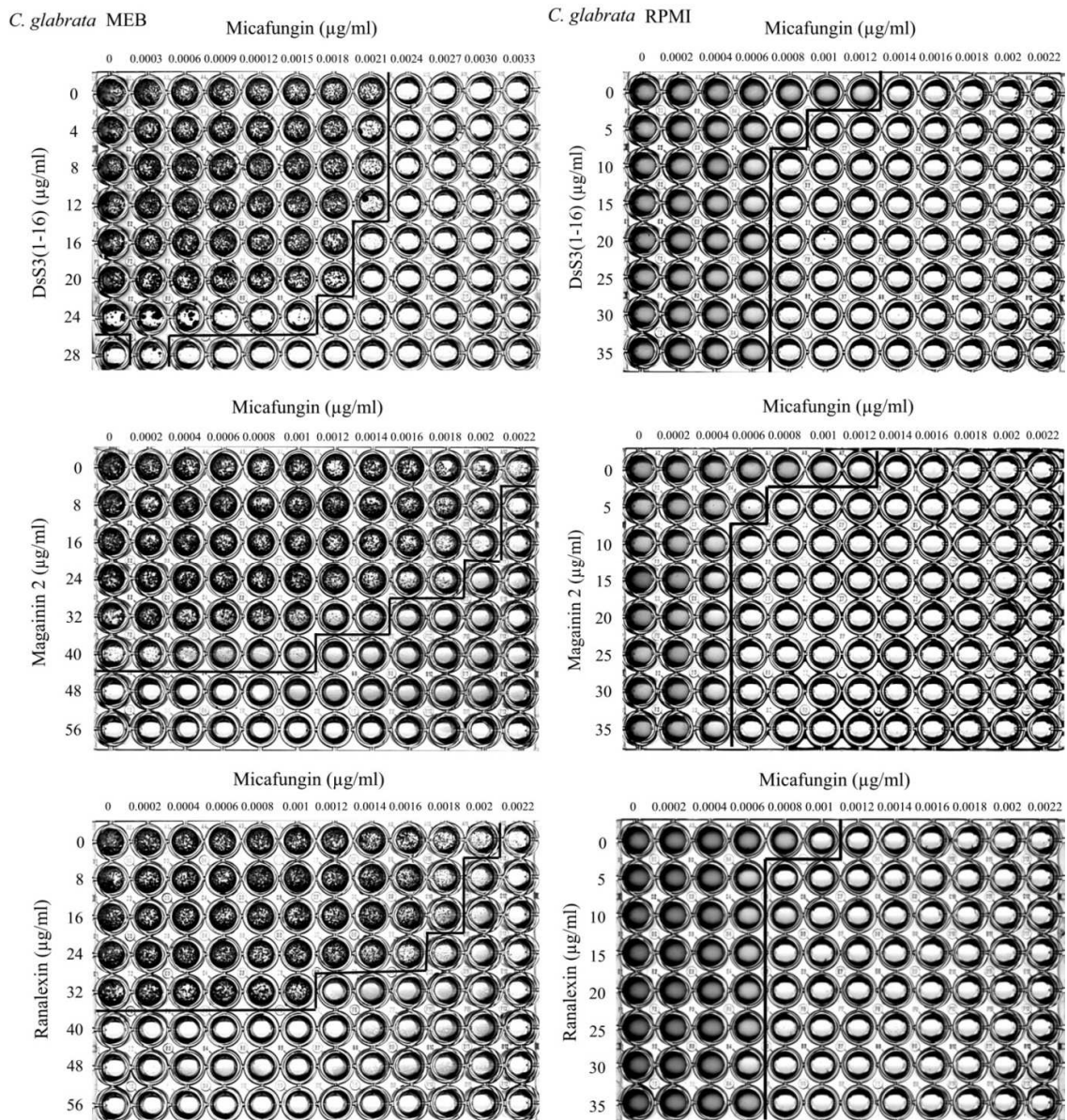
Figure 8. Representative checkerboard assays used to determine FICs for *C. glabrata* with AMP and Micafungin. Each experiment was carried out in triplicate and representative images for each are shown. Lines separate wells where growth was present from wells where growth was absent.
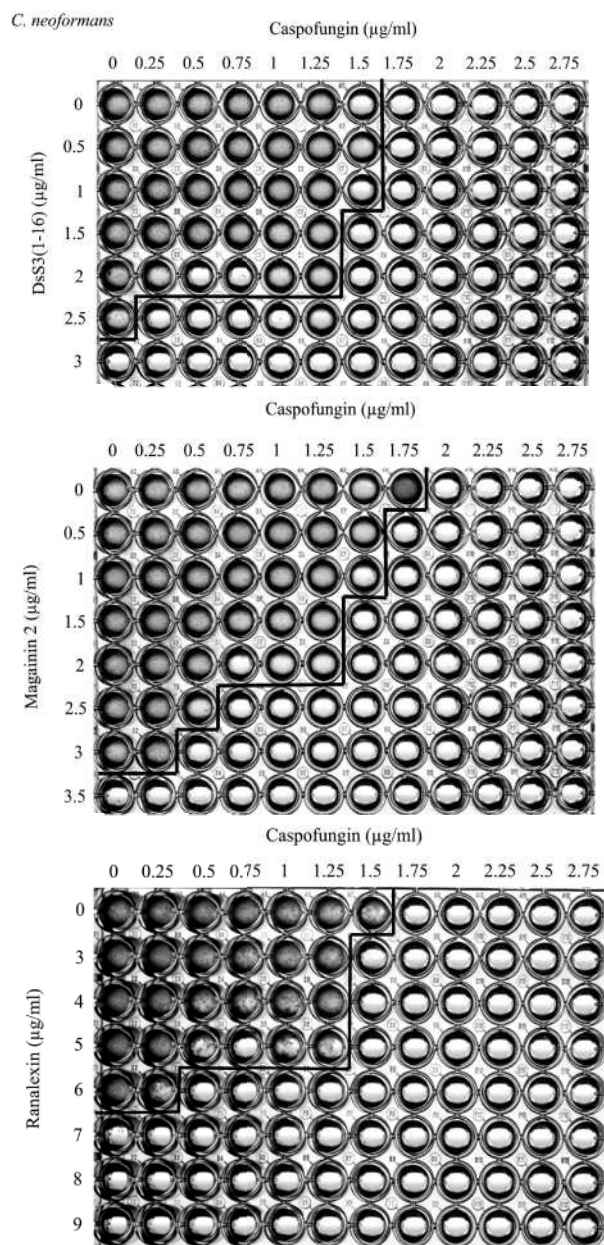
Figure 9. Representative checkerboard assays used to determine FICs for *C. neoformans* with AMP and Caspofungin. Each experiment was carried out in triplicate and representative images for each are shown. Lines separate wells where growth was present from wells where growth was present from wells where growth was present where growth was absent.

Appendix V: Disc diffusion assays
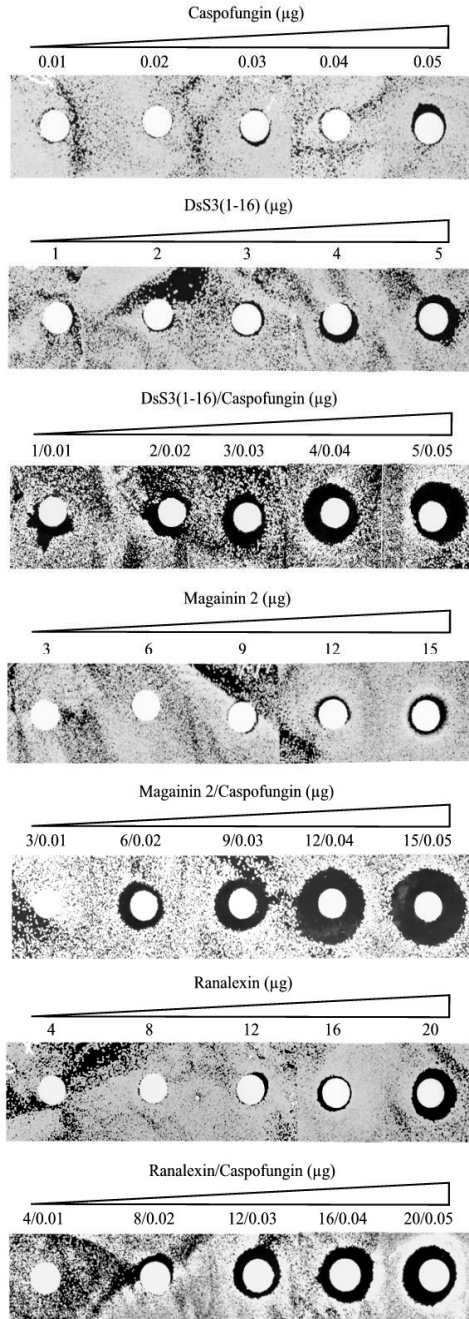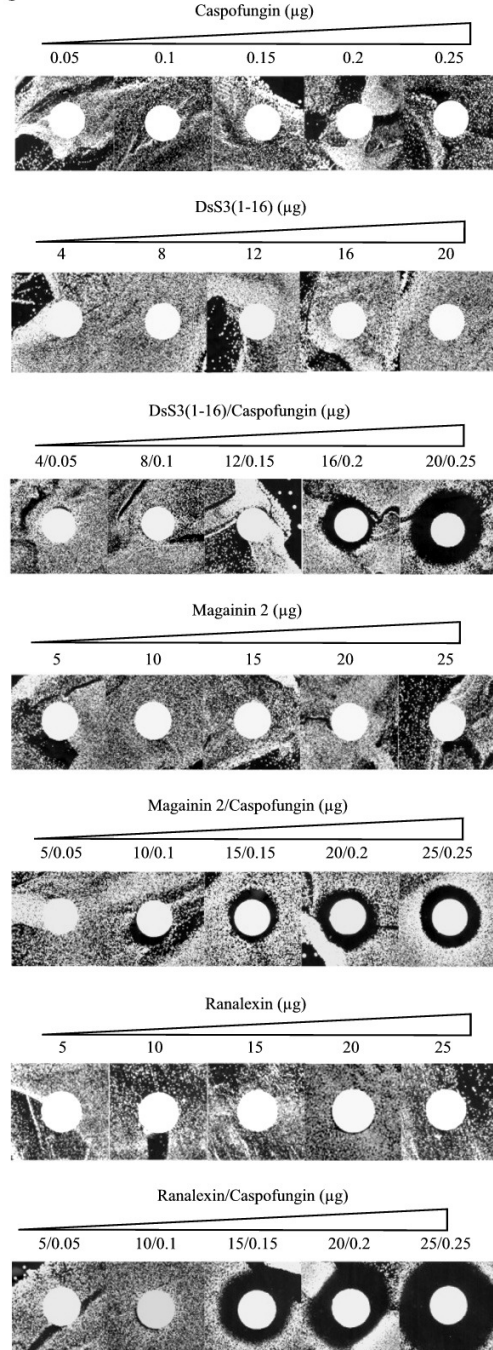
Figure 1. **Disc diffusion assays monitoring inhibition of *C. albicans* hospital isolate and *C. glabrata* with AMP and caspofungin. Discs were impregnated with increasing concentrations of peptide in the presence or absence of caspofungin. Plates were spread with mid-exponential phase culture. Each assay was carried out in duplicate.**
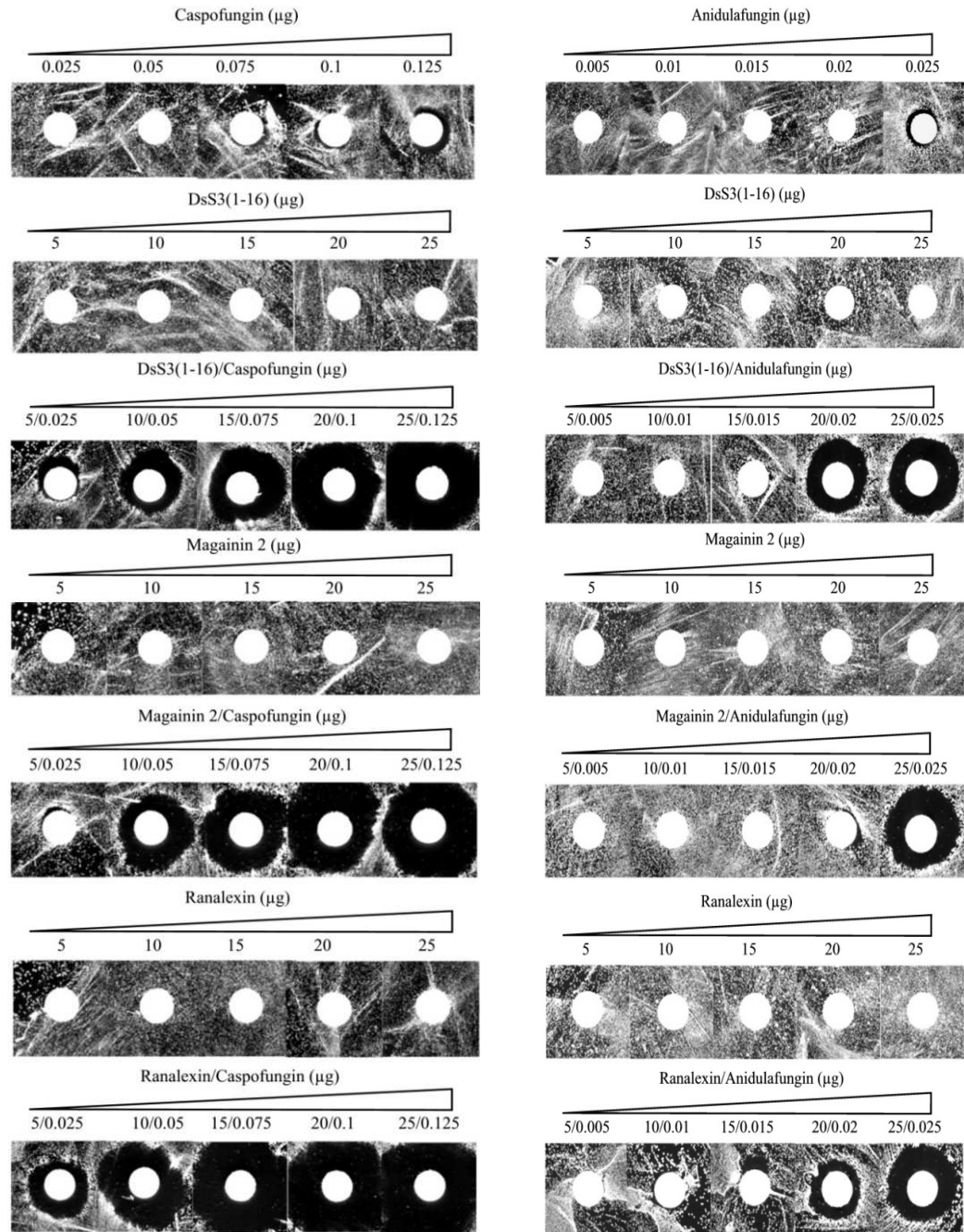
Figure 2. Disc diffusion assays monitoring inhibition of *C. albicans* hospital isolate with AMP and caspofungin/anidulafungin. Discs were impregnated with increasing concentrations of peptide in the presence or absence of caspofungin or anidulafungin. Plates were spread with mid-exponential phase culture. Each assay was carried out in duplicate.

# Appendix VI: MIC determination of *S. cerevisiae* deletion mutants
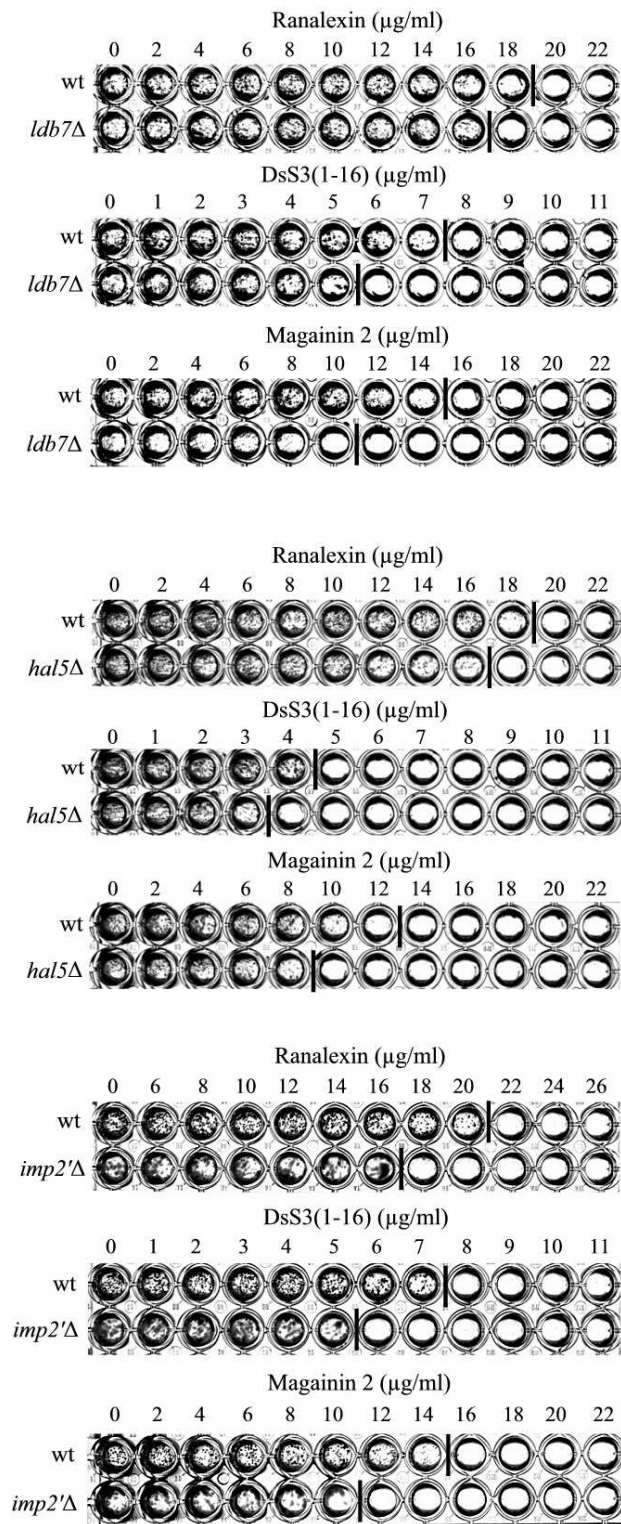
Figure 1. Representative checkerboard assays used to determine MICs for wt *S. cerevisiae*, *ldb7Δ, hal5Δ* and *imp2'Δ* with rana, DsS3(1-16) and mag 2. Experiments were carried out in duplicate and representative images for each are shown. Lines separate wells where growth was present from wells where growth was absent.

Appendix VII: Sensitivity of *IZH2* transformations to DsS3(1-16)
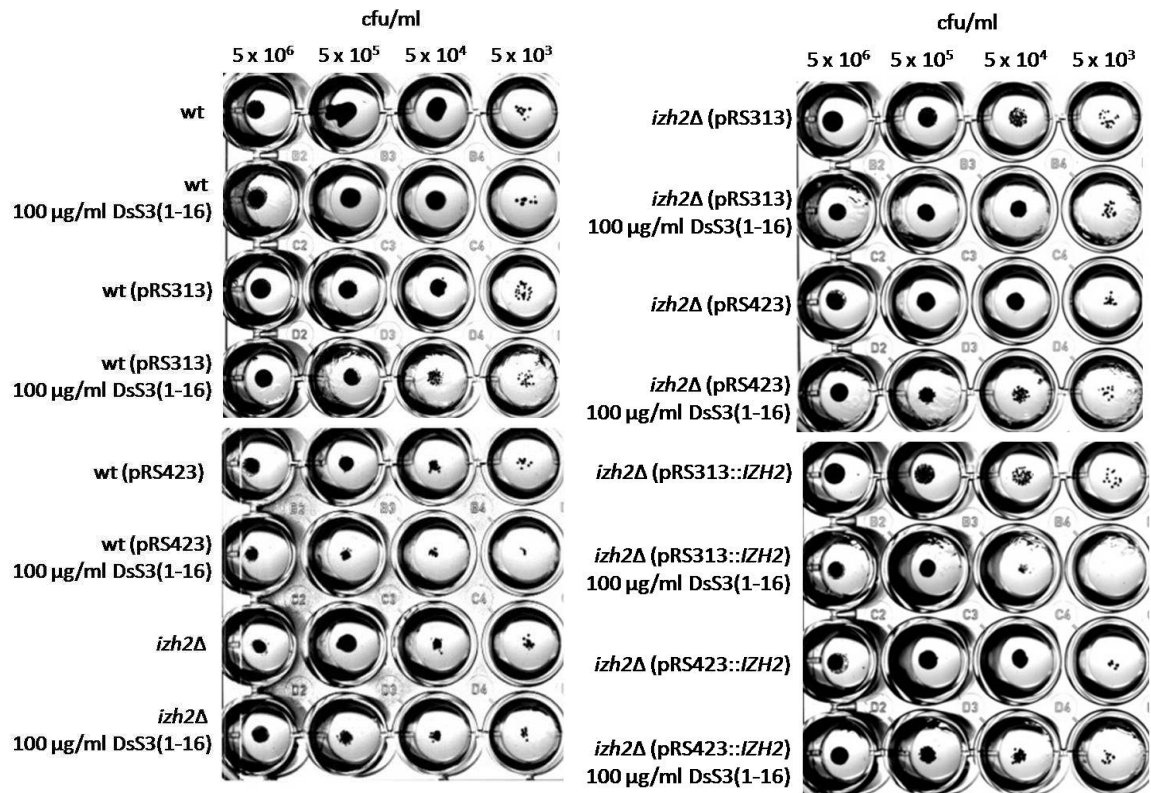
Figure 1. Growth of various concentrations of *S. cerevisiae* wt, *izh2Δ*, *izh2Δ*(pRS313) and *izh2Δ*(pRS423) on YNB agarose with or without 100 µg/ml DsS3(1-16). Experiments were carried out in triplicate and representative images for each are shown.

Appendix VIII: Publications

Harris, M., and Coote, P. "Combination of caspofungin or anidulafungin with antifungal peptides results in potent, synergistic killing of pathogenic *Candida albicans* and *Candida glabrata in vitro.*" *International Journal of Antimicrobial Agents.* **35** (4): 347-356.

Harris, M., Mora-Montes, H., Gow, N., and Coote, P. (2009) "Loss of mannosylphosphate from *Candida albicans* cell wall proteins results in enhanced resistance to the inhibitory effect of a cationic antimicrobial peptide via reduced peptide binding to the cell surface." *Microbiology*. **155**: 1058-1070.